Naval Command,
Control and Ocean
Surveillance Center RDT&E Division San Diego, CA
92152-5001

Technical Report 1716
January 1996

Environmental Analysis of U.S. Navy Shipboard Solid Waste Discharges: Report of Findings

D. Bart Chadwick
Charles N. Katz
Stacey L. Curtis
Dr. James Rohr
Marissa Caballero
Aldis Valkirs
Andrew Patterson

DISCLAIMER NOTICE

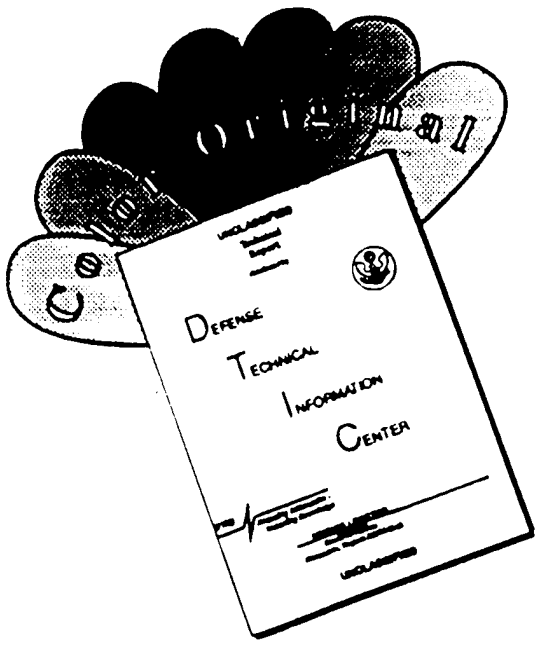

THIS DOCUMENT IS BEST QUALITY AVAILABLE. THE COPY FURNISHED TO DTIC CONTAINED A SIGNIFICANT NUMBER OF COLOR PAGES WHICH DO NOT REPRODUCE LEGIBLY ON BLACK AND WHITE MICROFICHE.

Technical Report 1716
January 1996

Environmental Analysis of U.S. Navy Shipboard Solid Waste Discharges: Report of Findings

D. Bart Chadwick
Charles N. Katz
Stacey L. Curtis
Dr. James Rohr
Marissa Caballero
Aldis Valkirs
Andrew Patterson

NAVAL COMMAND, CONTROL AND OCEAN SURVEILLANCE CENTER
RDT&E DIVISION
San Diego, California 92152-5001

K. E. EVANS, CAPT, USN
Commanding Officer

R. T. SHEARER
Executive Director

ADMINISTRATIVE INFORMATION

The work detailed in this report was performed by the Naval Command, Control and Ocean Surveillance Center RDT&E Division, Marine Environmental Quality Branch, Code 522, for Naval Sea Systems Command, Code 03R16. Funding was provided under program element 0603721N, Subproject S0401, accession number DN309084, and work unit ME40.

Released by
J. G. Govhoug, Head
Marine Environmental Quality Branch

Under authority of
R. H. Moore, Head
Environmental Sciences Division

ACKNOWLEDGMENTS

We would like to gratefully acknowledge the contributions made by Wayne Glad, Gordon Chase, Tom Knoebel, Dave Lapota, Debbie Duckworth, Gunther Rosen, Jon Groves, Bradley Davidson, Dr. Mark Hyman, Dr. Scott Jenkins, Dr. Russ Vetter, Larry Robertson, Dr. Mary Ann Moran, Coastal Resources Associates, Inc. (Dr. Tom Dean, Steve Carlson), Environmental Testing Associates (Dan Baxter), and Analytical Technologies, Inc.

PS

EXECUTIVE SUMMARY

This report summarizes the findings to date of work performed on the environmental analysis of pulped and shredded solid waste discharges from U.S. Navy ships. This study was requested as part of the Navy's effort to evaluate solid waste discharge compliance alternatives. Although the assessment is still ongoing, the present analysis suggests that there will be no significant adverse environmental impact from the discharges studied. The results of the ongoing studies will be integrated with findings presented here, and included in a follow-on report.

International regulations negotiated through the International Maritime Organization (IMO) have imposed restrictions pertaining to pollution from vessels in international waters. Regulation 5 of Annex V to the International Convention for the Prevention of Pollution from Ships, 1973, as modified by the Protocol of 1978 (MARPOL 73/78) prohibits the discharge of nonfood solid wastes into sensitive oceanographic and ecological areas, known as Special Areas. These Special Areas include the Baltic Sea, the North Sea, the Mediterranean Sea, the Wider Caribbean Region (including the Gulf of Mexico and the Caribbean Sea), the Antarctic area, the Black Sea, the Red Sea, and the "Gulfs" area (including the Persian Gulf). The U.S. Congress, through provisions of the Marine Plastic Pollution Research and Control Act (MPPRC) of 1987 and the Defense Authorization Act of 1994, requires that the U.S. Navy come into full compliance with MARPOL 73/78. The provisions call for compliance of all U.S. Navy surface ships in all enforced Special Areas by December 31, 2000, and for submarines by December 31, 2008. Currently, only the North Sea, the Baltic Sea, and the Antarctic areas are in force.

The Navy is in the process of researching alternatives for ways to comply with these restrictions and developing a compliance plan to propose to Congress. One alternative providing partial compliance to existing legislation consists of an equipment suite comprised of a plastics processor to handle plastics waste, pulpers for food and paper/cardboard products, and a shredder for metal and glass waste. This suite would be installed on all commissioned ships, with the exception of a few vessels whose waste generation rates would allow for temporary storage onboard. The equipment suite would be used not only in Special Areas but also in the open ocean as an improvement to current solid waste discharge practices.

The Naval Command, Control and Ocean Surveillance Center (NCCOSC) RDT&E Division Code 52 was tasked by the Naval Sea Systems Command (NAVSEA 03R16) to perform an environmental analysis of the pulper and shredder waste streams. The objective of this study was to determine to what extent, if any, Navy solid waste discharges lead to adverse marine environmental effects. The scope of the analysis was limited to nonplastic, nonfood solid waste, and therefore includes only the pulped paper and cardboard, and shredded metal and glass waste streams. The scope for this report was also limited to five of the Special Areas including the Baltic Sea, the North Sea, the Mediterranean Sea, the Wider Caribbean Region, and the Antarctic area. A subsequent report will include all of the Special Areas. This report presents the findings to date for the characterization of the waste streams and their expected fate and effects in the marine environment of Special Areas.

The study was approached primarily from a theoretical standpoint because few ships are installed with pulpers and shredders. A conceptual framework similar to that of an environmental risk assessment was used in which the material discharged was characterized with regards to its potential for biological impacts and in which the operational and receiving environments were characterized to determine the likely exposures. The analysis was approached for three spatial and temporal scales, including: a local scale, or single ship daily discharge case; a regional scale,

using an operational scenario that involves a battle group (BG) and an amphibious ready group (ARG) for a duration of 6 months; and a basin-wide, longer term assessment that considered Special Areas as a whole. Water column and sea floor processes were addressed in all cases.

The study involved a review of pertinent literature, characterization of the waste stream, model simulations, and field tests. The literature review focused on the regulatory framework of Special Areas, their environmental characteristics, the bulk waste stream constituents, general ocean discharge, and Navy vessel operational parameters. The waste stream characterization included physical, chemical, and biological assays as well as degradation and corrosion studies. Dispersion and fate modeling efforts entailed scaling analysis, ship wake dilution, and ambient dilution for the pulped material only. Small-scale field tests were conducted to develop test methodologies and to begin to validate the model simulations.

The findings of this study to date suggest that the discharge of paper and cardboard, and metal and glass waste streams as proposed will have no significant environmental consequences on a local, regional, or basin-wide scale in Special Areas. Furthermore, the findings support a conclusion that the discharge of these waste streams using pulpers and shredders is superior to current discharge practice utilized in open ocean environments. It must be kept in mind that this assessment is based on a few measurements, model simulations, and extrapolations to real-world conditions expected in Special Areas and as such, much of the conclusions are based on hypothetical considerations. The following key findings are the basis for these conclusions:

Key Findings of the Pulped Paper and Cardboard Waste Stream

- The pulped paper and cardboard is an organic material that is composed mostly of refractory cellulose. The pulped material was measured to be approximately 0.3% solids by weight of which approximately 92% is organic matter, and is low in nutrients compared to background organic matter. All of this indicates that the material will not be a significant source of nutients in the water column or the benthos and will most likely be avoided as a food source. Productivity should not be significantly enhanced and eutrophication should not be a major factor, however, microbial degradation may be hindered in nutrient limited ocean areas.

- The material contains no significant amounts of toxic chemicals. A 126 priority pollutant scan showed no pollutants at levels which would be expected to produce impacts and only trace amounts of zinc (6 $mg \cdot kg^{-1}$), acetone (2 $mg \cdot kg^{-1}$), and aliphatic hydrocarbons (6 $mg \cdot kg^{-1}$), which are well below threshold levels of concern for standard sediment criteria.

- On a mass basis, the waste stream is made up of predominantly large particles and most of the pulped material should settle to the sea floor where it will degrade through natural processes. Approximately 85% of the material is expected to sink within 1 to 10 days at average depths found in Special Areas with measured average sink rates of 0.5 $m \cdot min^{-1}$ for particles greater than 1000 μm. Another 12% will probably sink within 10 to 100 days while approximately 3% may remain in suspension, subject to microbial degradation and other processes in the water column. The measured degradation rate under optimal nutrient and temperature conditions was approximately 0.6% per day, however, the rate could be as low as 0.01% per day in cold, nutrient limited waters. The paper density was measured to be approximately 1.5 g/cm^3, indicating that density variations in the water column will not significantly affect sinking of particles greater than 200 μm in size. Approximately 95% of

the material will eventually be deposited on the sea floor. Therefore, exposure in the water column will be limited and the sea floor processes are assumed to be the dominant ones. No harmful effects have been seen in either regime given the expected waste concentrations.

- Discharge into the wake is the most critical factor in the dilution and dispersion of the pulped material. Modeling indicates that maximum concentrations of pulped paper following dilution in the wake will be approximately 0.2 $mg \cdot L^{-1}$, a dilution factor of 100,000 fold in a matter of minutes. Field measurements and modeling results support subsequent ambient dilution estimates up to 1,000,000 fold in approximately one hour. These levels are a fraction of background levels found in many ocean areas and well below any concentration found to have toxicity in laboratory bioassays.

- The potential impacts on water column and benthic biota tested occur only at concentrations significantly greater than would be found after discharge. Biological interactions tested with a large range of organisms from bacteria to small fish showed that the most sensitive response occurred in filter feeding sardines causing a temporary feeding interference effect at concentrations from 1 to 3 $mg \cdot L^{-1}$, or 5 to 15 times higher than found in the wake dilution. No biological effects were observed in any organism tested at concentration levels expected in the water column with wake dilution based on both particle and water phase testing. No biological effects were observed in two benthic organisms tested at concentration levels that would be expected in the sediments after 1000 ships had passed over the same location.

- Mass loading on an annual basis from regional and basinwide Naval operations is a miniscule fraction of other coastal inputs in Special Areas. Based on an operational scenario with an ARG and a BG deployed for 6 months in a 10,000 nm^2 area, the accumulated concentrations are well below those causing biological effects.

Key Findings for the Shredded Metal and Glass Waste Stream

- The shredded material is mostly composed of tin-coated steel cans (71% by weight) and glass (13% by weight). Minor components include aluminum cans, burlap bags, food waste, and paper labels. The elemental constituents of the metal and glass are not unlike those found in naturally occurring materials in the marine environment. Of these, only iron and tin are significantly enhanced in the waste stream relative to the concentrations found in typical marine sediments.

- The shredded material, discharged in burlap bags, sinks rapidly through the water column. This result indicates that the waste will have minimal impact in the water column and that its dominant fate and effects will occur on the sea floor. The proposed discharge method also appears to be an improvement over previous methods such as compacting which sometimes led to floating wastes. Based on the measured sink rates and estimates of shoreward transport in Special Areas, it is unlikely that the material will be a source of coastal litter if the bags are discharged outside the regulatory limits of 12 nmi or even 3 nmi.

- The ultimate fate of the shredded material is deposition, corrosion, and burial on the sea floor. Corrosion of the metal is likely to occur over a period of several years, although the rates can be highly variable. Corrosion is a process that will lead to a change in the aesthetic nature of the waste stream from a component of litter to a component more typical of sedimentary materials. The time scales for burial and redistribution of metal and glass waste

on the sea floor can be relatively long, ranging to hundreds of years for complete burial and degradation.

- Seawater leaching of the metal/glass was shown to cause some effects under laboratory conditions. However, the biological effects were shown to occur at concentrations that are estimated to occur within a few centimeters of the bag. Colonization of the metal and glass components in San Diego Bay over a year showed a highly diverse array of organisms, suggesting that many organisms are not negatively affected by the material.

- The effect of operating a large number of ships in a limited region as described above does not load the sea floor with bags at a significantly higher per unit area rate than already described for a single swath discharge. Any biological effects could therefore still be related to any that would be found within or near a single bag. These results could be altered if operational practices acted to concentrate the discharges in particular areas that are significantly smaller than an operational area. This suggests that operational discharge practices should be minimized in areas that are constantly traveled such as before and after leaving Navy ports.

- The annual input of the shredded metal/glass waste stream from U.S. Navy ships operating in Special Areas constitutes a tiny fraction of basin-wide inputs. It is estimated that it would take hundreds to billions of years of U.S. Navy discharges to match a single year discharge from other basin sources such as rivers or industrial discharges. The amount of material discharged annually by U.S. Navy ships would cover only a tiny fraction (billionths) of the sea floor.

- From a basin-wide perspective, there is at least a billion times more oxygen available in Special Areas than is needed to completely oxidize the annual discharge of metal components of the waste stream implying that it is improbable that the discharges will have any impact on the oxygen budget of any of the seas.

- Based on a steady-state analysis of the inputs and corrosion rates, the amount accumulated on the sea floor as a litter component would be roughly equivalent to about three years of discharges.

TABLE OF CONTENTS

LIST OF TABLES

LIST OF FIGURES

Figure 10-1. TBWAKE average dilution estimates as a function of distance from discharging vessel (frigate or aricraft carrier). Symbols represent pulped paper and cardboard discharge and lines represent dye discharge. Open symbols=unstratified, closed symbols=stratified, circle=10 kts, square=20 kts, triangle=25 kts. Solid line=20 kts unstratified, dotted line=20 kts stratified. Stratification was $2\pi \cdot N^{-1} \approx 500$ s.

Figure 10-2. TBWAKE minimum dilution estimates as a function of distance from discharging vessel (frigate or aircraft carrier). Symbols represent pulped paper discharge and lines represent dye discharge. Open symbols=unstratified, closed symbols=stratified, circle=10 kts, square=20 kts, triangle=25 kts. Solid line=20 kts unstratified, dotted line=20 kts stratified. Stratification was $2\pi \cdot N^{-1} \approx 500$ s.

Figure 10-3. Comparison of TBWAKE dilution estimates of pulped paper discharge from an aircraft carrier moving at 20 kts (10.3 $m \cdot s^{-1}$) for different ambient conditions. Solid line=Baltic Sea, dotted line=North Sea, open symbols=unstratified, solid symbols=stratified ($2\pi \cdot N^{-1} \approx 500$ s).

Figure 10-4. TBWAKE simulations of pulped paper particle concentration cross wake sections 5 km downstream of an aircraft carrier moving at 20 kts in unstratified (a-d) and stratified (e-h) conditions. Concentrations (gm^{-3}) are shown for 1, 1000, and 3000 μm (radius) particles and total particle load.

Figure 10-5. TBWAKE comparison of modeled and laboratory lateral wake-spreading rates. Closed symbols=tow tank measurements (Hyman et al., 1995), open symbols=TBWAKE numerical predictions.

Figure 10-6. TBWAKE comparison of wake dilution estimates of pulped paper discharge from an aircraft carrier moving at 10 kts (5.15 $m \cdot s^{-1}$). Computational simulation: circles=minimum dilution, triangles=average dilution, +=Csanady's 1981 estimation, x=IMO's (Delvigne, 1987) estimation. Open symbols=unstratified, solid symbols=stratified ($2\pi \cdot N^{-1} \approx 500$ s).

Figure 10-7. TBWAKE comparison of wake dilution estimates of pulped paper discharge from an aircraft carrier moving at 20 kts (10.3 $m \cdot s^{-1}$). Computational simulation: circles=minimum dilution, triangles=average dilution, +=Csanady's 1981 estimation, x=IMO's (Delvigne, 1987) estimation. Open symbols=unstratified, solid symbols=stratified ($2\pi \cdot N^{-1} \approx 500$ s).

Figure 10-8. TBWAKE comparison of wake dilution estimates of pulped paper discharge from an aircraft carrier moving at 25 kts (12.875 $m \cdot s^{-1}$). Computational simulation: circles=minimum dilution, triangles=average dilution, +=Csanady's 1981 estimation, x=IMO's (Delvigne, 1987) estimation. Open symbols=unstratified, solid symbols=stratified ($2\pi \cdot N^{-1} \approx 500$ s).

Figure 10-9. TBWAKE comparison of wake dilution estimates of pulped paper discharge from a frigate moving at 10 kts (5.15 $m \cdot s^{-1}$) Computational simulation: circles=minimum dilution, triangles=average dilution, +=Csanady's 1981 estimation, x=IMO's (Delvigne, 1987) estimation. Open symbols=unstratified, solid symbols=stratified ($2\pi \cdot N^{-1} \approx 500$ s).

APPENDIX LIST

LIST OF ACRONYMS

ASTM	American Society for Testing and Materials
ATI	Analytical Technologies Inc.
BAT	Best Available Technology
BC	Background Corrected
BOD	Biochemical Oxygen Demand
CCD	Charge-couple Device
CDNSWC/AD	Carderock Division Naval Surface Warfare Center Annapolis Detachment
Chl-a	Chlorophyll-*a*
CORMIX	CORnell MIXing Model for Continuous Discharge of a Heated Effluent
CNA	Center for Naval Analysis
C:N:P	Carbon: Nitrogen: Phosphorous Ratio
CNO	Chief of Naval Operations
COD	Chemical Oxygen Demand
DBASE IV	Database 4
DCM	Deep Chlorophyll Maximum
DGPS	Differential Global Positioning System
DOC	Dissolved Organic Carbon
ECLAC	Economic Commission for Latin America and the Caribbean
EMPSKD	Employment Schedule Data
EPA	Environmental Protection Agency
ERL	Effects Range Low
ESM	Enriched Seawater Medium
ETA	Environmental Testing Associates
GAR1	Small scale field test performed (date)
IAEA	International Atomic Energy Agency
IC	Inhibition Concentration
ICES	International Council for the Exploration of the Seas
ICP	Inductively Coupled Plasma
IDP	Initial Data Plane
IMCO	International Maritime Consultative Organization
IMO	International Maritime Organization
MED POL	Convention for the Protection of the Mediterranean Sea
MEPC	Marine Environment Protection Committee
MESC	Marine Environmental Survey Capability
MIKE21	Particle transport in coastal waters and seas
mpy	mil per year
MPPRCA	Marine Plastic Pollution Research and Control Act
MSC	Military Sealift Command
NAVSEA	Naval Sea Systems Command
NCCOSC	Naval Command, Control Ocean Surveillance Center
NCEL	Civil Engineering Laboratory, Naval Construction Battalion
NCSS	Naval Coastal Systems Station
NMFS	National Marine Fisheries Service
NOEC	No Observable Effects Concentration
NSF	National Science Foundation
NSFA	Naval Support Force Antarctica

ONR	Office of Naval Research
OTA	Office of Technology Assessment
PC	Polycarbonate
PMT	Photomultipler Tube
POC	Particulate Organic Carbon
psu	Practical Salinity Units
RV	Research Vessel
RSD	Relative Standard Deviation
SEDXPORT	Ocean dispersion model for sediment
SEM	Scanning Electron Microscopy
SIO	Scripps Institution of Oceanography
SSWD	Shipboard Solid Waste Discharges
STFATE	Short Term FATE model for dumping dredged material
TAPS	Tracor Acoustic Profiling System
TBWAKE	Model developed to simulate surface ship micro-bubble wakes
TOC	Total Organic Carbon
TOD	Total Oxygen Demand
TKN	Total Kjeldahl Nitrogen
TS	Total Solids
TSS	Total Suspended Solids
UCSD	University of California at San Diego
UNEP	United Nations Environmental Programme

1.0 INTRODUCTION

Recently enacted international regulations, as specified in regulation 5 of Annex V to the International Convention for the Prevention of Pollution from Ships, 1973, and modified by the Protocol of 1978 (MARPOL 73/78), will severely restrict the discharge of solid wastes from ships in MARPOL Special Areas in the future. These MARPOL Special Areas have been negotiated through the International Maritime Organization (IMO) and include the Baltic Sea, the North Sea, the Mediterranean Sea, the Wider Caribbean Region (including the Gulf of Mexico and the Caribbean Sea), the Antarctic area, the Black Sea, the Red Sea, and the "Gulfs" area (including the Persian Gulf). While the Naval Sea Systems Command (NAVSEA) is in the process of researching shipboard systems and procedures to comply fully with these regulations, it appears that viable technical solutions are still years away. NAVSEA is therefore developing, in parallel, a potential alternative for partial compliance using a suite of solid waste processing equipment to manage each waste stream in an effective and environmentally benign manner. The equipment suite consists of a plastics processor, two pulpers of different sizes for food and paper products, and a shredder for metal and glass. The Navy is in the process of deciding on a proposal to present to Congress which could include this equipment suite in order to allow the Navy to continue mission requirements and operations without undue restriction currently, and may prove to be an acceptable practice in the long term. However, the Navy must demonstrate that the proposed solid waste discharge will not place undue stress on the environment in order for Congress to inact legislative changes that will provide relief from full compliance in Special Areas.

This report provides a preliminary environmental analysis of selected shipboard solid waste discharges. Work is sponsored by NAVSEA 03R16 and performed by the Naval Command, Control and Ocean Surveillance Center, Research, Development, Test and Evaluation Division (NCCOSC RDT&E) Code 522. It is part of the Navy's effort to evaluate alternatives and decide upon a solid waste proposal to Congress that is environmentally sound, and technologically and economically feasible. In addition to this environmental analysis of shipboard pulper and shredder discharges, the Navy is also researching ways to handle waste onboard the vessels by means of destruction or storage and retrograde. The potential impact/non-impact of pulped and shredded solid waste discharges from Navy ships is discussed, and the preliminary theoretical and experimental findings for the environmental analysis of U.S. Shipboard Solid Waste Discharges (SSWD) is presented. Although this effort is ongoing, the required time frame necessitates preliminary documentation be submitted at this time. Further details will be forthcoming at the completion of this study.

1.1 Objectives and Scope

The objective of this study is to determine to what extent, if any, Navy solid waste discharges lead to adverse marine environmental effects. In order to accomplish this, a cooperative program to describe and quantify the thresholds and processes relevant to understanding the short-term and long-term impact of the Navy's proposed discharges was initiated. Due to constraints on time and resources, the study consists primarily of theoretical environmental analyses using literature reviews, laboratory data, modeling simulations, and selected small and large scale field tests.

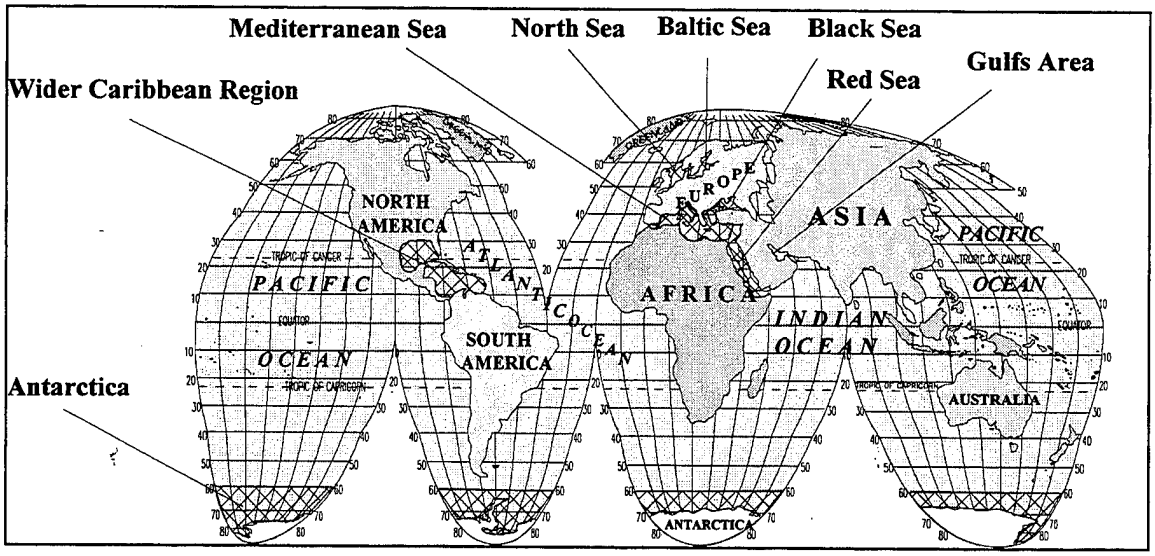

Figure 1-1. Map of the world showing MARPOL Special Areas under Annex V. Antarctica, North Sea, and the Baltic Sea are the only three Special Areas where IMO regulations are enforced.

The scope of this project is limited to issues concerning the discharge of nonplastic and nonfood solid waste from U.S. Navy ships in internationally designated Special Areas defined below. Because disposal of food wastes is allowed in Special Areas and plastics are banned in all ocean areas, neither have been tasked as a part of this assessment. Thus, the primary waste streams of concern for this project include pulped paper and cardboard, and shredded metal and glass. Discharge of these materials is prohibited within prescribed distances from shore and in Special Areas. Because this prohibition constitutes a hardship to the Navy in Special Areas, they will be the focus of this study and are detailed in the Special Area Rationale section. At the request of NAVSEA, the first five were the focus of this initial study and the remaining will be addressed in a subsequent report.

1.2 Background

Concern over the environmental degradation of marine habitats by anthropogenic activities has prompted international regulations, mandated by the U.S. Congress, which restrict and prohibit the discharge of solid waste from ships, particularly in MARPOL Special Areas. The U.S. Navy is reevaluating their current solid waste disposal practices to comply with the congressional legislation, and is proposing alternative procedures with the intention of allowing the Navy to maintain readiness without adversely affecting the quality of ocean environments in which naval vessels operate.

There are currently only three Special Areas where IMO regulations are enforced; these are the Baltic Sea, the North Sea, and the Antarctic area. The U.S. Navy is not currently discharging any solid waste into these regions (verbal communication, Center for Naval Analysis, CNA). In the other Special Areas, the Navy makes all attempts to comply with the MARPOL 73/78 regulations whenever possible. The proposed equipment to handle the paper/cardboard and metal/glass waste streams is currently not installed except as prototypes on the USS *George Washington*, the USS *Theodore Roosevelt*, the USS *Wasp*, and the USS *Vandergrift*. Therefore, current waste stream management varies according to the available equipment each vessel maintains. For the

variety of Naval vessels, a combination of incineration, compaction, storage and retrograde, and direct overboard disposal are all options currently in use.

NAVSEA has proposed a mix of solid waste discharge equipment to take the place of current methods for managing plastics, metal, glass, paper, cardboard, and food wastes. These new techniques of handling solid waste discharges are designed to minimize environmental impact and to ensure that the waste does not stay on the surface of the ocean after discharge. NAVSEA has detailed their proposed equipment mix and program strategy, including equipment types and numbers by vessel, along with reliability and processing rates, ship waste generation and storage requirements, backfit versus new construction requirements, program implementation schedules, and program implementation and operating costs (NAVSEA, 1993).

Four pieces of new equipment are being developed for shipboard use by the Carderock Division Naval Surface Warfare Center Annapolis Detachment (CDNSWC/AD); they are the plastics processor, the metal and glass shredder, and two sizes of combined food, paper, and cardboard pulpers. For this study, the shredder and pulpers serve as the prototype equipment providing the necessary waste streams for characterization, experimentation, and analysis.

Table 1-1. Typical shipboard waste generation rates (from NAVSEA, 1993).

Waste Stream	Waste Generation Rate (lbs/person-day)	Waste Density (lbs/ft^3)
Paper/Cardboard	1.11	6.0
Metal/Glass	0.54	11.8
Plastic	0.20	1.3
Food wastes	1.21	45.0

The NAVSEA plan presents shipboard waste generation rates and waste densities determined by actual surveys of naval vessels at sea, performed by CDNSWC/AD. Waste densities are preprocessed and estimated in air and will be less than those determined for processed waste in liquid. These rates are shown in table 1-1 (NAVSEA, 1993). These rates were used in this study, along with historical man-loadinging estimates from the archived employment schedule database from the Chief of Naval Operations (CNO), to estimate mass loading in each of the Special Areas.

Table 1-2. Typical shipboard waste composition (from Manzi, 1994).

Shipboard Solid Waste: Norfolk Naval Station	Weight Percentages (%)	Volume Percentages (%)
Plastics	9.84	15.00
Paper/Cardboard	39.25	59.50
Metal/Glass	12.41	9.28
Other Inorganics	7.50	4.75
Food	9.45	2.00
Other Organics	21.55	9.75

Typical solid waste discharges from shipboard-generated waste at the Naval Station, Norfolk have been characterized in a study performed at CDNSWC/AD (Manzi, 1994). This report provides basic information on percentages by weight and volume for the major constituents of the solid waste stream found at the Naval Station, Norfolk including food, other organics, cardboard, paper, metals, glass, plastics, and other inorganics. The percentages determined in this Norfolk study will differ somewhat from those found throughout the wide variety of ships at sea, and are used only as representative figures for the overall waste streams. These data, by weight and volume, are presented in table 1-2 (Manzi, 1994). The processing rates have also been determined and are shown in table 1-3 (NAVSEA, 1993).

Table 1-3. Processing rates of various waste processing units (from NAVSEA, 1993).

Equipment	Processing Rate (lbs/hr)
Large Pulper	500 paper/cardboard
	1,000 food wastes
	680 mixed
Small Pulper	100 paper/cardboard
	200 food wastes
	136 mixed
Metal/Glass Shredder	600 metal/glass
Plastics Processor	30

The following efforts were included are part of this study:

physical, chemical, and toxicological characterization of the waste streams in the laboratory; given that there was very little prior information in this area, obtaining this data was of primary importance

- a review of the oceanographic, ecological, and pollutant status of each of the Special Areas
- a review of the regulatory framework surrounding the concept of Special Areas, including scientific and other information available on how they became designated
- a review of past Navy operations in these areas
- a review of other studies on the dumping of waste materials in the oceans
- model simulations of the fate of material under a broad range of likely conditions, and
- field studies for model and laboratory validation, and to collect empirical data on dispersion and settling

To provide a framework for this analysis, the approach taken in this study was to form a conceptual model of the processes important in understanding the fate and effects of these waste streams in the marine environment in general, and particularly within Special Areas. Using the conceptual model as a framework, this study focuses on a number of processes and issues

pertinent to Special Areas that would provide the scientific basis for determining what impact, if any, there might be to these environments.

2.0 CONCEPTUAL FRAMEWORK

A conceptual framework for the study is described in this section. The section is broken down into three components: a statement of the problem, a set of conceptual models which incorporate processes and scales which may be important to the problem, and a description of the potential environmental issues which may arise as a result of these processes. The problem statement is not significantly different for any waste stream discharged into the ocean where the general goal is to determine the probability of adverse effects. However, the processes which determine the outcome to the problem depend on many diverse factors, which, for the ocean, are still poorly understood or difficult to measure. In this case, our conceptual models for the pulped and shredded waste streams are treated separately, as they contain significantly different materials and are delivered to the ocean in different manners, so are expected to have different fates, and may thus lead to different effects. The conceptual model will also vary as a function of the scale at which the system is considered, since the local effects of discharge from a single ship can be considerably different from the combined basin-scale effects due to many ships discharging over a long period of time. A conceptual model based on this basin-scale view is also considered. Many of the specific issues considered in this section were initially identified in the analysis of Swanson et al. (1994), while much of the basis for the general conceptual models described below draws on frameworks from previous studies of ocean disposal (e.g. Csanady, 1987; Brooks et al., 1987; Charnock et al., 1994), as well as knowledge of the Navy discharge plan (NAVSEA, 1993).

2.1 Problem Statement

Our formulation of the study is based on attempts to answer questions about the potential fate and effects of the waste streams. In this regard, this study follows the principles of environmental risk assessment using a dose/response model to evaluate the environmental significance of predicted exposures. A general statement of the problem is posed as,

To what degree, if any, do the materials discharged adversely effect the marine environment?

This broad question requires a scientific approach that attempts to answer specific questions regarding the characteristics of the waste stream, the characteristics of the receiving environment, and the manner in which the two interact. These can be broken down more specifically as follows:

Discharge Characteristics
1. What is being discharged?
2. How much is being discharged?
3. What are the discharge conditions?

Receiving Environment
1. What are the hydrographic conditions that will affect the fate of the discharge?
2. What are the biological systems and other endpoints that may be affected?

Interactions
1. Where does the material go?
2. How and at what rate is it dispersed?
3. At what level are biological systems exposed and for what duration?

Our understanding of the answer to the overall question of effects is thus based on the degree to which we can describe the discharge and the receiving system, and the level at which we can understand the interactions between the two. While discharge characteristics are relatively easy to define, the receiving environment varies widely across a broad range of Special Areas. There are constraints inherent in attempting to evaluate the potential outcome of an unlimited range of receiving water conditions. Thus, this study focuses on the processes thought to be important in controlling the fate and effects of the waste streams, and the range of oceanographic and environmental conditions which bound those found within the Special Areas. These dominant processes are described in the conceptual models below.

2.2 Conceptual Models

Local Scale Models

The local regime addresses relatively short term impacts due to a single ship or possibly a fleet of ships operating in an area of limited spatial extent. The physical processes associated with this scale are primarily related to near-field mixing, advection, and settling, while the biological issues are governed by acute exposure, grazing, and microbial degradation. This has parallels, for example, to previous studies of dredge spoil, acid waste, solid waste, and ballast water discharges by ships and barges which occurred over a limited time and area (Park and O'Connor, 1981; Farmer et al., 1975; Kress, 1993; EPA, 1991). The schematics for this localized regime are shown in figures 2-1 and 2-2 for the pulped paper/cardboard waste stream and the shredded metal/glass waste stream, respectively.

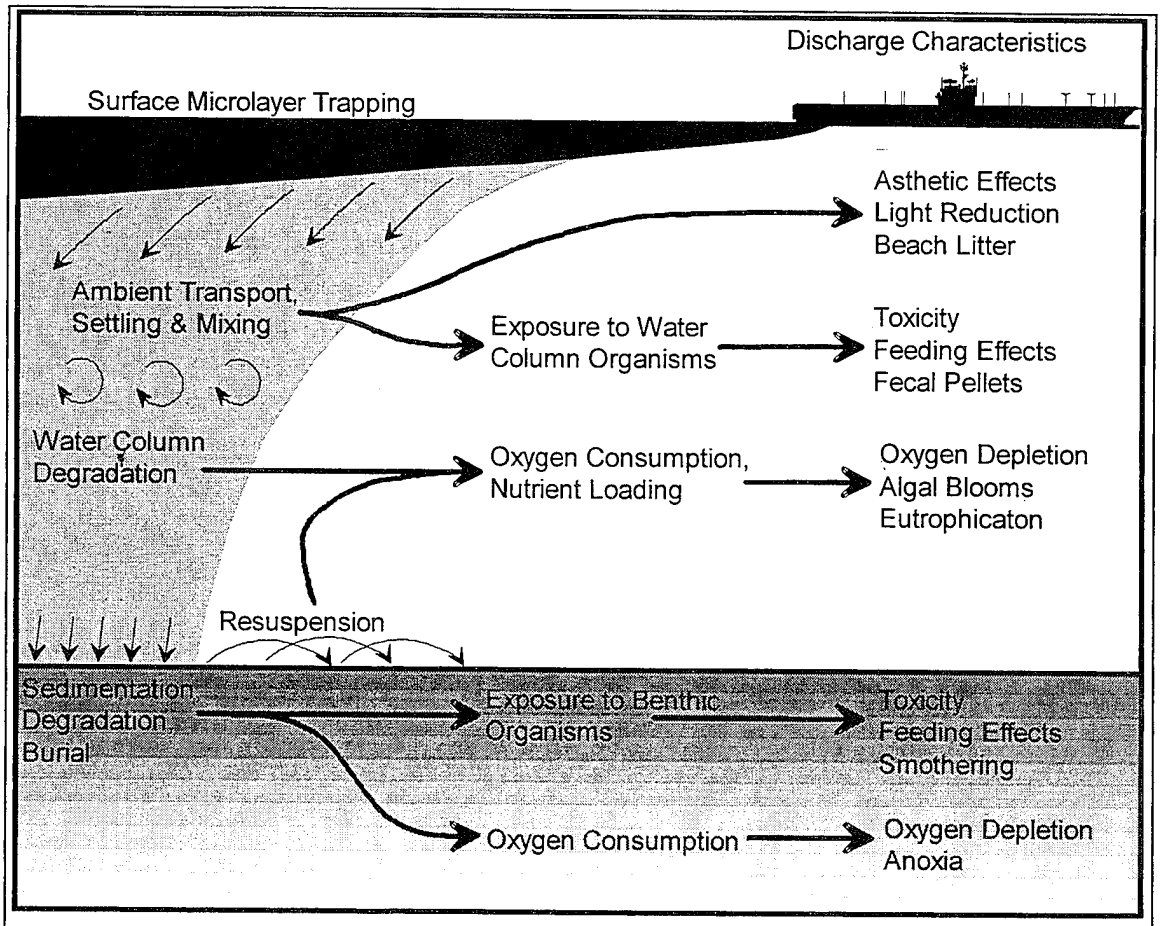

Figure 2-1. Conceptual local-scale model for the fate of ship-discharged pulped paper waste.

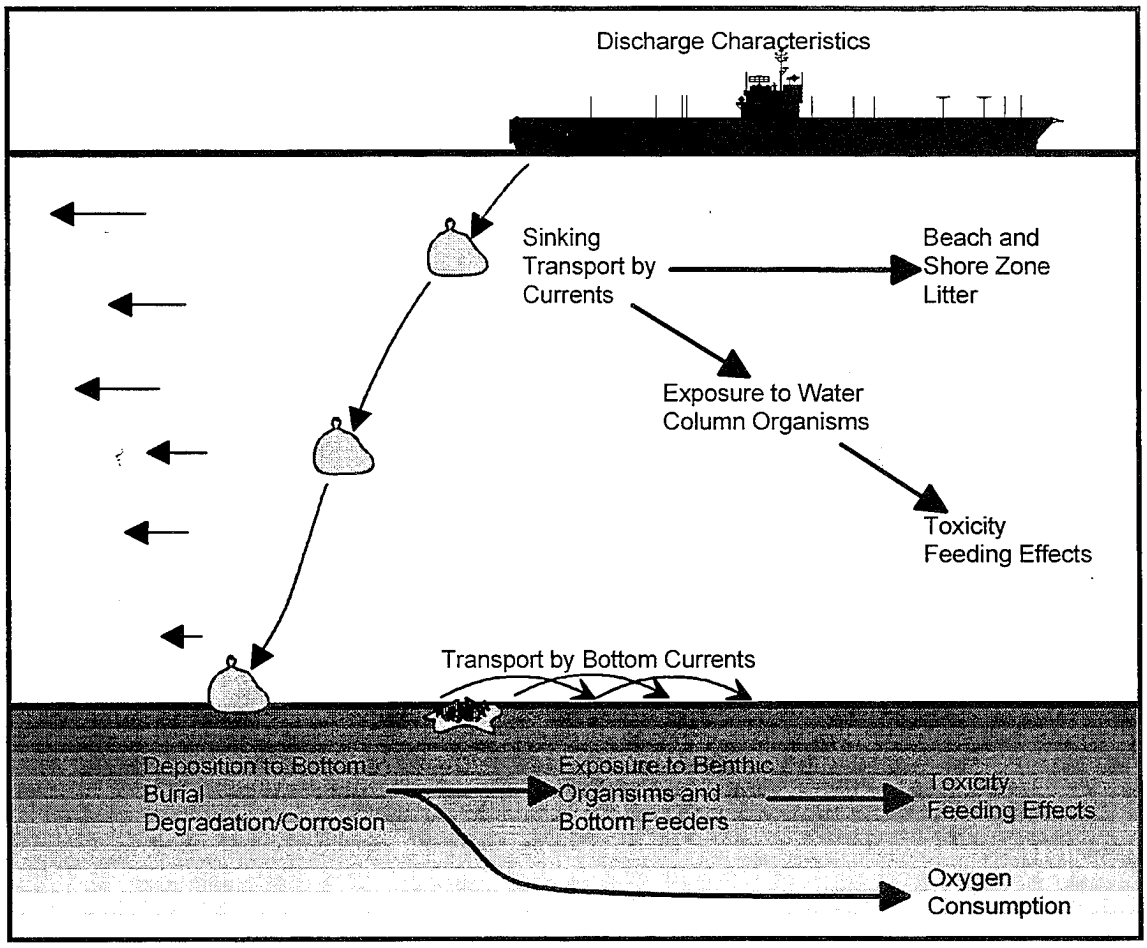

Figure 2-2. Conceptual local-scale model for the fate of ship-discharged shredded metal and glass waste.

Pulped Waste Stream Model. The pulper waste stream schematic incorporates the characteristics of the waste stream at the discharge point, the manner of discharge, transport and dilution effects due to the ship wake and the ambient flows, and deposition to the sea floor. First-order processes within the water column and sediment which may affect the fate of SSWD include degradation, deposition, burial, and resuspension. Potential detrimental effects include direct effects such as toxicity to water column and benthic organisms in terms of mortality, growth rate, and reproductive effects, feeding inhibition, oxygen depletion, and beach litter, as well as indirect effects such as eutrophication and corresponding algal blooms.

A simplified scenario for the life-cycle of the pulper discharge could be summarized as follows. The waste stream, composed primarily of particulate organic carbon in the form of cellulose, is discharged from the side of the ship. The waste stream is then diluted by the strong mixing in the ship wake in a very short time (i.e., minutes). Exposure to organisms in the water column can be assumed to begin at this point. Direct toxicity or feeding effects on particle feeders could occur at this time. Particles that are ingested may be assimilated or repackaged as fecal pellets and sink rapidly. The larger pulped particles will also begin to sink out preferentially, and all fractions of the waste stream will continue to dilute under the influence of ambient mixing. Material

remaining in the water column undergoes physical, chemical, and microbial degradation processes. Physical breakdown of the particles would lead to changes in the size distribution which may affect sinking. Chemical and microbial breakdown will consume oxygen and release CO_2 and nutrients. The oxygen demand associated with this breakdown could contribute to localized oxygen depletion in an oxygen limited region. The release of nutrients (primarily associated with components other than cellulose) may enhance primary productivity and lead to localized eutrophication. Eventually, some fraction of the material will reach the sea floor. This material may remain in place or may be redistributed by currents or bioturbation. Benthic organisms may be exposed during this period. Degradation will continue on the bottom but may be slowed significantly if the material is buried and removed from oxygen supplies.

Shredded Waste Stream Model. The model for the shredded metal/glass waste stream is considerably less complex. The shredded metal and glass are contained in a burlap disposal bag which does not trap air and allows the combined waste to sink quickly as a single unit. Thus the primary factors affecting fate of the shredder waste stream in the water column include the density and sinking characteristics of the bagged waste, the lateral transport that may occur during sinking, and short term exposure to water column organisms. It is anticipated that the shredded waste will reach the bottom rapidly, so that most of the processes which influence the fate and effects of the waste will occur at or near the sediment water interface. The primary factors to consider include burial, degradation (primarily due to corrosion), and possible transport by bottom currents. Potential detrimental effects include toxicity to benthic organisms, ingestion by benthic deposit feeders, oxygen uptake during corrosion processes, and beach and shore zone litter.

A typical scenario for the life cycle of the shredder discharge begins with the ejection of the bagged waste from the ship, containing primarily shredded tin cans, aluminum, and glass. The bags are then transported by currents as they sink rapidly to the bottom. The distance from the discharge point to bottom impact is dependent on current strength and water depth. Once the bags settle on the bottom, they will tend to stay in place except under very strong current conditions. At this point, benthic organisms may be exposed to the waste. Degradation of the bag material (burlap) and the corrosion of the metals will take place. The bag will decompose first and at some point, the metal/glass debris will be directly exposed on the bottom. These smaller components may be subject to transport and redistribution by currents. Eventually, much of the waste may breakdown or be buried. Hard materials may also provide a substrate for benthic colonization.

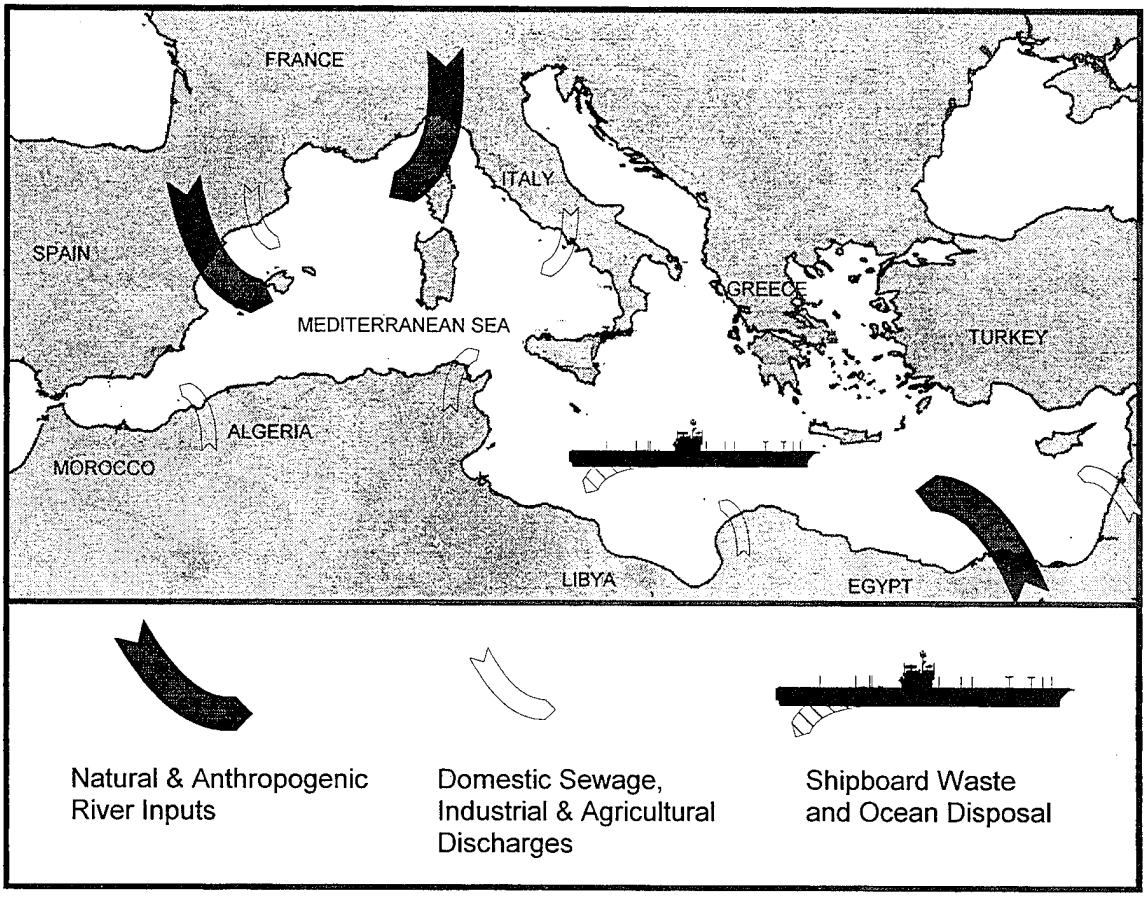

Figure 2-3. Conceptual basin-scale model for mass loading estimates and comparison to shipboard solid waste discharges in a typical Special Area.

Basin-Scale Model

The second regime involves a larger, basin-scale view of the problem. A schematic of the large scale model for a typical Special Area is shown in figure 2-3. This scenario incorporates the idea of large numbers of ships operating on broad spatial scales for extended periods of time. The primary processes addressed in this view include aspects of overall mass loading, sedimentation, litter, accumulation, and chronic low-level exposure. The goal of this approach is to provide a perspective on the relative contribution of ship discharges to the overall loading of regions or basins for constituents that are present in the SSWD. The primary components of the SSWD include organic cellulose materials from the pulper and inorganic metals and glass from the shredder. The basic constituents of this waste are present in most regions from a variety of anthropogenic and natural sources including river inflow, domestic sewage outfalls, industrial and agricultural discharges, and ocean dumping. Organic materials are also generated by natural processes within the water such as photosynthesis.

2.3 Technical Issues

Based on the problem statement, and the process schematics described above, a matrix of technical considerations for the project was developed. The key issues addressed are summarized in table 2-1. Issues are broken down as a function of potentially affected media (e.g., surface waters, sediments), and potential effects within those media (e.g., litter, ingestion, toxicity). Aspects for which little or no information was available prior to this study are highlighted. The technical approach for the project was developed from the concerns and issues posed by this conceptual framework. The specific aspects of the technical approach are described in detail in the following section.

Table 2-1. Summary of key issues related to the fate and effects of solid waste discharges from ships. Aspects for which little or no information was available prior to this study are highlighted.

Discharge Source	Discharge Conditions	Waste Stream Characteristics	Water Column Processes	Sea Floor Processes	Effects
Near-Field Pulper	Rate Period Location on Ship	Bulk Composition Physical Chemical Toxicological	Wake Mixing Ambient Mixing Ambient Currents Gravitational Settling Degradation	Deposition Rates Accumulation Resuspension Burial Degradation	Toxicity Feeding Effects Litter Oxygen Depletion Eutrophication Microlayer Enrichment Smothering Light Attenuation
Near-Field Shredder	Rate	Bulk Composition Physical Chemical Toxicological	Ambient Currents Gravitational Settling	Accumulation Transport Burial Degradation/Corrosion	Benthic Toxicity Litter Feeding Effects Ingestion Smothering
Basin-Scale	Ship Traffic Manning Rates	Bulk Composition Chemical	Special Area Characteristics	Sedimentation Rates Background Rates	Eutrophication Oxygen Depletion Liter

3.0 TECHNICAL APPROACH

The broad scope of the solid waste issue and the urgency of the required response, dictate that this initial assessment of the potential impact to the marine environment be approached primarily from a theoretical rather than an observational viewpoint. Additionally, since the Navy's proposed processing equipment suite has not yet been implemented except as prototypes aboard selected vessels, there is only limited opportunity for real data collection. Ongoing analyses will incorporate experimental measurements obtained during full scale field tests using a Navy frigate, however, the goal of this initial assessment was to isolate potential pathways and areas of impact using worst-case, order-of-magnitude estimates of loading, and conservative measures of physical and ecological response. This allows low-risk issues to be eliminated and subsequent evaluation to focus on the issues with the highest potential for environmental degradation in response to the Navy's proposed pulped and shredded waste streams. In addition, it will provide sufficient data with which to develop a preliminary environmental analysis using laboratory results projecting and extrapolating into real world conditions found in MARPOL Special Areas. A synopsis of the Special Areas, along with previous studies of ocean disposal for solid waste, dredge spoils, pulp mill effluent, and sewage contribute to the theoretical framework for understanding the processes important for this initial assessment, even though it is clear that these particular pulped and shredded waste streams are unique. Findings from the waste stream characterization form the basis for evaluation of overall mass loading for constituent compounds, potential exposure levels, and dispersal characteristics. In addition, they provide inputs to the wake and ambient dispersion models which constitute the basis for determining the fate of the pulped material as well as a predictive capability. Field tests on the pulped material provide data for verification and validation of the models as well as empirical fate measurements, and longevity tests on the shredded material indicate qualitatively the biological impact *in situ*.

In order to determine the potential impact on the marine environment due to Navy discharges, one must understand the discharge constituents and conditions, the fate of the material in the environment, and the ultimate effect it may have on biological, chemical, and physical processes resident in the area of discharge. The technical approach for this study incorporates the conceptual framework discussed in section 2.0, and is described below.

3.1 Discharge Conditions Composition and Waste Stream

Because little is currently known about their composition, characterization of the waste streams is an important first step. Basic knowledge of the physical, chemical, and biological characteristics of the waste stream are essential to better understand and predict the potential fate and effects of the material when it is discharged into the environment. Physical assays are required for prediction of dispersion, transport, exposure, bioavailability, and aesthetic considerations. Chemical and biological assays give an indication of the possible effects in the environment such as oxygen depletion, eutrophication, toxicity, feeding behavior, growth rate, and reproduction.

To characterize the discharge, this study relied on data found in the literature and data compiled from analysis and experimentation. Much of the basic rate, concentration, and composition information was derived from CDNSWC/AD information on the prototype pulper and shredder equipment. Actual samples from the prototype systems, both at CDNSWC/AD Detachment, and the USS *George Washington*, were used for all of the analysis. In general, attempts were made to obtain direct measurements data whenever possible, and representative estimates were used when necessary. Data for comparisons of both waste streams with other regional inputs were extracted

from the literature. The technical approach for determining the vessels operating characteristics and mass loading of both waste streams was to:

- estimate vessel movements and man-loadinging within each Special Area using archived EMPSKD data, and mass loading using those data in combination with waste generation rates provided by CDNSWC/AD (NAVSEA, 1993)

- incorporate other pertinent information relative to the operating speeds of the vessel, planned equipment suites, potential placement of the equipment onboard the ships, and operating scenarios based on discussions with cognizant contacts including NAVSEA 03V, CDNSWC/AD, CNA, and NRaD Liaison Office representatives

There are some issues which are specific to each waste stream, therefore the technical approach taken to characterize the pulp in waste stream attempted to:

- characterize the bulk composition of paper and cardboard with data extracted from the literature and to validate the information experimentally
- calculate particle concentration from the processing rates provided by CDNSWC/AD as well as to determine the concentrations experimentally
- analyze the chemical constituents and particle size and distribution experimentally

Our approach relative to the shredded metal and glass, with the expectation that they will generally sink rapidly to the bottom, has been to:

- classify the contents of the burlap bags into individual component percentages
- determine experimentally the volume, mass, and density of the samples provided
- determine experimentally the sinking velocity of the bags
- theoretically calculate the horizontal transport given average current speeds and depths within the Special Areas

3.2 Fate of Pulped and Shredded Waste Streams

As part of understanding the fate of the material, one must understand the receiving waters hydrodynamic and oceanographic characteristics as well as the regional sea floor processes. In addition, the ecology, pollution, and environmental status of the region of interest must be understood. Since there are numerous variations of the these conditions located within the Special Areas, our technical approach focused on the literature review to obtain this information. We then attempted to bound the range of environmental conditions by developing representative profiles for each of the Special Areas and evaluating the results in a comparative way. Given our current resources and time frame, this study was limited to this select number of cases which we believe represent the range of conditions found within the five Special Areas included to date.

The fate of the pulped and shredded waste streams has been approached separately due to the differing characteristics of the material. Relying on both theoretical and experimental data obtained from literature reviews, analysis, and field work, the following technical approach was used to determine the fate of both waste streams in the local and basin-wide scales.

Settling Characteristics. Settling velocity is an important parameter which was measured experimentally in a laboratory setting. An estimate of settling velocity could also be obtained via

field tests in a "real world" setting, at an increase of cost and resources; this approach will be incorporated into this study during the full-scale field work. Settling velocity will impact the duration of the biological exposure found in the water column, the degradation the material experiences while in the water column, the potential for litter washing onshore, and the ultimate dispersion and footprint of the material on the benthos. Based on measured settling velocities, efforts have been made to estimate sedimentation rates and total deposition using theoretical dispersion rates. Resuspension has been addressed to a limited extent through an analysis of the physical characteristics and similar studies from the literature. Dispersion modeling has been addressed to a large extent, both in the wake dilution case and the ambient case, as has degradation of the material, both in the water column and in the benthos. Each of these studies have initial results available which are included in this report. However, they are ongoing with significant efforts still to be accomplished to understand the respective processes. Each are addressed separately below in order to provide the adequate background material.

Dispersion Modeling. In order to reliably predict the dispersion and fate of material initially ejected into a ship's wake, properties effecting its transport (e.g., density, fall velocity, cohesiveness, moisture content, etc.), together with the essential dynamic wake and ambient features of the flow fields encountered must be determined. The flow in the wake of a ship, which is responsible for the initial dilution, is extremely complex, often being a nonlinear superposition of turbulent and shear flows, coherent vortex flows, free surface waves, bubble flows, and potentially internal waves (Reed et al., 1990; Meadows et al., 1990; Meadows et al., 1994). Furthermore, in order to reliably predict the long term dispersal and fate of the discharged material, the effect of possible bathymetric and ambient conditions occurring throughout the areas of interest must be known.

The hydrodynamic processes responsible for the dispersion and fate of Naval shipboard paper/cardboard discharges are best divided into two separate model studies. This separation arises due to the different nature, length and time scales of the hydrodynamic mixing, and has been the approach for analysis of industrial waste dumping from barges (Csanady, 1981) and tankers (Delvigne, 1987). One model was used to address mixing in the ship's wake over a period of minutes, where vigorous mixing results both from the drag of the ship and the stirring of the propellers. Initial wake dilutions on the order of 10^4 have been found in the wakes of barges (Csanady, 1981) and tankers (Delvigne, 1987). For comparison, initial dilution rates of 10^2 for sewage from a submerged outfall are considered good practice (Rawn et al., 1960). A second model was used to predict the subsequent ambient dilution of the paper/cardboard discharge over a period of days. Ambient diffusivities will depend primarily on wind, current, wave, swell, and density differences between the discharge and ambient ocean. Experiments have shown that ambient diffusion in the ocean may range from 10^{-5} to 10^{-2} $m^2 \cdot s^{-1}$ for vertical diffusivities and 10^2 to 10^5 $m^2 \cdot s^{-1}$ for horizontal diffusivities (Apel, 1987).

Because of the complex nature of predicting the dispersal and fate of particles discharged into the wake of a ship, several approaches are warranted (Fischer, 1979). These approaches may include: order-of-magnitude analysis, computer techniques, laboratory experiments, and field work. Computer modeling for wake mixing analysis is thought to be the best approach for this study, largely due to the present lack of full-scale wake mixing measurements for naval ships. Even with additional full-scale tests, which would be desirable, obtaining a full-scale database incorporating all relevant ships, discharge, and ambient conditions will remain prohibitively expensive. This study has tried to incorporate, where practical, as many of the other approaches as possible. For example, estimates made from semiempirical formula developed to predict the

dilution capacity of wakes behind barges (Csanady, 1981) and tankers (Delvigne, 1987) are compared with the present model results. In addition, tow tank tests investigating the spread of dye behind a model of a large Naval combatant have been made and used for comparison (Radcliff, personal communication).

Before choosing models to use for the wake and ambient conditions, NRaD conducted a model selection process. Several models were reviewed including: TBWAKE (a Navy model developed to simulate surface ship micro-bubble wakes); SEDXPORT (an ocean dispersion model for sediment, developed at the Scripps Institution of Oceanography (SIO); MIKE21 (a professional engineering software package for modeling particle transport in coastal waters and seas, developed by the Danish Hydraulic Institute); STFATE (a Short Term FATE model for dumping dredged material developed by the Army Corps of Engineers); and CORMIX (CORnell MIXing model for continuous discharge of a heated effluent).

Degradation. The environmental implications of waste paper releases into oceanic systems can be expected to depend on both the physical attributes of the waste (e.g., particle size, sinking rate) and the biological processing of the waste (e.g., degradation rate, food chain response). Relatively little is currently known about the biological fate of cellulose material in the open ocean or the cellulolytic abilities of natural oceanic bacterial assemblages, primarily because cellulose is not naturally abundant in such environments. Such information is critical, however, to gain a basic understanding of the ecological fate of cellulose particles released into the ocean, including where in the pelagic environment the bulk of decomposition is likely to occur, what the potential local impacts of waste releases are on marine food webs, and time frame necessary for complete decomposition of the waste material.

Cellulose is a natural and abundant component of coastal marine environments, and previous research in these systems provides a framework for design and interpretation of this microbial degradation study. It has been found, for example, that rates of mineralization of plant polysaccharides (cellulose and hemicellulose from wood and grasses) range from 0.2 to 2.0% d^{-1} (for particles <500 mm in diameter under aerobic conditions) in tropical and subtropical coastal marshes and mangrove swamps (Benner et al., 1984, 1985; Benner and Hodson, 1985). Temperature is an extremely important environmental determinant of polysaccharide decomposition rates in these systems, where cellulose decomposition rates increased by 3 to 4-fold when incubation temperatures were increased from 10° to 20 °C (Benner et al., 1986). This is known as a Q10 value, which refers to the increase in the rate of a biological process when the temperature increases by 10°C. Furthermore, decomposition kinetics of plant polysaccharides can be complex, in that mass loss does not follow a simple negative exponential (first order) model. Instead, the specific rate of decomposition continually decreases, so that no single decomposition parameter is appropriate for describing the complete degradation process (Moran et al., 1989a).

Decomposition rates of cellulose waste materials at sea will likely be influenced by factors not operating in shallow coastal systems that have served as the focus for previous studies. Because the background abundance of cellulolytic organisms is likely to be low in oceanic waters, bacterial community composition may constrain the rate of degradation, at least initially. Temperatures in the bulk of the ocean are lower than those in temperate and subtropical coastal systems, and particles will spend significant amounts of time at temperatures less that 1°C. Also, particle sinking rates will influence the temperature, pressure, and redox conditions experienced by the attached bacterial community. For example, larger particles (>500 mm diameter) sinking

at a rate of 50 to 100 $m \cdot d^{-1}$ are likely to move out of the upper mixed layer in less than one day and reach the sea floor (with 1-2°C temperatures and ~500 atm pressure) in 40 to 80 days. By contrast, smaller particles (<50 mm in diameter) sinking at rates of approximately 1 $m \cdot d^{-1}$ may stay in the warmer surface waters for several weeks. It is evident, therefore, that studies specific to the pelagic environment are needed in order to understand and realistically model the fate of cellulose wastes in the ocean.

The general mechanism by which organic particles are degraded in seawater is, quite surprisingly, still poorly understood and much debated (Smith et al., 1992). Observations of naturally occurring particles in the ocean surface waters have shown that most particles in the sea are heavily colonized by bacteria (Alldredge and Gotschalk, 1990). However, measurements of bacterial growth rates using radiotracer techniques indicate that the attached bacteria grow very slowly (Ducklow et al., 1982; Simon et al., 1990). If bacterial growth and respiration were the only sinks of particulate carbon, then such slow rates suggest that it would take months to years for complete degradation of organic particles, and therefore that much of the particulate material in the upper ocean would sink to the sea floor undegraded, which is generally not observed. It has recently been hypothesized that attached bacterial communities have intense hydrolytic activities, even though they are not growing rapidly (Smith et al., 1992). According to this hypothesis, the bacteria are releasing extracellular enzymes and thereby solubilizing particles at rates much faster than predicted from bacterial growth alone, and thus much of the particulate material is being released as partially-degraded soluble material. If so, the hydrolytic activity of attached bacteria would result in more of the particle mass being solubilized before it reaches the sea floor. This controversy over the decomposition of natural particles is highly relevant to determining the fate of cellulose wastes at sea, particularly with regard to the rate at which the cellulose particles disintegrate and the amount of particulate material that survives passage through the water column.

Cellulose particle degradation by marine bacterioplankton can best be studied by taking an integrated approach which includes several independent and complementary methods for measuring rates of particle decomposition, and for understanding the mechanisms by which decomposition occurs. Direct measures of particle mass loss as well as measures of bacterial production, bacterial respiration, and hydrolytic enzyme activity at the particle surface are used in this study. Because much of our current understanding of bacterial decomposition of particles in the sea comes from the use of radiotracer methodology to measure rates of bacterial growth, and because this methodology has several potential artifacts associated with its use (including isotope dilution problems and inexact estimation of critical carbon conversion factors), a new, more direct method is being developed and used for measuring bacterial growth on cellulose particles. This method is based on flow-cytometric quantification of the dilution of fluorescent staining in actively dividing cells.

The Office of Naval Research (ONR), in collaboration with other divisions within the Navy, has expressed interest in research aimed at evaluating the ecological fate and effect of released cellulose waste materials. ONR and NAVSEA are jointly funding this effort to evaluate the microbial degradation of the Navy's pulped cellulose waste steam in order to better understand the technical and scientific issues discussed above, and to aid in the overall environmental analysis of the Navy's proposed methods of discharging this waste stream. This work is being accomplished by Dr. Mary Ann Moran and her colleagues in the Department of Marine Sciences at the University of Georgia. Initial results of this effort are included in this report; completed findings will be provided upon completion of the study.

Shredded Metal and Glass

Settling Characteristics. Settling velocity for the shredded waste stream has been tested experimentally in San Diego Bay using bagged samples provided by CDNSWC/AD. A calibrated pressure sensor was used to determine the depth and time with very repeatable results. An estimate of transport in various ocean currents and depths was then calculated accounting for the transient and the steady-state drift. This was done assuming the bags remained intact; no estimates to date have been made with regard to bags which may break on impact with the water. Accumulation and burial have both been addressed theoretically using ship traffic data and estimates of mass loading, as well as regional data within the Special Areas on sedimentation rates and types, and bottom flow.

In addition to the qualitative longevity test conducted on the bags in San Diego Bay, a specific study on corrosion was performed by NRaD materials experts. This study is provided in Appendix G, and the technical approach is included below.

Corrosion. With regard to influencing marine benthic habitats, it is important to know how long this material will persist in the environment, or conversely the corrosion rate of the material. The glass is crushed into small pieces which will reach the bottom fairly quickly and, although it will persist for quite some time, it is relatively inert. Therefore, the focus of this study concerned the shredded metal products. Since the metal waste will corrode and release its constituent elements to the environment, it is important to know the composition of the waste and the rate at which the various materials are released into the water column. Because conditions in the marine environment may differ from location to location, it is also important to know how the corrosion rates depend on these varying conditions.

Corrosion effects in seawater are the primary concern of this study; however, in general terms corrosion can be categorized into eight types of related, but somewhat different processes (Fontana, 1986). Four of these processes are important for this study. Uniform attack occurs as direct oxidation over a wide area of metallic surface. Uniform attack allows for corrosion at rates that can be measured relatively reliably. The corrosion rate (expressed as mass of metal oxidized per unit time) is proportional to the surface area of the corroding metal. To a large extent, mild steel undergoes uniform attack when it is immersed in seawater. Pitting is a kind of localized attack that often occurs on metals, such as aluminum, that naturally resist corrosion due to the formation of passive oxide films. While the eventual rate of corrosion in a pit is determined by the rate of reduction of oxygen (usually at a surface away from the pit), a pit requires some kind of initiation process to start the pit formation. Thus the overall rate of corrosion on a pit-forming metal like aluminum may depend on factors other than the dissolved oxygen concentration. Pitting is assisted by the presence of chloride ion, so salinity may also be a factor in pitting corrosion rates. Crevice corrosion (and related filiform corrosion) occurs in small openings such as joints and under defects in nonmetallic coatings. Corrosion on coated metals will begin with crevice or filiform corrosion that progresses under the coating and eventually results in the rupture of the coating due to the build up of corrosion products. Filiform corrosion is common on coated food and beverage cans that are exposed to the atmosphere. In seawater this type of corrosion would be expected to lead to the destruction of coatings and the exposure of the metal underneath to direct attack.

The most reliable information about corrosion in seawater comes from the direct exposure of samples in the ocean environment. Well characterized samples (for chemistry, metallurgy, and surface condition) are carefully measured and weighed before exposure. Good studies also record the exposure conditions (O_2 concentration, pH, temperature, flow rates) and their variation in time. After exposure, the samples are cleaned to remove the corrosion products and any marine fouling, then weighed. Cleaning methods can be mechanical, chemical, or both, but standard methods are used to assure reproducibility in the measurements (American Society for Testing and Materials (ASTM) method for cleaning samples). Corrosion rates are usually reported in mpy (thousandths of an inch) via the formula:

$$mpy = \frac{534W}{\rho AT} \qquad \text{(Eq. 3-1)}$$

where W is the weight loss in milligrams, ρ is the density of the sample in $g \cdot cm^{-2}$, A is the area of the specimen in square inches, and T is the exposure time in hours. Reporting corrosion rates in this manner is useful for the assessment of corrosion damage for structural materials. Since we are interested in the total amount of material corroded we must take into account the surface areas and densities of our samples.

In this study, due to limited time and resources, a general corrosion review was performed, and measurements of the samples provided by CDNSWC/AD were conducted. The qualitative longevity test in the bay gave indications of corrosion and fouling under particular conditions found in San Diego Bay. However, it was not intended to provide the quantitative data possible using the above methodology. If it is warranted, further quantitative studies could be performed in a range of oceanic conditions which would be more representative of ocean areas of interest.

Since much of our corrosion data are extracted from the literature, a general synopsis of seawater corrosion studies is provided for the readers information. The most widely cited studies of corrosion in seawater were undertaken by the Naval Civil Engineering Laboratory (NCEL) Construction Battalion, Port Hueneme, California. The studies involved the exposure of about 20,000 samples of 475 different metal alloys at three depths in the Pacific Ocean. An exhaustive summary of the results was published (Reinhart, 1976). Some of these results, and the results of many other studies, are summarized (with references) in *Corrosion of Metals in Marine Environments* (Beavers et al., 1986), compiled by the Metals and Ceramics Information Center. A study has also been conducted to compare the corrosion of mild steel in polluted and unpolluted seas (Shimada et al., 1975). The effect of water flow velocity on the corrosion of steel has also been examined (Peterson and Lennox, 1984). These studies conclude that the main factor influencing the corrosion rate for carbon steel is the dissolved oxygen concentration. This is subject to the caveats that excessive flow rates will increase the corrosion rate substantially, and that in polluted waters with high sulfide concentration (and a correspondingly low oxygen concentration) the corrosion rates will be significantly higher than normally predicted from the oxygen concentration. In addition to Reinhart (1976), studies on the corrosion of aluminum over a five year field period (Ailor, 1969) and laboratory studies (Dexter, 1980) indicate an increase in the corrosion rate of aluminum with depth. The reasons, however, are poorly understood.

The bulk of the Navy's metal waste stream consists of food and beverage containers. Food containers are designed to keep the outside environment away from the food products. These containers must themselves prevent a breach of the container from corrosion that is initiated either from the outside environment or from the inside by the food product. Under most

conditions tin is more noble than iron and provides a barrier coating to prevent corrosion. The steel sheet used in tin-plated containers is usually a mild steel with very low concentrations of additional elements. A mild steel has a carbon content of less than 0.2% (in the case of steel for cans, less than 0.14%) and about 0.5% manganese.

In some cases, the tin plating is not sufficient to prevent the corrosive action of some food products. In addition to the tin plating, organic coatings, referred to as enamels in the industry, are also used. The enamels are often oleoresins (natural products) or epoxies (synthetic products), but other coatings can be used. Coatings can be used on the interior surface of the can only, but are sometimes present on both the interior and exterior surface. An interesting but slightly dated discussion about tin container technology is given in the *Metals Handbook* (Brick et al., 1961).

Many beverages are distributed in aluminum cans. Modern aluminum cans are deep drawn from 3004 alloy sheet. The lids on the cans are stamped from type 5182 sheet. The 3004 alloy contains about 1.0% manganese and 1.0% magnesium. The 5182 alloy contains about 0.3% manganese and 4.0% magnesium. Highly corrosive cans always have organic coatings on the inside. The outside of the cans, however, are usually coated only with decorative paint that does not completely cover the metallic exterior.

The chemistry of the corrosion products from these containers in the ocean environment is influenced by the same factors that control the rates of corrosion themselves. While a detailed discussion of the marine chemistry of these corrosion products is beyond the scope of this study, a simplified discussion of the chemical reactions and fates of the major chemical elements and products follows.

Iron: Because of the presence of dissolved oxygen in the ocean, iron in this environment exists almost completely in the Fe(III) oxidation state. In spite of the high concentration of chloride in seawater, chloride complexes of Fe(III) are not a factor in the distribution of iron. The very small solubility product of $Fe(OH)_3$ (about 10^{-37}) guarantees that at the near neutral pH levels in seawater most iron exists as solid or colloidal $Fe(OH)_3$. This iron must ultimately end up in the ocean bottom sediment and undergo dehydration to more stable forms such as Fe_2O_3 (Horne, 1969).

Manganese: Manganese can exist in seawater in oxidation states of Mn(II), Mn(III), or Mn(IV) depending on the oxidative potential of the seawater. Since manganese is only a trace element in seawater, yet is common in ocean sediments, most manganese must precipitate. The major precipitates of manganese are believed to be $MnCO_3$, $MnO(OH)$, and MnO_2.

Aluminum: Aluminum chemistry in the oceans can be quite complex. Aluminum is a major element in the earth's crust and in ocean sediments. To a large extent, at ocean pH levels, any aluminum produced by the corrosion of metallic aluminum probably ends up as insoluble $Al(OH)_3$.

Magnesium: Magnesium is a major component of seawater. Concentrations of 1300 $\mu g \cdot mL^{-1}$ are typical.

Tin: Tin is easily oxidized from the Sn(II) state to the Sn(IV) state. At ocean pH levels the Sn(IV) probably exists as insoluble SnO_2. Tin is less abundant naturally in the ocean than the

other major constituents and may be subject to different concerns in the benthic habitats than the commonly found elements.

3.3 Effects of Pulped and Shredded Waste Streams

Effects of concern fall under the categories of biological interaction, aesthetic degradation, habitat impairment, interference with local industry such as fisheries, and possible bioaccumulation which could endanger human health. Potential stressors need to be evaluated, particularly in sensitive oceanographic and ecological environments. If an area is already experiencing environmental degradation, whether by natural or anthropogenic causes, the effects may be more severe than otherwise warranted. A thorough analysis must consider effects which are short-term, long-term, local, regional, or basin-wide, as well as those which are species specific or range over a variety of species. Within this assessment, these variations will be addressed based on experimental data on biological interactions of pulped and shredded materials with only representative species indicative of each level of the food web.

When amounts and types of anthropogenic products are increased it is possible that ecosystems in estuaries and semienclosed embayments where water circulation is restricted could be affected. However, this may not occur in open oceans or semienclosed seas because of their large water volume and relatively active circulation. To date the research in off shore open ocean areas or semienclosed seas is quite limited with regard to biological effects on major components of marine ecosystems. In this study, biological effects have been tested in the laboratory and extrapolated to potential impacts in the Special Area seas. Below is a description of the biological interaction studies which are being performed as part of this study.

Biological interaction includes feeding interference and toxicity effects which can lead to reproductive changes, growth rate impairment, and mortality, all of which can in turn cause population changes. This study to date has focused on feeding interference, toxicity, and to some extent growth rate and mortality. The approach has included a wide range of organisms, choosing representative species throughout the world oceans rather than specific ones found in each of the Special Areas. These species include phytoplankton, bacteria, algae, amphipods, polychaetes, zooplankton, mysid shrimp, silver side minnows, and sardines.

Laboratory toxicity screening consists of several methodologies for both water column and benthic organisms. Because some of the organisms are found in both the water column and the benthos, the tests in this analysis are discussed in terms of the liquid-phase, or elutriate effects, and the solid phase, or particle effects. Results of toxicity screening are often difficult to interpret and it is often difficult to compare one test with another. However, standardization provides a means to draw comparative conclusions regarding toxicity. By performing a suite of tests, the combined results lend more confidence to the interpretation. Toxicity screening is generally used to provide a rapid means of assessing the potential toxicity of a test solution under controlled environmental conditions. Standard tests have been developed using phytoplankton, algae, shrimp and fish, and experimental research tests are being developed and used for comparison with existing standards. Mortality or functional reduction of the test organisms are typically measured, and an effect on 50% of the animals is the common parameter tested. The test concentration that causes 50% mortality is called the lethal concentration (LC_{50}) or Lethal Dose (LD_{50}), and in the case of functional impairment it is called the effective concentration (EC_{50}) or inhibition concentration (IC_{50}). Replicates of all tests are typically done for statistical comparison.

In this study solid phase tests were conducted on polychaetes and amphipods because they are important components of most benthic marine communities and there are proven, widely used protocols for laboratory assays with these species. In addition, live animals are readily available from commercial suppliers. Elutriate tests were conducted on bioluminescent bacteria and phytoplankton, mysid shrimp, and minnows. These test species were chosen for the importance they hold in the food web, the sensitivity they have to contaminants, and the coverage of the widest range of species feasible.

Zooplankton are generally defined as free-living heterotrophic organisms too small and/or weak to move independently of major ocean currents. A wide variety of invertebrate taxa ranging from protists to large jelly fish occur in the plankton for the duration of their lives, and other invertebrates and fish are zooplanktonic as larvae. Zooplankton inhabit all layers of the ocean down to the greatest depth sampled, but are most concentrated near the surface. Zooplankton species play very important roles in food webs as major consumers of bacteria and phytoplankton, an important food source for diverse carnivores (particularly the juveniles of most commercially important fish), and as nutrient regenerators.

Copepods are among the dominant macrozooplankton (>200 μm in size) in most marine environments. Because of their numerical importance and linkages, significant changes in their abundances or feeding rates can affect the abundances of other marine organisms in ecosystems. The macrozooplankton species used for this study are *Calanus* and *Acartia* because they represent common species found in both open ocean and near-shore estuarine conditions. Feeding interference was studied specifically, and mortality was derived secondarily from the experiments. Growth rate experiments were also performed on *Polykrikos kofoidi*, a ubiquitous heterotrophic microzooplankton (20-200 μm). This work is being conducted by Dr. Mike Mullin and Dr. Hae Jin Jeong at SIO, La Jolla, California.

Pulp wastes themselves, and/or leached chemicals, may affect ingestion rates of copepods on suitable prey by clogging the predators' feeding apparatus or by toxic action, thereby altering their feeding behavior, growth, and reproduction rates. If copepods living and feeding near the surface can survive in various densities of pulp slurry and then recover their feeding rates on suitable prey after pulp waste has sunk or been dispersed, the wastes will not significantly affect the ecology of copepods. The tests conducted during this study were designed to specifically study these issues.

Small, pelagic, clupeoid fishes (sardine, anchovy, herring, menhaden) are an important link in most coastal pelagic ecosystems. These organisms harvest the carbon found in phytoplankton and zooplankton and convert it to a large standing stock of small migratory schooling fishes. In turn, these species are the forage base for larger predacious fishes (tuna, salmon, rockfish), seabird populations (pelicans, gulls, terns), and marine mammals (dolphin, seal, sea lion). On a weight basis, clupeoid fisheries are the most important fisheries world-wide. Presently the sardine biomass is estimated to be about 340,000 metric tons.

Fish such as the Pacific sardine can reach this high biomass because they feed lower on the food chain than larger predacious fishes. They typically subsist on a diet of phytoplankton and zooplankton. Sardine can feed by two different methods. If the prey organisms are large enough, sardine will strike at and ingest individuals. If the organisms are smaller but abundant, they will filter-feed. They use cartilaginous extensions on their gill rakers to filter water as it passes through the gills and collect the organisms trapped on the gill rakers. The size of the particles trapped depends on the size of the sieve created by the gill rakers. This varies with species and

the size of the individual fish (Blaxter and Hunter, 1982). Compared to invertebrate filter-feeders (clams, oysters, mussels), little is known about the filtration process in clupeoid fishes. The fish feeding experiments being conducted by Dr. Russ Vetter at the National Marine Fisheries Service (NMFS), La Jolla, California, are designed to address issues relative to filter feeding processes, as well as growth rate and mortality. Biochemical measures may be addressed at a later time.

Having discussed the biological interaction concerns of this study, other concerns including aesthetic degradation, habitat impairment, interference with local industry, and bioaccumulation are addressed briefly below.

Aesthetic concerns include litter washing up on beaches, floating garbage, and water turbidity. These have all been approached both from a theoretical and experimental point of view. The technical approach used in this study has been to determine what the sinking velocities of the two waste streams are, and to analyze the dispersion and transport given the oceanographic conditions in the Special Areas.

Habitat impairment can include effects such as eutrophication, oxygen depletion, "smothering the benthos," and creating inhabitable zones where accumulation has taken place. All ocean areas are subject to natural variation, and determining the effect of the pulped and shredded waste streams must be done with the specific location in mind, as well as by estimates of basin-wide impacts. This work has been accomplished using chemical analysis of the material along with knowledge of the Special Areas obtained through the literature reviews.

Interference with industries such as fisheries could occur if either the material directly harms the species of interest, or if the food web was significantly altered, leading to reduced sources of nourishment. Each of these issues are being addressed in the studies being conducted at SIO and NMFS.

Bioaccumulation, although mentioned as a possibility, has not been addressed due to the minimal potential of occurrence. An assessment of the bulk constituents, the chemical composition, and the mass loading have not warranted significant investigative effort regarding this issue.

3.4 Environmental Analysis

The question we addressed in this study is whether the Navy's proposed solid waste discharges will have an impact in the MARPOL Special Areas. Our approach has been to quantify the discharges in terms of physical and chemical characteristics, and biological response. We then have attempted to predict the fate of both waste streams from a physical, chemical, and biological perspective, and to determine the effect that they may have in a laboratory setting, followed by extrapolations to the expected environment. The analysis is based on using the theoretical, laboratory, and limited field data collected, and projecting the estimations to the "real world."

Using all of the collected data, whether obtained experimentally or theoretically, we formed an overall analysis of the impact to the representative ocean environments found within the MARPOL Special Areas. Specifically, the potential impact of both the pulped and shredded waste stream was addressed from the aspects of discharge conditions, waste stream characteristics, water column processes, and sea floor processes. This was an interdisciplinary activity, involving oceanography, ecology, toxicology, environmental chemistry, and marine biology, as well as computer modeling and hydrodynamics. The environmental criteria we

addressed are basic issues found in the definition of pollution: degradation of the marine habitat, biological effects, aesthetic impairment, and interference with marine industries such as fishing or tourism. Many of these criteria could be determined directly, however, some criteria such as population variation and bioaccumulation require longer term assessment and will be included in the ongoing effort in terms of worst case sensitive endpoint review from existing literature and studies.

During this analysis we took into account the existing ecological, oceanographic, geological, and industrial nature of the region, along with the Navy's projected mass loading. We used standards of comparison for evaluating biological response, and existing methodologies for ocean disposal and monitoring. We also considered a range of spatial scales that the Navy's discharges may impact, from the local single ship case to an regional operational scenario and the basin-wide scale. With the use of simulation we were able to extrapolate results to a variety of ocean areas using known input conditions. This report presents the findings to date for this project, with a final report at the completion of the various ongoing studies.

4.0 GENERAL OCEAN DISCHARGE STUDIES

Examination of the ocean waste disposal literature provides a context for U.S. Navy solid waste discharges within the broad view of ocean pollution in general. Some reports concerning shipboard waste disposal are available. Others address related topics such as ocean dumping of municipal waste in deep waters, biological processes associated with ocean dumping, general physical oceanographic processes concerning dispersion of liquids and solid matter in the oceans, and legal actions by nations taken to reduce the deposition of wastes in the oceans. Since accumulation of waste from ship disposal in open waters results in small sporadic inputs to an essentially boundless site, studies identifying specific effects of waste accumulation from ships in the benthic environment were not found. In this overview we will discuss some issues identified in the above topics.

Literature references to the Navy's plans for shipboard waste reduction and handling document the comprehensive approach adopted by the Navy to reduce or eliminate various forms of shipboard waste by both handling procedures and technological improvements (Committee on Merchant Marine and Fisheries House of Representatives, 1993; Smookler and Alig, 1992). Compliance target dates were established and procedural details were provided.

Waste handling and disposal issues faced by the Navy are common to cruise ships as well. In addition to having to cope with waste from as many as 2,500 passengers and 800 crew members on a large vessel, the cruise industry has the additional problem of finding ports with suitable waste handling facilities. The designation of the Wider Caribbean area as a Special Area where any overboard disposal is prohibited and recent heavy fines of as much as $500,000 have caused the cruise industry to seriously consider its waste handling and disposal practices. Increased passenger awareness has also focused attention on dumping incidents (Committee on Merchant Marine and Fisheries House of Representatives, 1993). Steps taken to address waste handling issues include installation of onboard processing equipment (grinders, shredders, compactors, and incinerators) and operational and management procedures. A commitment to invest in shoreside facilities for handling waste has also been pledged.

General Fate of Waste in the Sea. Waste disposed in the ocean, if not liquid or buoyant, will eventually sink to the benthos. Some general oceanic processes which will affect liquid or solid wastes are described by Kester et al., (1985). Unique oceanographic features of the sea include a large dilution capacity, and a long residence time of deep seawater which may be on the order of 100 years. Liquid waste disposal and subsequent dilution is enhanced by discharging the waste into the turbulent wake of a moving vessel (Kester et al., 1985). Solid waste such as dredged material and fly ash may form areas of localized contamination on the sea floor, and mobilization of these wastes may also occur gradually.

The general process of waste dispersion with time from release at the surface to descent to depths results in increasing widespread dispersion at lower concentrations. A waste stream entering the ocean surface will be mixed and advected in surface waters. With further penetration into deeper waters mixing and advection will continue at a slower rate as a result of reduction in current flows and turbulent diffusion. The loss of wind-driven mixing below surface waters decreases horizontal mixing. In previous experiments, dye placed at depths of 300 m and 1000 m was dispersed horizontally with a diffusion velocity of 0.1 $cm \cdot s^{-1}$, or 10 times slower than the expected rate in the ocean mixed layer. Eddy kinetic energy from current meter records has been shown to be less energetic at 500-2000 m depths than in the upper 100 m (Kester et al., 1985).

Slow settling particles (10^{-3} cm·s^{-1}), in general, will be retained in the surface layer by vertical mixing. Extensive horizontal mixing will occur with particles settling at less than 10^{-2} cm·s-^{1}, and years may be necessary to reach the ocean floor. Clay, fine silt, and portions of sewage sludge are examples of this. Incorporation into larger particles is necessary for such waste elements to settle to the benthic environment (Kester et al., 1985). Only a small portion of degradable organic matter dispersed in the surface layer may reach the ocean floor. The flux of carbon to sediment traps at 500 m was only 4% of the carbon fixed by productivity in the overlying waters (Kester et al., 1985). Benthic organisms effectively utilize carbon reaching them; however, the extent to which waste may be added before natural degradation processes are altered is not known.

If they may be assimilated into the benthic environment, particles eventually reach the ocean floor by formation of flocculant particles or through incorporation into zooplankton fecal matter. Some biological characteristics of the deep ocean benthos, such as extremely slow organism growth rates, small population sizes, long generation times, low fecundity, limited dispersal, and low recruitment rates, suggest that recovery following perturbation may be quite slow (Kester et al., 1985) and these sediments have been shown to slowly recolonize after perturbation.

It is generally assumed that the health of the open ocean is better than near-shore waters and estuaries (Office of Technology Assessment (OTA), 1987). In the open ocean few documented impacts can be attributed to waste disposal activities, in part because fewer wastes have been disposed of in open ocean waters. Physical processes tend to dilute and disperse pollutants, and there is less susceptibility to hypoxia and eutrophication (OTA, 1987). The oxygen reservoir in the ocean is very large and it is not likely that oxygen depleting wastes could ever be discharged in a volume large enough to significantly alter oceanic oxygen concentrations (Kester et al., 1985). Open ocean waste disposal has generally been associated with alkaline or acid industrial wastes, sewage sludge, and dredged material (OTA, 1987). Physical processes and the large buffering capacity of ocean waters act to disperse and neutralize such wastes.

The issue of transport of wastes from specific dump sites into the food chain has been considered from a modeling point of view. In general the mass transport of a contaminant as this relates to its concentration field is determined primarily by physical processes followed in importance by geochemical and biological processes (International Atomic Energy Agency (IAEA), 1983). Contaminants from waste dumping which find their way to benthic sediments may be released into the benthic boundary layer above and further dispersed into overlying waters horizontally and vertically. In a near field situation, concentrations of contaminants may be expected to be higher in the proximity of sources. In order to sustain levels of production sufficient to provide a fishery likely to be harvested by man, the minimum area required may be on the order of 100 square kilometers or more (IAEA, 1983). On such a scale, the distribution of contaminants in the extreme near field is of diminished importance since fishery species must feed over a larger area resulting in lower accumulation. In terms of food chain accumulation, it is not realistic to expect that, at each level, organisms have fed only on other organisms which have fed only in areas of peak contamination.

Deep-Sea Dumpsites. Deep-sea dumpsites with depths of 4000 m have been used in Europe for disposal of industrial waste, sewage sludge, and low-level nuclear waste. Four deep-ocean dumpsites have received industrial and sewage waste in the United States (Kester et al., 1985). Aqueous solutions or dilute suspensions dumped in at deep-sea dumpsites have typically had densities in the range of 1.01 to 1.15 g·cm^{-3} and initial dilutions exceeding 1000 times that of the

dumped waste. Subsequent dispersion occurs in the oceanic mixed layer. In winter months when a seasonal pycnocline is absent, wastes may be detected at depths of 100 m, but above the permanent pycnocline of the deep ocean. If dumping occurred over the continental shelf, wastes would have reached the sea floor in most areas (Kester et al., 1985). The physical parameters of the waste mentioned above are significantly different from those of the waste streams under consideration and will vary accordingly. However, this material is provided for background because of the limited nature of similar studies.

Most studies concerning biological responses to waste disposal have been associated with near-surface planktonic organisms since waste disposal occurs mainly in the upper layers of the ocean. Continental shelf research has focused on benthic species. Studies with surface planktonic species have found: 1) no histological evidence of damage to euphausiids, 2) short-term, small-scale shifts in phytoplankton species composition in waste plumes, 3) loss of zooplankton fecundity in a waste plume, and 4) no effects of an at-sea incineration plume on plankton (Kester et al., 1985). The chemical nature of the waste plume and the term of exposure are factors of prime concern in such studies making it difficult to draw any general conclusions. Clearly some toxic effects may be anticipated from acute exposure to a waste plume of a sufficiently toxic nature. The scope of exposure and subsequent effects would then be limited by dilution of the plume to nontoxic levels.

Sludge Disposal/Monitoring. Investigations of sludge disposal sites have revealed various findings. At a sludge disposal site in the Firth of Clyde, Scotland, benthic faunal distribution was related to a gradient of increasing organic enrichment from dumping. The study area was 6 km^2 with a depth of 70-80 m. Up to $1.55 \cdot 10^6$ metric tons of sludge per year was allowed to be dumped at this site. Sludge rapidly reached the benthic environment settling at a rate of 20 $g \cdot m^{-2} \cdot d^{-1}$, or 1-2 orders of magnitude higher than the highest levels of natural carbon input to inshore sediments (Capuzzo and Kester, 1987). Long term monitoring of this environment did not show any large accumulation of sludge in the center of the site, however. The study indicated that adaptation at the community level was a progressive process involving continuous species replacement. It was concluded that if discharges were maintained at the level studied an environmentally hazardous situation was unlikely.

In another sludge dumping study conducted at a site in the Elbe estuary over a 20 year period a highly unstable but resilient community structure was found (Capuzzo and Kester, 1987). Approximately 250,000 tons of sludge were dumped at this site in 14.5 to 19.5 m of water from 1961 to 1981. Population fluctuations were caused by primarily biotic factors, such as life cycle and settlement patterns, predation, and crowding. It was concluded that a minimum of five years of study was necessary to observe any effects from activity such as sludge dumping. Shorter study periods risk false conclusions regarding short-term events which may be part of normal randomness concerning community structure.

Gibbs and Angelides (1989) reported large differences in the distribution of oxidizable and reducible metals in both digested and undigested wastewater sludges from a 20 m dumpsite in the New York Bight. Larger flocculates (flocs) formed during dumping of digested sludges had higher concentrations of oxidizable metals, while the smaller flocs had higher concentrations of reducible metals. In undigested sludge flocs, the larger flocs had high concentrations of oxidizable metals. The maximum organic-bound metal concentrations were found in the slowest settling flocs. Considering settling velocities ranging from >6 $cm \cdot min^{-1}$ to 0.7 $cm \cdot min^{-1}$, Gibbs and Angelides (1989) calculated that the fast settling flocs at the 20 m dumpsite would reach the

bottom in 5.5 hours after dumping. In terms of the fate of metals found in undigested sludge, it was noted that slow settling microflocs are transported much farther in the ocean than fast settling flocs. These smaller flocs would also remain in suspension longer. Digested sludge disposal results in more organic-bound metals settling near the dumpsite via rapid settling of large flocs.

Monitoring at or near the 106 Mile Ocean Waste Dumpsite (Deep Water Municipal Sewage Sludge Disposal Site) has not shown any serious short-term impacts on marine resources (OTA, 1987). Since 1961 various industrial wastes were dumped there reaching nearly 5 million metric tons in the early 1970s. Dumping then declined to approximately 200,000 metric tons in the mid-1980s. Long-term impacts may not be detected, however, due to the expense and difficulty of monitoring. Since municipal sewage sludge dumping will likely increase substantially with diversion from the New York Bight, the uncertainty of long-term effects will remain.

Since 1986 sewage sludge has been dumped at the 106 Mile Site at depths of 2340 to 2740 m (Hill et al., 1993). Sewage sludge has been discharged at this site at the rate of approximately $8 \cdot 10^6$ wet tons per year since 1988. Model predictions using current data and experimental settling velocities indicate that a maximum flux of 60 $mg \cdot m^{-2} \cdot day^{-1}$ would occur at the southwestern site corner decreasing to 25 and 1 $mg \cdot m^{-2} \cdot day^{-1}$ at 50 and 350 km to the southwest, respectively. Little material is predicted to reach the continental shelf with fine sludge particles being widely dispersed in the water column. Using bacterial endospores as an indicator of sewage sludge contamination, Hill et al., (1993) found parts of the 106 Mile Site to be contaminated. The contaminant distribution was broadly consistent with model predictions..

The topic of human health risk from ocean dumping at a hypothetical deep-water dumpsite has also been discussed (Lipton and Gillett, 1991). A model utilizing estimates of uncertainty regarding contaminant bioaccumulation, commercial fish landings, and seafood consumption was used to estimate carcinogenic health risk from organic pollutants such as PCB's. Parameter variability and uncertainty, particularly in bioaccumulation estimates, was demonstrated to lead to several orders of magnitude variation in estimated risk values. This study was based on the underlying assumption that a definite link between dumpsite contaminants and the human food chain existed. Current risk management thresholds were bracketed by these risk distributions, indicating that under some highest risk conditions and assumptions ocean disposal of municipal sludges may pose a risk to human health. The assumptions under which the modeling was conducted were associated with a defined dumpsite. It should be noted that such conditions would not be present in the open ocean where vessel waste disposal would occur.

Conclusion of Ocean Discharge Methodology Review. Monitoring of deep ocean dumping sites has not indicated any serious short-term impacts on marine resources. It has been noted that several years of monitoring are necessary to begin any appraisal of environmental effects due to dumping. It can be anticipated that such a task would be even more difficult in the open ocean, if at all possible.

Several studies were reviewed regarding ocean disposal, including ocean dumping of municipal wastes and shipboard waste. The studies in general do not relate directly to the Navy's unique waste streams and operations in Special Areas, however, they do give an indication of disposal procedures, biological processes, and general physical oceanographic processes involved. The Navy's solid waste discharge will be evaluated in this study according to specific

parameters including wake and ambient dilution, conditions of the receiving environment, and ecological response.

Enhanced dilution of shipboard waste from moving vessels, the large dilution capacity of the deep sea, widespread dispersion with settling, and less susceptibility to hypoxia and eutrophication are all factors which would act to minimize waste accumulation and undesirable ecological effects from shipboard dumping.

Pulp Mill Effluent Review. Some investigation of literature concerning the process of reducing waste paper products to fine particulate matter for disposal purposes was performed to identify possible similarities with pollutants created during the wood and paper producing processes, recognizing that simply grinding waste paper products for disposal would not be expected to create waste liquors such as those produced during the production processes. Since pulp mill processes typically discharge effluent to water bodies of restricted flow, or to moving streams and rivers where rapid dilution may take place, subsequent toxicity to receiving water organisms is heavily influenced by hydrological conditions. Clearly, discharge to waters where rapid dilution may take place is more comparable to discharges from moving vessels at sea than discharging to water bodies with restricted circulation. A review of the literature (McLeay, 1987) provided background information on the following topics:

Effects. Acute toxicity of pulp and paper mill effluents is generally attributed to resin, fatty acids, and chlorinated phenols. In 96-h LC_{50} studies with juvenile rainbow trout, untreated pulp mill effluents were normally acutely lethal. Dilutions of 100:1 to 20:1 tend to eliminate acute toxicity. Treatment such as fiber removal did not reduce acute lethal toxicity. The dilution factors cited above would rapidly be exceeded during shipboard discharges from vessels underway. Additionally, the toxic resins, fatty acids, and chlorinated phenols would not be components of the ground particulate discharge from Naval vessels. Parameters such as pH, alkalinity, and hardness can influence toxic effects of pulp and paper mill effluents. Modifying effects of salinity and seawater chemistry are not currently understood.

Where mill effluents are discharged to water bodies with restricted circulation, observed fish mortality has often accompanied oxygen depletion. Limited circulation and flushing has led to detrimental effects on plankton communities as well. Clearly such conditions would not be present in open ocean waters during ground paper refuse disposal.

Some evidence has been found for flavor effects in fish exposed to pulp mill effluent (>1%) in poorly mixed waters for periods of hours to days. The off-flavors imparted by mill effluents were rapidly eliminated following movement by the fish to clean water. This cause and effect relationship would not be expected to occur in open unrestricted ocean waters.

Information is lacking on the toxic effects of dilute (<2%) mill effluents on the reproduction, development, and disease of estuarine or marine species.

Fate. Cellulose is a reasonably abundant, naturally occurring substance in the marine environment. Found in such materials as the tunics of tunicates, vascular plant tissues (sea grasses and outwashed terrestrial plants), and within cell walls of dinoflagellates, cellulose exists throughout the world's oceans in varying concentrations.

As a relatively indigestible polysaccharide, the ultimate fate of the cellulose matrix in a pulped paper marine discharge depends on a number of factors. Primary among these are the availability and efficiency of cellulase producing protozoa and bacteria in digesting the cellulose molecules and the rate of burial of cellulose in marine sediments. A number of marine organisms have developed mean to digest cellulose, via microorganism production of cellulase. However, like most enzymes, cellulase activity is governed by prevailing physical and chemical conditions. In high pressure, cold environments off the deep ocean, cellulase activity is lower than in shallower and warmer coastal waters. While digestion of cellulose may be fairly rapid (hours to days), such as in the gut of sea turtles foraging on seagrasses in warm tropical and subtropical waters, under other circumstance, the process may also take years or decades and may even be stopped altogether. The regular persistence of ancient wooden ship carcasses on the bottom of northern seas, and the occurrence of cellulose in many marine microfossils are an indication that cellulose may persist indefinitely under certain conditions. Even in relatively shallow waters, such as at the discharges of pulp mills in the cool waters of the northern Pacific, fibrous mats supporting an extensive amount of cellulose material may persist for decades without appreciable signs of consumptive decay (K. Merkel, personal communication).

5.0 REGULATORY FRAMEWORK

The International Convention for the Prevention of Pollution from Ships, 1973, as modified by the Protocol of 1978, thereto MARPOL 73/78, addressed issues pertaining to pollution by ships in international waters. The 1973 document was negotiated through the International Maritime Consultative Organization (IMCO), now the International Maritime Organization (IMO). The Convention was an attempt to eliminate ship-source pollution from all sources through one mechanism, and was in response to the growing international environmental awareness, particularly concerning pollution as a result of oil spills. This international treaty characterizes seas of concern as Special Areas; enclosed or semienclosed seas which lack wind, tidal, or current action to effectively flush out water and pollutants on a regular basis. The treaty endorses Annex I designed to prevent the discharge of oil, Annex II focusing on preventing the discharge of noxious liquid substances carried in bulk, and Annex V impeding discharge of ship-generated garbage (including paper, cardboard, metal, glass, plastic, rubber, and food wastes) into the marine environment. The Marine Environmental Protection Committee (MEPC), a subsidiary body of the Assembly of the IMO, monitors implementation of MARPOL 73/78. The Coast Guard administers and enforces Annexes I, II, and V on the national level.

5.1 MARPOL 73/78 Annex V

Annex V of MARPOL 73/78 restricts and prohibits discharge of solid wastes in coastal areas and in Special Areas throughout the world. The legislation became effective 31 December 1988. Outside Special Areas it requires a prohibition on the discharge of plastics and distance-from-shore restrictions for solid waste discharges depending on physical state (comminuted, or ground, versus non-comminuted). Inside Special Areas it requires a prohibition of plastic and nonfood solid waste and distance-from-shore restrictions on food waste depending on physical state.

A Special Area is defined in Annex V as "...a sea area where, for recognized technical reasons in relation to its oceanographical and ecological condition and to the particular character of its traffic, the adoption of special mandatory methods for the prevention of sea pollution by garbage is required" (IMO, 1992). The existence of the mentioned characteristics must first be proven for a sea to merit the status of a Special Area. Delimitation of a sea is determined by the countries bordering the area and is adopted by all states concerned. One of the following conditions in each category should be satisfied in order to designate a region of special concern:

- Ecological conditions
  - endangered species
  - productivity
  - spawning, breeding, nursery areas
  - critical habitats

- Oceanographic conditions
  - circulation
  - residence time
  - ice state
  - wind

- Vessel traffic characteristics

For the purposes of MARPOL 73/78 Annex V the Special Areas are the Baltic Sea, the North Sea, the Mediterranean Sea, the Wider Caribbean Region (including the Gulf of Mexico and the Caribbean Sea), the Antarctic area, the Black Sea, the Red Sea, the Gulf of Oman, and the "Gulfs" area (including the Persian Gulf) (IMO, 1992). Of these, the IMO has only effected the regulations in three regions: the Baltic Sea, the North Sea, and the Antarctic area. As requested by NAVSEA, this study will focus on issues related to the first five of the Special Areas listed above and the particular concerns which motivated their designation. Subsequent analysis of the other regions will be forthcoming. All of the Special Areas, including those proposed and in force, are shown graphically in figure 1-1. The five areas discussed in this study are also indicated.

Procedures for the Designation of a Special Area. A proposal to designate a given sea as a Special Area is submitted to IMO for consideration and reviewed by MERC. The proposals contain a draft amendment to MARPOL 73/78 providing the formal basis for the designation of an area as a Special Area along with a background document addressing scientific and applicable criteria. All coastal states must be in agreement with the scientific documentation. Designation can only become effective when adequate reception facilities are provided for ships by the coastal states bordering said region. Special Area restrictions take effect one year after IMO notifies signatory states of an areas certification to place it in force.

5.2 Impact of MARPOL 73/78 Annex V on the U.S. Navy

The regime of Special Areas has been designed for the purpose of environmental protection. To minimize pollution two main methods of protection have been established: control of discharge processes and shipboard operational control.

Although MARPOL 73/78 Annex V exempts public vessels from complying, the U.S. Congress enacted legislation through the Marine Plastic Pollution Research and Control Act (MPPRCA) of 1987 which establishes the following major requirements for the Navy (NAVSEA, 1993):

- Total ban on discharge of plastics anywhere at sea
- Prohibition on all solid waste discharges in Special Areas
- Prohibition on discharge of solid waste near land

The Navy has requested relief from Congress and has requested the following three main elements (NAVSEA, 1993):

- Extension of the compliance deadline to 31 December 1998
- Permission to discharge nonplastic, nonfloating processed solid waste in Special Areas
- Exemption for submarines to permit continuation of current practice of discharging sinkable compacted slugs

The NAVSEA Program Plan of 1993 proposes that the Navy's Report to Congress establishes the following policy commitment as quid pro quo:

- No discharge of plastics anywhere
- All nonplastic solid waste will either be held onboard, or processed into sinkable form prior to discharge

- In addition to MARPOL Special Areas, processing of solid waste will occur whenever surface ships are in the open ocean

Table 5-1 summarizes current regulatory discharge policy and the policy proposed by the Navy.

Table 5-1. Policy Comparison: Regulatory Discharge Policy Versus Navy Proposal.

Regulatory Policy	**Navy Proposed Policy**
	MARPOL Special Areas
Discharge of all plastics are prohibited	Discharge of all plastics are prohibited
No discharge within 12 nmi (* Caribbean)	No discharge within 12 nmi
Food waste may be discharged >12 nmi	Nonfloating trash & garbage may be discharged >12 nmi
*Caribbean - comminuted food wastes (<25 nmi) may be discharged >3 nmi	
Discharge of all other garbage prohibited	
	Other Ocean Areas
	U.S. Coastline:
Discharge of all plastics are prohibited	Discharge of all plastics are prohibited
Floating dunnage discharged >25 nmi	No discharge within 3 nmi Pulped trash & garbage (food waste) may be discharged >3 nmi
Food waste and garbage discharged >12 nmi	Nonfloating solid waste may be discharged >12 nmi
Comminuted food waste and garbage (<25 nmi) discharged >3 nmi	Foreign Coastline:
	Discharge of all plastics are prohibited
	No discharge within 12 nmi
	Open Ocean (>25 nmi):
	Discharge of all plastics are prohibited
	All nonfloating, nonplastic solid waste may be discharged >25 nmi

5.3 Special Area Rationale

To be classified as a Special Area all bordering countries must determine why that region mandates special interest. Mandatory methods for the prevention of sea pollution by garbage are required in Special Areas due to sensitive oceanographical and ecological conditions, and to the particular character of the vessel traffic within the region. Presented in this section are the specifics that provided the rationale for selecting five of the Special Areas: the Baltic Sea, the North Sea, the Mediterranean Sea, the Wider Caribbean Basin, and the Antarctic area. These concerns include all of the primary criteria for establishing a Special Area: oceanographic and ecological sensitivity, and specific ship traffic concerns. The other Special Areas will be covered in a subsequent report.

Baltic Sea. The preparation for the Baltic Sea to be designated a Special Area was delineated during the 1973 Helsinki Convention. Information was complied and presented by government experts from countries such as Denmark, Finland, Germany, Poland, Sweden, and Russia. Together, these experts formulated the following summary of concerns which was proposed during the 1973 convention and accepted 1 October 1989.

- Its geographical character as an enclosed sea body has an extremely slow and irregular exchange of deep water with other ocean waters.
- The water in the Baltic Sea is cold, which markedly slows down the chemical and biological degradation of certain pollutants.
- Aeration of the deep water in the Baltic Sea is very slow because of marked stratification of water masses; this also slows down degradation of certain pollutants.
- The prevailing anaerobic conditions in some regions favor the growth of certain microorganisms that generate hydrogen sulfide; consequently, adding adverse affects on low level food chain inhabitants (Zmudzinski, 1989).
- The stagnation of the deep water in the different basins of the Baltic Sea proper causes accumulation of some substances, especially persistent pollutants. These pollutants are reintroduced into the surface layers during eventual turnover.
- The concentrations of certain pollutants in organisms of the Baltic Sea are much (in certain cases ten times) higher than in the marine environment of the open seas.
- Organisms in the Baltic Sea are of either true marine or true fresh water origin. Living in the brackish water of the Baltic Sea constitutes in itself an environmental stress upon which all other pressures are added. Environmental pollutants even in low concentrations could act as such additional pressures.

North Sea. The countries bordering the North Sea submitted a proposal for declaring the region a Special Area under the provisions set by MARPOL 73/78 Annex V during the Second Ministerial Conference in 1984 (Ijlstra, 1988). The MEPC of the IMO agreed to the proposal during the twenty-sixth session held in September 1988. A report presented at the conference entitled the "Scientific and Technical Working Group on the Quality Status of the North Sea"

provided key scientific documentation which led to the adoption of the North Sea as a Special Area and contained the following summarized designation criteria:

- The impact on the ecology has been severe in the North Sea primarily due to urbanization; a shift from long-living to short-living species has taken place.

- The North Sea is a semienclosed geological area with characteristic concerns regarding residence time and stratification. The geological and geomorphological structures, characteristic of the North Sea, provide a great variety of wildlife habitats susceptible to contaminants (Lee, 1988). Inputs discharged from rivers do not mix with the entire volume of the sea generally remaining close to the coast resulting in poor flush time for pollutants in coastal regions (Sebek, 1990).

- The North Sea has supported a highly productive fishing industry, yielding a record catch in 1974 of 3.44 million tons, annual average for the region is given at 2.5 million tons, or about 5.3% of the total world catch of fish (The World Bank, 1990). This once thriving industry has been increasingly depleted of salmon, sea trout, flounder, and eel which support worldwide markets.

- The area supports a variety of shore birds, sea birds, and wildfowl which winter there; numbers are documented at 4.2 million (Evans, 1987).

- Due to anthropogenic causes, significant changes to the marine environment have already occurred including some sea mammals and fish species disappearing completely, sea grass communities disappearing, and the amount of algae increasing dramatically (Stefels, 1991).

- The area encompasses a large array of vessel traffic contributing to the continuous pollution problem located within both estuarine waters and the sea itself. Traffic is so heavy that there can be 300 or more merchant ship movements per day in the Straits of Dover making it one of the most congested seaways in the world (Lee, 1988).

Caribbean Sea. The Convention for the Protection and Development of the Marine Environment of the Wider Caribbean Region (Earthscan, 1983) provided the framework to the IMO MEPC for the designation of the Wider Caribbean as a Special Area under the provisions of MARPOL 73/78. The Wider Caribbean includes the Caribbean itself, the Gulf of Mexico, and a number of other seas and bays extending as far south as French Guiana. All coastal states bordering the region of concern in attendance produced scientific and socio-economic documentation required by the IMO for applicable classification. The nations of the region are committed to take all appropriate measures to prevent, reduce, and control pollution of the area caused by discharges from ships, and for this purpose, to ensure rules and standards are established by the international organization. The MEPC established a different standard for the discharge of victual waste for the Wider Caribbean region than for other Special Areas. The disposal of victual wastes which have been passed through a comminuter or grinder shall be made as far as practicable from land, but in any case not less than 3 nmi from the nearest land (U.S. Coast Guard, 1994).

The amendments designating the Wider Caribbean as a Special Area under Annex V were adopted by the MEPC on 4 July 1991, by resolution MEPC 48(31). They were subsequently accepted on 4 October 1992, and entered into force for party states on 4 April 1993. The Wider

Caribbean region Special Area designated under Annex V is not yet enforceable due to a lack of adequate reception facilities in states party to MARPOL 73/78. The discharge requirements will become effective for the Wider Caribbean region Special Area once each party to MARPOL 73/78, whose coastline borders the Special Area, certifies that reception facilities are available and the IMO establishes an effective date.

The following summarizes the criteria for the Wider Caribbean region Special Area designation:

- Oceanographic conditions in the Wider Caribbean region, with the exception of ice conditions, meet all of the MEPC criteria for Special Area status. Most of the water in the Caribbean is below sill depth. Studies show long residence time caused by low flushing rates restrains pollutants from adequately dispersing (Davidson, 1989). Winds and currents, distinctive of the Caribbean Sea, serve as a vehicle for transporting water-borne and air-borne pollution from coastal areas (Frankenhoff et al., 1977).

- Adverse wind patterns cause significant effects on floating debris resulting in offshore movements independent of the direction of currents.

- Because the Caribbean waters are nearly enclosed by land, marine debris becomes confined and concentrates thus posing a signification problem for the area's marine animals, fisherman, and beach users (Garrity et al., 1993).

- Numerous species of marine mammals, birds, reptiles, amphibians, fishes, plants, corals, and other invertebrates found throughout the Wider Caribbean region are known to be threatened and in danger of extinction.

- The Caribbean region contains both areas of high productivity as well as rare and fragile ecosystems such as coral reefs, mangroves, and wetlands which are highly sensitive to the effects of pollution.

- Heavy maritime traffic, such as cruise liners and oil tankers, consistently contribute to ship discharges of pollution.

- Increasing human population and development activity in the area has the potential to contribute significant additional pollutants.

Mediterranean Sea. Delegates convened for the 1976 Barcelona Convention, originally the second conference of the Convention for the Protection of the Mediterranean Sea (MED POL), and developed criteria which led towards the designation of the Mediterranean Sea as a Special Area under MARPOL 73/78 Annex V. Scientific data were supplied by 83 institutions and 16 countries. All party states, with the exception of Albania, agreed and presented conclusions to the IMO MEPC based on the following characteristics:

- The enclosed nature of the Mediterranean Sea hinders tidal movements and currents. In addition, the shallow undersea ridge running from Sicily to Tunisia further limits water exchange.

- Dispersal rate is slow because of the lack of circulation resulting in prolonged residence time for pollutants.

- The Mediterranean Sea lacks a continental shelf and has a low level of suspended natural nutrients. Mixing of warmer, less saline water with deeper, colder waters is limited. Therefore, nutrients that move into deep water generally do not return to the surface and affect primary productivity.

- Various species of endangered and threatened marine and bird populations reside in and along the coastal areas of the Mediterranean Sea. Urbanization has resulted in the loss and reduction of habitat essential for breeding.

- Poorly controlled fishing has led to the depletion of many commercial fish stocks; futhermore, destruction of habitats such as seagrass beds and coastal wetlands limits breeding and spawning.

- High urbanization concentrating along coastal boarders of the Mediterranean Sea contributes to pollution runoff. Over 120 cities dot the coastline with over 100 million residents; an additional 100 million tourists come every year to visit its shores. An estimated 80% of the municipal waste enters the sea either inadequately processed or entirely untreated (The World Bank, 1990).

- Major rivers discharge into its waters. Rivers carry into the sea about 85% of its land-based pollution (industrial, sewage, fertilizer, and pesticide runoff).

- Heavy maritime traffic of an annual estimate of 220,000 vessels contributes to the ongoing high rate of pollution (The World Bank, 1990).

Antarctica. The amendments designating the Antarctic area as a Special Area under Annexes I and V of MARPOL were adopted by MEPC on November 1990 by resolution MEPC 42(30). They entered into force for party states, including the United States, on 17 March 1992. The resolution required that the designation of the Antarctic as a Special Area take effect the day the amendments entered into force to ensure a timely and adequate protection of the area.

The amendments do not call for the establishment of waste reception facilities within the Special Area as is mandated in other Special Areas under annexes of MARPOL 73/78. It was agreed at the 15th Antarctic Treaty Consultative Meeting of October 1989 that there should be no discharge of oily residues and mixtures of garbage in the Antarctic area either ashore or into the sea. Flag states whose ships enter the Antarctic area must ensure that adequate reception facilities are provided (U.S. Coast Guard, 1994).

Designation of the Antarctic as a Special Area and protected as such was based on the Protocol on Environmental Protection to the Antarctic Treaty adopted 4 October 1991. The following summarizes criteria for designation of the Antarctic as a Special Area.

- The Antarctic is the last major region of the planet close to its pristine condition.

- Over 98% of the surface is ice covered; any exposed rock and soil remains below freezing except for short periods in the summer (Benninghoff, 1985).

- Strong winds, which are characteristic of the Antarctic especially in winter, can move dust and diaspores great distances.

- The Antarctic is a home for a variety of unique and sensitive species including many that are endangered and threatened.

- Antarctic research has made many important scientific contributions and is critical to our understanding of global ecological and environmental problems.

- Observations conducted in 1992-1993 found the lowest ozone levels and the largest ozone "hole" in this region. Because of the highly sensitive condition of the region, it is vulnerable to any adverse environmental damage (The Antarctic Environmental Protection Act of 1993).

6.0 SPECIAL AREA CHARACTERISTICS

This section of the report is a review of the Baltic Sea, Caribbean Sea, Mediterranean Sea, North Sea, and the Antarctic Ocean. The reviews were performed to obtain background on the special oceanographic, ecological, pollution, and vessel traffic conditions in these areas. Much of the information gathered forms the basis for their inclusion as MARPOL Special Areas. For each area, an attempt was made to tabulate quantitative data of pertinent physical, chemical, and biological parameters that could be used as guides for comparing SSWD to background conditions or other inputs to Special Areas. It was not possible to obtain numbers for all parameters in all areas. Furthermore, because there is a high degree of variability even within a single Special Area, a "typical" or average number was used, even though its meaning is somewhat limited. The data for each area, except the Antarctic, are shown in tables 6-1 through 6-4.

Table 6-1. Representative oceanographic characteristics of the Baltic Sea.

Parameter	Value	Value	Reference(s)
	Layer 1	Layer 2	
Current Velocities ($cm \cdot s^{-1}$)	5	2	Voipio, 1981/Defense Mapping Agency, 1990
Salinity (psu)	5	15	Voipio, 1981
Temperature (°C)	10	5	Voipio, 1981/Defense Mapping Agency, 1990
Density (sigma-t)	3	12	Voipio, 1981/Defense Mapping Agency, 1990
Layer Thickness (m)	40	400	Voipio, 1981/Defense Mapping Agency, 1990
TSS Background ($mg \cdot L^{-1}$)	3	0.5	Brügmann, 1992
TSS Nearshore Inputs ($kg \cdot yr^{-1}$)	$5 \cdot 10^{9}$		Lajczak, 1993
Si O_4-Si ($mmole \cdot m^{-3}$)	5	50	Voipio, 1981
PO_4-P ($mmole \cdot m^{-3}$)	0.1	0.5	Voipio, 1981
PO_4-P Nearshore Inputs ($kg \cdot yr^{-1}$)	$5.4 \cdot 10^{7}$		Helsinki Commission, 1987
NO_3 -N ($mmole \cdot m^{-3}$)	0.5	3.5	Voipio, 1981
N Nearshore Input ($kg \cdot yr^{-1}$)	$9.4 \cdot 10^{8}$		Helsinki Commission, 1987
TOC ($mg \cdot L^{-1}$)	5		Broman, 1990/Voipio, 1981
POC ($g \cdot m^{-3}$)	0.2		Broman, 1990/Voipio, 1981
DOC ($mg \cdot L^{-1}$)	5		Broman, 1990/Voipio, 1981
BOD_5 ($mg \cdot m^{-3} \cdot d^{-1}$)	2		Voipio, 1981
BOD_5 Nearshore Input ($kg \cdot yr^{-1}$)	$1.7 \cdot 10^{9}$		Helsinki Commission, 1987
Residence Time (yrs)	35		Voipio, 1981
Primary Production ($g\ C \cdot yr^{-1}$)	$34 \cdot 10^{12}$		Voipio, 1981
Zooplankton Production ($g\ C \cdot yr^{-1}$)	$4.4 \cdot 10^{12}$		Voipio, 1981
Phytoplankton Biomass ($g \cdot m^{-2}$)	2		Voipio, 1981
Zooplankton Biomass ($g \cdot m^{-2}$)	15		Voipio, 1981
Surface Area (km^2)	$3.75 \cdot 10^{5}$		Voipio, 1981
Average depth (m)	60		Voipio, 1981
Max Depth (m)	460		Voipio, 1981
Volume (km^3)	$2.2 \cdot 10^{4}$		Voipio, 1981
1% light depth (m)	20		Voipio, 1981
Mass loading of solids ($mt \cdot yr^{-1}$)	10^{6}		Voipio, 1981
Sedimentation Rate ($mm \cdot yr^{-1}$)	1		Voipio, 1981

Table 6-2. Representative oceanographic characteristics of the Caribbean Sea.

Parameter	Value	Reference(s)
Surface Current Velocity ($cm \cdot s^{-1}$)	75	Joannessen, 1968
Deep Current Velocity ($cm \cdot s^{-1}$)	50	Joannessen, 1968
Surface Salinity (psu)	36	Joannessen, 1968
Deep Salinity (psu)	35	Parr, 1937
Surface Temperature (°C)	27	Joannessen, 1968
Deep Temperature (°C)	4	Wust, 1964
Surface Density (sigma-t)	23.5	Joannessen, 1968
Density (sigma-t)	27.8	Joannessen, 1968
Sfc Layer Thickness (m)	100 m	Joannessen, 1968
TSS Nearshore Inputs ($kg \cdot yr^{-1}$)	$3.2 \cdot 10^{11}$	Jones and Amador, 1993/ Earthscan, 1983
TOC Inputs ($kg \cdot yr^{-1}$)	$2.5 \cdot 10^{9}$	Blough et al., 1993
DOC ($mg \cdot L^{-1}$)	0.5	Blough et al., 1993
PO_4-P ($mg \cdot m^{-3}$)	15.5	Muller-Karger et al., 1989
Surface NO_3-N ($mg \cdot m^{-3}$)	35	Muller-Karger et al., 1989
N Nearshore Inputs ($kg \cdot yr^{-1}$)	$8 \cdot 10^{8}$	Muller-Karger et al., 1989/ Wust, 1964 Calculated
Surface O_2 Background ($mL \cdot L^{-1}$)	5	Wust, 1964
Deep O_2 Background ($mL \cdot L^{-1}$)	6	Wust, 1964
Primary Production ($g\ C \cdot m^{-2} \cdot yr^{-1}$)	180	Underwood, 1989/Muller-Karger et al., 1964
Primary Production ($g\ C \cdot yr$)	$4.58 \cdot 10^{8}$	Muller-Karger et al, 1989 Calculated
Phytoplankton Biomass ($mg\ Chl \cdot m^{-3}$)	0.25	Muller-Karger et al., 1989
Zooplankton Biomass ($mL \cdot m^{-3}$)	0.25	Muller-Karger et al., 1989
Surface Area (km^2)	$2.51 \cdot 10^{6}$	Kjerfve
Surface Area w/Gulf of Mexico (km^2)	$4.24 \cdot 10^{6}$	Sverdrup, 1942
Average depth (m)	2600	Seiwell, 1938
Max Depth (m)	7680	Kjerfve
Volume (km^3)	$6.53 \cdot 10^{6}$	Kjerfve Calculated
Sedimentation Rate ($mm \cdot yr^{-1}$)	0.028	Seibold and Berger, 1982

Table 6-3. Representative oceanographic characteristics of the Mediterranean Sea.

Parameter	Value	Reference(s)
Current Velocities ($cm \cdot s^{-1}$)	150	Defense Mapping Agency, 1991
Salinity (psu)	37	Defense Mapping Agency, 1991
Temperature (°C)	14-26	Defense Mapping Agency, 1991
Density (sigma-t)	27	Defense Mapping Agency, 1991
Sfc Layer Thickness (m)	75	Sverdup et al., 1942
TSS Background ($mg \cdot L^{-1}$)	2	Saydam, et al., 1984
TSS Nearshore Inputs ($kg \cdot yr^{-1}$)	$3.5 \cdot 10^{11}$	UNEP, 1989
Si O_4-Si ($mmole \cdot m^{-3}$)	54	Estrada, 1990
PO_4-P ($mmole \cdot m^{-3}$)	0.01	Estrada, 1990
P Nearshore Inputs ($kg \cdot yr^{-1}$)	$3.6 \cdot 10^{8}$	UNEP, 1989
N Nearshore Input ($kg \cdot yr^{-1}$)	$1 \cdot 10^{9}$	UNEP, 1989
TOC ($mg \cdot L^{-1}$)	2	Palanques et al., 1990
POC ($g \cdot m^{-3}$)	1	UNEP, 1989
DOC ($mg \cdot L^{-1}$)	1	UNEP, 1989
TOM Nearshore Inputs ($kg \cdot yr^{-1}$)	$2.5 \cdot 10^{9}$	UNEP, 1989 Calculated
BOD_5 Nearshore Input ($kg \cdot yr^{-1}$)	$3.3 \cdot 10^{9}$	UNEP, 1989
COD Nearshore Input ($kg \cdot yr^{-1}$)	$8.6 \cdot 10^{9}$	UNEP, 1989
Fe ($ug \cdot L^{-1}$)	0.25	UNEP, 1989
Residence Time (yrs)	80	UNEP, 1989
Primary Production ($g\ C \cdot m^{-2} \cdot yr^{-1}$)	50	UNEP, 1989
Primary Production ($kg\ C \cdot yr^{-1}$)	$3.6 \cdot 10^{13}$	UNEP, 1989
Surface Area (km^2)	$2.5 \cdot 10^{6}$	UNEP, 1989
Average depth (m)	1500	UNEP, 1989
Max Depth (m)	5100	UNEP, 1989
Volume (km^3)	$3.7 \cdot 10^{6}$	UNEP, 1989
1% light depth (m)	100	UNEP, 1989
Typical distance to coast (km)	370	UNEP, 1989
Mass loading of solids ($mt \cdot yr^{-1}$)	$350 \cdot 10^{6}$	UNEP, 1989

Table 6-4. Representative oceanographic characteristics of the North Sea.

Parameters	Value	Reference(s)
Current Velocities ($cm \cdot s^{-1}$)	50	Otto et al., 1990
Salinity (psu)	35	Postma et al., 1989
Temperature (°C)	5/15 (winter/summer)	Otto et al., 1990
Density (sigma-t)	28/26 (winter/summer)	Otto et al., 1990 Calculated
Sfc Layer Thickness (m)	25	Defense Mapping Agency, 1990
TSS Background ($mg \cdot L^{-1}$)	1.0	Eisma, 1990
TSS Nearshore Inputs ($kg \cdot yr^{-1}$)	$20 \cdot 10^9$	Eisma, 1990
SiO_4-Si ($mg \cdot m^{-3}$)	140	Brockmann et al., 1990
PO_4-P ($mg \cdot m^{-3}$)	20	Brockmann et al., 1990
PO_4-P Nearshore Inputs ($kg \cdot yr^{-1}$)	$1.23 \cdot 10^8$	WRC TR182, Norton, 1982
NO_3-N ($mg \cdot m^{-3}$)	70	Brockmann et al., 1990
NO_3-N Nearshore Inputs ($kg \cdot yr^{-1}$)	$9.70 \cdot 10^8$	WRC TR182/Norton, 1982
TOC Inputs	1%	Estimated
POM ($mg \cdot L^{-1}$)	0.2	Eisma, 1990
POM Nearshore Inputs ($kg \cdot yr^{-1}$)	$3.5 \cdot 10^9$	Eisma, 1990
BOD_5 Nearshore Inputs ($kg \cdot yr^{-1}$)	$1.14 \cdot 10^9$	WRC TR182/Norton, 1982
Residence Time (yrs)	2	Otto et al., 1990
POM Production	$135 \cdot 10^6$	Eisma, 1990
Surface Area (km^2)	$5.75 \cdot 10^5$	Hardisty, 1990
Average depth (m)	90	Portman, 1989
Volume (km^3)	$5.4 \cdot 10^4$	Hardisty, 1990
1% light depth (m)	20	Otto et al., 1990

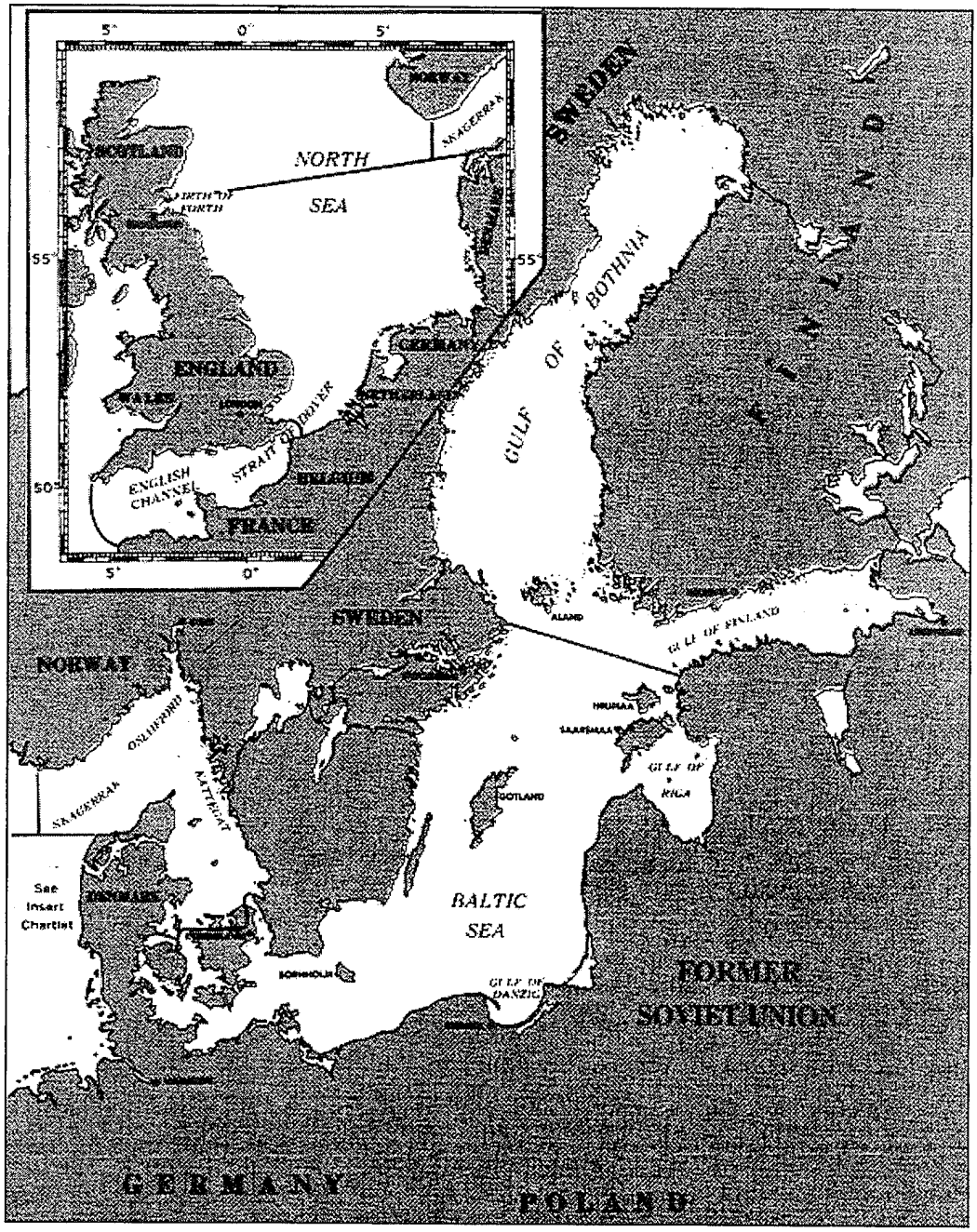

Figure 6-1. General area map of the Baltic and North Sea regions (Defense Mapping Agency, 1990).

6.1 Baltic Sea

General Description. The Baltic Sea, surrounded by Sweden, Finland, Poland, Germany, Denmark, Lithuania, Latvia, Estonia, and the Russian Federation is one of the largest brackish water areas in the world (figure 6-1). It is shallow, with an average depth of 55 m and a

maximum depth of 459 m. The sea has a meridional extension of more than 1500 km and a latitudinal extent of about 650 km, a surface area of approximately 400,000 km^2, and a volume of 21,000 km^3. The Baltic Sea is a very peculiar ecosystem because of its brackish nature and almost permanent stratification. This peculiarity results from very slow water exchange with the adjacent North Sea and an exceptionally high amount of freshwater inflow (approximately 1to 2% per year by volume). Because of slow exchange, water in the Baltic Sea has a residence time of 35 to 40 years, leading to accumulation in water, sediments, and biota of discharged pollutants.

Physical Oceanography. The hydrography and oceanographic conditions of the Baltic Sea have been reviewed by Voipio (1982), Kullenberg (1981), and Jansson (1972). A dominant feature of the oceanography is a marked permanent salinity stratification. Fresh-water supply generates a brackish surface layer which eventually flows out through the Danish Sounds into the North Sea. Water from the North Sea flows in at depth to produce a more saline deep water layer. This layering along with seasonal changes of temperature and river runoff produce a very stable vertical stratification throughout the year. The depth of the halocline varies from about 30 to 80 m depending on location, but is typically 10 to 20 m thick. A seasonal thermocline usually develops between 15 and 20 m. Temperatures above the thermocline can range from 0 to 15°C, while below temperatures normally range from 4 to 6°C. The northern part of the Baltic is ice covered during much of the winter.

Outflow of water from the Baltic to the North Sea is driven by sea-level differences across the Danish Sounds. Inflow of water is driven by both horizontal salinity gradients and by episodic meteorological conditions. The special meteorological conditions can create very strong but short-lived pulses of inflow that generate successive renewal of the bottom waters. These bottom waters have a residence time varying between two and five years depending on their density.

The permanent circulation in the Baltic is very weak and is driven predominantly by freshwater inflow. Mean currents are on the order of a few $cm \cdot s^{-1}$ and are typically cyclic. Wind-induced motion, however, can produce currents up to 200 $cm \cdot s^{-1}$ and is a major factor affecting vertical mixing. Although storms are frequent and often persistent, the mean winds are generally weak. Thus, the mean circulation appears to be mainly estuarine and thermohaline in nature, with a high frequency meteorological component.

Chemical Oceanography. The Baltic Sea has a salinity range of 1 to15 psu with a general distribution of increasing concentrations from north to south. Conservative elements are typically in ratios similar to those found in the open ocean, with the exception of calcium which is relatively high as a result of riverine input. A permanent oxygen deficiency below the halocline is a result of the limited circulation and vertical stratification. This deficiency leads to frequent anoxic conditions and the production of hydrogen sulfide in the bottom waters. Anoxic conditions can exist over long periods of time (years) until the intrusion of relatively oxygen rich North seawater replenishes the bottom water during the special meteorological events previously mentioned.

The nutrient chemistry and eutrophication of the Baltic Sea have been particularly well studied by Ferm (1991), Nehring and Matthäus (1991), Schiewer (1991), Cederwall and Elmgren (1990), Elmgren (1989), Voipio (1981), and Jansson (1972). Large changes have been observed over the last two decades. Since the turn of the century the Baltic phosphorous load has increased about eightfold and the nitrogen load about fourfold. Coastal discharges from land account for 90% of

the total phosphorous load and 50% of the nitrogen loads. Atmospheric deposition accounts for the majority of the other inputs.

Trace metals have shown a fivefold increase in the Baltic over the last 50 years. The increase has been tied to fossil fuel burning and subsequent atmospheric deposition. There is a high correlation of trace metals with particulate organic matter either through active biological uptake or through nonbiogenic adsorption. The majority of metals are ultimately deposited into the underlying sediments.

The high dissolved organic content of the Baltic results in a yellow to yellow-brown color of its waters. This is caused by the high dissolved organic matter content that is derived from decomposition of biological matter, riverine input of humic substances, and the exceptionally large input of organics from municipal and industrial wastes, especially those from the pulp and paper industry. However, organic matter input from anthropogenic sources is estimated to be only 2% of the total standing stock. This suggests that changes in biological production, such as those that occur from eutrophication, will have the greatest impact on organic matter distributions.

Ecology. The ecology of the Baltic is marked by exceptionally low species diversity. Because the hydrographical conditions are very peculiar and even extreme, many marine species are excluded from the Baltic Sea. Furthermore, the Baltic is a geologically young sea and few endemic species have evolved. The low diversity of plankton is demonstrated by the low number of copepods which make up the majority of biomass in most sea areas. Copepods are estimated to be represented by 800 species in other oceans but are represented by only 8 in the Baltic. Only 145 macroscopic animals occur in the Baltic while 200,000 species occur in other seas. Since the ecosystems are simple with few species and few links between them, small environmental changes can lead to severe imbalances.

Primary production of organic matter shows marked regional variation caused by variations of nutrient levels and the length of the growing period. Light conditions and duration of sea-ice cover are decisive for the seasonal development of vegetation and ecosystem functions along with nutrients. Consumers, which are composed of heterotrophic pelagic and benthic organisms, are dependent on sinking organic matter from the euphotic zone.

As a result of eutrophication, the corresponding production has generally increased since the 1920s; it is unclear if phytoplankton production has increased over this time period. However, it is estimated that zooplankton biomass has increased 50%, sedimentation of organic matter has increased by 60%, benthic macrofauna above the halocline has increased by three to fivefold, and fisheries yield have increased tenfold.

Pollution Status. There is an extensive literature base on the inputs and effects of pollutants in the Baltic Sea which include Wulf and Rahm (1993), Kautsky (1992), Schmidt (1992), Hallberg (1991), Slaczka (1990), Andrulewicz and Rohde (1987), Melvaslo (1981), and Kullenberg (1977) as well as the articles already cited. The pollutants studied have included trace metals, nutrients, chlorinated hydrocarbons, pesticides, oil, sewage, radioactive inputs, and industrial waste materials. Of these, the effects of eutrophication have been the most well-documented and considered to be the Baltic Sea's largest pollution problem.

As a result of its restricted horizontal and vertical exchange, the Baltic is particularly susceptible to anthropogenic inputs. The most important hydrographic environmental parameters are salinity and oxygen which have a direct affect on spawning behavior, the development of larvae, and the migration activity of fish. Eutrophication has an indirect impact on the biology by first favoring production of the plankton which in turn enhances fish production. As the biomass from the euphotic zone settles to the bottom it is decomposed by oxygen consuming bacteria, leading to anoxia. Anoxic conditions ultimately lead to a reduction in the size of habitat available to demersal fish and other aerobic organisms. It is estimated that the macrobenthos over an area of 100,000 km^2 has been wiped out by anoxic conditions caused by eutrophication.

Past practices of waste dumping, such as the dumping of scrap iron, autos, containers and garbage, and munitions are now prohibited. Dumping from frequent shipping resulted in tracks of dumped ship garbage, e.g., in 1968 about 400 m^3 garbage·day^{-1} was dumped by ferries traveling between Denmark and Sweden (Voipio, 1981).

It is clear that limited circulation and flushing to the open ocean, or in this case to the North Sea, has created unique oceanographic conditions that have already been significantly impacted by man. The unusual nature of its ecological diversity and simplistic food chain links makes the Baltic even the more susceptible to anthropogenic impacts.

6.2 North Sea

General Description. The North Sea is a shallow, semienclosed sea located between the British Isles and the mainland of Northwestern Europe (figure 6-1). Britain, the Orkney, and Shetland Islands form the western border, with Denmark and Norway to the west, and France, Belgium, the Netherlands, and Germany to the south. The major sea connection is to the Atlantic via the Norwegian Sea on the north. Exchange with the Atlantic is also effected through the English Channel to the southwest, and connection to the Baltic is via the Skagerrak, Kattegat, and Danish sounds to the east. The North Sea, with an area of approximately 575,300 sq. km, a maximum length of about 1100 km (Strait of Dover to Unst), a maximum width of about 675 km (Scotland to Denmark), and an average depth of 74 m represents about one six-hundredth of the surface area of the world's oceans. Depths are generally shallow in the south (50 m), sloping deeper to the north (200 m) with extreme depths along the Norwegian coast of 750 m in the Norwegian Trench and Skagerrak.

Physical Oceanography. The physical oceanography of the North Sea was recently reviewed by Otto et al., 1990. General descriptions of the circulation and hydrography are described in Sverdrup et al., (1942), Laevastu (1960, 1963), Lee and Ramster (1968), Lee (1970, 1980), Hill, (1973), Saetre and Mork (1981), and Sundermann and Lenz (1983). Systematic studies of North Sea oceanography have been carried out since about the turn of the century (Smed, 1983), primarily under the international coordination of the International Council for the Exploration of the Sea (ICES).

On short time scales, the dominant process determining water level, current velocities, mixing, and transport in the North Sea is the semidiurnal M_2 tide. The resulting tidal amplitudes and water velocities are generally highest in the south and west (2-3 m, 0.5-2 m·s^{-1}) and lowest along the Norwegian coast (<1 m, 0.1 m·s^{-1}). On longer time scales, the wind, other tidal harmonics, and to a lesser extent density driven flow also exert considerable influence on the circulation through the induction of residual flows superimposed on the oscillatory tidal currents. The

combined action of the tidally averaged, wind driven, and baroclinic circulation results in a residual flow field which determines, to first order, the long-term transport processes of the North Sea. The characteristic residence time of a conservative tracer or pollutant discharged in the North Sea ranges from about 100 to 1000 days as a function of the residual transport and the turbulent diffusion generated by the tidal currents. Much of the tidal energy is dissipated in turbulent motion generated by friction at the sea bottom. This is particularly true in the shallower coastal and southern regions of the sea. In these regions, the water column may remain well mixed for much of the year, while in much of the northern portion of the sea stratified conditions may prevail, especially during the summer months.

This stratification is a result of both the deepening of the water column, which reduces the turbulent mixing of the tides, and seasonal heat flux through the sea surface. Minimum surface temperatures occur in February, and range from about 7°C in the northwest to 2°C in the south. In summer the warmest water occurs in the south (17°C) while the northern waters remain relatively cool (11°C). Variations in salinity result from the interaction of direct river runoff of about 370 $km^3 \cdot yr^{-1}$ and influx from the Baltic via the Skagerrak of about 530 km^3/year with the oceanic inflows through the Norwegian Sea and the Straits of Dover. Salinity variations are generally small, with typical levels of about 35 psu, thus the primary mechanism for stratification is via temperature variations. Near the coast, salinities may drop below 35 psu but are typically greater than 30 psu. Vertical distribution is typically uniform with maximum variations along the Norwegian coast of about 2 to 3 psu.

Pollution Status. Chemical pollution of the North Sea was recently reviewed by Portman (1989) and Salomons et al., (1988). Chemical pollutants in the North Sea tend to cover the broad spectrum of compounds related to inputs from the highly industrialized countries surrounding the sea. Metal inputs are thought to be generally on the decline, with primary sources including atmospheric deposition, rivers, direct discharge, dredge and sewage sludge disposal, and industrial wastes. The most reliable data for metal and organic contaminants is based on levels in fish and shellfish from ICES coordinated monitoring programs. The conclusion of these studies was that at current levels the contaminants measured present no serious threat to human health via consumption, but that no clear statement could be made as to the potential threat to marine organisms.

Nutrient loadings and distributions have been described by Brockmann et al., (1990). In the oceanographic sense, the term nutrients generally refers to the biologically available inorganic forms of nitrogen, phosphorus, and silica. In the surface layer where photosynthesis is active, nutrients generally have maximum concentrations during the winter when incoming radiation is low, and may be completely exhausted during the summer growth season. Primary external sources of nutrients are from river inflow, atmospheric exchange, and coastal discharges, especially in the Southern Bight and German Bight where most of the river discharge is concentrated.

Observation and monitoring of litter has been reported for the North Sea proper (Dixon and Dixon, 1983), and for the beaches and coasts of northwest Europe (Dixon and Dixon, 1981). These studies indicate that the primary source of this litter is from routine disposal of garbage from ships. Distributions of various litter components including plastics, paper and cardboard, wood items, metal and glass, and netting show that these products are widely distributed throughout the North Sea. Plastics were the most common item, followed in decreasing order by paper and cardboard, wood, metal and glass, and netting. These estimates are only for floating

debris and probably underestimate some items, especially glass and metal. In a review of contaminant inputs to the North Sea, Grogan (1984) estimated that more than 500 mt of metal and a similar amount of glass are disposed into the sea by ships each year. Little is known about the direct effects of litter pollution. Most of the documented damage to marine organisms is mechanical in nature, relating to entanglement. Adverse effects due to ingestion of plastics and other debris has also been documented (Kastelein and Lavaleije, 1992). In comparison to other sources, Grogan (1984) described the inputs from ships as insignificant except with respect to shore littering.

Ecology. The ecology of the North Sea has been reviewed descriptively by De Wolf and Zijlstra (1988), in terms of modeling efforts (Fransz et al., 1991), fisheries (McIntyre, 1988), marine mammals (Reijnders and Lankester, 1990), and benthos (Rees and Eleftheriou, 1989; McIntyre, 1978).

North Sea fisheries are among the most productive in the world. The annual catch yields about $3.5 \cdot 10^6$ tons which accounts for about 5.3% of the world's total commercial fish harvest. Principal fish stocks include herring and mackerel (approximately 50%) with the remaining contribution primarily from pout, cod, sand eels, whiting, haddock, and plaice. Many fisheries appear to be declining as the result of overfishing. There is also evidence of pollution effects on commercial and other fish species.

The underlying ecological strength of the fishery stems from high productivity at lower trophic levels due to nutrient delivery by strong tidal mixing in the North Sea. This nutrient supply supports the development of phytoplankton often manifested in spring and summer blooms. Increasing frequency of phytoplankton blooms (e.g., *Phaeocystis pouchetii*), especially in the southern regions of the North Sea and the eastern English channel, have led to concerns about eutrophication, water discoloration, shellfish poisoning, and other ecosystem effects. In response to this primary productivity, there is also a rich diversity of zooplankton within the North Sea. Copepods, such as *Calanus finmarchicus* in the north and the smaller *Temora longicrnis* in the south, represent a primary pillar in the overall food web. Phytoplankton, zooplankton, and fisheries dynamics are thus strongly interrelated and externally dependent on physical exchange and mixing processes.

Information on population and health status of marine mammals in the North Sea is rather sparse. Resident stocks include the grey and common seal, the harbor porpoise, the white beaked, white-sided, and bottlenose dolphins, and the pilot, minke, and killer whales. Several other species have been encountered in the North Sea but are not considered indigenous. In general, the number of these top predators is thought to be declining due to interactions with both pollution and fisheries (Reijnders and Lankester, 1990).

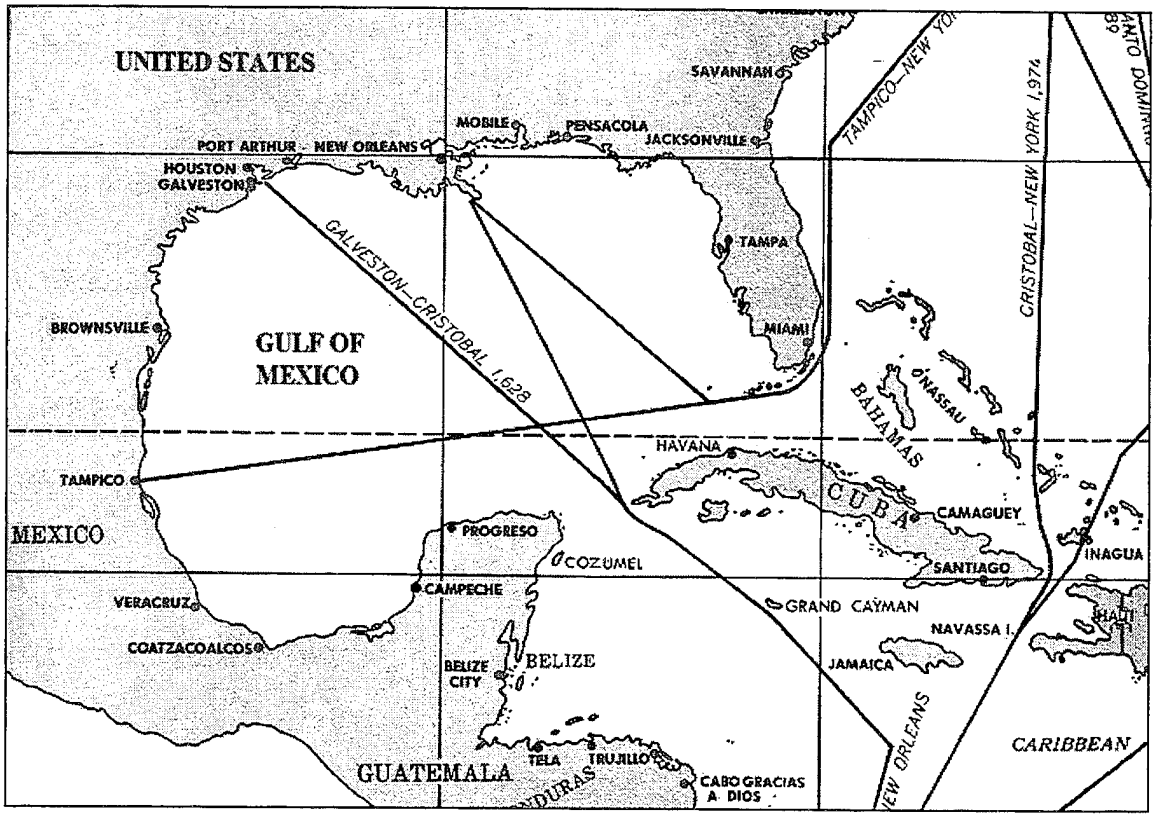

Figure 6-2. General area map of the Caribbean Sea region (Defense Mapping Agency, 1988).

6.3 Caribbean Sea

General Description. The Caribbean Sea (figure 6-2) consists of a number of deep basins including, from east to west, the Venezuela Basin (5600 m), the Columbia Basin (4500 m), the Yucatan Basin (4600 m), and the Mexico Basin (4400 m). The basins are separated by ridges rising generally less than 1000 m below sea level and thus permitting significant communication with the open ocean (Sverdrup et al., 1942). The overall shape is that of a wide and somewhat irregular channel with the eastern end opening toward the tropical part of the North Atlantic. The northern boundary, represented by the islands of Cuba, Haiti, and Puerto Rico, is broken by several passages (Sverdrup et al., 1942). If the Gulf of Mexico is included, the total surface area is calculated to be $4.24 \cdot 10^6$ km^2 where 80% of the water is deeper than 1800 m and half is deeper than 3600 m. The Caribbean Sea and the southern half of the Gulf of Mexico are tropical environments experiencing little seasonal change (Clark, 1992).

Physical Oceanography. The general circulation of the region is dominated by the Caribbean Current which runs east to west through the Caribbean proper and northwards through the Gulf of Mexico. Seasonal loop currents are present in the Gulf of Panama and the Gulf of Mexico, and strong currents run eastward through the Florida Straits and join the Gulf Stream. In general, this strong, clockwise current system provides effective flushing of the Caribbean proper and portions of the Gulf of Mexico.

The average sea surface temperature in the Caribbean is 27 °C with a seasonal fluctuation of about 3°C. A permanent thermocline is found over much of the area at a depth of about 100 m. The stable thermal structure limits upwelling and vertical mixing, hence much of the area is deficient in nutrients (Clark, 1992). North Atlantic waters pass freely through the Caribbean Sea at depths less than about 800 m, but mixing is restricted at greater depths (Sverdrup et al., 1942). Below the upper water, a considerable amount of Antarctic Intermediate Water enters the Caribbean Sea. The water at the intermediate salinity minimum is mainly of South Atlantic origin (Nielsen, 1925; Parr, 1937). The intermediate salinity minimum decreases in intensity in the direction of flow. In the eastern Caribbean Sea (about 68°W) the average minimum salinity is 34.73 psu, while in the Yucatan Channel the average minimum salinity is 34.88 psu. The increase is due mainly to vertical mixing within the moving water mass (Seiwell, 1938).

The deeper waters are divided into basins of which the Venezuela and Colombia basins in the eastern Caribbean Sea, and the Cayman Trough and the Yucatan Basin in the western Caribbean Sea are the most important. The renewal of deep water in the Venezuela Basin is relatively rapid since oxygen content is high, having an average value of approximately 5.1 $mL \cdot L^{-1}$ at a depth of 2500 m (Seiwell, 1938). The renewal of deep water in the Cayman Trough and the Yucatan Basin is apparently even more rapid since average oxygen content at 2500 m is between 5.5 and 6.0 $mL \cdot L^{-1}$. Deep water salinity is uniform averaging 34.98 psu (Parr, 1937).

Chemical Oceanography. Nutrient concentrations in the offshore marine waters tend to be extremely low. These levels may be an order of magnitude less than those seen in temperate waters. As a result, the net productivity of the water column primary producers is severely limited. Accordingly, phytoplankton biomass is low and water column clarity is high (UNESCO, 1983). Little nitrate ($<<0.2$ μM NO_3-N) is present in the upper 50 m (Muller-Karger et al., 1989). In waters below about 140 m nitrate concentrations are 2.5 to 10.0 μM, and below 400 m levels >25 μM are seen. Phosphate concentrations are variable in surface waters (0.0 to 0.06 μM PO_4-P) and increase with depth (0.5 to 1 μM at 250 m). Near land masses and in upwelling regions, surface nutrients are more abundant. For example, the upwelling system near Margarita Island provides abundant nutrients which cause diatom-dominated blooms, and consequently, a large fishing industry (Muller-Karger et al., 1989).

Ecology. While the shallow waters of the Caribbean are known for low biological production rates, they are characterized by high levels of benthic production (UNESCO, 1983). Highly productive coastal ecosystems of mangroves, seagrass, and coral reefs typify shallow Caribbean waters providing habitat for a large and diverse fauna, as well as nursery grounds for prawns and fish (Clark, 1992). Mangrove forests develop where fresh water mixes with seawater along swampy, tropical shorelines. They are found throughout the Caribbean region with the largest concentrations occurring on the shores of Columbia and Venezuela. Mangroves also provide nursery areas for fish, shellfish, shrimp, and crabs. The root systems act as efficient traps for particles and pollution, primarily from land sources but potentially from offshore as well. This trapping effectively clarifies the surrounding waters thus protecting reef and seagrass habitats.

Extensive seagrass meadows exist in the shallow water regions of the Caribbean. High concentrations are found on the Bahaman banks, U.S. Gulf coast, Jamaica, Cuba, Mexico, Belize, Honduras, Nicaragua, Costa Rica, Panama, Columbia, and Venezuela coasts. The dominant species is usually *Thalassia testudium* (Turtlegrass). Like mangroves, seagrasses provide habitat for many other species, trap sediments and pollutants, and provide erosion control. Seagrass

productivity is particularly sensitive to changes in temperature and light. Thus any process which leads to reduced light levels could potentially impact the status of seagrass habitat.

Coral reefs are found from southern Florida and the Gulf of Mexico throughout the Caribbean with the densest regions in the Bahamas and off Belize. The barrier reef off of Belize is second in size only to the Australian Great Barrier Reef. The reefs generally grow in waters of 50 m depth or less, and require stable temperatures around 23°C. As with seagrasses, light and temperature are strong controlling factors over the growth and development of coral reefs. Water column particulate matter such as silt or pulped material can, therefore, influence reef habitat by reducing water clarity or by directly smothering the coral polyps. Recently, wide spread coral bleaching has been reported in large areas of the Caribbean including Columbia, Puerto Rico, the Virgin Islands, the Cayman Islands, Jamaica, the Bahamas, Haiti, Florida, Bermuda, and the Gulf of Mexico. Although the cause of this recent bleaching event is still under debate, previous events have been linked to alterations in temperature, salinity, light, food depravation, siltation, and tidal exposure.

Pollution Status. Pollution in the Caribbean Sea is a shared concern of many neighboring countries. In 1977 a joint project to develop an action plan for environmental management for the wider Caribbean region was agreed upon by the Economic Commission for Latin America and the Caribbean (ECLAC), and the United Nations Environmental Programme (UNEP, 1985). The Cartageña Convention was concluded under the UNEP Regional Seas Programme and came into force in 1986 (Freestone, 1991). A mandate to negotiate a protocol on Specially Protected Areas and Wildlife was set. A central feature of the agreements involved commitments to conserve Special Areas and species both within national jurisdictions as well as on a regional basis. A permanent Scientific and Technical Committee was also established.

While the scope of pollution in the Caribbean Sea is perhaps not as well documented as in other regional seas, some sources of pollution may be identified. The Caribbean Sea may be considered similar to the Mediterranean Sea in that both have a heavy amount of maritime traffic, important tourist industries, and high levels of coastal contamination. An estimated 85% of the ocean contamination in Latin America and the Caribbean is caused by human activity on land. Of this contamination, 90% remains in coastal waters and ecosystems such as mangrove swamps, seagrass beds, and coral reefs (UNEP, 1990).

Hydrocarbon pollution via spills has been estimated to total more than 500,000 tons per year in the seas and oceans of Latin America and the Caribbean. Marine transport was responsible for more than 28% of these incidents (UNEP, 1990). In the Western Caribbean Sea 38% of plankton samples were polluted with tar balls likely originating from ship bilges (Wyatt, 1982).

Pollution of Caribbean beaches by various discarded consumer items has been reported (Cruz et al., 1990). Along the Mosquitia Coast of Honduras 123.4 kg of debris per km of beach was estimated. Materials of polymer origin accounted for 91.5%, glass bottles for 7.4%, and aluminum cans for 0.94%. Plastic pellets and tar balls were also found. Cruz et al., (1990) concluded that the materials were carried by the Caribbean currents from the Antilles and beyond. Along Panamanian beaches 43% of beach debris originated from Panama, other Caribbean countries contributed 31%, while 16% was from the U.S. The remaining 10% was from more distant sources (Garrity and Levings, 1993). The majority of debris (82%) was polystyrene foam and other plastic material related to consumer or household uses. No evidence of substantial input from industrial, recreational (cruise liners), or offshore commercial fishing

sources was found. Some dumping of household debris from small vessels was observed. In a recent review (Pruter, 1987), the major inputs of plastic debris to the oceans generated from ships, rivers, municipal drainage systems, and beach goers. The major types of debris were identified as fishing gear, packaging material, convenience items, and raw plastics.

From an oceanographic perspective, the Caribbean Sea above the sill depth is not subject to restricted circulation and long residence time as are other Special Areas. Its sensitivity appears to stem from the oceanographic conditions which lead to the development of specialized ecological communities such as coral reefs. These communities may then be particularly sensitive to perturbations outside the normal range of oceanographic conditions brought on by either natural or anthropogenic events. It is because of this sensitivity, and because of the dependence of the Caribbean economy on these natural assets for both tourism and fisheries, that the Caribbean has received consideration for Special Area status under MARPOL. The risk of such impacts is thought to be increased for the Caribbean due to the high vessel traffic of both commercial and tourist vessels in the region.

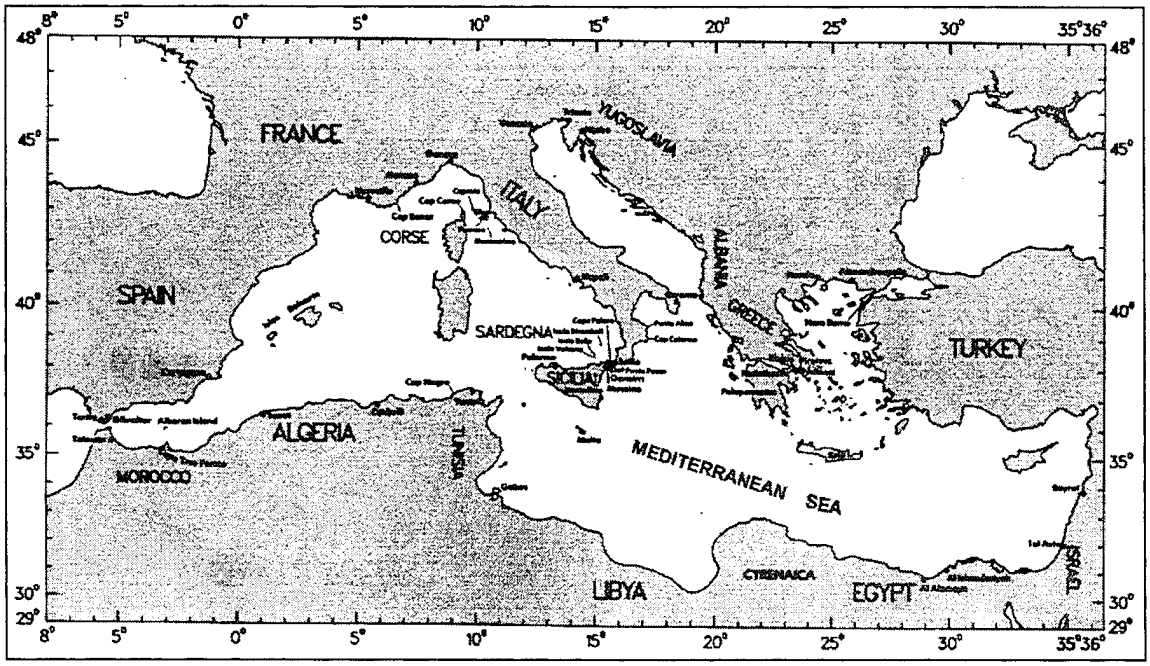

Figure 6-3. General area map of the Mediterranean Sea region (Defense Mapping Agency, 1991).

6.4 Mediterranean Sea

General Description. The Mediterranean Sea is bordered by 18 countries from the continents of Europe, Asia, and Africa (figure 6-3). The sea has a maximum east-west extent of 3800 km and a maximum north-south extent of 900 km, although the farthest point away from land is only 370 km. The sea covers an area of about $2.5 \cdot 10^6$ km^2, has an average depth of 1500 m, and has a

volume of approximately $3.7 \cdot 10^6$ km^3 (UNEP, 1989). Its maximum depth is 5100 m. The length of its coastline, including its many islands, is estimated at $4.6 \cdot 10^4$ km.

The Mediterranean is a semienclosed sea. It connects with the Atlantic Ocean on its western extent through the Strait of Gibraltar, with the Red Sea on its southeastern extent through the Suez canal, and with the Sea of Marmara to the northeast through the Dardanelles. The Strait of Gibraltar is the largest of these openings at 15 km wide and a sill depth of 290 m. The opening to the Suez is 120 m wide and 12 m deep, while that of the Dardanelles varies from 450 m to 7.4 km wide and is 55 m deep.

The sea consists of two major basins, the Western and Eastern, each of which is made up of a series of interacting sub-basins and seas. The Western Mediterranean, roughly a third of the surface area, consists of the Alboran Sea, the Algero-Provencal basin, the Ligurian Sea, and the Tyrrhenian Sea. The Eastern Mediterranean, covering the remaining two-thirds of the surface area, consists of the Adriatic, Ionian, Aegean, and Levant Seas. The major interconnection between the Western and Eastern basins is through the Strait of Sicily.

There is large variation in climate across the Mediterranean. The climate changes from damp and temperate in the north to an extreme arid condition in the south. The large mountains surrounding most of the sea (except in the southeast) exert an influence on the climate, and ultimately the sea's ecology. In particular, the variation in amount and location of precipitation is influenced by this topography. Rainfall intensity and duration generally decrease from west to east and from north to south. Seasonal rainfall is maximum in spring and autumn, with a distinct minimum in summer. Dry winds, primarily from the north and west, produce a strong evaporative influence over the entire sea. This evaporative effect is maximum during winter and spring. In contrast to the distribution of rainfall, both the air and sea-surface temperatures increase from west to east and from north to south.

The major rivers entering the Mediterranean are the Ebro, Rhone, Po, and Nile. These combine to produce an annual freshwater inflow estimated at 10^3 km^3 and a sediment input of $5 \cdot 10^7$ mt. Because of the irregular coastline, torrential rivers draining small areas do occur on a seasonal basis and can be important locally. Over 90% of the inflow from rivers occurs along the northern coast.

Physical Oceanography. Given the warm and sunny climate of the region, the oceanography of the Mediterranean is marked by a hydrological imbalance in which evaporation exceeds fresh water input from precipitation and runoff. The imbalance is mainly compensated (87%) by net inflow of Atlantic surface water through the Strait of Gibraltar, with a smaller amount (13%) coming in through the Dardanelles. Water exchange through the Suez Canal is negligible. This results in a surface current system that is dominated by a steady eastward flow of Atlantic surface water along the African coastline. As surface water migrates east, numerous counterclockwise eddies spin off, moving water up into the various northern basins. There is no return of surface water. Instead, the return of water occurs by an east to west flow of subsurface water (described below). This deeper water spills over the sill at Gibraltar and becomes the source of Upper Deep Water in the North Atlantic, a water mass that can be traced for considerable distances.

Owing to the high evaporative effects, vertical convection controls the vertical distribution of salinity and temperature, as well as other dissolved components. Waters of the Mediterranean

are exceptionally high in salinity with surface values ranging from 36 psu in the west to 39 psu (Defense Mapping Agency, 1991) in the east. With the formation of high salinity water comes an increase in density, particularly during winter when surface temperatures decrease. This results in large scale vertical convection when surface waters sink. This also results in the formation of three distinct water mass layers: a surface layer, the Levantine Intermediate Water, and the Mediterranean Deep Water. Sverdup et al., (1942) suggested a fourth transition layer between the Intermediate Water and the Deep Water. Inflow of the Atlantic surface water replaces this sinking surface water, while outflow of deeper water, principally the Levantine Intermediate Water, completes the mass balance.

The surface layer thickness, defined by a temperature minimum in the Western Basin and by a slow temperature decrease in the eastern basin, varies between 75 m and 300 m (Sverdrup et al., 1942). Mean surface temperatures vary seasonally from 14°C in winter to 26°C in summer. Temperatures can, however, reach as high as 30°C in the far reaches of the Eastern Basin in summer and as low as 5°C in the northern reaches of the Adriatic in winter. Spatially, temperatures generally increase from west to east. The surface temperature-salinity variations result in surface densities that typically are lowest in summer (25 σ_t) and highest in winter (29 σ_t). Density generally increases west to east and south to north, although the influence of the Po River can lead to relatively large variations within the Adriatic.

The Levantine Intermediate Water, 300 to 600 m, is characterized by temperature and salinity maxima at roughly 400 m. The bottom of this layer, at roughly 600 m, is characterized by rapid decreases in both temperature and salinity. The water of this layer is formed in the inner part of the Mediterranean and then spreads to the west. The Deep Water, present at depths below 600 m, is relatively more homogeneous than the other layers. It has a temperature of approximately 13 to 15°C and a salinity of 38 to 39 psu.

Surface current velocities vary a great deal throughout the sea as result of variations in tidal state, localized and seasonal wind patterns, and freshwater inflow. Mean current speeds are, however, fairly consistent throughout the year at about 0.5 kts. Although the mean current flow trend is east-southeast, there are numerous gyres that setup throughout the sea. Even though the semidiurnal tidal amplitudes are low, averaging about 0.6 m, tidal current velocities can be quite significant. Tidal current speeds of up to 3 kts are common, and speeds up to 4 and 5 kts occur through many of the narrow constrictions such as the Strait of Messina (Defense Mapping Agency, 1991). Current speeds are also altered locally and seasonally by the winds as well as by localized freshwater runoff, such as in the Adriatic. These effects can also lead to significant variations in the general current velocities.

As stated previously, the Mediterranean is a semienclosed sea. Each of its interconnections with surrounding seas and oceans is through narrow and shallow openings. Because of its restricted flow interchange, deep basins, and strong vertical convective processes, the residence time of water is estimated at roughly 80 years (UNEP, 1989).

Chemical Oceanography. Except for salinity and nutrients, the chemistry of the Mediterranean is quite similar to that of the adjacent Atlantic. The general distribution of dissolved chemicals is determined by the strong vertical convection and the generalized circulation pattern described above. In the case of salinity, evaporative effects result in exceptionally high values relative to the Atlantic. In the case of nutrients, exceptionally low values are found. This occurs because the natural recycling of nutrients from deep waters is limited by the continual wash-out of

materials along with deep water through the Strait of Gibraltar. Furthermore, Atlantic surface waters entering the sea are relatively low in nutrient content, having already been used up. Thus the Mediterranean is "self-cleansing" with respect to eutrophication by losing nutrient rich deep water and gaining nutrient poor surface water.

Although the region is in general oligotrophic, proximity to nutrient sources such as large rivers and urban discharges (mainly along the northwestern shore) does lead to localized eutrophication. With the influx of nutrients from various sources, biological productivity is enhanced in the surface waters. The production leads to a much higher than normal fallout of organic matter, resulting in an increased oxygen consumption in the deep water. This condition can lead to anoxic conditions in the deep water and underlying sediments with a negative impact to the benthos. The extent to which this occurs in the Mediterranean is, however, limited to its peripheral embayments.

According to Saydam et al. (1984), total suspended loads measured throughout the surface waters of the northeastern Mediterranean ranged from 0.06 to 5.4 $mg \cdot L^{-1}$. The average value for near-shore stations was 2.1 $mg \cdot L^{-1}$ while the average value for off-shore stations was 1.6 $mg \cdot L^{-1}$. There were, however, significant seasonal differences in which summer and fall values were typically a factor of two lower than those measured in the spring. The increased levels were attributed to particulate matter generated by primary production. The increase in particulates was observed along with an increase in dissolved oxygen at rate of approximately 1 $mg \cdot L^{-1}$ TSS : 1 $mg \cdot L^{-1}$ DO_2.

The organic matter content of the waters and suspended particles of the Mediterranean is generally low as a result of low biological productivity. Dissolved organic carbon (DOC) values range from 0.5 to 1.5 $mg \cdot L^{-1}$, while particulate organic carbon (POC) values are about 1 $mg \cdot L^{-1}$. Only about 0.1 $mg \cdot L^{-1}$ of the POC are living organisms (UNEP, 1989).

Nutrients, dissolved oxygen, particulate suspended matter, and chlorophyll-*a* have been shown by Moraitou-Apostolopoulou (1985) to commonly have a vertical distribution that is related to the development of a deep chlorophyll maximum (DCM) (described in more detail below). This distribution results in mid-depth minima of nitrate-nitrogen and silicate-silicon, as well as mid-depth maxima of nitrite-nitrogen, oxygen, cell counts, and chlorophyll-*a*. Phosphate-phosphorus, however, was low and typically nondetectable throughout most of the euphotic zone.

Ecology. Although rich in biological diversity, the Mediterranean is relatively poor in terms of the abundance of organisms. This is a direct result of nutrient limitation and the resulting low primary production. Maximum primary production is typically associated with the DCM and is found at the lower limit of light requirements and increased nutrient levels, at roughly 100 m (UNEP, 1989). In the western Mediterranean, Estrada (1985) measured maximum total phytoplankton cell counts of about 200 $cells \cdot mL^{-1}$ and typical chlorophyll-*a* levels of 0.9 $\mu g \cdot L^{-1}$ (maxima as high as 2 $mg \cdot L^{-1}$ were observed) at the depth of the DCM. The maximum cell count was driven principally by diatoms, although dinoflagellates dominate the cell counts above and below the DCM.

Primary production tends to be higher in colder years as a result of deeper mixing and a larger area of deep water production. High productivity can occur locally, particularly at river mouths and along the coast in winter as a result of nutrient influx. In these areas and in regions of

upwelling, high production leads to a high organic matter flux to the sediments which can result in anaerobic conditions in the sediments and bottom waters. The highest primary production levels in the Mediterranean are observed in the spring off the Egyptian coast under the influence of the Nile.

The zooplankton of the Mediterranean show a great homogeneity both quantitatively and qualitatively (Moraitou-Apostolopoulou, 1985). Both the biomass and the variety of the most important species are found to be similar in both the eastern and western basins (Moraitou-Apostolopoulou, 1985). The most important species are copepods followed by the cladocerans. The majority are atlantomediterranean, a small portion being endemic. Standing stocks are equivalent to the biomass values of the offshore temperate Atlantic, although it has been difficult to determine biomass numbers.

Endemic species make up a relatively high percentage of the total species present in the Mediterranean. The numbers include 25 to 50% of sessile groups, 13% of crustaceans, and 10% of fishes. This implies that the Mediterranean has been a center of evolution. The geological evolution of the Mediterranean along with its climatological fluctuations may have played a role in the rich diversity of its ecosystems. The diversity of environmental conditions within the Mediterranean, particularly abiotic ones such as temperature, has also led to a large community diversity.

Low primary production and a low standing stock of bottom-dwelling organisms provides no opportunity for the development of a big fisheries industry. However, because of the large surrounding human population, there is an exceptionally high demand which has resulted in the development of a large number of small-scale fisheries. It has also led to high prices and overfishing. There is a very large number of demersal and pelagic species exploited. In terms of tonnage, the leading catches are herrings, sprat, and anchovies. There is also a good sized fisheries for mollusks and crustaceans such as lobster, crab, and shrimp. The most important nonedible marine species are corals and sponges.

Pollution Status. Evidence suggests that except for some localized areas, neither organisms nor the waters of the Mediterranean are seriously contaminated. However, because of its large area and because assessment efforts have not been made over a long period of time, a comprehensive assessment of the state of pollution in the Mediterranean is somewhat lacking. Of the numerous studies that have been conducted, the major contaminant issues appear to be related to nutrients as they affect eutrophication, oil discharge, and litter.

Nutrients. Of the possible elements associated with discharges into the Mediterranean, excess nutrients and the resultant eutrophication process appear to be the most widespread problem. However, the Mediterranean as a whole does not appear to have a problem with eutrophication because of the removal process in the deep water described previously. Eutrophication is the process by which the addition of nutrients, principally phosphorus and nitrogen, results in accelerated growth of the phytoplankton and phytobenthos. The extreme condition caused by the accelerated growth can lead to anoxia, death of aquatic organisms, and conditions of putrefaction. These conditions are marked by high turbidity and changes in water color ranging from red to brown ("red tide"). It should also be noted here that in some circumstances eutrophication can have beneficial effects by enhancing fisheries production.

Eutrophication tends to be a local problem mainly occurring along the coastline as a result of land-based releases including river input, agricultural runoff, and domestic-industrial waste water input. River inflow of nutrients is by far the largest source (75%) of the total estimated inputs of $8 \cdot 10^5$ mt $N \cdot yr^{-1}$ and $3.22 \cdot 10^5$ mt $P \cdot yr^{-1}$ (UNEP, 1989). In contrast, the domestic and industrial inputs are only about 10 to 20% of the total input while agricultural runoff is about 10% of the total. Nutrient influx can affect large areas along the coast, particularly in areas with large sources and restricted circulation. The north-western portion of the Adriatic Sea is usually used as an example, with its large nutrient source in the Po River (Waste Discharge into the Marine Environment, 1982).

Marine Litter. The sources, effects, fate, and current levels of litter in the Mediterranean are reviewed in UNEP, (1991). The review covers "persistent" litter such as plastics, metal, and glass, etc. For the purposes of this review, food debris and paper cartons were considered "nonpersistent" and were not discussed. Much of the information regarding litter in the Mediterranean is derived from estimates based on few quantitative studies. Furthermore, the heterogeneous nature of the litter in terms of material type, size, units of measure, and the methods employed in quantification, result in a large variability in the estimates. Some of the major findings are, however, considered below.

Based on a qualitative assessment of the litter found along the Mediterranean coastline, the majority of litter is believed to be derived from land, principally debris left by beach goers. However, there is no quantitative estimate of this input. The other main source of debris is that which is discarded from ships. Of the $6.6 \cdot 10^8$ $kg \cdot yr^{-1}$ estimated for ship-borne trash, 97% was derived from merchant ships while 1.5% ($1 \cdot 10^7$ $kg \cdot yr^{-1}$) was derived from military ship activity.

Quantitative assessment of coastal litter ranges widely from 0.5 to 1100 pieces/frontal meter of coastline. The major component of coastal debris (by piece) was typically plastic. The amount of floating debris estimated from at-sea counts ranged from 0.12 to 2000 pieces/km^2 and was mainly composed of plastic. A very rough estimate of seabed litter is 29 kg km^{-2}. On a per piece basis, plastic is the dominant material composing coastal and floating litter, although Gabrielides et al. (1991) suggest that plastics were also dominant on a weight basis. The wood component of seabed litter predominates over that of plastic and metal, and glass follows distantly as smaller components of the nonfloating litter.

The factors controlling the distribution of litter are 1) proximity to sources such as population centers and shipping lanes, and 2) dispersion forces such as winds and currents. However, the exact nature of the relationship of these factors to the distribution of litter has not been well studied.

The deleterious effects of marine litter include entanglement and ingestion by marine organisms (including birds), damage to free navigation through entanglement of ship propellers etc., and damage to beaches by deterioration of their aesthetics. The effects on the marine ecology and on vessel operations has not been well documented. Although difficult to quantify, the effect on beach aesthetics is potentially very damaging since the Mediterranean coast is one of the largest tourist destinations in the world.

Ship Traffic. Ship traffic in the Mediterranean can be characterized as heavy. Annual traffic in the Mediterranean of ships that are more than 100 gross registered tons is estimated at 220,000 vessels (The World Bank, 1990). About 2000 merchant ships are in the Mediterranean at any

one time. Of these, 250 to 300 are oil tankers. Some 22% of the total world petroleum traffic transits through the Mediterranean (UNEP, 1989).

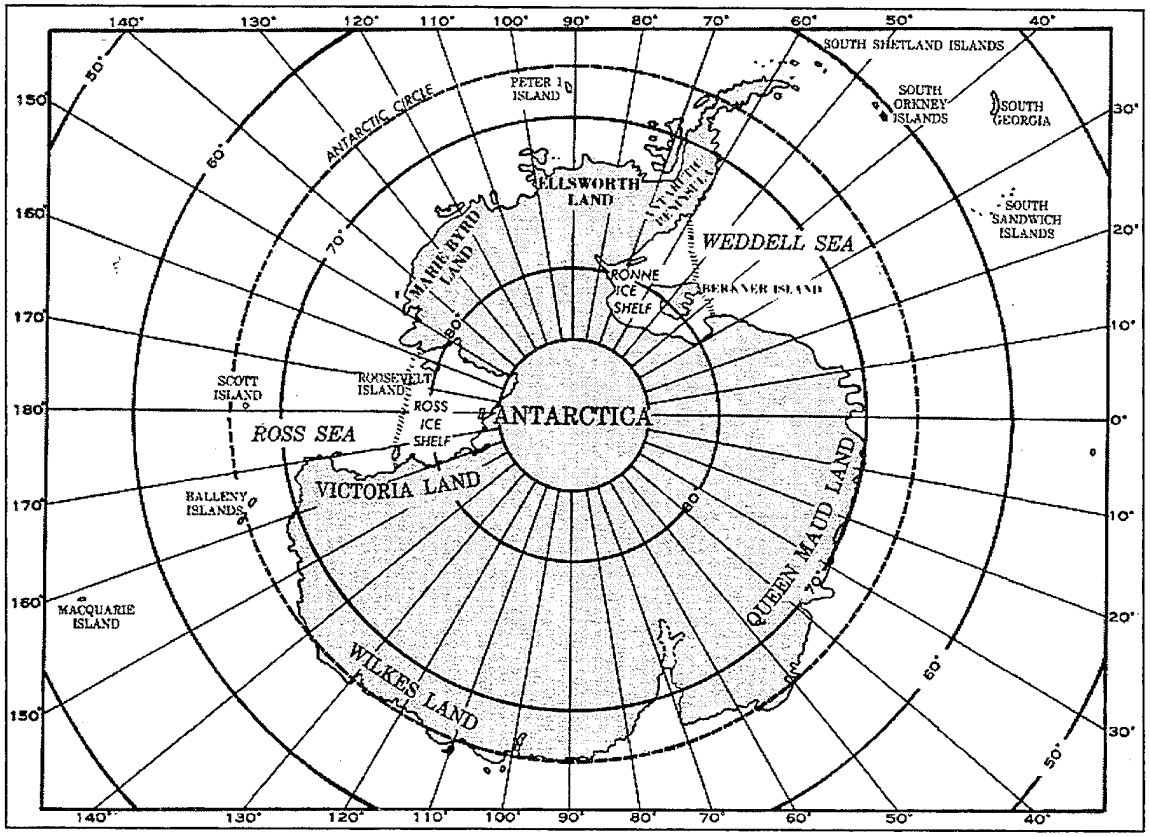

Figure 6-4. General area map of the Antarctic region (Defense Mapping Agency, 1992).

6.5 Antarctica

General Description. The Antarctic is defined by the Antarctic Treaty as the area south of latitude 60°S and thus includes the Antarctic Continent and surrounding waters (figure 6-4). The continent is geographically isolated, with the closest land, Campbell Island, roughly 700 km away. Along with geographical isolation, the exceptionally harsh climate conditions have left this area virtually uninhabited by man. As such, the environment is pristine relative to anywhere else in the world.

Antarctic waters cover approximately $3.6 \cdot 10^7$ km^2. The continental shelves are relatively narrow and deep. Average widths are 30 km while average depths at the shelf edges reach 500 to 900 m, a factor of 2 to 4 times the world average shelf depth (Defense Mapping Agency, 1992). Seaward of the shelf, water depths increase to as much as 5000 m.

Physical Oceanography. The Antarctic waters are a sum of the southernmost portions of the Pacific, Atlantic, and Indian Oceans. The Weddell, Bellingshausen, Amundsen, and Ross Seas

are found adjacent to the Antarctic continent. The configuration of land and water permits a circumpolar oceanic flow which is on the order of 10% of the world's seawater (Defense Mapping Agency, 1992). This current moves easterly at approximately 0.5 $m \cdot s^{-1}$, completely encircling Antarctica to depths that may reach the ocean bottom. Smaller gyres from the East Wind Drift current can form in bays such as the Weddell, Ross, and Bellingshausen Seas.

The waters of the Antarctic are cold and dense. Surface water temperatures are almost everywhere less than 2°C and range to -1.9°C moving toward the continent. In the marginal sea areas, salinity typically ranges from 33 to 34 psu. The range in density is 26.5 to 27.5 σ_t.

Antarctic cold water merges with warmer tropical water and downwells beneath the warmer waters at the Antarctic Convergence. The Antarctic Convergence separates the heavier, colder Antarctic water to the south from the lighter, warmer but more saline water to the north. The boundary lies at about 50°S in the Atlantic sector, and between 50°S and 60°S in the Pacific sector marked by steep horizontal temperature and salinity gradients at the surface waters (Defense Mapping Agency, 1992). North of the Antarctic convergence, salinity changes little during the year. South of the convergence, melting of sea ice during spring and summer causes a great deal of variation in surface waters. Melting pack ice may produce local areas of low salinity (33.5 to 33.8 psu). Pack ice may form as far as this boundary, although this is rare.

Between the Antarctic continent and the Antarctic Convergence, a zone of upwelling is found known as the Antarctic Divergence. This is an area of significant biological activity (Defense Mapping Agency, 1992). More than half of the world's ocean bottom water originates here as a result of ice formation when dense seawater sinks to the ocean bottom and moves northward. Seasonal pack ice forms from the freezing of seawater, varying in areal coverage by several fold between summer and winter. The maximum extent of the pack ice varies from 17 to $20 \cdot 10^6$ km^2. In the spring and summer months the ice recedes south to the coastline. In February the pack ice reaches a minimum coverage varying from 2.4 to $5.1 \cdot 10^6$ km^2 (Glasby, 1990). In addition to being an important influence on world climate conditions, pack ice provides habitat for many seals and penguins.

Chemical Oceanography. Nutrients are not limiting factors affecting productivity in most of the Ross Sea and McMurdo Sound. Dissolved inorganic phosphates, silicates, and nitrates are abundant all year due to vigorous circulation, particularly of upwelled deep water. The concentrations relative to temperate waters are high (Keys, 1984). However, localized depletion of nutrients can occur at the ice edge during spring melting when intense biological activity ensues (Lizotte and Sullivan, 1992). A high degree of oxygen saturation is observed in Antarctic surface waters as a result of the high degree of vertical convection (Gordon, 1971). The amount of saturation typically decreases as a function of depth from as much as >100% to between 50 and 60%.

Suspended sediment concentrations in the Ross Sea and McMurdo Sound are typically between 2 and 4 $mg \cdot L^{-1}$. These concentrations can increase substantially in near-shore areas during the summer and fall from meltwater stream input (Keys, 1984) and in areas of upwelling. The depth of 1% irradiance level was observed to vary from 35 to 109 m as a result of changing phytoplankton biomass (Tilzer et al., 1994).

Ecology. Primary production measurements made in recent years clearly demonstrate that the highly productive Antarctic waters are the result of inshore waters and not oceanic regions

(El-Sayed, 1977). Average primary production rates for the region at 0.134 $gC \cdot m^{-2} \cdot d^{-1}$ (Holm-Hansen et al., 1977) along with light limited conditions through half the year suggest the term high productivity needs qualification.

As mentioned above, the Antarctic Divergence upwelling creates an area of high biological activity. During the summer, 24 hours of sunlight and the high nutrient levels produce a high degree of primary productivity, particularly in coastal regions and along the ice edge areas. A short food web is focused on krill as the key species which provide the link between primary productivity and marine mammals and birds. Krill comprise approximately half of the standing crop of zooplankton. Estimates of the krill standing crop vary from $125 \cdot 10^6$ to $6 \cdot 10^9$ mt with densities reaching 33 kg m^3. From primary production estimates, a standing crop of 250 (annual average) to $600 \cdot 10^6$ mt (summer average) may exist (Defense Mapping Agency, 1992).

The size and density of Antarctic krill (*Euphausia superba*) allows economically practical harvesting by man at approximately 80,000 to 90,000 mt y^{-1} (Defense Mapping Agency, 1992). Since krill are at the center of the Antarctic food web, their abundance directly effects the higher levels of multiple predators. Krill may be considered a sensitive species by virtue of their numbers and position in the Antarctic food web, and thus, pollution detrimental to their existence must be controlled.

Other zooplankton such as copepods, amphipods, and chaetognaths are not considered as important as krill in the Antarctic food web, possibly due to a more dispersed distribution. Squid and fish occupy a level between krill and top mammalian and bird predators. Squid may be considered a potential fishery due to their concentration near the Antarctic Convergence. Fish stocks are generally not a likely harvest resource as they do not apparently occur in sufficiently dense pelagic aggregations. Environmental knowledge of Antarctica remains incomplete, however. Knowledge of interaction between sea ice and the marine ecosystem, between marine ecosystems and terrestrial ecology, and the extent to which components of the marine ecosystem are vulnerable to pollution remains inadequate (Glasby, 1990).

Vessel Traffic. Shipping is most frequent in the Drake Passage between Antarctica and South America. Vessels too large to pass through the Panama Canal, such as commercial oil tankers, use this route. Passage is usually north of the Antarctic Convergence. Tour cruise ships visit the Antarctic Peninsula during summer, typically to areas where bird rookeries and seal colonies are located (Defense Mapping Agency, 1992).

Pollution Status. Limited anthropogenic impacts have occurred in the past with the exception of harvesting of mammals such as whales and seals. Current scientific activities and tourism also have little impact on the marine environment. Impacts previously noted were local. For example, a small number of birds and seals are lost to scientific collecting. Other activities such as helicopter overflights and foot expeditions are restricted (Defense Mapping Agency, 1992). These activities are now either regulated or the species are protected by legislation.

Water quality has been detrimentally affected on a local scale by garbage disposal, sanitary wastes, and solid wastes in coastal waters. Small oil spills from vessel traffic may threaten the health of local biota (Defense Mapping Agency, 1992). Antarctic organochlorine environmental contamination at extremely low levels has been recorded from sources of human activity outside of Antarctica. Impacts from these contaminants are not known. Organochlorine compounds such

as DDT and PCB's have been found in krill, although at concentrations that do not pose a human health hazard (Defense Mapping Agency, 1992).

Seaborne litter is present at the Subantarctic islands, being most frequent on windward shores and least frequent on leeward shores. This pattern is also seen in the semienclosed waters of Port Ross in the Auckland Islands (Glasby, 1990). A land-based origin of the litter is unlikely, since the islands are nature reserves with permit restricted entry. The composition and country of origin of the persistent synthetic litter indicates that it is introduced by commercial fishing activity.

7.0 OPERATIONAL PROFILES

7.1 Methods

The CNO archived database contains vessel traffic information in specified regions throughout the world. This database, entitled employment schedule (EMPSKD) data, is obtainable in classified form from the Officer in Charge, CNO of the World Wide Military Command and Control System (WWMCCS) Operations Support Detachment (N311ND). As part of this study, records were obtained for four Special Areas: the North Sea, the Baltic Sea, the Mediterranean Sea, and the Wider Caribbean Basin. CNO has no EMPSKD data for the Antarctic area because Navy ships do not routinely travel there.

The EMPSKD database was searched using a DBASE IV browser by the NRaD Liaison Office. The search parameters were designed to include all ship operations within each sea by year, for the years 1984 through 1993. The results were broken down to include the ship class, port of call, and number of days at sea within each Special Area. All in-port days were excluded from the results.

Using estimates of the number of crew per ship type and the solid waste generation rates per crew member (NAVSEA, 1993), estimates of mass loadings to each Special Area resulting from U.S. Naval operations were calculated.

In addition, the NRaD Liason Office assisted with basic information on ships complements and vessel traffic patterns, the Center for Naval Analysis (CNA) assisted with data on battlegroup configurations and current operational trends, and CSNSWC Annapolis Detachment, as well as NAVSEA, assisted with Navy discharge practices and planned equipment configurations and operations.

7.2 Results

Operational trends for U.S. Navy vessels have been reviewed in each of the Special Areas delineated in this report. These areas include the Baltic Sea, the North Sea, the Mediterranean Sea, the Wider Caribbean Basin, and the Antarctic region. Some data are presented for the Persian Gulf areas as well because it was available from the CNA. However, that region as a whole will be addressed in a subsequent report. These results include man-loadinging estimates in the Special Areas for the years 1984 through 1993, predications of average man-loadinging given historical estimates, assumptions on vessel traffic patterns, current and proposed Navy discharge practices, predicted equipment operations on various ship classes, and CNA operational analysis results which included basic battlegroup configurations in seas of interest.

Table 7-1. Estimates of yearly man-loadinging in each of the Special Areas from 1984 to 1993. Estimated average yearly man-loadinging for four Special Areas was derived from historical EMPSKD data using days-at-sea for the vessel classes multiplied by published man-loadinging figures for that particular vessel type. The Antarctica is not included because CNO has no historical data for that region.

YEAR	BALTIC	NORTH	MEDITERRANEAN	CARIBBEAN
1984	15,803	57,205	3,886,761	2,666,037
1985	34,444	32,494	3,769,876	2,805,352
1986	44,842	55,622	4,080,554	2,331,005
1987	9,590	32,417	3,462,308	2,359,215
1988	27,963	52,629	2,603,916	2,772,279
1989	22,756	13,777	3,574,395	2,673,288
1990	18,251	13,429	2,949,366	3,436,550
1991	13,260	7,270	3,456,390	2,048,381
1992	17,370	4,894	3,016,463	2,438,000
1993	25,467	53,280	3,573,470	1,973,116
AVERAGE	23,000	32,300	3,437,000	2,550,000

Estimated average yearly man-loadinging for four Special Areas was derived from historical EMPSKD data using days-at-sea for the vessel classes multiplied by published man-loadinging figures for that particular vessel type. The Antarctic is not included because CNO has no historical data for that region. There is little, if any, Navy vessel traffic, with only an occasional Military Sealift Command (MSC) vessel transiting on support missions. The Navy did support research activities in the area, and still does have a Naval Support Force Antarctica (NSFA) based out of Port Hueneme, CA, but they are scaling down support and conduct air, rather than sea, operations. According to verbal communication with NSFA, all solid waste is shipped out of Antarctica on commercial vessels contracted by the National Science Foundation (NSF), which conducts most of the research there. No solid waste is discharged in the area, and although one can theoretically predict an environmental impact if discharges were made, there are no substantiating mass loading figures to work with. The results of the historical yearly man-loadinging estimates, as well as the averages used for predictive purposes in this study, are presented in table 7-1.

There is far greater U.S. Navy ship traffic in the Mediterranean Sea and the Wider Caribbean Basin than the Baltic and North Seas. Currently, the more operationally important Special Areas are the Mediterranean Sea, the Wider Caribbean Basin, and the Persian Gulf areas. These areas have not been enforced as Special Areas to date, however, the Baltic and North Seas have implemented their status as Special Areas, and there is currently no U.S. Navy solid waste being discharged in those regions. This is also true of the Antarctic region.

The rounded averages shown in table 7-1 have been used to determine average mass loading estimates for the bulk pulped and shredded material, and for estimating typical analytical measures such as chemical oxygen demand, biochemical oxygen demand, and nutrient loading. These man-loadinging estimates, based on historical data, can be used to predict future loading.

However, operational patterns vary with time around the world depending on political events, therefore these numbers should be considered "order of magnitude" estimates. Time and resources have not allowed for detailed statistical review of ship traffic to date, however, site specific analysis can be approached theoretically using typical operational scenarios.

In general, U.S. Navy ship traffic tends to be spatially dispersed (verbal communication, Paul Speer, CNA). Even if ships are traveling between the same ports, over time they most likely choose somewhat different routes or participate in exercises which bring them to varying areas. It is reasonable to assume that their discharges are spread within a region rather than accumulating in one spot or path. In gross terms, mass loading can be approached as a basin-wide effect. There are exceptions to this, however, particularly in instances where there is a designated test range that is used commonly, or a specific event such as an invasion force that brings several ships to one location for a period of time. In these instances, one cannot consider the discharge to be regional or basin-wide, but rather local, and accumulation in a relatively small area must then be considered. In recent years there have been a few such events in the Caribbean region, in the Persian Gulf, and in parts of the Mediterranean Sea.

CNA has been tasked to study SSWD with respect to zero discharge. They have analyzed current solid waste discharge issues, including operations in Special Areas, solid waste generation, potential shipboard retention, and the possibility of retrograde. The following pertinent information was presented by CNA (February 1994) and discussed in subsequent conversations. The Navy has a significant solid waste discharge problem in certain operationally important areas such as nearshore off of Haiti, or in small sea operations such as the Adriatic Sea. This makes it necessary to practice retention/retrograde today. Although the Baltic and North Seas are not as operationally important, vessels in those areas also experience the hardship of retention/retrograde because they are not currently discharging their solid waste. The main issue is the number of days between ports where shore services can be obtained. Using snapshots of data for the years 1988 and 1993, it was found that, in general, there is no evidence that underway periods are shorter now than during the Cold War. To the contrary, it appears that where transits of 1 to 7 days used to be more common, there are fewer in the 1 to 7 day range and more of higher duration, even as high as 25 days or greater depending on ship class. There may be fewer vessels at sea at any one time, but the duration does not appear to be decreasing. This creates a significant solid waste handling issue when it cannot be discharged overboard, and according to CNA there is no evidence that solid waste retention is getting any easier. This will be addressed in detail in the CNA Zero Discharge Analysis Report, where documentation including retention volume figures for various numbers of days at sea for several ship classes is provided. These data support our estimates of potential discharges, and the overall mass loading to the environment. In addition, they provide general scenarios where the potential local environmental impact may be assessed. Typical battlegroup configurations for the three most important Special Areas are presented below; these data are representative of operations in 1993, although they change over time. The various ships assigned to a region are not always transiting at the same time; at-sea man-days/year estimated in this study will be lower than the vessel complement sums.

MEDITERRANEAN SEA - 6TH FLEET

Generally, battlegroups operate with an aircraft carrier and support ships, some of which are full-time and others which are on a "tether" within a distance of the main group. A typical battlegroup consists of full-time:

1 CV/N

1 6th Fleet flagship (AGF)
2 combatants
1 ARG (LPD, LSD and LHA or LHD or LPH)
1 T-AFS
1 AS
1 AD
4 SSN's
And on tether:
6 combatants
1 AOE

WIDER CARIBBEAN BASIN
Permanent deployments are generally counter-drug forces including:

3 combatants
2 T-AGOS

In addition, there are several exercises conducted in the Wider Caribbean Basin each year.

PERSIAN GULF AREAS - NAVCENT
1 CV/N
5 combatants
1 T-AO
1 T-AFS
And on tether:
3-4 combatants
1 ARG (LPD, LSD and LHA or LHD or LPH)

The Navy currently practices a variety of ways to process solid waste. Depending on the area and the vessel, various methods such as compaction, incineration, retention, retrograde, or discharge may be used. Prototypes of equipment, proposed as the interim solid waste processing suite, are currently installed for testing purposes on the USS *George Washington* and the USS *Theodore Roosevelt*, and plans are being made for other test platforms. Eventual plans are made for installing the equipment (plastics processor, pulpers, and shredder) on all commissioned vessels by 1998, with the exception of a few smaller classes of vessels which will retain material in "odor barrier" bags if possible, and a number of post-1998 installations scheduled during new construction (NAVSEA, 1993).

Because of varying size and throughput requirements, there will be two pulper sizes. The larger vessels (CV/N class generally) will have more than one of each of the processors on board. The planned equipment mix and concepts, production and installation schedule, processing rates and duration, equipment design mission duration by class, and other details are provided in the solid waste program plan (NAVSEA, 1993). The equipment parameters vary widely for different ship classes. For instance, hours of operation for the shredder range from 0.1 to 2.8 per day, for the large pulper they range from 1.0 to 10.8 per day, and for the plastic processor they range from 1.5 to 12.2 per day. This, of course, is dependent upon man-loadinging, waste generation, and equipment mix. It is beyond the scope of this study to delve into the details found in the NAVSEA plan. However, of specific interest are the FFG and CVN classes because they provide a range for extremes of solid waste generation. In addition, these two classes were useful because they have been fully characterized for modeling purposes. Later, in the Analysis

section, an operational scenario will be addressed using several ship classes, and the waste generation and equipment parameters will be discussed in more detail for those particular vessels.

The FFG class, with a full complement of 220 persons, will have 1 shredder, 1 small pulper, and 1 plastics processor. Daily hours of operation are 0.2, 3.8, and 1.5, respectively. Waste generation in lbs/day is as follows: metal/glass-119, paper-244, food-266, and plastic-44. At the other extreme, the CVN class with a full complement of 6286 persons, will have 2 shredders, 3 large pulpers, and 7 plastics processors. Daily hours of operation are 2.8, 7.1, and 6.0, respectively. Waste generation for this class in lbs/day is as follows: metal/glass-3394, paper-6977, food-7606, and plastic-1257 (NAVSEA, 1993). The number of each equipment type may change as plans are further refined, but they provide an overall basis from which to determine mass loading, to simulate discharge and dispersion dynamics, and to discuss possible effects on the environment.

8.0 PULPER WASTE STREAM CHARACTERIZATION

Two types of pulper samples were obtained from the prototype small pulper system run at CDNSWC/AD. The first set was obtained in July 1994. The samples were mixtures of various pulped paper materials and Severn River water. The mixtures included: 1) all white office paper, 2) all cardboard (nonwaxed), 3) an equal mixture of white paper, magazines, and newspaper, 4) an equal mixture of white paper, cardboard, magazines, and newspaper, and 5) background river water. The samples were collected in cleaned 20 L polyethylene carboys, frozen, and shipped overnight to NRaD. The samples were kept frozen until they were split into 1 L containers prior to analysis.

The second type of pulper samples came to us as bulk pulped material that had been dewatered such that the wet/dry ratio was approximately 6:1. This material was received in January, just prior to field work (GAR1). This material was kept frozen until used in field work and further chemical and biological analyses.

8.1 Chemical Analyses

8.1.1 Methods

Pulper samples were analyzed for conventional chemical constituents and components that might be considered harmful contaminants. The first set of measurements included Total Organic Carbon (TOC), five-day Biochemical Oxygen Demand (BOD_5), Chemical Oxygen Demand (COD) Total Solids (TS), Total Kjeldahl Nitrogen (TKN), Total Phosphate as phosphorus (PO_4), Nitrate plus Nitrite as nitrogen (NO_3+NO_2), and Ammonia as nitrogen (NH_3). The second set of measurements included the List of 126 Clean Water Act (CWA) Section 307(a) Priority Toxic Pollutants. All chemical analyses were performed by Analytical Technologies Inc. (ATI), utilizing Environmental Protection Agency (EPA) methodologies or equivalent methods. Quality assurance and quality control such as reagent blank, blank spikes, matrix blanks, and method detection limits were performed in accordance with the specific EPA method guidelines.

The chemical analyses were performed on three separate batches of samples. The first batch of samples, sent out on 17 August 1994, included four replicates of each sample type. The samples were prepared for analysis by thawing, and then blending the water/paper mixture for 30 seconds to homogenize the samples as requested by ATI. The first batch of samples was analyzed for TOC, BOD_5, TS, COD, TKN, and PO_4. The four replicate samples were denoted with a "-1" through "-4" suffix with the following sample identification numbers:

P1 Background Severn River water
P2 All white office paper
P5 All cardboard (nonwaxed)
P6 Equal mixture of white paper, magazines, and newspaper
P8 Equal mixture of white paper, cardboard, magazines, and newspaper

Sample material left over from the 20 L carboys was placed into a number of 1 L containers (uniquely designated with a suffix "-1" through "-n" and maintained frozen until further analysis).

The second batch of samples, sent to ATI on 27 January 1995, included a single sample of each of the samples as designated above: P1, P2, P5, P6, and P8. These samples were analyzed for NH_3, NO_3+NO_2, and PO_4.

The third batch of samples sent to ATI (7 June 1995) was composed of the bulk dewatered pulped paper. These samples were analyzed for EPA priority pollutants.

Table 8-1. Conventional chemistry results for pulper samples obtained from the prototype small pulper at CDNSWC/AD. Concentrations are in $mg \cdot L^{-1}$ except for TOC values which are in percent by weight.

Sample ID	*Sample Type*	*BOD_5*	*COD*	*PO_4*	*TKN*	*NO_3+NO_2*	*NH_3*	*Solids*	*TOC*
P1-1	River Water	<5	344	0.11	1.10	-	-	7210	0.02
P1-2		<5	383	<0.1	1.10	-	-	7360	<0.01
P1-3		<5	295	<0.1	1.30	-	-	7250	0.02
P1-4		<5	310	<0.1	1.30	-	-	7020	<0.01
P1-5		-	-	<0.1	-	0.14	<0.2	-	-
P2-1	White Paper	365	196	0.16	2.50	-	-	9510	0.15
P2-2		340	595	0.31	2.20	-	-	9980	0.12
P2-3		343	501	0.32	1.30	-	-	10100	0.22
P2-4		273	3500	<0.1	1.40	-	-	10400	0.16
P2-5		-	-	0.19	-	0.43	<0.2	-	-
P5-1	Cardboard	187	569	<0.1	1.90	-	-	9650	0.20
P5-2		193	1550	0.11	2.30	-	-	10400	0.11
P5-3		125	221	<0.1	2.60	-	-	9160	0.11
P5-4		167	753	<0.1	2.60	-	-	8970	0.16
P5-5		-	-	0.15	-	0.15	<0.2	-	-
P6-1	Mixed Paper	63	1300	0.39	2.80	-	-	10400	0.10
P6-2		222	344	<0.1	2.50	-	-	9900	0.25
P6-3		153	993	0.22	2.90	-	-	10500	0.24
P6-4		88	151	<0.1	2.20	-	-	9920	0.25
P6-5		-	-	0.21	-	0.16	<0.2	-	-
P8-1	Mixed Paper	135	245	0.37	2.30	-	-	11700	0.30
P8-2		280	202	<0.1	3.10	-	-	12100	0.27
P8-3		311	212	0.52	2.60	-	-	11700	0.58
P8-4		186	151	0.29	3.90	-	-	11500	0.27
P8-5		-	-	0.43	-	<.05	<0.2	-	-

8.1.2 Results

Results of the chemistry analyses performed on the pulped material slurries provided by CDNSWC/AD are shown in tables 8-1 and 8-2. The original data reports from the laboratory are in appendix A. Concentrations in all tables are reported in $mg \cdot L^{-1}$ except for TOC which is reported as percent. table 8-1 shows all the data for the measured parameters BOD_5, COD, PO_4, TKN, NO_3+NO_2, NH_3, TS, and TOC. Data are presented for both the background river water used to make the slurries, as well as for the pulped-paper/water slurry mixtures using various paper compositions. As such, the pulped-paper/water slurry data represent the combined amounts found for both the water and paper material.

Table 8-2. Averaged conventional chemistry results for pulper samples obtained from the prototype small pulper at CDNSWC/AD. Concentrations are in $mg \cdot L^{-1}$ except for TOC values which are in percent by weight. Concentrations in the bottom row have been normalized to particle mass by dividing the average concentration of the constituent by the background corrected solids content. BC=background corrected data.

Sample Type	BOD_5	COD	BC COD	PO_4	BC PO_4	TKN	NO_3+NO_2	NH_3	Total N	BC Total N	Solids	BC Solids	TOC	BC TOC
River Water	<5	333	-	0.11	-	1.20	0.14	<0.2	1.34	-	7210	-	0.02	-
White Paper	330	1198	865	0.25	0.14	1.85	0.43	<0.2	2.28	0.94	9998	2788	0.16	0.14
Cardboard	168	773	440	0.13	0.02	2.35	0.15	<0.2	2.50	1.16	9545	2335	0.15	0.13
Mixed Paper	132	697	364	0.27	0.16	2.60	0.16	<0.2	2.76	1.42	10180	2970	0.21	0.19
Mixed Paper	228	203	0	0.40	0.29	2.98	<.05	<0.2	2.98	1.64	11750	4540	0.36	0.34
Average	**214**	**718**	**417**	**0.26**	**0.15**	**2.44**	**0.25**	**NA**	**2.63**	**1.29**	**10368**	**3158**	**0.22**	**0.20**
% rsd	40%	57%	85%	43%	73%	19%	64%	NA	12%	24%	9%	30%	44%	48%
Normalized to particle mass ($mg \cdot kg^{-1}$):														
	$6.8 \cdot 10^4$		$1.3 \cdot 10^5$		$4.8 \cdot 10^1$					$4.1 \cdot 10^2$				62.7%

Table 8-2 shows the average values for each paper slurry type as derived from the data in table 8-1. Overall averages are shown at the bottom of each chemical parameter column. Included in this table are Background Corrected (BC) values for each of the chemical constituents which are calculated by subtracting the average river water values from the average values for each of the slurries. Thus, the BC values reflect those amounts associated with the pulped material only. These are amounts are 214 $mg \cdot L^{-1}$ BOD_5, 417 $mg \cdot L^{-1}$ COD, 0.15 $mg \cdot L^{-1}$ PO_4, 1.29 $mg \cdot L^{-1}$ N (includes: $TKN+NO_3+NO_2$), 3158 $mg \cdot L^{-1}$ TS, and 0.2% TOC. The variability of the chemical components in the pulped material, expressed as the percent relative standard deviation (standard deviation/mean·100) is also included in the table. These values ranged from 12% to 85% depending on the constituent, and were typically about 42%. The composition of the solid paper portion of the samples can be obtained by normalizing the background corrected concentrations to the amount of total solids. The averages for these values are shown in table 8-2.

The results of the priority pollutant scans (on a dry weight basis) were all below the detection limit of the analyses performed except for zinc at 5.6 $mg \cdot kg^{-1}$, acetone at 1.8 $mg \cdot kg^{-1}$, and a few aliphatic hydrocarbons between C_{16} and C_{20} at 6 $mg \cdot kg^{-1}$. Full results can be found in the data reports included in appendix A.

It appears that the pulped material is mainly composed of organic carbon with very little nitrogen or phosphorous. The ratio of C:N:P (by weight) in the pulped material alone is roughly 2000:1.3:0.15. When this is compared to marine organic matter which has a C:N:P ratio of roughly 41:7.2:1 (Redfield, 1934), it can be seen that the pulped cellulose would be a relatively poor source of carbon because of the lack of corresponding nutrients. This suggests that the material would not be the best source of carbon to marine bacteria, and that degradation would likely be hindered where nutrient conditions were limiting.

Another important observation is that the slurry produced was approximately 0.3% pulped solids by weight. Although slightly less than expected from a pulper run under optimum conditions, this result verifies the expected end-of-pipe discharge conditions in terms of bulk material.

The BOD_5 and COD values, which were 214 and 417 $mg \cdot L^{-1}$, respectively, are another important aspect of the waste stream. The BOD_5 values (normalized to mass of solids) are consistent with published values for cellulose at approximately 0.08 $g \cdot g^{-1}$ BOD_5 (Pitter and Chudoba, 1990) when taking into account the amount of dilution of the slurry (0.3%). They are also relatively lower than those found in sewage treatment effluent not subjected to primary treatment, e.g., 485 $mg \cdot L^{-1}$ (Pyewipe, 1992-1994), although somewhat higher than effluents from treatment works having advanced treatment (Harris County, 1994). However, the COD value normalized to the mass of solids (table 8-2) of 0.13 $g \cdot g^{-1}$ is considerably lower than the theoretical total oxygen demand (TOD) value of 1.18 $g \cdot g^{-1}$ required for complete oxidation of cellulose. This may be due to incomplete oxidation in the COD test as suggested by Pitter and Chudoba (1990).

The amount of organic carbon and relatively high surface area to volume ratio of the particles generated in the pulping process is sufficient to generate the levels of BOD_5 and COD indicated above. It should be noted that although cellulose has the same basic molecular makeup as starch, the BOD_5 of starch is 7 times greater at approximately 0.62 $g \cdot g^{-1}$ (Pitter and Chudoba, 1990). This suggests a substantially lower degradability of the cellulose relative to starch because of structural differences.

The priority pollutant scans suggest that there are no contaminants in the pulped material at any appreciable level. The presence of zinc at 6 $mg \cdot kg^{-1}$ dry weight is a factor of 25 below the Effects Range Low (ERL) threshold for zinc in sediments (150 $mg \cdot kg^{-1}$, Long, et al., 1995), a guideline for concentrations representing minimal toxicity effects. It is also well below the 9608 $mg \cdot kg^{-1}$ screening level guideline for sediments, using Puget Sound Sediment Management Standards (1991), one of the only sources for sediment quality guidelines. The presence of aliphatic hydrocarbons at the low levels observed do not indicate anything other than background values that would naturally be present in the marine environment, and as such, do not constitute a contaminant.

There are no water or sediment quality criteria for acetone. The only hazard criterion available for comparison is the Material Safety Data Sheet value for an oral rat toxicity at 9750 $mg \cdot kg^{-1}$ (LD_{50}), although the source of acetone in this scan is unknown and is relatively common laboratory cross contaminant. Concerning the priority pollutant measurements, it should be kept in mind that the compounds measured may potentially be a result of their presence in the river water used for pulping the material at CDNSWC/AD rather than from the material itself.

8.2 Physical Analyses

8.2.1 Methods

The pulper samples obtained from CDNSWC/AD were analyzed for a variety of physical characteristics including settling velocity, particle size, and density. The settling velocity and density measurements were conducted in-house while the particle size analyses were performed by an outside contractor, Environmental Testing Associates (ETA). A number of the 1 L subsamples were analyzed in these analyses as described below.

Settling Velocities. Settling velocities of pulped paper were determined on three types of samples during five different experiments. Two cardboard subsamples (P5-10 and P5-3), two white paper subsamples (P2-3 and P2-9), and one mixed paper (with cardboard) subsample (P8-10) were used for these experiments. The experiments were run by dumping a sample into a three-meter high, 9.8 cm diameter settling column filled with fresh water of known density. Various fractions of the paper material were collected as a function of time in removable cups at the bottom of the column. The fractions collected were then weighed and their densities determined as indicated below.

The general design of the settling experiments was as follows. Prior to the start of an experiment, the sample volume, its temperature, and the water column temperature were measured. Samples were then poured into the top of the three-meter settling column at time zero. At various time intervals described below, valves situated at distances of 300 cm (Valve 1), 255 cm (Valve 2), and 209 cm (Valve 3) from the top were closed, thus isolating the material into separate fractions. The material collected below Valve 1, designated Fraction 1, fell 300 cm in the time interval measured. The material below Valve 2, designated Fraction 2, fell 255 cm in the time interval measured. Fraction 3, the material collected below Valve 3, fell 209 cm in the specified time interval. After these three fractions were collected and transferred to other containers, the remaining material was remixed in the column by introducing air bubbles throughout and then allowed to stand overnight for 16 hours. The amount of material collecting below Valve 1 over the 16 hours was then isolated as Fraction 4. The material left suspended

above Valve 1 at that point was collected as Fraction 5. Estimates were made of potential material losses at each of the various transfer steps.

The weight of material settling in Fractions 1 through 4 was determined by transferring it into drying dishes and weighing the dried material. To reduce the volume of water collected within the removable cups, most of the water had to be siphoned off. This was usually done after allowing the samples to stand for at least as long as the original settling interval, to reduce any loss of material within the siphoned water. The samples were then transferred into drying pans (about 200 mL of water left) and allowed to dry overnight. After drying, the samples were transferred to preweighed pans by scraping with a razor blade. The final dried material was then weighed on an electronic balance. Losses at each of the steps were also quantified. The material collected as Fraction 5 was filtered onto a glass fiber filter (1.2 μm nominal pore size) and weighed after drying.

The time intervals chosen for each of the experiments were based on a subjective estimate of how much material appeared to have been collected. The time intervals for white paper experiments were 8, 16, 36, and 960 minutes. The time intervals for cardboard and mixed paper experiments were 4, 12, 32, and 960 minutes. Because the time intervals were discrete and relatively long, settling velocities were calculated using the distance settled divided by the midpoint of the time interval. Thus the actual velocities are only an estimate within the time span of the interval.

Density Analyses. The density of various paper products as well as that of the individual fractions from the above settling experiments was determined using electronic weighing. Individual samples of photocopy (white) paper, cardboard, and newspaper were used to determine bulk material densities, while the material collected from the settling column was used to determine densities specifically from the pulper samples.

Densities were determined using a modified weighing method described in the density analysis kit from Mettler Toledo Inc. The procedure made use of a Mettler model ME33360 density determination kit using a Mettler model AE240 top loading analytical balance. The determination is based upon the principle that the buoyancy of any object is proportional to the volume it displaces and the density of the medium which contains it. Thus the procedure involved weighing a paper sample in air and also while immersed in a liquid of known density, in this case ethanol, to ensure that the particles would be well saturated and sink onto the weighing pan.

The original dry paper samples were split into multiple subsamples for replicate measurement determinations. Each of the subsamples were initially weighed in quantities of approximately the same mass (0.025g). To ensure that all moisture was removed, these preweighed paper subsamples were dried in aluminum weighing pans at 70°C for 2 hours. They were then stored in a desiccator and allowed to equilibrate to ambient room temperature.

The samples were handled at all times with steel tweezers to avoid contamination from skin moisture or oils. The paper was first weighed in air. It was then removed from the balance. Often, a very small mass of paper material was left behind in the balance weighing pan. Quantitative removal was difficult due to the small size of some of the fiber particles. For this reason the weight of the fibers left behind was also recorded and eventually subtracted from the original air measurement. This correction was usually quite small. Following the weight

determination in air, the samples were immediately weighed while immersed in 100% ethanol. Measurements were not recorded until the weight stabilized and the maximum amount of trapped air was displaced. This occurred after 2 to 20 minutes. The paper was submersed inside a small aluminum bowl with a volume of approximately 3 mL. The temperature of the ethanol was continuously measured with a glass mercury thermometer.

The porous paper samples were well wetted by the ethanol. However it should be assumed that something less than 100% of the trapped air was displaced. The air buoyancy may have caused a systematic error by slightly underestimating the wet weight and thereby slightly overestimating the density.

The paper density at a given temperature was calculated as follows:

$$\text{Paper Density} = [(\text{dry weight})/(\text{dry weight-wet weight})] \cdot \text{density of the liquid}$$

Particle Size Analysis. Particle size analysis was performed by ETA. One-liter subsamples of pulper material P2, P5, P6, and P8 were sent to ETA on 27 January 1995. The samples were analyzed for particle size using both microscopic and settling column techniques. As a result of the physical breakup of the paper material into small pieces, a large range of particle sizes could be visually observed. These ranged from individual fiber fragments to large clumps. Because of the variety in particle sizes and structures, categories of particle "type" were devised to describe them. A naming convention was devised to describe various group structures as follows:

Fiber-paper:	particle with an aspect ratio of ≥5:1
Particle-paper:	particle with an aspect ratio of <5:1 (tightly bound fibers as in original material)
Bundle:	3 or more fibers contacting each other and in a parallel arrangement (loosely bound fibers)
Matrix:	3 or more fibers intersecting each other or attached to a central point (loosely bound fibers)

Microscopic examination involved filtering diluted pulper samples ($1:1.8 \cdot 10^5$), preparing them onto slides, then counting and sizing particles observed under a magnification of 50X. Counting rules were as follows:

1. A total of 100 paper structures greater than 5 divisions (49.5μm) are counted at a magnification of 50X.
2. The largest structure on the first slide analyzed is sized first to account for a negative bias in counting large structures.
3. Fields are established using the "left" edge of a grid line, tabulating every third structure crossing the vertical cross-hair.
4. After every fifth structure counted, the slide is moved to the next horizontal grid square.
5. After every 25 structures counted, a new slide (comprising a different quarter section of the same filter) is counted.
6. All numerical size distribution statistics are based on the arithmetic mean diameter.
7. The estimated mass distribution is based on particle volume (formula for a sphere) in each size category, and does not take into account particle specific gravity.

In the settling column method, a 25 mL aliquot of a pulper sample was diluted to 100 mL then placed into a 175 cm column of fresh water. The accumulation rate of fibers reaching the bottom of the column was determined by measuring time and accumulation height. Particle sizes were then computed employing hydrodynamic equations for settling velocities according to Stokes Law, with a drag coefficient for spherically shaped materials and a material density of 1.5 $g \cdot cm^{-3}$.

8.2.2 Results

Settling Velocities. Settling velocities of pulped paper were determined during five experiments. Individual experiment results are tabulated in tables 8-3 through 8-7. Because of the discrete sampling times utilized (e.g., 4, 12, 32, and 960 minutes), the experiments provide only a coarse settling velocity as a function of mass fraction. Based on the time intervals chosen, settling velocities ranged from 0.4 to 150 $cm \cdot min^{-1}$.

Table 8-3. Results of settling velocity experiment for sample P5-10, cardboard pulp.

Settling Experiment 1

Sample P5-10 White Paper Only
Experiment Run 8/25/94
Starting Sample Temp = ?
Starting Column Temp = 25°C
Column Water Density = 0.99707
Sample Volume = 900
Column Height = 300

Fraction 'FRAC'	Cutoff Time (min)	Fall Distance (cm)	Settling Velocity ($cm \cdot min^{-1}$)	Weight Collected (g)	Percent of Total (%)	Cum Percent Total (%)
1	4.0	300	150.00	0.557	24.85	24.85
2	12.0	255	42.50	0.883	39.41	64.26
3	32.0	209	13.06	0.403	17.98	82.25
4	960.0	198	0.41	0.279	12.42	94.67
5	NA	NA	NA	0.120	5.33	100.00
Totals				2.242	=2.49 $g \cdot L^{-1}$	

Table 8-4. Results of settling velocity experiment for sample P2-9, white paper pulp.

Settling Experiment 2

Sample P2-9 White Paper Only
Experiment Run 8/26/94
Starting Sample Temp = ?
Starting Column Temp = 22.5°C
Column Water Density = 0.9976
Sample Volume = 905
Column Height = 300

Fraction 'FRAC'	Cutoff Time (min)	Fall Distance (cm)	Settling Velocity ($cm \cdot min^{-1}$)	Mass Collected (g)	Percent of Total (%)	Cum Percent 'FRAC' 1-5 Only (%)
1	8.0	300	75.00	0.460	17.28	17.62
2	16.0	255	31.88	1.370	51.47	70.12
3	360.0	209	11.61	0.415	15.59	86.01
4	960.0	198	0.41	0.299	11.22	97.46
5	NA	NA	0.00	0.066	2.49	100.00
"Loss"	NA	NA	NA	0.052	1.96	
Totals				2.663	$=2.94\ g \cdot L^{-1}$	
'FRAC' 1-5 Only				2.611	$=2.88\ g \cdot L^{-1}$	

Table 8-5. Results of settling velocity experiment for sample P5-3, cardboard pulp.

Settling Experiment 3

Sample P5-3 Cardboard Only
Experiment Run 8/30/94
Starting Sample Temp = 21.9°C
Starting Column Temp = 24°C
Column Water Density = 0.9973
Sample Volume = 900
Column Height = 300

Fraction 'FRAC'	Cutoff Time (min)	Fall Distance (cm)	Settling Velocity ($cm \cdot min^{-1}$)	Mass Collected (g)	Percent of Total (%)	Cum Percent 'FRAC' 1-5 Only (%)
1	4.0	300	150.00	0.821	25.26	28.69
2	12.0	255	42.50	1.237	38.05	71.92
3	32.0	209	13.06	0.490	15.09	89.06
4	960.0	198	0.41	0.264	8.10	98.26
5	NA	NA	0.00	0.050	1.53	100.00
"Loss"	NA	NA	0.00	0.364	11.19	
Pan Loss	NA	NA	0.00	0.026	0.78	
Totals				3.251	$=3.61\ g \cdot L^{-1}$	
'FRAC' 1-5 Only				2.862	$=3.18\ g \cdot L^{-1}$	

Weighted average sinking velocity = 63.69 $cm \cdot min^{-1}$
Recovered TSS Amount/Chemical Analysis TSS (Fraction 1-5 Only) = 1.36

Table 8-6. Results of settling velocity experiment for sample P2-3, white paper pulp.

Settling Experiment 4

Sample P2-3 White Paper Only
Experiment Run 8/31/94
Starting Sample Temp = 28.5°C
Starting Column Temp = 24.2°C
Column Water Density = 0.9972
Sample Volume = 934
Column Height = 300

Fraction 'FRAC'	Cutoff Time (min)	Fall Distance (cm)	Settling Velocity ($cm \cdot min^{-1}$)	Mass Collected (g)	Percent of Total (%)	Cum Percent 'FRAC' 1-5 Only (%)
1	8.0	300	75.00	0.641	19.72	20.90
2	16.0	255	31.88	1.437	44.18	67.71
3	36.0	209	11.61	0.464	14.25	82.82
4	960.0	198	0.41	0.423	13.00	96.59
5	NA	NA	0.00	0.105	3.22	100.00
"Loss"	NA	NA	NA	0.183	5.64	
Totals				3.253	$=3.48\ g \cdot L^{-1}$	
'FRAC' 1-5 Only				3.070	$=3.29\ g \cdot L^{-1}$	

Weighted average sinking velocity = 32.40 $cm \cdot min^{-1}$
Recovered TSS Amount/Chemical Analysis TSS (Fraction 1-5 Only) = 1.11

Table 8-7. Results of settling velocity experiment for sample P8-10, mixed paper and cardboard pulp.

Settling Experiment 5

Sample P8-10 Mixed Paper with Cardboard
Experiment Run 9/20/94
Starting Sample Temp = 20.1°C
Starting Column Temp = 26.1°C
Column Water Density = 0.9968
Sample Volume = 925
Column Height = 300

Fraction 'FRAC'	Cutoff Time (min)	Fall Distance (cm)	Settling Velocity ($cm \cdot min^{-1}$)	Mass Collected (g)	Percent of Total (%)	Cum Percent 'FRAC' 1-5 (%)
1	4.0	300	150.00	1.583	35.73	35.73
2	12.0	255	42.50	0.823	18.57	54.30
3	32.0	209	13.16	1.396	31.50	85.80
4	960.0	198	0.41	0.617	13.93	99.72
5	NA	NA	0.00	0.012	0.28	100.00
Totals				4.431	=4.79 $g \cdot L^{-1}$	

Weighted average sinking velocity = 65.66 $cm \cdot min^{-1}$
Recovered TSS Amount/Chemical Analysis TSS = 1.06

Visible particles observed in four of the five experiments reflected rapid sinking material ranging from 108 to 188 $cm \cdot min^{-1}$ resulting in the highest rate observed for the mixed paper sample (experiment 5). The average weight percent of material collected during each of the time intervals for all experiments were: 25.56 %, 40.10 %, 19.52 %, and 12.16 %. These mass fractions correspond to average sink rates of 120, 38.25, 12.48, and 0.41 $cm \cdot min^{-1}$, respectively. The weighted average sinking velocity (average velocity·mass fraction) for all experiments was 48.5 $cm \cdot min^{-1}$. This weighted average sinking velocity ranged from 32 $cm \cdot min^{-1}$ for white paper to 65.7 $cm \cdot min^{-1}$ for mixed paper.

Measurement accuracy of the mass fraction data was checked in two ways in these experiments. Because the methods employed in the experiments resulted in some loss of pulped material during each of the many analysis steps, the losses were estimated by measuring amounts lost in the scraping pans and in volumes decanted or siphoned off during the volume reduction steps. These losses were determined to be generally less than 10%. Losses from scraping pans were determined to be less than 1%, and losses during siphoning and/or container transfers were measured between 2 and 11%. A second way to estimate accuracy was to compare the recovered material in the experiments to the amounts measured by chemical analyses (TS). For all experiments, the average amount recovered in the settling experiments was within ±10% of the amount determined in the TS measurements.

The above analyses provide a key element in understanding the fate of this material in the marine environment. The majority of pulped paper particles sink reasonably quickly. Although not all the material was observed to sink even after a day, the mass fraction likely to remain suspended in the water column is less than 3% based on the average amount of material unaccounted for in the first

four settling fractions. Qualitatively, the largest particles were observed to fall the fastest, while those particles settling the slowest were typically the smallest.

It should be kept in mind that this evaluation was performed on material that had been frozen and well saturated, and thus had undergone physical processes that it would not normally be subjected to. The effect of these processes would tend to increase the likelihood of complete saturation as well as to increase the relative number of smaller particles. The effect of incomplete saturation and creation of smaller particles would manifest itself in slower sinking rates. However, indications from personal observations of the pulped paper effluent suggest that most of the material is indeed well saturated upon discharge and sinks (Drake et al., 1994). The fact that the pulper acts to efficiently wet the material prior to discharge is a very positive result from a sinking point of view. The effect on the size distribution is unknown but is thought to be a minimal effect on the overall distribution.

Table 8-8. Density of white paper and cardboard materials obtained from printed photocopy paper, a new cardboard box, and the pulped paper slurries used in the settling experiments. Densities were determined by weighing the materials drying in air and while immersed in ethanol of known density.

Sample Type	Description	Density (g/cm^3)
White Paper[a]	Printed photocopy paper	1.342
Cardboard[a]	New cardboard box	1.434
White Paper[b]	Printed photocopy paper	1.501
Cardboard[b]	New cardboard box	1.515
Density from Settling Experiment 1		
P5-10 Cardboard	Fraction 1	1.43
	Fraction 2	1.48
	Fraction 3	1.52
	Fraction 4	1.56
Density from Settling Experiment 2		
P2-9 White Paper	Fraction 1	1.59
	Fraction 2	1.92
	Fraction 3	1.56
	Fraction 4	1.51
Density from Settling Experiment 3		
P5-3 Cardboard	Fraction 1	1.46
	Fraction 2	1.54
	Fraction 3	1.51
	Fraction 4	1.47
Density from Settling Experiment 4		
P2-3 White Paper	Fraction 1	1.483
	Fraction 2	1.461
	Fraction 3	1.613
	Fraction 4	1.70
Density from Settling Experiment 5		
P8-10 Mixed Paper	Fraction 1	1.471
P8-10	Fraction 2	1.567
P8-10	Fraction 3	1.318
P8-10	Fraction 4	1.633

Average of all settling experiment density measurements: 1.52 gcm^{-3} ± 8% rsd.

a Determined by weighing dry then immersed in ethanol

b Determined by weighing immersed in ethanol then dry

Density Analyses. The average density of pulped paper, derived from all measurements, was 1.52 $g{\cdot}cm^{-3}$ with a relative standard deviation (rsd) of 8% (see table 8-8). This includes density analyses made on the material used during the settling experiments as well as those from the bulk paper products. The range in densities was 1.34 to 1.70 $g{\cdot}cm^{-3}$. The average for white paper, cardboard, and mixed paper was 1.60, 1.50, and 1.50 $g{\cdot}cm^{-3}$, respectively. The observed differences were not statistically significant (95% confidence level, 6 degrees of freedom). There were no trends observed in the density values determined for each of the four settling fractions. Thus, the density

of material falling the fastest was no different than material settling at slower rates. For purposes of comparison to the density measurements made in this study, the CRC Handbook of Chemistry and Physics (1972) states that cellulose has a density between 1.27 and 1.61 $g \cdot cm^{-3}$. The density measured for this material is sufficiently high enough that density differences found in seawater should be insignificant from a settling viewpoint.

Difficulties in making the density measurements are mainly related to sufficiently wetting the pulped paper. Although the use of ethanol in the analysis was used to enhance the density differences of the paper from the measuring medium, it also appeared to increase the wetting efficiency as well. How fast the pulped paper wets may be an important process in ensuring the material sinks quickly.

Table 8-9. Particle size data based on microscopic analysis. Sizes are the midpoint of the hydrodynamic diameter size bins. Values given in each size bin are the percent of the total number of particles in the sample.

By Particle Numbers (%):

Particle size (μm)	23	47	94	188	375	750	1500
White Paper	8	29	24	18	12	6	3
Cardboard	1	33	29	15	9	12	1
Mix w/o cardboard	7	39	25	16	10	2	1
Mix w/ cardboard	1	34	26	21	12	5	1
Average	4.3	33.8	26.0	17.5	10.8	6.3	1.5
% rsd	88.8%	12.2%	8.3%	15.1%	14.0%	67.1%	66.7%

Table 8-10. Particle size data based on microscopic analysis. Sizes are the midpoint of the hydrodynamic diameter size bins. Values given in each size bin are the percent of total mass of particles in the sample.

By Particle Mass Fraction (%):

Particle Size (μm)	23	47	94	188	375	750	1500
White Paper	0.0	0.0	0.2	1.8	7.9	22.2	67.8
Cardboard	0.0	0.0	0.2	1.2	4.6	44.4	49.5
Mix w/o cardboard	0.0	0.1	0.4	2.5	10.4	18.7	67.9
Mix w/ cardboard	0.0	0.0	0.2	2.1	5.7	19.4	72.6
Average	0.0	0.0	0.3	1.9	7.2	26.2	64.5
% rsd	NA	200.0%	40.0%	28.8%	35.9%	46.8%	15.8%

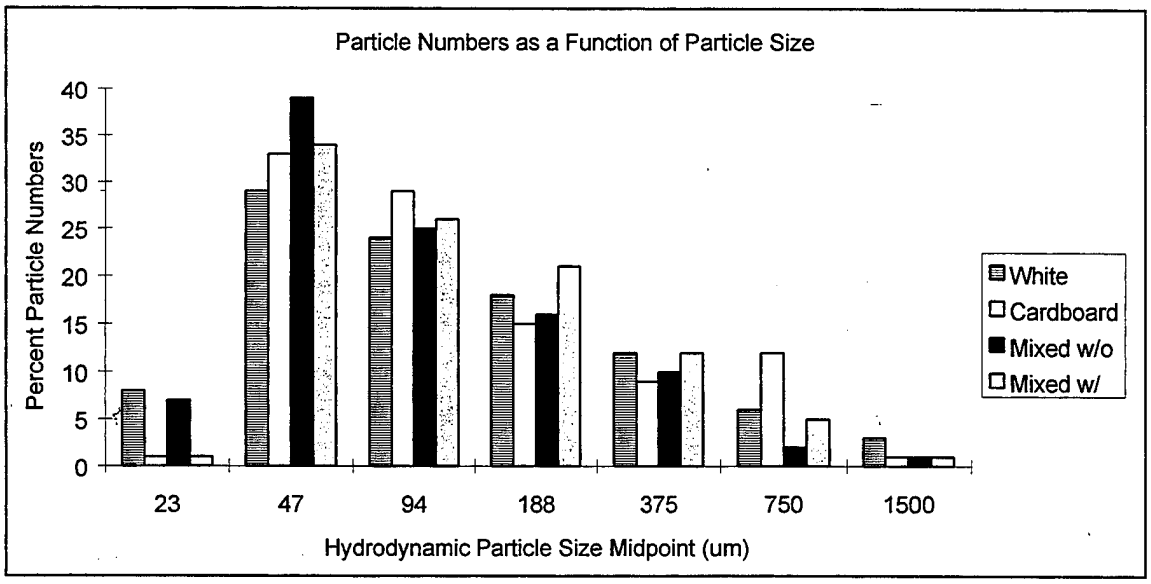

Figure 8-1. Numerical distribution of particles as a function of particle size for pulped white paper, cardboard, mixed paper with (w/) and without (w/o) cardboard based on microscopic analysis.

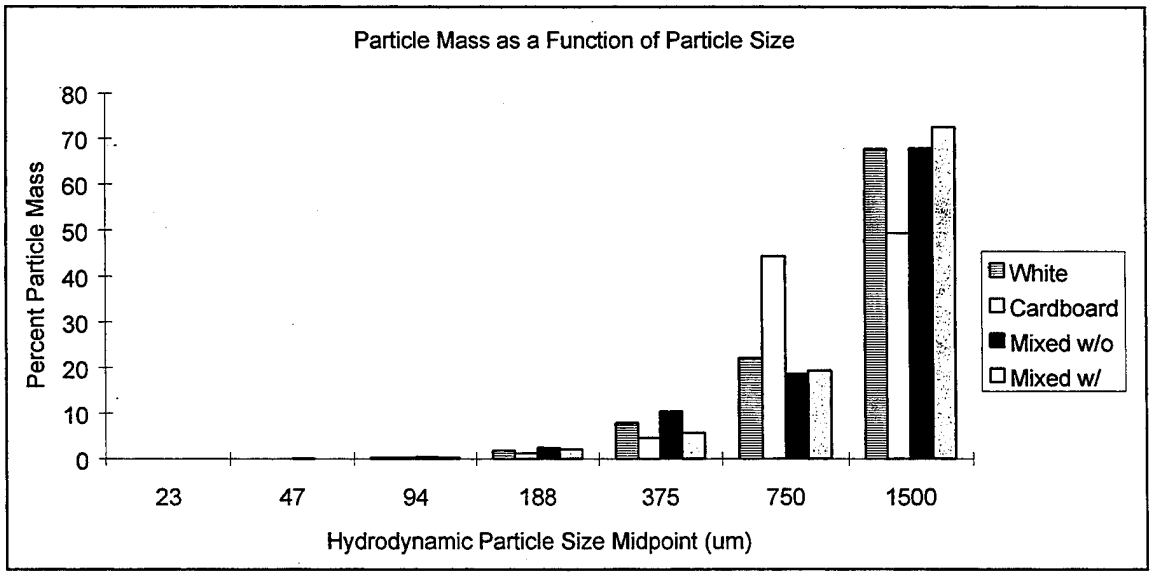

Figure 8-2. Mass distribution of particles as a function of particle size for pulped white paper, cardboard, mixed paper with (w/) and without (w/o) cardboard based on microscopic analysis.

Particle Size Analysis. Particle size data provided by ETA are tabulated in appendix B. The microscopic analysis data are summarized in tables 8-9 and 8-10 and in figures 8-1 and 8-2. Because the paper particles are not spherical, a standard application of Stoke's Settling Law to the

settling column results (see Methods) was not useful for determining particle size. Thus, these data will not be discussed further. Understanding the term "particle size" is difficult because the particles are highly nonuniform in shape. This is a result of the pulping process in which a variety of structures composed of one to many individual fibers are created. Because the paper is made up of long thin fibers, the pulped structures that are formed are composed of criss-crossed fibers forming highly irregular shaped surfaces. Therefore, the size measurements used here require some definition.

The term hydrodynamic size is used here to describe the particles as if they were equivalent spheres. This size determination is most important in assessing transport processes such as settling velocity and dispersion characteristics. The hydrodynamic diameter is defined as follows: ϕ_{hyd} = length·sphericity, where sphericity = $(\text{thickness}^2/(\text{length}\cdot\text{width}))^{0.333}$. Other measures of size such as fiber diameter, or surface area/particle are more important when considering biological interactions as these are the dimensions expected to be "seen" by the organisms. These measures will also be used in the following discussion.

The hydrodynamic particle diameters observed in the microscopic analysis ranged from about 16 to 2000 μm. Although most of the particles were small (94μm and less), most of the mass was contained in the larger particles (see figures 8-1 and 8-2). The mean hydrodynamic diameter for the four samples was 170 μm, while the mean fiber diameter was 21.5 μm. Table 8-10 shows the mass distribution for each of the discrete size bins. The largest size bin (1500 μm midpoint) can be seen to contain most of the mass, typically greater than 65%. The particle surface areas ranged from 0.15 to 0.30 mm^2 and averaged 0.25 mm^2. It again should be pointed out that the particle size analyses were performed on pulped material that had been previously frozen. The expected effect of freezing then thawing the samples would be to increase fiber breakdown. Thus, these results might be slightly skewed toward the smaller sizes, if at all.

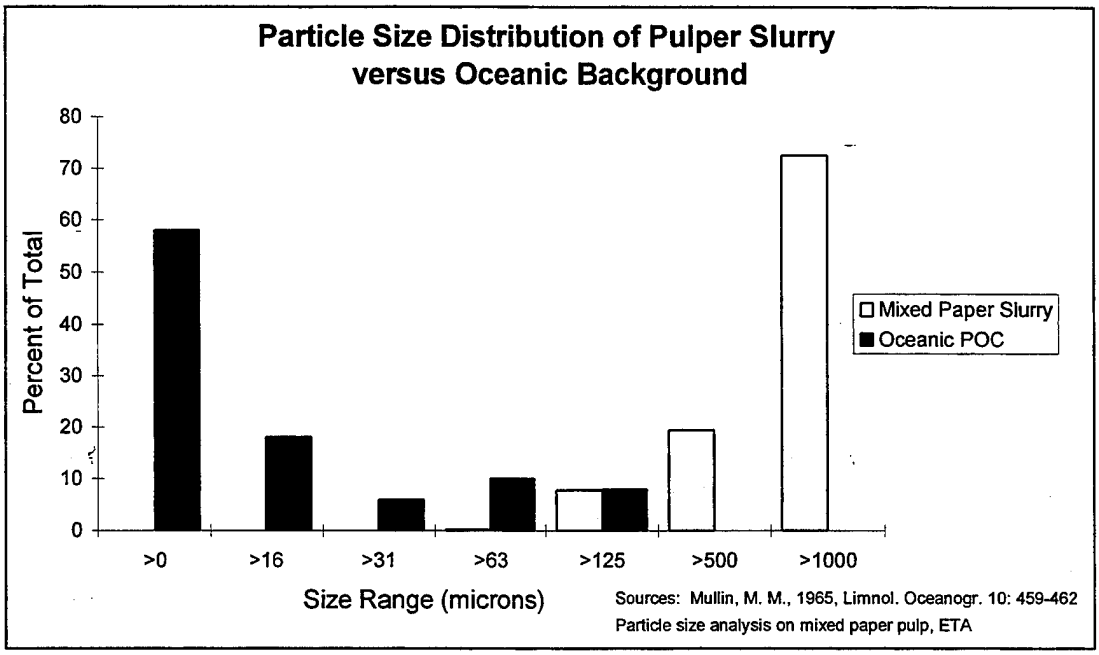

Figure 8-3. Comparative mass distribution as a function of particle size for mixed paper slurry and oceanic background particulate organic carbon (Mullin, 1965).

The particle sizes observed for the pulped material are relatively high compared to background particulate organic carbon in the ocean (figure 8-3). Although there is some overlap around 100 μm, the majority of pulped material (by mass) are particles larger than 1000 μm. The size of particles and their surface area has important implications regarding their fate in the sea. As seen earlier, the larger the particle size, the faster it sinks. Therefore, the pulped paper would fall out of the water column much more quickly than natural particulate matter, indicating that it would have less time to be remineralized in the water column. This along with its more refractory chemical nature would suggest that the majority of the material would likely settle to the sediment without undergoing major changes. The high surface area of the particles make them more susceptible to bacterial colonization. This can ultimately lead to changes in sinking rates by changing the effective size and shape of particles, depending on how fast colonization takes place. This can also lead to higher degradation rates once colonized.

8.3 Biological Interactions

8.3.1 Methods

Measured effects of pulped material on marine organisms were carried out in a variety of ways. Standard EPA and specialized bioassay experiments were performed to determine if there were toxic and/or other deleterious effects of pulped material on a variety of marine organisms. The bioassays were performed using both a particulate-phase (particle and seawater mixtures) and a liquid-phase (elutriate) of the pulped paper. The liquid-phase is based on effects caused only by the soluble components of the material once mixed with seawater. Because bioassay tests range in their sensitivities to specific toxicants, a variety of tests and test species were included for the broadest measure of effects possible. Effects on the feeding habits of ubiquitous marine organisms were also considered because of the potential for pulped material to act as a food source or food substitute.

The tests were designed to look at potential effects in a range of species including bacteria, phytoplankton, zooplankton, pelagic fish, and benthic organisms. These experiments included: Liquid-Phase Bioassays using Microtox, QwikLite, Algae, Mysid and Minnow tests; Particulate-Phase Bioassays using Amphipod and Polychaete Bioassays; Zooplankton Interactions using *Calanus*, *Acartia,* and *Polykrikos kofoidi;* and Clupeoid Feeding Studies using Sardines. The Liquid-Phase Bioassays were performed in-house, while the other experiments were performed by outside agencies. Follow-on work, described in section 14.0, describes plans for future work concerning these and related studies.

Standard methods were employed whenever possible in these analyses to provide a basis of comparison to other work performed in the field. However, much of this methodology is somewhat arbitrary and designed to answer specific regulatory questions or issues. To span both the data comparison issue and the special needs of this project, additional methods and conditions were employed. In particular, bioassays are usually conducted at high concentrations of test solution to generate a dose-response curve that can then be related to expected conditions in the environment. In high enough concentrations, a response can be elicited from most any test solution, and thus it was felt that a more realistic parameter would be the level at which there is no effect from the test solution. Therefore, most tests were run at multiple test solution concentrations to determine a no effects level.

Liquid-phase Bioassays

A series of static-renewal EPA acceptable bioassays, in addition to a suite of Microtox and QwikLite Bioluminescence Assays, were conducted to estimate the potential effects of elutriates of the pulped paper material. The materials were tested with mysid shrimp (*Mysidopsis bahia*), the minnow (*Menidia beryllina*), the bioluminescent dinoflagellate (*Gonyaulax polyedra*), the bioluminescent bacteria (*Photobacterium phosphoreum*), and the marine chain diatom (*Skeletonema costatum*, clone "Skel"). The marine diatom was used for the chlorophyll assays. Bioassay organisms representing different phyla were chosen and tested where a toxic response found might represent a potential "risk" to the marine environment. *M. bahia* was chosen because it represents a species that is found both in the water column and on sediments, while the minnow *M. beryllina* was chosen to represent a pelagic or swimming species. The phytoplankton chain diatom species and the dinoflagellate were used to observe any potential effect on primary producers in marine waters. The endpoints measured were survival in the mysids and minnows (LC_{50}), inhibition of bioluminescence of *G. polyedra* (IC_{50}), inhibition of lumnescence in *Photobacterium phosphoreum* (EC_{50}) bacterium (IC_{50}), and biomass or chlorophyll fluorescence inhibition (IC_{50}) in the diatom tests. In all cases, an attempt was also made to determine a No Observable Effects Concentration (NOEC). The original report and data for each of these experiments is presented in appendix C.

Test Equipment Preparation for Mysids and Minnows. All test chambers were constructed from borosilicate glass beakers with lids. All beakers were washed with a critical cleaner and rinsed with 10% nitric acid. Three deionized water rinses followed each cleaning procedure. All acute toxicity tests with the mysids were conducted in 300 mL beakers with 200 mL of dilution water. The minnows were maintained in 400 mL beakers with 250 mL of dilution water. The diatom assay required 125 mL Erlenmeyer flasks containing 25 mL of test solution. The bioluminescent assays used spectrophotometric grade cuvettes containing approximately 3 mL of test solution.

Source and Acclimation of Test Species. Several days old *M. bahia* and *M. beryllina* were acquired from Aquatic Indicators, St. Augustine, Florida, by overnight mail. Both the mysids and minnows were slowly acclimated in a 25°C water bath and transferred by pipette to several holding tanks with filtered (0.45μm) seawater. The dilution water used in testing was obtained from the NCCOSC Biological Effects Program bioassay facility located near the mouth of San Diego Bay. Water was filtered through a coarse sand filter prior to final filtration (0.45μm). The test animals were slowly acclimated to the test water salinity of 33 parts-per-thousand over several days. All test animals were fed daily with freshly hatched *Artemia* brine shrimp.

The marine diatom, *S. costatum* (clone "Skel") was obtained from the UCLA, Hopkins Marine Station. The cultures were maintained on an enriched seawater medium (ESM) using filtered (0.20 μm) seawater. Raw seawater was collected from the Scripps Institute of Oceanography pier pump system in La Jolla, California. Aliquot samples of the stock were routinely placed into fresh media to maintain high cell densities. The diatoms were cultured at room temperature (~25°C) under cool white fluorescent bulbs at a light intensity of approximately 4000 lux for 12 hours per day.

Seawater Extraction of Pulped Paper Materials. Test solutions were attained by leaching the pulped paper material in filtered seawater for 1.5 hours. This was done with a 30 minute mixing period followed by a 1 hour settling period (Elutriate Preparation, EPA protocol, 1991).

A 25% elutriate was prepared (EPA protocol, 1991) by subsampling 1 L of filtered seawater exposed to 250 g of the homogenized material (1:4 ratio). This 25% elutriate was then used as the 100% test solution. For testing purposes and to determine a dose-response curve, the 100% test solution was diluted with filtered seawater by half until reaching 6.25%. The test solutions for all assays conducted ranged between 100% and 6.25% elutriate. In cases of expected extreme toxicity, a 5% elutriate was prepared (50 $g \cdot L^{-1}$). A dry:wet weight conversion factor (1:6.3) was used because of the high percentage of water in the material. Additional assays with the paper pulp were conducted to determine a no effect level of exposure using a 0.01% elutriate (0.630 $g \cdot L^{-1}$). The supernatant was carefully removed from the material with the use of a mesh filter. The elutriate resulting from leaching was then used to make dilutions of the test solution. In the first three assays where mysids were exposed to an elutriate of paper pulp, suspended solids were suspected of causing effects. The elutriates were then centrifuged following the leaching procedure. Centrifugation was performed for 7 minutes at 1800 rpm at 25°C on a Damon IEC Centra-8R Centrifuge.

Experimental Test Design and Procedure for *Mysidopsis bahia* and *Menidia beryllina*. These assays were conducted to test for potential effects arising from exposure to the leachates using 96 hour static renewal acute test procedures. EPA test protocols were followed for the mysid and minnow bioassays (U.S. EPA, 1988). For acute bioassays, test chambers used for the mysids and minnows were typically 300 and 400 mL beakers filled with 200 and 250 mL of solution, respectively. The average ages of the animals were 5 and 13 days at the start of the bioassays for mysids and minnows, respectively. Ten mysids and minnows were placed in each beaker with two replicates for each concentration. Each assay began when test species were distributed to test beakers containing 50 mL of filtered seawater (0.45 μm). Specimens were pipetted from holding tanks into test beakers. Test solutions of the appropriate percentage were added to each beaker to a final volume of either 200 or 250 mL. All animals were fed newly hatched *Artemia* brine shrimp daily. The test beakers were covered with glass lids and placed in

a temperature controlled bath at 25°C. Solutions were renewed every 24 hours at which time fecal material was removed and seawater chemistry measurements were recorded. Survival was recorded every 24 hours. Dissolved oxygen, pH, and temperature were measured daily. Minimum requirements for test acceptability for dissolved oxygen are 40% saturation for acute tests. The seawater temperature must not fluctuate more than ±2°C.

Test concentrations of 100%, 50%, 25%, 12.5%, and 6.25% with a seawater control were used for both materials in the mysid acute tests and the minnow acute tests. Percent survival was calculated and graphed. A probit analysis was performed to estimate LC_{50} values, where appropriate. All data were analyzed using TOXIS II and PRODAS statistical programs.

Experimental Test Design and Procedure for Diatom Biomass (Fluorescence) in *Skeletonema costatum* (Clone "Skel"). Prior to testing, monocultures of *Skeletonema* were maintained in ESM in 2 L borosilicate Erlenmeyer flasks under a light regime of 12:12 hours (light:dark) at a light intensity of approximately 4000 lux from cool white fluorescent bulbs. Culture temperature was maintained near 19°C. This bioassay was conducted in accordance with the American Society for Testing and Materials Standard Guide for Conducting Static 96-hr Toxicity Test with Microalgae (E 1218) (ASTM, 1992). At the beginning of each bioassay, 400 mL of diatom stock was introduced into three replicate Erlenmeyer flasks containing a combined 150 mL of leachate and filtered seawater for the controls and different concentrations of the test solution. The dilution water was collected from the pumped seawater system at the pier of the Scripps Institute of Oceanography in La Jolla. All seawater was filtered with membrane filters to 0.2 μm and enriched as the stock cultures. Materials were tested at concentrations of 100%, 50%, 25%, 12.5%, and 6.25% with seawater controls.

The control groups received no test solution leachates and did not exhibit background fluorescence. A Turner model 112 fluorometer was used to measure *in-vivo* fluorescence from the diatom cells. The fluorometer was equipped with a combination T-5 lamp, a red-sensitive photomultiplier tube (R-136), a blue excitation filter (5-60), and a red filter (2-64) to detect fluorescence at wavelengths >640 nm. Chlorophyll *a* fluorescence has maximum emission at 663 nm. The instrument was blanked between readings with filtered (0.45 μm) seawater. All flasks were read within 1 hour after the introduction of the diatoms into the flasks and at 24-hour intervals for a period of 96 hours. The measured fluorescence is directly related to cell number and to the presence of viable diatom cells relative to the leachate concentration. Mean relative fluorescence, standard deviation, and the coefficient of variation were calculated for each control and leachate concentration. Relative fluorescence, calculated as a percentage of control values, was plotted over time during the test.

Experimental Test Design for Microtox (Bioluminescence) Assay. The Microtox Bioassay System is an acute toxicity test utilizing a specially cultured bioluminescent bacteria (*Photobacterium phosphoreum*). The test is employed for the determination of a dose-response curve, from which the inhibition concentration (IC) of test solution causing a specified effect is found. The method measures the effect on the bioluminescent light output of the bacteria as they are challenged by the test solution. Observations of light output are recorded at 5 and 15 minutes of exposure. This test is usually used as a screen test for toxic effects. Three trials of the paper pulp assay were performed with four dilutions and a control. Five minute and 15-minute readings were taken. The EC_{50} was determined graphing the calculated Microtox statistic on log/log paper. Also, the percent reduction of light output at the 100% leachate dilution was calculated.

Experimental Test Design for QwikLite (Bioluminescence) Bioassay System. The QwikLite Bioassay also measures the inhibition of light emitted by the bioluminescent dinoflagellate, *Gonyaulax polyedra*, exposed to a test solution. The test lasts 96 hours and results are expressed as the percent of control in which all dilutions are compared to the controls. Results were reported as the IC_{50} when a dose-response was evident.

Testing of the dinoflagellates was accomplished by placing individual cuvettes containing the test material, media, and cells into a darkened test chamber which was attached to a photomultiplier tube (PMT). The QwikLite bioassay system uses a 2-inch diameter 8575 PMT with an S-20 response used in the photon count mode. The top of the test chamber is removable and houses a small adjustable motor which drives a stainless steel shaft terminating in a plastic propeller. The propeller is seated into the cuvette and as the contents are stirred, bioluminescence is generated and measured by the PMT. Each test period is completed at 24-hour intervals until completion of the bioassay. Mean light output (PMT counts) is calculated for each experimental group and control. Light output means are then graphed as light output (percent of control) as a function of time. All graphs represent the data collected after 96 hours of exposure.

Particulate-Phase Bioassays

Benthic Species Tests. Two species of benthic organisms were tested for potential toxic effects of pulped cellulose. These were the amphipod *Grandidierella japonica* and the polychaete *Neanthes arenaceodentata.* These were selected because 1) they are representatives of polychaetes and amphipods that are important components of most marine benthic communities, 2) there are proven, widely used protocols for laboratory assays with these species, and 3) live animals are available from commercial suppliers. These tests were performed by Coastal Resources Associates (CRA), using their Standard Operating Procedures TS 009.00 and TS018.00 (see appendix D).

The tests performed on both species were similar except for the length of exposure and sediment type. The tests were conducted in two different sediment types: fine sand and silty sand. The organisms were placed into chambers containing uncontaminated sediment and filtered seawater, and then were allowed to acclimate for 1 hour. A stock solution of pulped material (0.1% by volume wet weight) was prepared by diluting the paper slurry provided in filtered seawater. Varying amounts of this stock solution were then slowly poured into each chamber, providing enough pulped material to result in a 0.01, 0.1, and 1 mm layer on the sediment surface. These layer thicknesses were chosen based on highly conservative scenarios in which 100, 1000, and 10,000 aircraft carriers, each pulping at maximum capacity and traveling at 18 kts, discharged onto the same 100 x 1 m area.

The amphipods were exposed for a period of 10 days while the polychaetes were exposed for 96 hours. The chambers were renewed each 48 hours with newly prepared filtered seawater to maintain appropriate water quality parameters. This was done by carefully siphoning off about 80 to 90% of the seawater, then replenishing it so as to not disturb the pulped paper layer. A statistically derived estimate of the concentration of the slurry that is lethal to 50% of the test species exposed (LC_{50}) was then determined from these results. In addition to these analyses, TOC and grain size of the sediments were analyzed to determine if these parameters had any

effects on the results. In all cases replicate samples and analyses were used to obtain appropriate statistical confidence in the results.

Zooplankton Interactions. The effects of pulped material on zooplankton were investigated at SIO. Two types of zooplanktonic copepods, *Calanus* and *Acartia*, were subjected to various concentrations of pulped material to determine its potential effect on feeding. The experiments were designed to test three interaction hypotheses including the impact of feeding in the presence of particles, the ability to recover from any impact of feeding in the presence of particles, and the impact on feeding in the presence of slurry leachate. Four experiments were devised to test the following hypotheses:

> $H_0$1- copepod ingestion rate is independent of the presence of pulper slurry, (experiments 1 and 2);
>
> $H_0$2- ingestion rates of copepods that had been previously incubated with pulper slurry are not significantly different than those never exposed to the slurry (experiment 3); and
>
> $H_0$3- copepod ingestion rates in seawater, which had previously been in contact with pulped slurry for 24 hours then removed by filtration, are not significantly different than in seawater never contacting slurry (experiment 4).

Experimental Organisms And Conditions. The dinoflagellates *Gymnodinium sanguineum* and *Gonyaulax polyedra*, and common copepods *Acartia* spp. and *Calanus pacificus* were chosen for these experiments. *G. sanguineum* and *G. polyedra* are common red-tide dinoflagellates and known as prey for *C. pacificus* and *Acartia* spp. They were grown in enriched f/4 seawater media without silicate at room temperature (20-23°C) with continuous illumination of 100 $\mu E \cdot m^{-2} \cdot s^{-1}$ from cool white fluorescent lights. Cultures in exponential growth phase were used for feeding experiments.

Adult female *C. pacificus* were collected from the coastal waters off La Jolla, California, using a 303 μm mesh net. Adult female *Acartia* spp. were collected from the waters of Mission Bay, California, using a 54 μm mesh net. The copepods were maintained at 15°C in 1 gallon jars with *G. sanguineum* or *G. polyedra* in filtered seawater for at least two days before experiments.

To initiate an experiment, copepods were rinsed with filtered seawater, and 5 healthy female *Calanus* (experiments 1, 3 and 4), or 8 female *Acartia* spp. (experiment 2), were transferred into 500 or 270 mL polycarbonate (PC) bottles, respectively. Three 1 mL aliquots from a *G. sanguineum* or *G. polyedra* culture were counted to determine density, then added to PC bottles in the appropriate concentrations using volume dilution with an autopipette. The wet weight of slurry was measured on a microbalance and added to the appropriate PC bottles to obtain the various concentrations (ratio of wet weight of slurry to weight of seawater). Slurry inside the bottles was not homogeneously distributed, even though bottles were rotated. Duplicate control bottles containing only *G. sanguineum* or *G. polyedra* and duplicate experiment bottles containing *G. sanguineum* or *G. polyedra* and slurry at all slurry concentrations were used in all experiments. Actual initial concentrations of *G. sanguineum* or *G. polyedra* were measured in one extra control bottle by counting and removing more than 200 individual cells with a Pasteur micropipette.

Experimental and control bottles were placed on rotating wheels at 0.9 rpm under dim light at 15°C for 16 to 20 hour. After incubation, 2 mL aliquots from each bottle were transferred into multiwell chambers for counting *G. sanguineum* or *G. polyedra* cells (after serial dilution where necessary). Copepods were sieved through a 101 μm mesh and counted. Ingestion rates (prey ingested copepod^{-1} hour^{-1}) of copepods on *G. sanguineum* or *G. polyedra* were calculated using the equations of Frost (1972) from final concentrations of prey in bottles with and without *Calanus* or *Acartia.*

Experiment 1 and 2 Design. These experiments were designed with similar intent but involved different species of copepods and phytoplanktonic food. In experiment 1 *Calanus* and *G. sanguineum* were used, while *Acartia* spp. and *G. polyedra* were used in experiment 2. The concentration of phytoplankton was initially constant in all experimental containers, while slurry concentrations of 0.05, 0.1, 0.3 and 0.6% (wet weight) were added; the period of measurement was 24 hours.

Experiment 3 Design. In experiment 3, *Calanus* and a 0.6% slurry (a concentration which caused a large reduction in ingestion rates in experiment 1) were incubated for 24 hours as in experiment 1. After the 24-hour incubation time, the *Calanus* were sieved onto a 101 μm mesh, counted, and transferred into new bottles containing only *G. sanguineum* cells without slurry. New duplicate control bottles containing only *G. sanguineum* were used. The bottles were again incubated for 24 hours as described above, and cells and *Calanus* were counted.

Experiment 4 Design. In experiment 4, 0.6% slurry in filtered seawater was kept at 15°C for 24 hours. The slurry was then screened out through a GF/C glass fiber filter, and the filtrate seawater was transferred into four new bottles. *G. sanguineum* was added to all four bottles, and 5 female *Calanus* were added to two of these. Controls were similarly treated using seawater which had not been exposed to slurry. Bottles were incubated for 24 hour as described above, and cells and *Calanus* were counted.

Microplankton Growth Rates

A dense population of the ubiquitous, heterotrophic dinoflagellate *Polykrikos kofoidi*, originally collected at the Scripps pier and maintained in culture, was used for specific growth rate tests in the presence of pulped paper slurry. Specifically, the specific growth rate was determined by incubating 50 actively swimming *P. kofoidi* cells, with *G. polyedra* as prey (84 *G. polyedra*·mL^{-1}) in the presence of slurry at 0, 0.05, 0.1, 0.3, and 0.6% wet weight concentrations. Triplicate experiment bottles were set up at all slurry concentrations. Three mL of f/4 media were added into each bottles to keep *G. polyedra* cells healthy. Actual initial concentrations of *G. polyedra* were measured in one extra bottle by removing and counting more than 100 individual cells with a Pasteur micropipette. Experimental bottles were placed on rotating wheels at 0.9 rpm under a 13:11 hour light-dark cycle of illumination with approximately 50 μm·m^{-2}·s^{-1} of cool white fluorescent light at 19°C for 47 to 53 hours. The final concentrations of *P. kofoidi* were measured by counting all cells in multiwell chambers under a dissecting microscope by removal with a Pasteur micropipette. The specific growth rate of *P. kofoidi*, μ(d^{-1}), was calculated as:

$$\mu = \ln\frac{P_t / P_0}{t} \qquad \text{(Eq. 8-1)}$$

where P_0 is the initial concentration of *P. kofoidi* and P_t is the final concentration after time t.

Clupeoid Feeding Studies. The effects of pulped material on filter and selective feeding fishes was investigated at NMFS. *Sardinops sagax* (sardines) were chosen as they are ubiquitous in the upper water column in most of the Special Areas, and because as filter feeders, they are more likely to interact and sustain deleterious effects from the presence of this material in the water column. In these initial studies, the sardines were tested only for feeding interactions. Follow-on work is described in section 14.0.

Pacific sardines collected from trawls made off the coast of San Diego were purchased from a San Diego bait dealer. After appropriate sorting for size and age, the fish were placed in four 1700 L control tanks to acclimate them to filter feeding conditions using 24 to 48-hour-old *Artemia* nauplii as food (sardines can feed both by filter feeding and by ingestion). The fish were fed daily at 0800 with approximately 233 nauplii· L^{-1}. This amount was expected to be sufficient to maintain the nutritional requirement of the sardines which were thought to consume between 1.7% and 5.0% of their body weight per day.

Once acclimated, the sardines in three of the four tanks were subjected to pulped paper-seawater slurries in the amounts of 3, 15, and 30 mg dry weight of paper·L^{-1}, respectively. A fourth tank was maintained as a control and remained free of pulped paper throughout the study. The pulped-paper slurry, prepared 24 hours in advance, was added to each of the three tanks every other day, 10 to 15 minutes before adding the *Artemia*. The fish were exposed to the slurries and *Artemia* for a period of 8 hours, after which the tanks were drained down for cleaning, then refilled with clean seawater. During the exposure periods the tanks were kept in a recirculating mode, and the paper was kept in suspension using a pumping system. During nonexposure periods the tanks were run in flow-through mode with fresh seawater. The tests were conducted over a 14 day period.

The fish were monitored daily for feeding behavior, general health and appearance, and feeding interactions. The feeding interactions were quantitatively determined by measuring the amount and rate of nauplii and pulped paper consumed under each exposure condition. This was done by weighing and identifying the stomach contents of the fish at the end of the experiment. To determine how well the pulped material stayed in suspension during each feeding period, and to monitor feeding rates, four 250 mL subsamples of tank water were taken at 1, 2, 3, 4, 6, and 8 hours after exposure. The water was filtered through predried and weighed filters, and the number of nauplii on the filters were counted under a dissecting microscope. The filter was then dried and weighed to obtain the total weight of paper and *Artemia* left in suspension.

Tests performed just prior to the submission of this report utilized the same methods described above except that: 1) the concentrations of pulped paper slurry tested were 1.0, 0.1, and 0.01 mg·L^{-1}; 2) the fish were exposed every day rather than every other day although feeding effects were measured every other day over a two hour period; 3) the amount of nauplii introduced was increased to 863 per liter so that the fish maintained their body weights throughout the experiments; and 4) tests were run for extra two days in the absence of paper slurry to test recovery of ingestion rates.

8.3.2 Results

Liquid-Phase Bioassays

Effects of Paper Pulp on *Mysidopsis bahia.* Three assays, using 5% elutriates that were not centrifuged, resulted in 15% to 60% mortality at the lowest concentration (6.25%), and lethality in all higher concentrations of test solution. No dose-response was observable. Suspended solids in the elutriate possibly contributed to these effects. Consequently, no LC_{50} was observed in *M. bahia* from this material leachate and further assays were performed after centrifugation of the elutriate. A NOEC value for these tests was not applicable because effects were observed at all test dilutions. The three assays performed using a 0.01% elutriate showed no dose-response. The NOEC for these tests was greater than 100% of the 0.01% leachate.

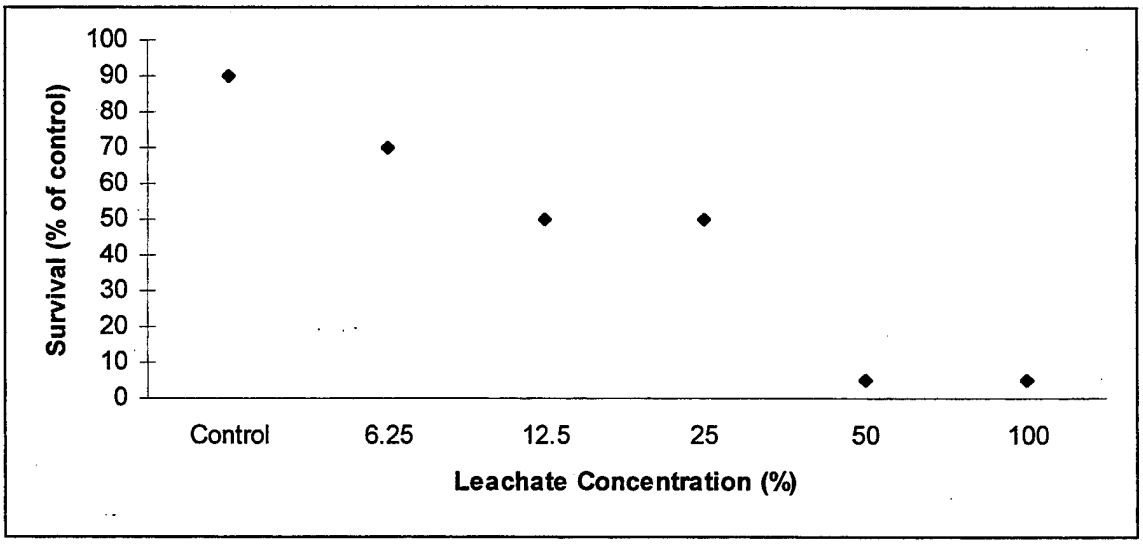

Figure 8-4. Survival of *Mysidopsis bahia* exposed to dilutions of 5% pulped paper elutriate for 96 hours. LC_{50}=22% of the 5% elutriate. NOEC not applicable because effects were observed at all test dilutions.

When the elutriate was centrifuged, two of three assays resulted in LC_{50} values of 22% and 32% test solution at 96 hours of exposure, an example of which is shown in figure 8-4. The third assay resulted in total lethality (97.5% mortality) in concentrations of 12.5 through 100%. No LC_{50} value was possible to determine in *M. bahia* from the third assay of this leachate. After 96 hours of exposure, a NOEC value was not applicable to two of the three assays. In the third assay the NOEC was 6.25% (of the initial 5%) leachate.

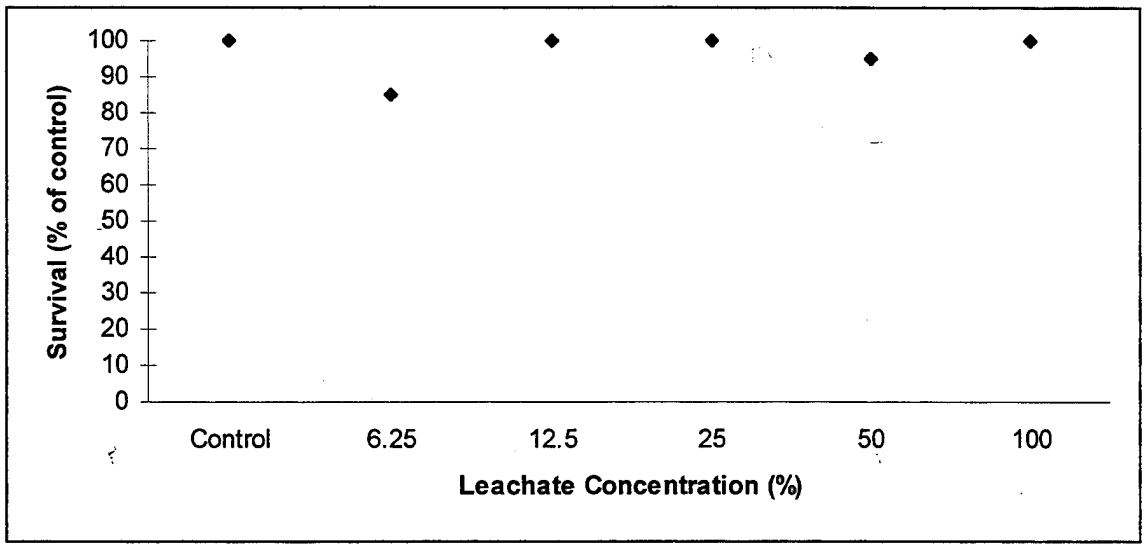

Figure 8-5. Survival of *Menidia beryllina* exposed to dilutions of 5% pulped paper elutriate for 96 hours. No toxicity was noted at any test dilution. NOEC is taken as 100% because no effects were observed at any dilution.

Effects of Paper Pulp on *Menidia beryllina.* In three assays conducted with 5% leachate, no significant mortality occurred in any test concentration (example shown in figure 8-5). No LC_{50} value was determined in *M. beryllina* from this material leachate. After 96 hours of exposure, the NOEC value was a 100% solution of the initial 5% leachate in each of the three assays.

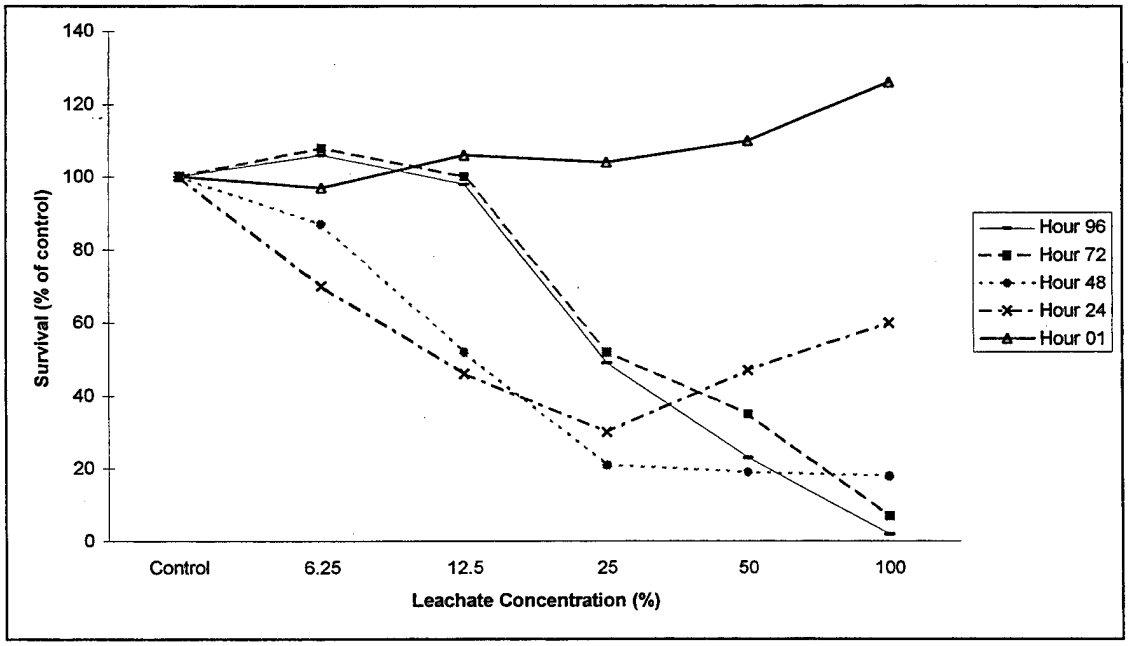

Figure 8-6. Relative fluorescence of *Skeletonema costatum* for 1, 24, 48, 72 and 96 hour exposures of 5% pulped paper elutirate. IC_{50}=25% and NOEC =12.5% of the 5% elutriate. No effects were observed after the first hour of exposure but were observed at 24 hours and beyond.

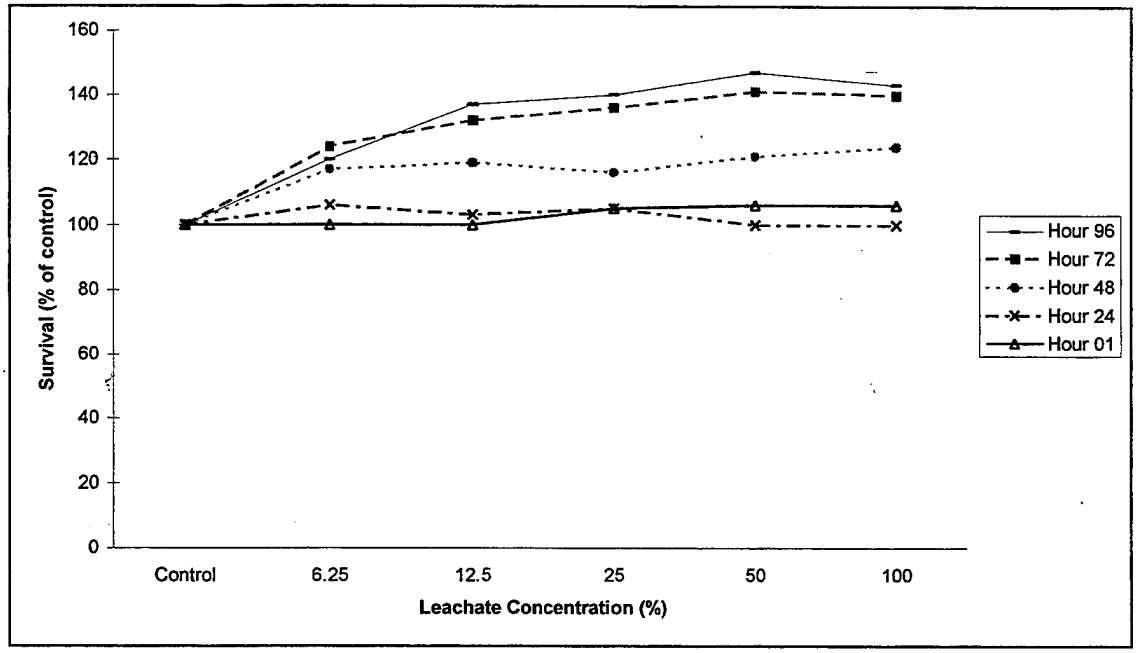

Figure 8-7. Relative fluorescence of *Skeletonema costatum* for 1, 24, 48, 72 and 96 hour exposures of 0.01% pulped paper elutirate. No toxicity was noted at any test dilution. NOEC is taken as 100% because no effects were observed at any dilution.

Effects of Paper Pulp on *Skeletonema costatum* (Clone "Skel"). Three assays with 5% leachate resulted in dose-responses where the IC_{50} values at 96 hours of exposure were: 12.5 to 25%, 25% (figure 8-6), and 25 to 50% dilutions of the initial 5% leachate, respectively. No decline in plant biomass was observed under any dilution after the first hour of exposure. However, biomass declined consistently with increasing concentration of test solution thereafter until the assays ended at 96 hours. The NOEC values in two of the three assays were 12.5% and 25% dilutions of the initial 5% leachate. One assay conducted with 0.01% initial leachate concentration resulted in no decrease of biomass (figure 8-7). A slight enhancement of growth was observed in conjunction with increased test solution. No IC_{50} value was determined with *S. costatum* from this leachate. After 96 hours of exposure, the NOEC value was a 100% solution of the initial 5% leachate.

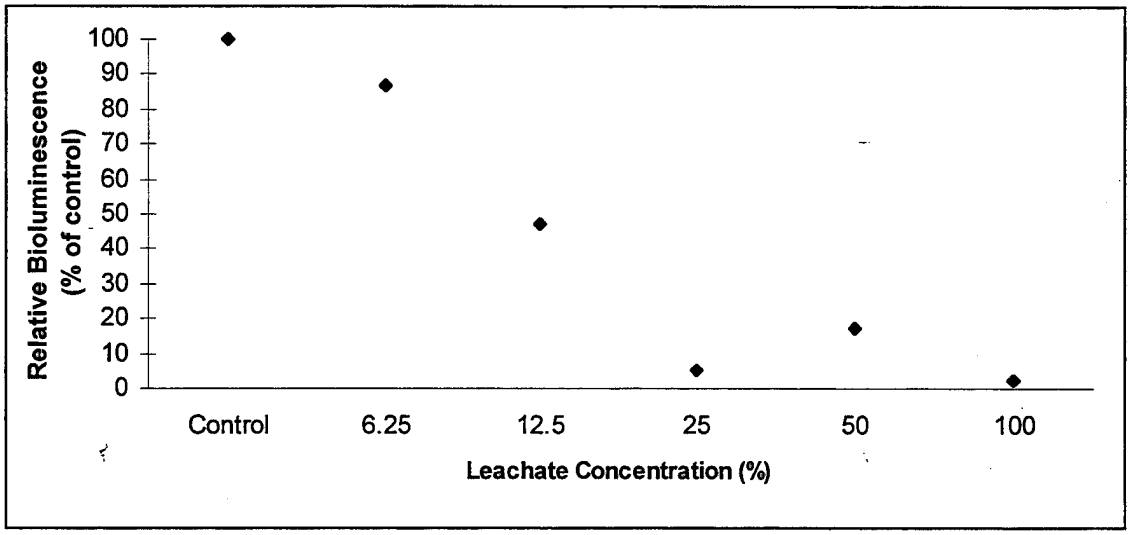

Figure 8-8. Relative bioluminescence of *Gonyaulax polyedra* exposed to dilutions of 5% pulped paper elutriate for 96 hours. LC_{50}=27.69% of the elutriate. NOEC not applicable because effects were observed at all test dilutions.

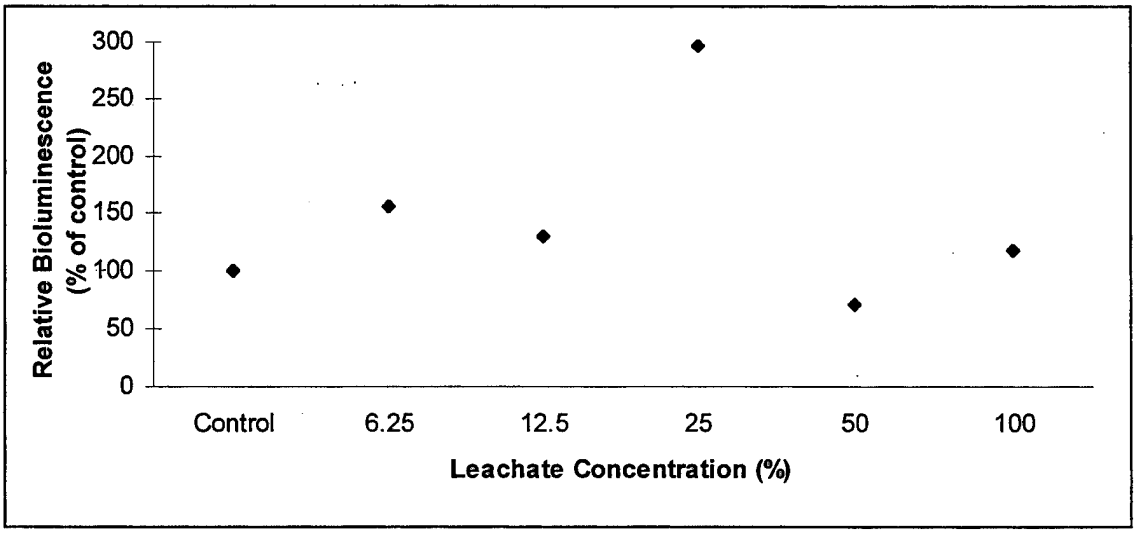

Figure 8-9. Relative bioluminescence of *Gonyaulax polyedra* exposed to dilutions of 0.01% pulped paper elutriate for 96 hours. Poor dose response, NOEC is taken as 100% because no effects were observed at any dilution.

Effects of Paper Pulp on *Gonyaulax polyedra.* One assay resulted in a dose-response curve with an IC_{50} of 27.7% after 95 hours of exposure (figure 8-8). No NOEC value was applicable. One assay test at 0.01% initial leachate resulted in variable levels of bioluminescence (figure 8-9). A poor dose-response resulted in no observable IC_{50} value. After 96 hours of exposure, a NOEC value was observed at a 100% solution of the initial 0.01% leachate.

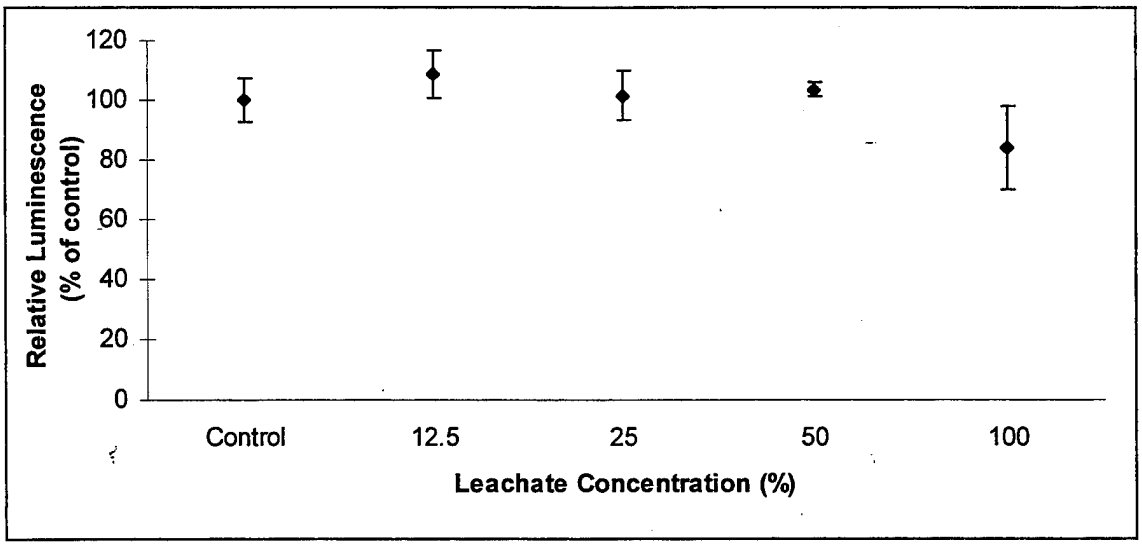

Figure 8-10. Relative luminescence of *Photobacterium phosphoreum* exposed to dilutions of 5% pulped paper elutriate for 15 minutes. NOEC=50% of the 5% elutriate.

Effects of Paper Pulp to *Photobacterium phosphoreum* (Microtox). Trials 1 and 2, using 5% leachate, showed a 5-minute EC_{50} value in both those trials which were at or exceeded 100%, the maximum dilution tested. The third trial showed no toxicity as the control and the 100% leachate solution readings were essentially the same. The 15-minute readings in Trial 1 were inconclusive for determining EC values because all mean readings for the dilutions, except 100%, exceeded the control mean (figure 8-10). This yielded only one usable point, and a dose-response curve could not be plotted. After 15 minutes of exposure, the NOEC value was a 100% solution of the initial 5% leachate in each of the three trials.

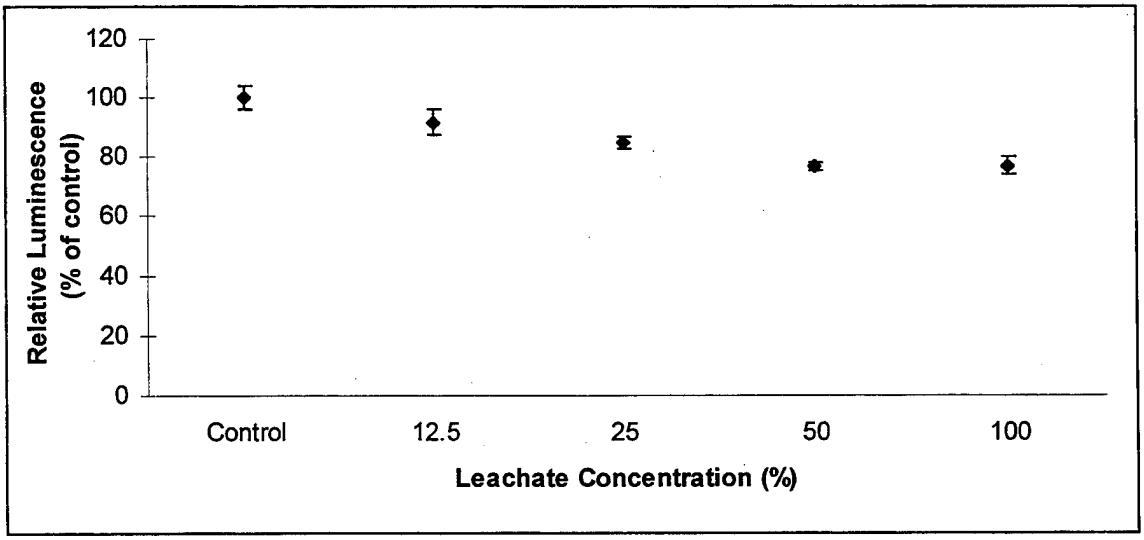

Figure 8-11. Relative light output for *Photobacterium phosphoreum* exposed to dilutions of 0.01% pulped paper elutriate for 15 minutes.

A 0.01% paper pulp leachate was tested using four concentrations and a control for exposure periods of 5 and 15 minutes (figure 8-11). No EC_{50} value was noted, although a 20% reduction of light output occurred at the 100% leachate solution exposure. A NOEC value was not applicable for the 15-minute exposure.

Table 8-11. Summary of pulped paper elutriate test results. Elutriate concentration is percent by weight of pulped paper added to seawater to make the test solution. The endpoints measured were survival in the mysids and minnows (LC_{50}), inhibition of bioluminescence of *G. polyedra* (IC_{50}), inhibition of lumnescence in *Photobacterium phosphoreum* (EC_{50}), and biomass or chlorophyll fluorescence inhibition (IC_{50}) in the diatom tests.

	Elutriate Concentration	
Test Species	5%	0.01%
Mysidopsis bahia	LC_{50}= 22-32% NOEC=6.25%	LC_{50}>100% NOEC=100%
Menidia beryllina	LC_{50}>100% NOEC=100%	Not Tested
Skeletonema costatum	IC_{50}=12.5-50% NOEC=12.5-25%	IC_{50}>100% NOEC=100%
Gonyaulax polyedra	IC_{50}=27.7% NOEC=NA	IC_{50}>100% NOEC=100%
Photobacterium phosphoreum	EC_{50}>100% NOEC=100%	EC_{50}>100% NOEC=NA

Complete results of the above bioassays are tabulated and graphed in appendix C and summarized in table 8-11. The above results suggest that the no observable effects levels for pulped paper for each of the species tested is between 0.01% and 5% initial leachate. At the 5% leachate level, there is a range of effects including light reduction in *G. polyedra*, mortality in *M. bahia*, and biomass loss in *S. costatum*. The effects noted with three test organisms, and the lack of effects in the others, is consistent with their known relative sensitivities. The variations observed within each test are typical of these bioassays and point to the need to consider multiple tests as well as replicates of each type of test.

To utilize these laboratory bioassay results in an attempt to understand the potential effects on organisms in the field, it is necessary to identify the actual exposure (magnitude and duration) levels in the field. This, of course, is a function of the dispersion characteristics of the liquid (seawater) waste stream. Another consideration is the amount of time that the pulped paper is in contact with the seawater prior to being exposed to the organism. The above tests used an elutriate that placed the particles in contact with the seawater for 1.5 hours. The seawater used in the pulping operation then discharged over the side would likely have been in contact on the order of minutes rather than hours. Thus, the elutriate conditions utilized are conservative estimates of the initial conditions that would be found in the discharge seawater.

Particulate-Phase Bioassays

Benthic Species Tests. No effects were observed in the amphipod or polychaete tests. Results of the 96-hour polychaete test showed no significant difference in survival between the controls and the highest concentration tested, a 1-mm layer of paper slurry ($P<0.05$, Dunnett's test). A 95 to 100% survival rate was seen in all test containers. Results of the 10-day amphipod test showed no significant difference in survival between the controls and the highest concentration tested, a 1 mm layer of paper slurry ($P<0.05$, Dunnett's test). The paper slurry also showed no effect in the organisms' ability to rebury in new sediment after completion of the test ($P<0.05$, Dunnett's test).

The survival rate of amphipods was poor (50-60%) in both controls and dilutions with the paper slurry added. The high mortality was likely due to the organisms being stressed and in a weak condition when starting the test. The organisms used were small, and were collected following a wet winter when amphipod population densities were depressed.

There was no apparent effect of grain size on the toxicity of the paper slurry. There were no toxic effects of the paper slurry in either sediment sample. Fine sand and silty sand were collected for testing based on a visual examination of sediments in the field. Coarse sand was not used in the tests because amphipods cannot bury effectively in coarse sediments and do not survive well. However, grain size analysis and total organic carbon content indicated that the two samples of sediment differed only slightly. Both were composed of 96 to 97% sand and 3 to 4% silt and clay, but the silty sand sample was somewhat higher in total organic carbon (861 verses 552 $mg \cdot kg^{-1}$). In the amphipod test, the fine sediment was composed of 96% sand and 4% silt and clay, while the silty sediment was composed of 92% sand and 8% silt and clay. The TOC was slightly higher in the silty sediment (1190 verses 1040 $mg \cdot kg^{-1}$). There were no effects observed from the paper slurry in either sediment sample.

Zooplankton Interactions

Results are shown here relating specifically to the three hypotheses formulated. The complete report of this portion of the study can be found in appendix E.

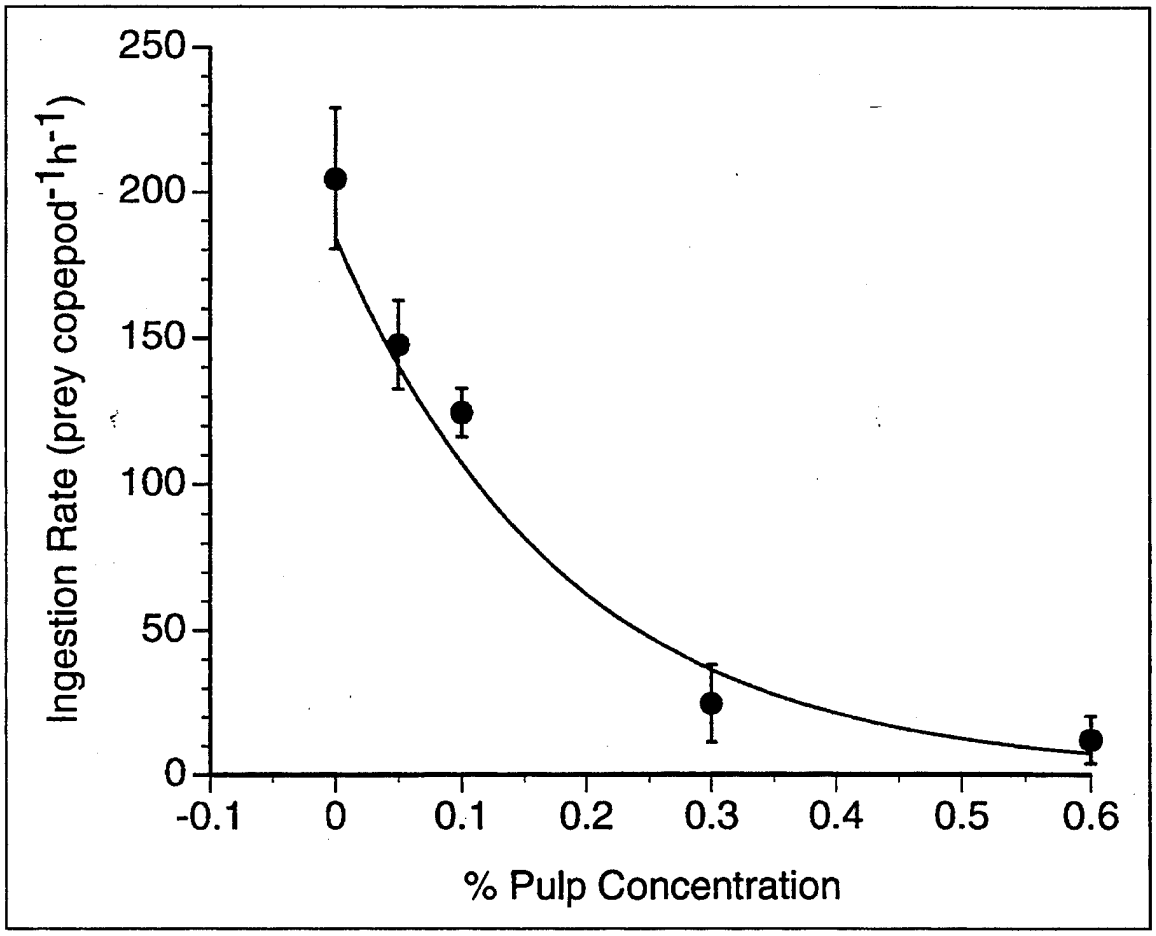

Figure 8-12. Ingestion rates of *Gymnodinium sanguineum* by *Calanus pacificus* under varying pulped paper concentrations. Symbols represent treatment means ±1 standard error.

Test of H_o1-(copepod ingestion rate is independent of the presence of pulper slurry). With increasing slurry concentration, the ingestion rates of *G. sanguineum* by *C. pacificus* exponentially decreased from 205 to 12 prey *Calanus*$^{-1}$ h^{-1} (see figure 8-12). Ingestion rates of *G. sanguineum* by *C. pacificus* were significantly reduced by slurry (ANOVA, $p < 0.005$; Zar 1984). Therefore, H_o1 can be rejected when *G. sanguineum* and *C. pacificus* were prey and predator. Ingestion rates at slurry concentrations of 0.05% and 0.1% (wet weights) were not significantly different from those without added slurry ($p > 0.05$), but they were significantly depressed at slurry concentrations >0.3% wet weight ($p < 0.05$).

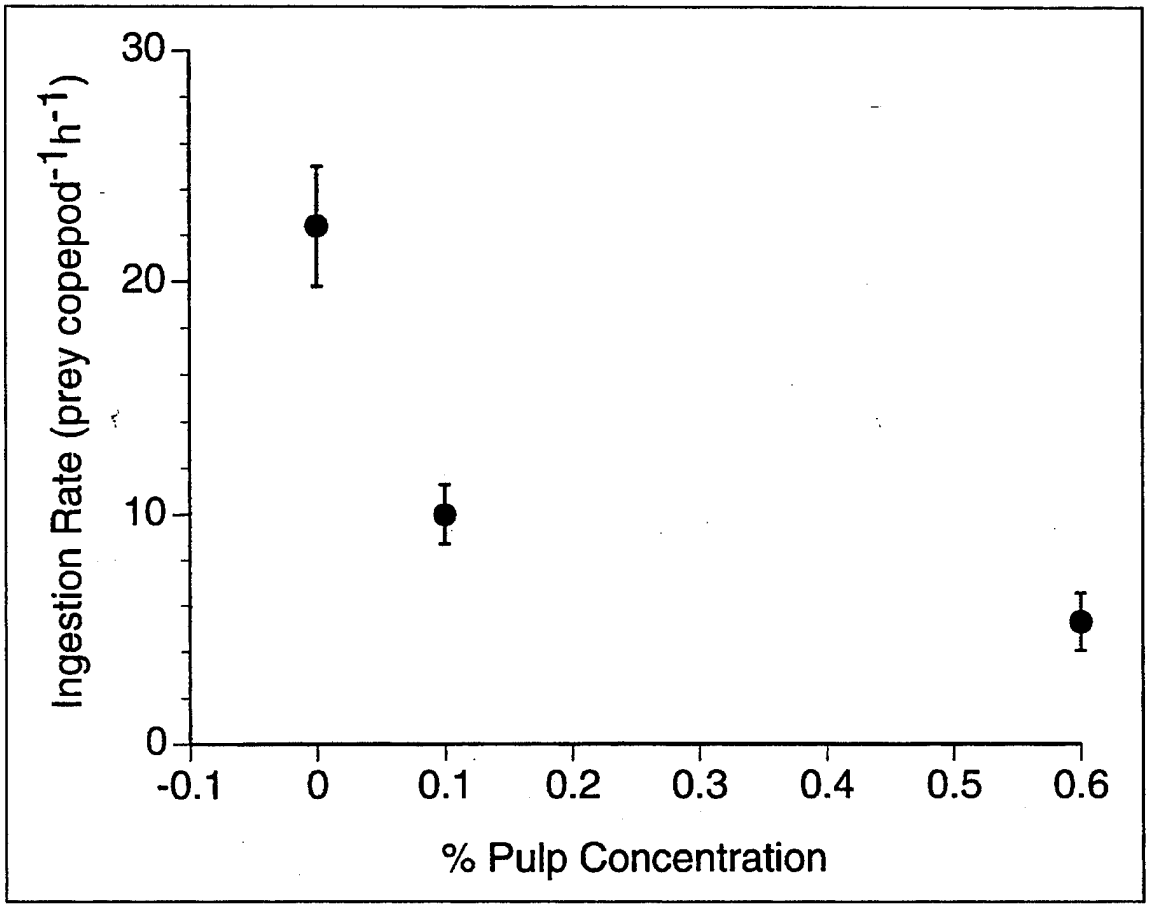

Figure 8-13. Ingestion rates of *Gymnodinium polyedra* by *Acartia* spp. under varying pulped paper concentrations. Symbols represent treatment means ±1 standard error.

With increasing slurry concentration, the ingestion rates of *G. polyedra* by *Acartia spp.* also decreased from 22 to 5 prey *Acartia*$^{-1}$ h^{-1} (see figure 8-13). Ingestion rates of *G. polyedra* by *Acartia* spp. were significantly reduced by slurry (ANOVA, $p < 0.05$). Therefore, H_o1 can also be rejected when *G. polyedra* and *Acartia spp.* were prey and predator. The ingestion rate at a slurry concentration of 0.1% (wet weight) was not significantly different from that without added slurry ($p > 0.05$), but was significantly depressed at 0.6% wet weight ($p < 0.05$).

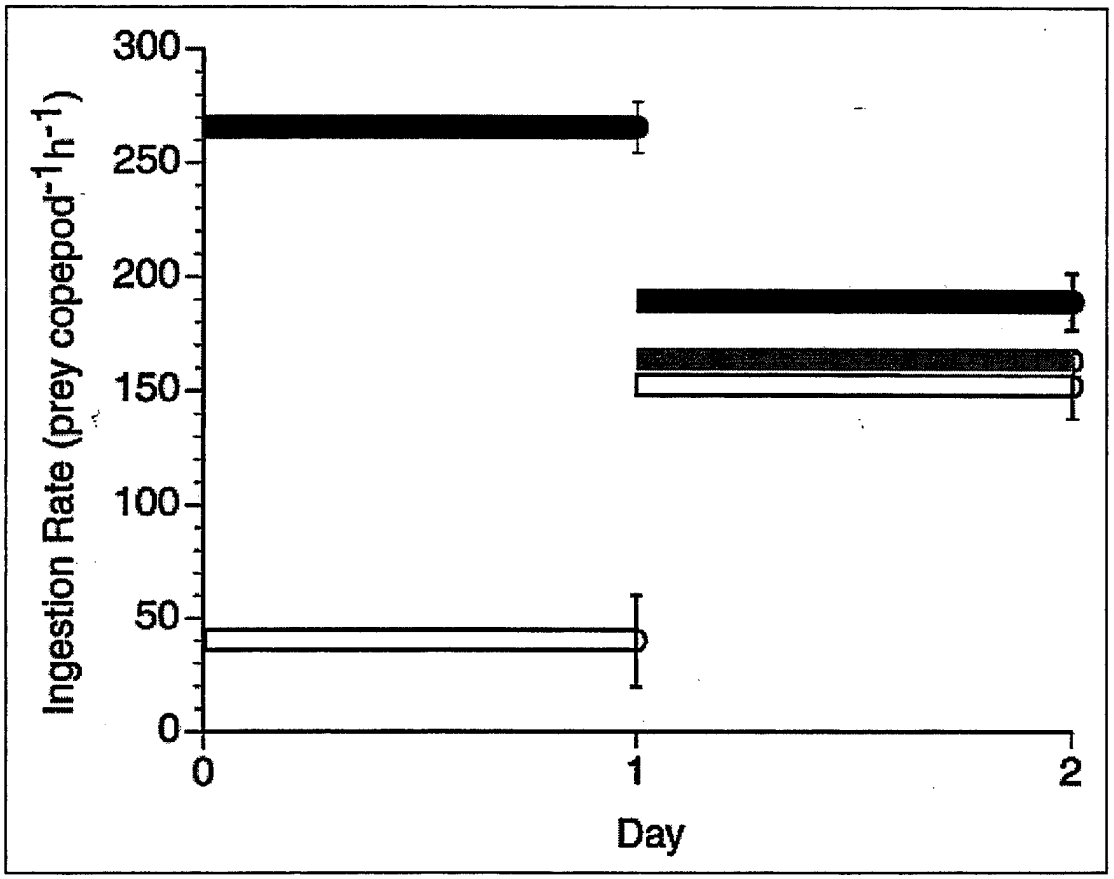

Figure 8-14. Effect of prior exposure of pulper pulped paper on ingestion rate of *Gymnodinium sanguineum* by *Calanus pacificus*. Symbols represent treatment means ±1 standard error. Black bars: incubated without slurry in both day 1 and 2 (initial *G. sanguineum* concentrations in day 1 and 2 were 183 and 117 ml^{-1}, respectively). Open bars: 0.6% slurry (wet weight:wet weight) in day 1 and none in day 2. Gray bar: pulped paper free seawater in which pulped-paper had been soaked for 24 hours then removed by filtration.

Test of H_o2-(ingestion rates of copepods that had been previously incubated with pulper slurry are not significantly different than those never exposed to the slurry). In experiment 3, after the first day incubation, the ingestion rate of *Calanus* on *G. sanguineum* incubated with the slurry concentration of 0.6% (wet weight) was significantly different from that without slurry (figure 8-14, two-tailed -t test, $p < 0.05$), and similar to the result in experiment 1. However, the ingestion rate of *Calanus* originally incubated with 0.6% (wet weight) slurry for 24 hours and then transferred into new bottles containing *G. sanguineum* without slurry was not significantly different from that of the *Calanus* continuously incubated without slurry. Therefore, H_o2 cannot be rejected. The results show that *Calanus* recovers its feeding rate when the slurry disappears.

Test of H_o3-(copepod ingestion rates in seawater, which had previously been in contact with pulped slurry for 24 hours and then removed by filtration, are not significantly different than in seawater never contacting slurry). The ingestion rate of *Calanus* in slurry-free seawater, in

which slurry had been soaked for 24 hours and then removed by filtration, was not significantly different from that in seawater never contacting slurry ($p > 0.05$, gray bars in figure 8-14).

These results suggest that the zooplankton tested were not adversely affected when in the presence of pulped paper at concentrations less than 0.3% wet weight, equivalent to a concentration of 0.05% on a dry weight basis. At concentrations above this, the zooplankton become physically hindered from reaching their prey, which affects their ingestion rates. As such, there is no direct harm to the organism. Nor is this effect long-lasting, as the plankton recover to normal ingestion rates once the physical barriers are removed. The issue that again needs to be addressed is the length and magnitude of exposure in the natural environment. These are addressed through modeling and measuring the particle dispersion fields. The zooplankton also do not appear to be affected by the soluble portion of the pulped paper at an elutriate concentration of 0.1% dry weight (in contact with the seawater for 24 hours). As in the bioassay test above, dispersion of the liquid-phase of the discharge needs to be considered to put limits on the potential exposures.

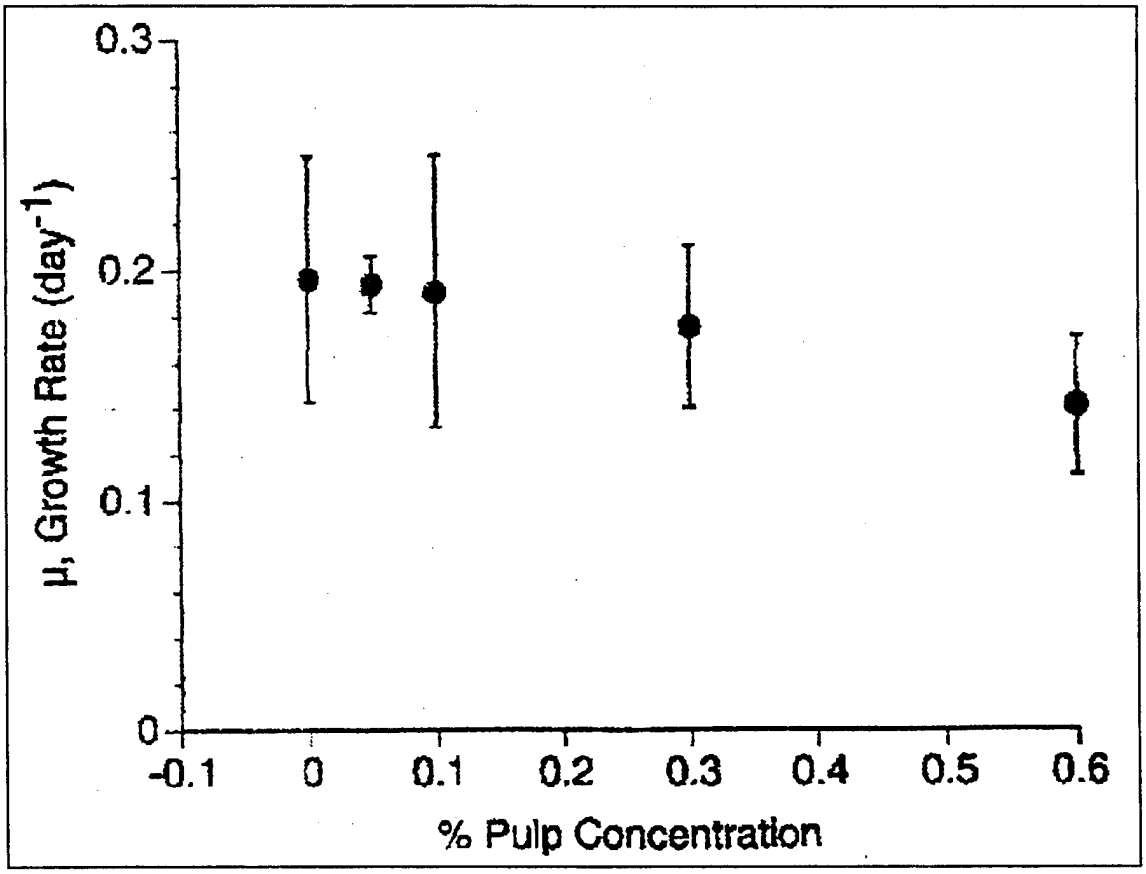

Figure 8-15. Specific growth rates of *Polykrikos kofoidi* feeding on *Gonyaulax polyedra* as a function of pulped paper concentration. Symbols represent treatment means ±1 standard error.

Microplankton Growth Rates. With increasing slurry concentration, the specific growth rates of *P. kofoidi* on *G. polyedra* decreased from 0.196 to 0.142 d^{-1} (figure 8-15). However, this

decrease in rates was not statistically significant (ANOVA, p >0.1: Zar, 1984). Therefore, the presence of slurry does not affect the population of *P. kofoidi.*

Clupeoid Feeding Studies

Three different results were derived from the these experiments. These relate to behavior, feeding interactions, and growth and mortality. The complete report can be found in appendix F.

Behavior. Feeding behavior was subjectively monitored using obvious visual changes in gill flaring. Feeding was categorized subjectively into three groups: active filtering, passive filtering with occasional gulping, and little or no feeding. The control tank group showed active filter-feeding throughout the experiments. Fish subjected to the 15 and 30 mg·L^{-1} pulped paper concentrations actively filtered in the first hour after food was introduced. In the next hour the feeding was reduced to passive filtering and gulping, and then reduced further to little or no feeding for the remainder of the feeding period, even though abundant prey were available. Another observation made of the fish subjected to the two highest test concentrations with filtering was that they did not maintain tight schooling behavior as did the other two tanks.

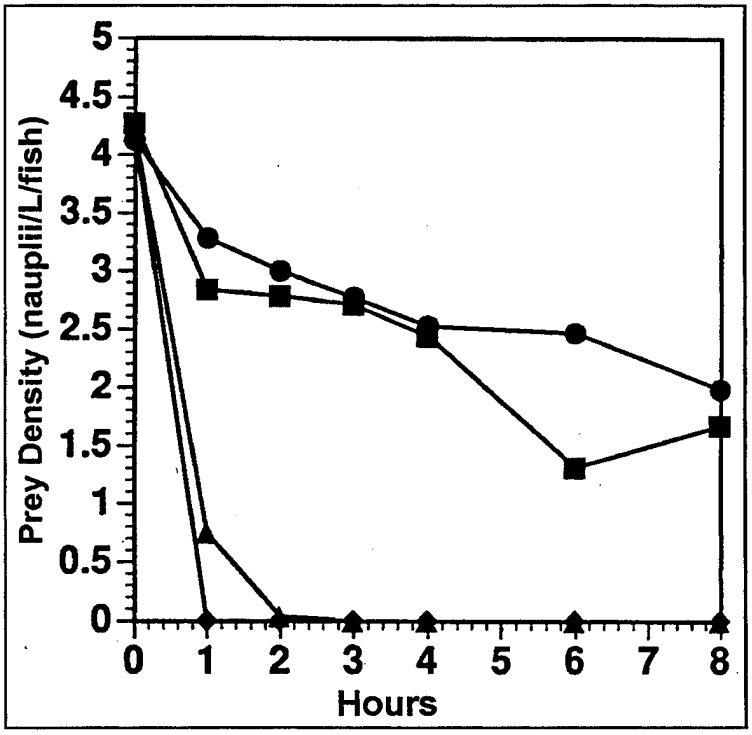

Figure 8-16. Effect on the ability of the Pacific Sardine to filter-feed on *Artemia* nauplii over time at 3, 15 and 30 mg L^{-1} pulped paper concentrations.

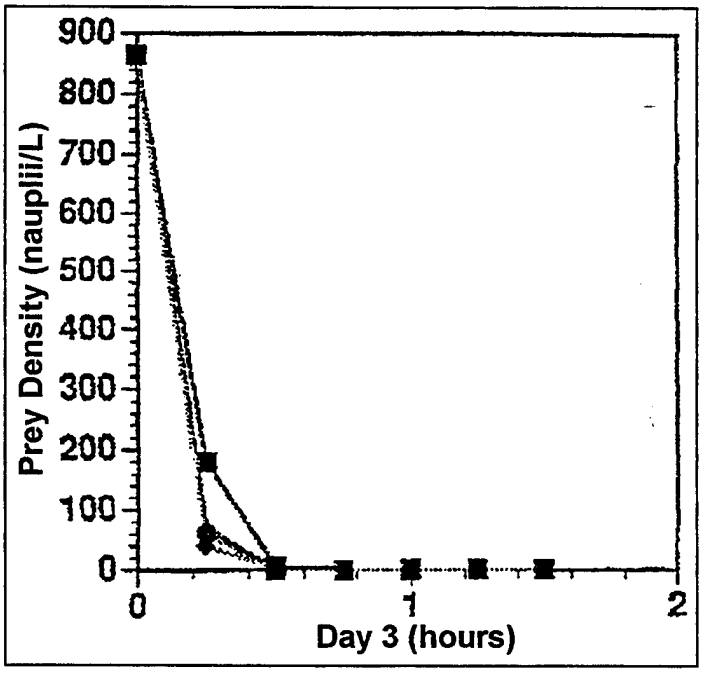

Figure 8-17. Effect on the ability of the Pacific Sardine to filter-feed on *Artemia* nauplii over time at 0.01, 0.1, and 1.0 mg L^{-1} pulped paper concentrations.

Feeding Interactions. All three test concentrations of pulped paper, 3, 15 and 30 mg·L^{-1}, resulted in a significantly negative effect on the ability of the Pacific Sardine to filter-feed on *Artemia* nauplii. There was a dose-dependent effect on filtering success with all concentrations in which the rate of food ingested fell off with increasing pulped paper concentration, an example of which is shown in figure 8-16. At 30 mg·L^{-1} there was almost complete inhibition of feeding success. In an attempt to find a no effects level, similar tests run at 1.0, 0.1, and 0.01 mg·L^{-1} showed adverse effects only at the 1.0 mg·L^{-1} level; see figure 8-17. The 0.1 mg·L^{-1} and lower concentrations clearly had no effects on feeding. Additionally, fish exposed to the slurries and then allowed to feed two extra days in the absence of slurry had ingestion rates equivalent to those of the controls indicating that the fish quickly recovered to normal feeding levels.

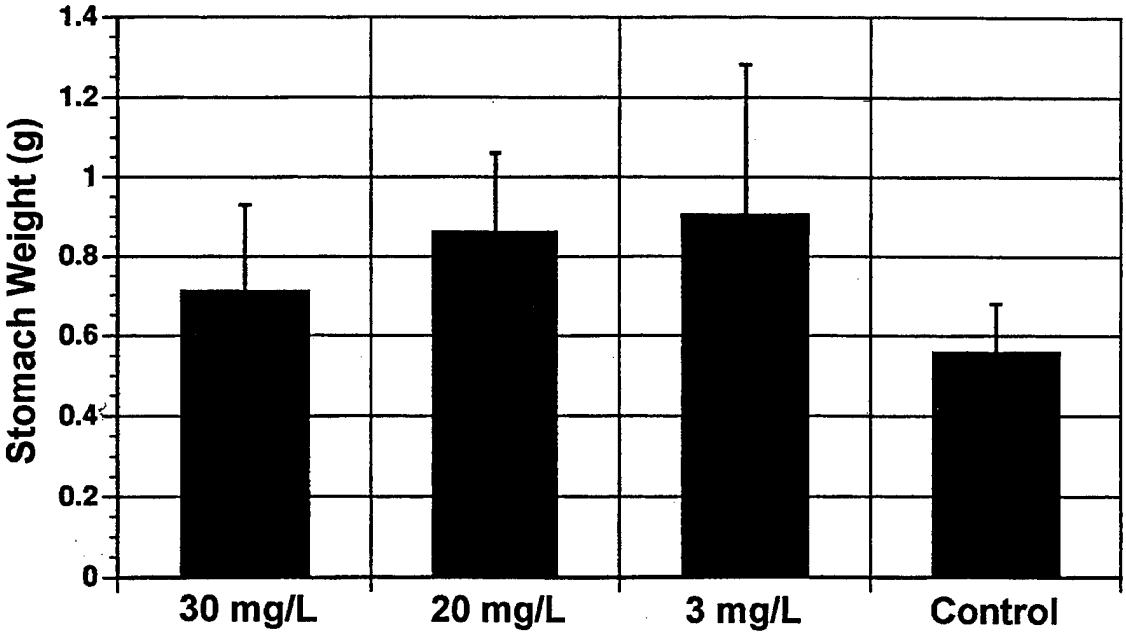

Figure 8-18. Stomach weights of Pacific Sardines after feeding in various pulped paper concentrations.

Based on the analysis of stomach contents, all treatment groups (3-30 $mg \cdot L^{-1}$) ingested paper along with nauplii (figure 8-18). The amount of paper ingested appeared to increase with decreasing pulped paper concentration, although the differences were not statistically significant. This result appears related to the observed feeding behavior. As the treatment concentrations decreased, the fish spent more time actively filter-feeding, and thus received more paper along with their food. The paper was also observed within the intestines of the fish as paper plugs. These intestinal plugs had an outward appearance as lumpy protrusions on many of the fishes abdomens. The effects of the paper plugs within their intestinal tracts is unknown. There was no evidence of paper fiber digestion in either the intestines or in the fecal material. No data were yet available on stomach contents of the fish exposed to 0.01-1 $mg \cdot L^{-1}$ slurries although there was no outward indication of intestinal plugging.

Growth and Mortality. All 3 to 30 $mg \cdot L^{-1}$ treatment groups had a significantly higher mortality rate (about 18%) than the control, although this effect was dose independent. Also, all groups lost weight during the experiment, an indication that either the estimated requirement of 1.7% body weight/day minimum was too low, or that the estimated filtering capacity was too high. In either case, the decrease in body weight indicates insufficient food supply and this certainly added a stress on the fish under all conditions. The effect of this added stress on the results is unknown. However, the 0.01-1 $mg \cdot L^{-1}$ slurry experiments were performed with a higher concentration of nauplii, and there was no mortality in any treatment suggesting that mortality was possibly related to sufficient food availability.

It appears that clupeoid feeding can be affected by the presence of pulped paper at exposure concentrations at or exceeding 1 $mg \cdot L^{-1}$. Although the tests were run for roughly 2 weeks, the exposures were made with a duration of only 2 hours. The NOEC appears to be between paper

particle concentrations of 0.1 and 1 mg·L^{-1}. Even at the 1 mg·L^{-1} level, the fish recovered to normal ingestion rates after a day, suggesting that even if the fish were exposed to particle concentrations sufficient to cause a feeding effect, they would be able to recover to normal feeding habits very quickly. These results suggest that clupeoid feeding may be a limiting factor with regard to acceptable concentration levels of pulped paper particles, as all other particle tests showed no effects at concentrations below 1 mg·L^{-1}.

8.4 Degradation Analyses

8.4.1 Methods

The degradation studies, being conducted at the University of Georgia, were designed to look at three aspects of bacterial degradation of cellulose slurries. The first approach focused on measuring decay constants for various categories of cellulose waste under conditions representative of oceanic sites within Special Areas. Initial results of this first phase have been completed and included in this report; the second and third will be completed and reported in a subsequent report. The second approach will focus on the effect of the wide size range of particles making up the paper slurries on rates of degradation. The third approach will focus on the rates of cellulose decomposition mediated by a variety of indigenous microbial populations in seawater samples collected from around the globe. The methods and results for the first of these approaches are included below, and information regarding future work can be found in section 14.0.

Special Area Conditions. These microbiological studies focused on measuring decay constants for various categories of cellulose wastes under conditions representative of oceanic sites within Special Areas. The laboratory conditions were chosen based on seasonal variations and vertical profiles from representative Special Areas (the Baltic Sea, the Mediterranean Sea, and the Caribbean Sea). Eventually, they will span a range of temperatures from 4°C to 28°C, a range of inorganic nitrogen concentrations from 0 (trace levels) to 5 μM, and a range of inorganic phosphorus concentrations from 0 (trace levels) to 1 μM. To date, decay rate measurements have been completed for the highest temperature and nutrient conditions using white paper slurries.

In this experiment, paper slurries were added to Pyrex flasks and suspended in natural seawater freshly collected from the Georgia nearshore at concentrations of 1 mg (dry weight)·mL^{-1}. The seawater was amended with 5 μM N (as nitrate and ammonium) and 1 mM P (as phosphate). Flasks were incubated at 28°C while shaking at 200 rpm. All analyses were conducted in triplicate.

Rates of bacterial decomposition were measured by two methods. Gravimetric determinations involved harvesting the flasks after a 1 month degradation period, filtering flask contents through a 0.8 micron pore-size Nuclepore filter, and determining the weight of the remaining cellulose. This method is the simplest to perform but is also relatively insensitive, so it is used only as a gross measure of degradation rates.

The second method involved measuring rates of bacterial protein production via 3H-leucine incorporation. Subsamples (1.7 mL) were removed at daily to weekly intervals from the incubations and placed in 2-mL microcentrifuge tubes. 3H-Leucine was added at tracer levels (a final concentration of 20 nM, and bacterial cells were allowed to incorporate the leucine for a 1-hour period. After the incubation period, the macromolecules were fixed and precipitated by the

addition of trichloroacetic acid. Precipitated bacterial protein was assayed via scintillation counting to determine rates of incorporation of 3H-leucine into bacterial cellular material. Rates of leucine incorporation were converted to bacterial carbon assimilation values and ultimately degradation rates. These rates are based on the specific activity of the leucine and use theoretical relationships between the incorporation of leucine by bacteria and the formation of new bacterial cellular material.

In addition to the above decomposition rate measurements, numbers of bacterial cells were tracked periodically in the incubation flasks. Subsamples (5 mL) were removed from the flasks and subjected to mild sonication for 1 minute to gently dislodge cells from the cellulose particles. Sonicated samples were diluted with sterile, particle free water, filtered onto 0.2 micron pore-size blackened Poretics membrane filters and then stained for 3 minutes with 0.01% acridine orange, a fluorescent dye that intercalates into bacterial nucleic acid and allows the cells to be visualized by epifluorescence microscopy. Two subsamples were removed from the flask at each sample point and ten microscope fields were counted from each replicate.

Size Interactions. The cellulose particles in the waste slurries span a fairly large size range (from 30 μm to over 3 mm in diameter) and, upon release into the ocean, will sort in the water column based on size and sinking rate. Thus it is important to determine whether decomposition rates will vary with size and surface area:volume ratio of the particles. In an initial study to determine the appropriate size categories to use in these studies, a mixed paper slurry was size fractionated into five categories by resuspension in distilled water and sequential filtration through a series of sieves and polyethylene mesh screens with 2 mm, 1 mm, 500 μm, and 150 μm openings. Particles caught on the 2 mm sieve were repeatedly resuspended and refiltered to ensure that smaller particles were not attached to larger ones and that the sieve openings were not being occluded.

Composition of the Cellulose Particles. Although the paper slurries contain cellulose as the primary constituent, inorganic fillers which are added to pulped wood during the paper making process will also be a component of the particulate matrix. Clays, calcium carbonate, and titanium dioxide are among the most commonly used fillers and are usually added to improve the whiteness and the printing properties of the paper. In most paper-making processes, fillers account for 15% or less of the total weight of the finished paper.

White paper and mixed paper slurries were analyzed for inorganic content by filtering subsamples through a Whatman GF/F glass fiber filter, rinsing thoroughly with distilled water, drying at 110°C, and weighing. The filters were then combusted at 550°C for 4 hours to remove all organic materials, and the weight of the remaining inorganic fraction was determined. The elemental composition of the paper slurries (carbon, hydrogen, and nitrogen (CHN)) were determined on a Perkin-Elmer 240C CHN analyzer.

8.4.2 Results

The intent of the initial decomposition studies was to estimate the upper bounds of the decomposition rates that can be expected in seawater when temperature is optimal and inorganic nutrients are available in excess. Based on gravimetric measurements, rates of decomposition of white paper particles averaged 15.9% (+ 4.8%) over a 32 day period. Based on 3H-leucine incorporation, rates of decomposition averaged 11.2%. Assuming that bacterial decomposition of cellulose particles occurs via first order kinetics, the measured rates translate into a decay constant

(k) of approximately -0.005 d^{-1}. Thus the organic matter in white paper slurries has a minimum half life of 139 d (4.3 months) in the ocean. The half life is expected to be longer if environmental conditions are suboptimal for some or all of the decomposition period.

During the 32 day time period, bacterial numbers varied from $7.8 \cdot 10^6$ mL^{-1} to $4.0 \cdot 10^7$ mL^{-1}. These numbers are significantly higher than numbers commonly found in coastal seawater (approximately $2 \cdot 10^6$ mL^{-1}) and reflect the additional substrate added to the seawater in the form of cellulose particles. Microscopic examination of the flask contents reveals that most of the bacteria were attached to the particle surfaces rather than free living.

Size fractionation of the mixed paper slurry into five categories, based on passage through sieves or screens with 2 mm, 1 mm, 500 μm, or 150 μm openings, showed that most of the particles do not pass the largest size sieve. We found that 97.8% of the particles, by weight, were retained on the 2 mm mesh. The 1 to 2 mm category contained 1.4% of the particle weight, the 500 micron to 1 mm category contained 2.3% of the weight, the 150 to 500 micron category contained 1.1% of the weight, and the <150 micron category contained 0.4% of the weight. These results are similar to those from microscopic examination of the pulped paper in which most of the mass is contained within the large size particles. Larger particles were observed in this analysis, mainly as a result of differences in the methodology and size bins chosen for analysis.

Chemical analysis revealed that the white paper and mixed paper particles were 92% organic matter by weight. Thus the biologically nonreactive inorganic fillers used in the paper-making process (clays, calcium carbonate, or titanium dioxide) can only make up a small percentage (<8%) of the particle weight. CHN analysis indicated that nitrogen content of the particles is extremely low (below detectable levels) for the white paper slurry and only 0.02% of the weight for mixed paper. The weight ratio of carbon to nitrogen (C:N ratio) is therefore >1000, a value which is much higher than the optimal C:N ratio for a bacterial substrate (C:N of 15 or less). These results corroborate the chemical analyses discussed earlier in which the C:N ratio calculated was 1540:1. These data suggest that inorganic nitrogen availability in seawater may be a critical factor determining rates of particle degradation in the ocean. Future nutrient manipulation experiments will provide a direct mechanism to address this question.

9.0 SHREDDER WASTE STREAM CHARACTERIZATION

9.1 Physical Analyses

Five bags of shredder material were obtained from operations performed aboard the USS *George Washington* on 21 April 1994. The material was shipped frozen to NRaD overnight. The bags were subsequently kept frozen except when they were analyzed for content identification/mass fraction, volume/density, frontal area, fall velocity, and long-term monitoring. The five bags were numbered 1 through 5 corresponding to the sequence in which they were generated. All measurements were made on Bags 3, 4, and 5, except for the long-term monitoring which was performed on Bags 1, 2, and 3.

9.1.1 Methods

Content Identification/Mass fraction. The bags were opened for visual inspection and identification of the contents. The material was divided into broad categories of material types. These included burlap (bag material), glass, paper, aluminum, organics (typically food wastes), and tin-plated steel cans. Materials were weighed on a triple-beam balance to determine the mass of each category.

Volume/Density. The volumes of the bags were determined by placing them into fresh water (density of 1 $g \cdot cm^{-3}$ assumed) and measuring the volume of water displaced. The density of each bag was calculated by dividing the mass of each bag (measured above) by its volume.

Frontal Area. To determine a drag coefficient, the frontal area of the bags was measured by tracing their outline onto graph paper as they sat on the ground. Axial dimensions of the frontal area, measured as if the bags were elliptical in shape, were also measured using a tape measure.

Fall velocity. Fall velocities were determined by attaching a pressure transducer to each bag and dropping them into seawater (San Diego Bay) with an approximate density of 1.023 $g \cdot cm^{-3}$. The velocities were measured over a vertical distance of about 12 m. The pressure transducer data were recorded on a computer at 20 Hz.

9.1.2 Results

Table 9-1. Shredder bag components by weight and weight fraction. Bags were collected from the USS *George Washington* in 1995.

	Weight				Fraction			
BAG #	3 (g)	4 (g)	5 (g)	Mean (g)	3 (%)	4 (%)	5 (%)	Mean (%)
Burlap	437	401	427	421	8.3	9.3	8.6	8.75
Glass	701	6	0.0	236	13.4	0.1	0.0	4.50
Paper	63	118	66	82	1.2	2.8	1.3	1.76
Aluminum	29	223	0.0	84	0.6	5.2	0.0	1.92
Organics	294	56	0.0	117	5.6	1.3	0.0	2.31
Tin Cans	3720	3483	4484	3896	70.9	81.3	90.1	80.76
Total	5245	4286	4977	4836	100	100	100	100

Content Identification. The contents of three shredder bags were physically separated and weighed to determine the individual mass fractions of each component. Results are tabulated in table 9-1 and shown graphically in figure 9-1. The average bag weight was 4.8 kg. The materials observed were generically categorized as tin cans, burlap, glass, aluminum, organics, and paper. The major constituent of the shredder material was tin can food containers, making up between 70% and 90% by mass. Most of these were sliced open, twisted and bent into nonflattened shapes. The next most common material, by weight, was the burlap bag used as the waste stream container. Glass was the third most common material by weight, although it was completely absent in one of the bags. Aluminum (mostly as beverage cans), organics (mostly as miscellaneous food wastes), and paper (mostly as miscellaneous container labels) each made up roughly another 2% of the waste stream. Like glass, aluminum and organics were not always present in the shredder bags.

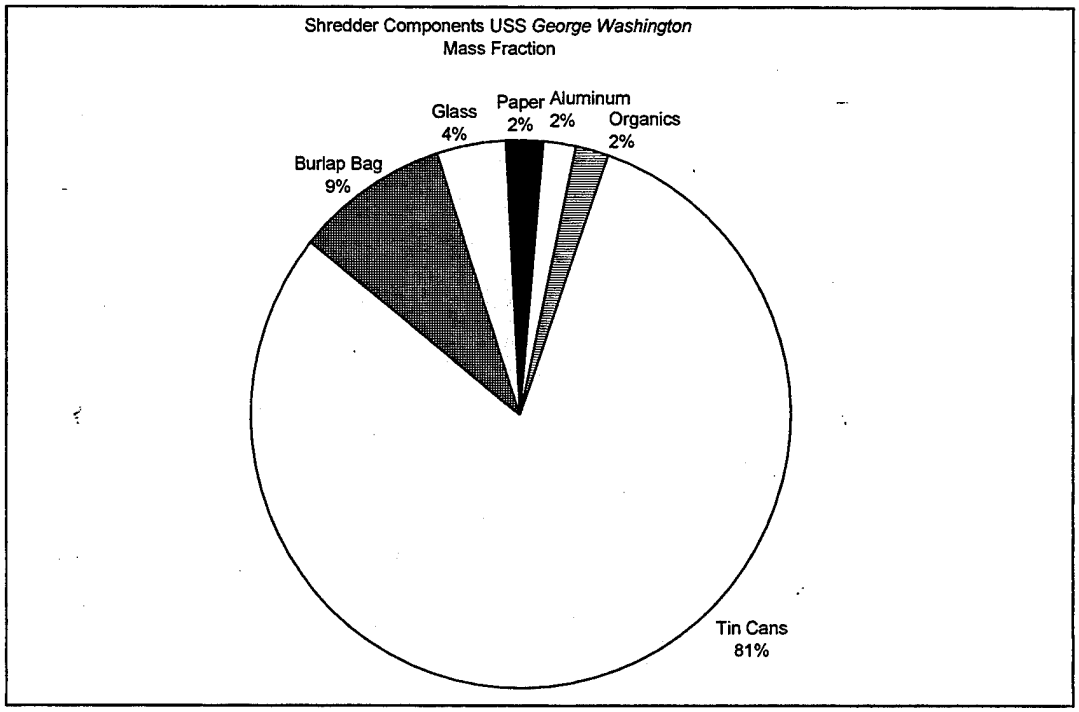

Figure 9-1. Average component makeup of three shredder bags from USS *George Washington* by mass fraction.

Table 9-2. Shredder bag density, frontal area, and fall velocities. Bags were collected from the USS *George Washington* in 1995.

Bag	Displacement (L)	Density ($g \cdot cm^{-3}$)	Frontal Area (cm^2)	Fall Velocity ($m \cdot s^{-1}$)
3	2.5	2.098	1923	0.591
4	2.0	2.176	2052	0.521
5	2.3	2.164	2242	0.508
Average	2.3	2.146	2072	0.540

Volume/Density. The volumes displaced by the three bags analyzed were 2.5, 2.0, and 2.3 L. Based on the these measurements and the total weight of material in each bag, the average density was calculated as 2.15 $g \cdot cm^{-3}$ (table 9-2). The calculated densities do not appear to be reasonable when comparing them to known densities of iron (7.86 $g \cdot cm^{-3}$), aluminum (2.7 $g \cdot cm^{-3}$), glass (2.4 $g \cdot cm^{-3}$), and paper (1.54 $g \cdot cm^{-3}$), or when using a low estimate for the density of the burlap and organics at 0.7 $g \cdot cm^{-3}$. Using the mass fractions along with these known or estimated densities would give a combined density of roughly 6.0 to 6.7 $g \cdot cm^{-3}$. The volume displacement calculation is a source of error in the density analysis which was based on very small (~3/8) and difficult to read

height changes. Although this is likely the dominant source of error, any trapped air within the material during measurement would have resulted in an overestimate of the volume displacement and hence would result in an underestimate of the density. However, other minor sources of error in the comparison results from not knowing the density of the organics and burlap, and from not knowing the amount of organics attached to the cans. In the case of one bag, vegetable grease attached to the tin cans was counted as tin can and not as organics, and thus would overestimate the density. In any event, it is probably safe to assume that the measured densities are lower than actual by a factor of 2 to 3.

Frontal Area. The bag frontal area (the area that would likely present itself to settling in the water column) was determined to be between 1920 and 2240 cm^2 with an average area of 2070 cm^2. Making this measurement by either tracing the bag outline as it sat on the ground, or using an ellipse as an estimate of the shape produced similar results. These measurements of frontal surface area are not only useful for calculating a drag coefficient that can be used to estimate lateral transport, but also can be used for determining the size of its impact area when making mass loading estimates.

Fall Velocities. Settling velocities of bags dropped into San Diego Bay ranged from 0.51 to 0.59 $m \cdot s^{-1}$ and averaged 0.54 $m \cdot s^{-1}$. The velocities were constant after 2 s suggesting that the time to fully flood the bag and reach terminal velocity was negligible when considering settling rates. This result indicates that the bags sink relatively quickly. This along with the estimate of density suggests that they would sink unimpeded through the water column given any seawater stratification condition.

9.2 Biological Interactions

9.2.1 Methods

Although shredded metal and glass material will not remain in the water column for very long, after reaching the bottom, it is expected that some of the material will solubilize. To determine whether there are any effects from this liquid-phase, the shredder bags were subjected to the same suite of elutriate tests described above in section 8.3.1.

9.2.2 Results

Effects of Shredded Metal on *Mysidopsis bahia*. Three assays conducted at an initial 5% leachate level resulted in no significant mortality. No dose-response was observed. No LC_{50} was observable in three tests with *Mysidopsis bahia* using this leachate. After 96 hours of exposure, the NOEC value was a 100% solution of the initial 5% leachate in each of the three assays.

Effects of Shredded Metal on *Menidia beryllina*. Three assays conducted at the 5% initial leachate level resulted in no mortality in any test concentration. No LC_{50} was observed in tests with *Menidia beryllina* using this material leachate. After 96 hours of exposure, the NOEC value was a 100% solution of the initial 5% leachate in each of the three assays.

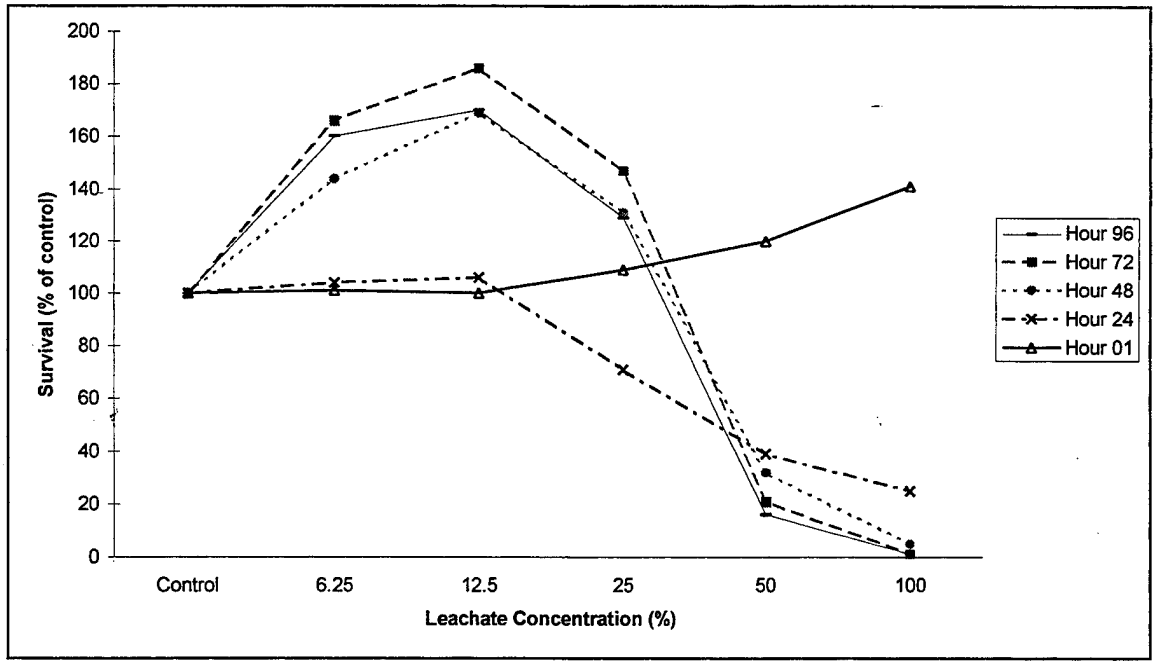

Figure 9-2. Relative fluorescence *Skeletonema costatum* for 1, 24, 48, 72, and 96 hour exposures of 25% shredded metal elutriate. IC_{50}=58.8% and NOEC=25% of the elutriate.

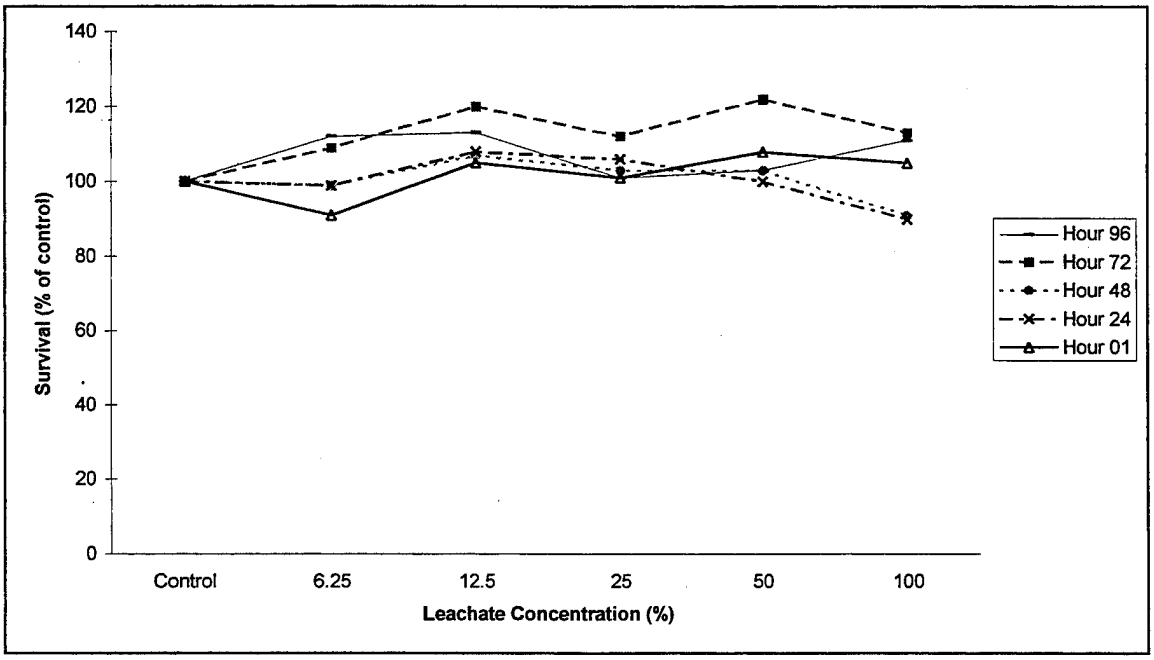

Figure 9-3. Relative fluorescence of *Skeletonema costatum* for 1, 24, 48, 72, and 96 hour exposures of 5% shredded metal elutriate. No toxicity was noted. NOEC=100% because no effects were observed at any dilution nor at any duration.

Effects of Shredded Metal to *Skeletonema costatum* (Clone "Skel"). A 25% shredded metal leachate assay resulted in a dose-response and an IC_{50} value at a 59% dilution of the initial 25% leachate (figure 9-2). After 96 hours of exposure, the NOEC value was equal to a 25% dilution of the initial 25% leachate. One assay at the 5% initial leachate level resulted in no decline or enhancement of plant biomass (figure 9-3). No IC_{50} was observable in tests with *Skeletonema costatum* using this leachate. After 96 hours of exposure, the NOEC value was a 100% solution of the initial 5% leachate.

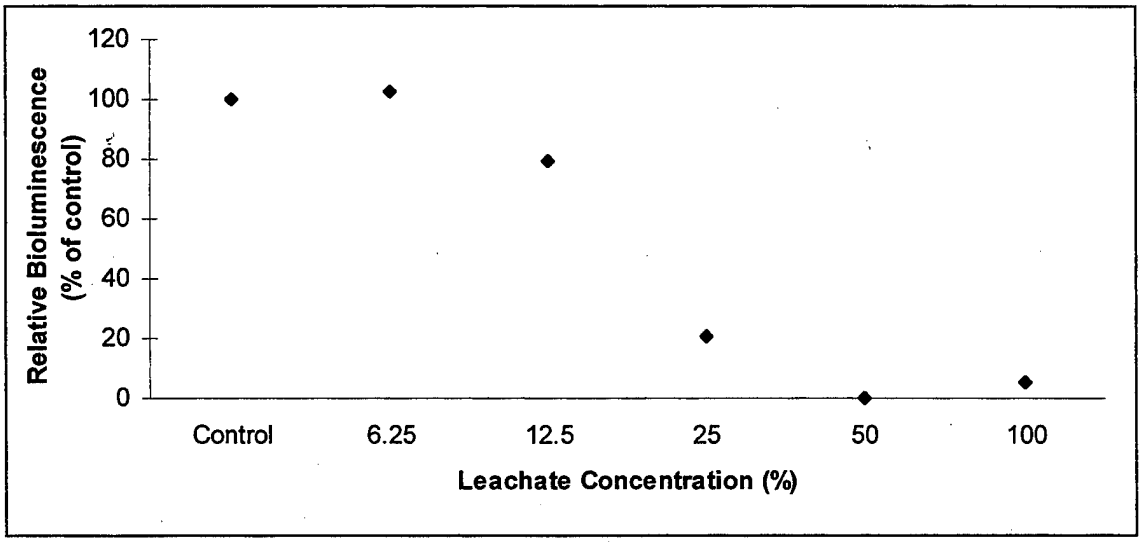

Figure 9-4. Relative dose response of *Gonyaulax polyedra* represented as a percentage of control exposed to dilutions of 25% shredded metal elutriate for 96 hours. IC_{50}=18.8% and NOEC=6.25% of the 25% elutriate.

Effects of Shredded Metal to *Gonyaulax polyedra.* A 25% leachate resulted in a dose-response curve and an IC_{50} value at 96 hours at a 18.8% dilution of the initial 25% leachate (figure 9-4). After 96 hours of exposure, the NOEC value was determined to be a 6.25% dilution of the initial 25% leachate. One assay conducted at the 5% initial leachate level resulted in a dose-response curve and an IC_{50} value at 96 hours at a 18.7% dilution of the initial 5% leachate (figure 9-5). An NOEC value was not applicable after 96 hours of exposure.

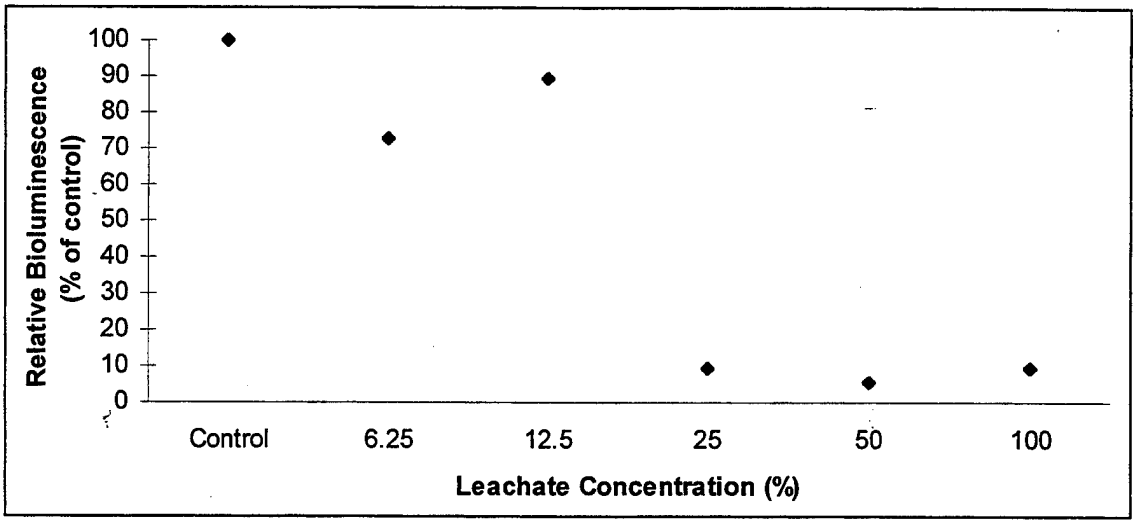

Figure 9-5. Relative dose response of *Gonyaulax polyedra* represented as a percentage of control exposed to dilutions of 5% shredded metal elutriate for 96 hours. IC_{50}=18.7% of the 5% elutriate. NOEC not applicable because effects were observed at all test dilutions.

Effects of Shredded Metal to *Photobacterium phosphoreum* (Microtox). A 25% metal leachate, centrifuged and noncentrifuged, was tested using four dilutions and a control for 5 and 15 minutes of exposure time. Only one trial was performed. The centrifuged sample appeared more toxic than the noncentrifuged sample. This may have been due to enhanced stimulation in the noncentrifuged sample which contained a white residue. This white material resembled vegetable shortening, and was observed on some of the metal pieces used to produce the leachate. The 5 and 15 minute EC_{20} values for the centrifuged sample were 27.5% and 46%, respectively. Both EC_{50} values exceeded 100% leachate. The 5 and 15 minute EC_{20} values for the noncentrifuged sample were 89% and 80%, respectively. The EC_{50} values for both the 5 and 15 minute tests exceeded 100%. A NOEC value was not applicable after 15 minutes of exposure due to an effect observed in the lowest concentration tested.

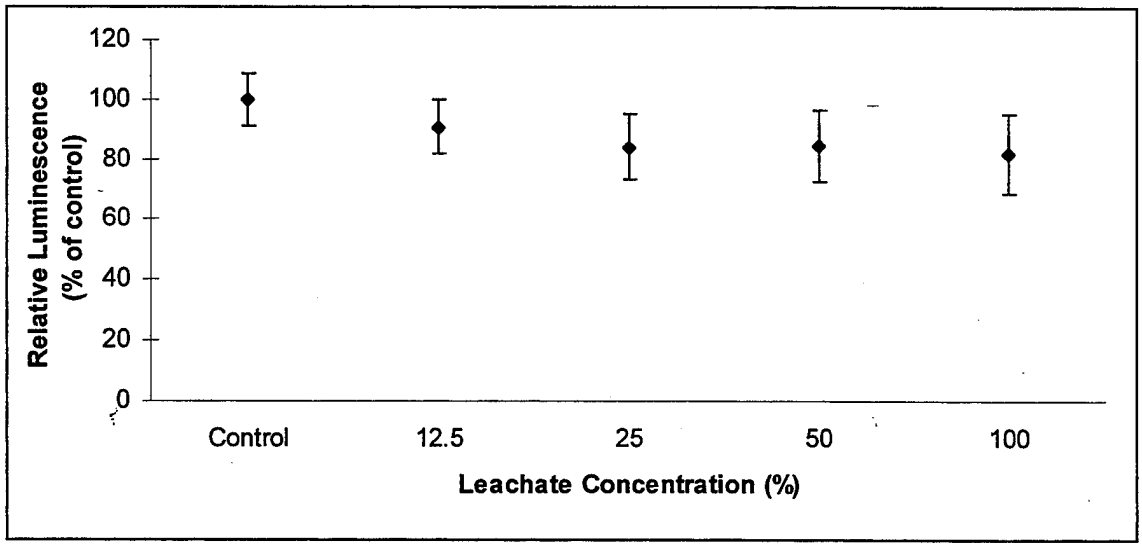

Figure 9-6. Relative light output for *Photobacterium phosphoreum* exposed to dilutions of 5% shredded metal elutriate. NOEC not applicable because effects were observed at all test dilutions.

A centrifuged 5% metal leachate was tested using four dilutions and a control for 5 and 15 minutes of exposure (figure 9-6). After 5 minutes an EC_{20} value at a 44% dilution of the initial 5% leachate was observed. No EC_{50} was noted although there was a 23% reduction in light output at a 100% solution of the initial 5% leachate. After 15 minutes, of exposure, no EC_{20} or EC_{50} value was noted and only a 13% reduction of light output occurred in the 100% solution of the initial 5% leachate. An NOEC value was not applicable after 5 or 15 minutes of exposure due to effects observed in the lowest concentration tested.

Table 9-3. Summary of pulped paper elutriate test results. Elutriate concentration is percent by weight of pulped paper added to seawater to make the test solution. The endpoints measured were survival in the mysids and minnows (LC_{50}), inhibition of bioluminescence of *G. polyedra* (IC_{50}), inhibition of lumnescence in *Photobacterium phosphoreum* (EC_{50}), and biomass or chlorophyll fluorescence inhibition (IC_{50}) in the diatom tests.

	Elutriate Concentration	
Test Species	25%	5%
Mysidopsis bahia	Not Tested	LC_{50}>100% NOEC=100%
Menidia beryllina	Not Tested	LC_{50}>100% NOEC=100%
Skeletonema costatum	IC_{50}=59% NOEC=25%	IC_{50}>100% NOEC=100%
Gonyaulax polyedra	IC_{50}=18.8% NOEC=6.25%	IC_{50}=18.7% NOEC=NA
Photobacterium phosphoreum	EC_{50}>100% NOEC=NA	EC_{50}>100% NOEC=NA

Complete results of the above bioassays are tabulated and graphed in appendix C and summarized in table 9-3. The above results suggest that the NOEC level for shredder material in most of the species tested was between 5% and 25%. At the 5% elutriate level, only *Gonyaulax polyedra* appeared to show an effect. This is likely the result of its high sensitivity to dissolved metal concentrations. It also suggests that further tests be run to confirm the result and to obtain a better estimate of NOEC.

As discussed previously, these laboratory bioassay results are useful in understanding the potential effects on organisms in the field only when actual exposure (magnitude and duration) levels in the field are determined. In the case of the shredder bag waste stream, the bags are likely to settle onto the bottom without producing any effects within the water column. Once deposited on the bottom any solubilized material would quickly be diluted by the surrounding water. To determine exposure, the concentration at a fixed distance away from the surface of the shredder material and an assumed fixed volume could be used to calculate what the effective elutriate concentration would be. The 25% or 5% elutriate concentration levels tested would certainly be concentrations found within the bag itself, and only within a small volume surrounding the material inside the bag. All the above results showing some effect would therefore only be applicable to the area within the bag.

The biological interaction tests were designed to look at effects and not their cause(s). Although the leachates were not tested chemically, the presence of the potentially toxic Sn coatings on the steel cans suggest a likely causitive agent. This analysis could be pursued although a full analysis for toxic agents could be costly, especially in light of the minimal effects observed at environmental concentrations.

9.3 Long-Term Monitoring and Corrosion Analyses

Long-term Monitoring Methods. A qualitative study of degradation of shredder bags was carried out. This was done by dropping the bags into San Diego Bay and monitoring them visually over time with an underwater video system. Three bags numbered 1 through 3, were placed on the bottom off NRaD pier 159 on 6 July 1994. They were placed on a mostly sand bottom at a depth of about 4 m at mid-tide. Tidal height variation is approximately 2 m. The bags were visually inspected with a video recorder at random time intervals to observe any degradation, biological growth, or silting over. On 30 May 1995, some pieces of the shredded material were brought up for visual inspection and sent off for corrosion analysis.

9.3.1 Methods

Table 9-4. Sample descriptions of metal components randomly selected and analyzed for the corrosion study. These samples are shown in figure 9-7.

Sample Label	Description
A	Tin-plated can lid
B	Tin-plated can lid
C	Tin-plated can body with attached bottom; can interior is white
D	Tin-plated can body
E	Pepsi® can body and top lid
F	Coca Cola® can body and top lid
G	Sunkist Orange® can body and top lid
H	Pepsi® can body
I	Tin-plated can body

Metal components from one of the shredder bags were randomly selected for corrosion analysis. The samples of shredded food container waste that were received for analysis in the materials laboratory are shown in figure 9-7. Sample descriptions are given in table 9-4.

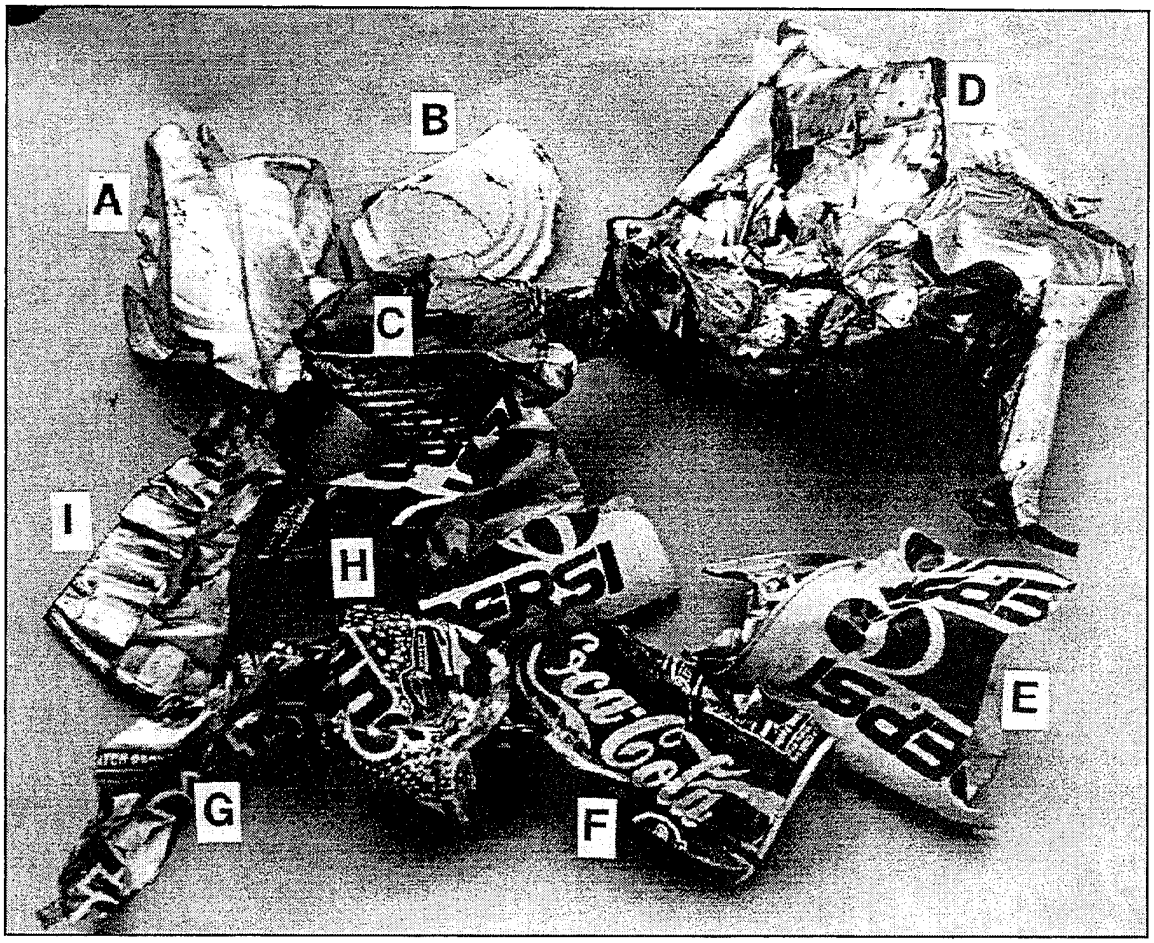

Figure 9-7. Samples of shredded metal/glass waste received for analysis.

The samples consisted of some tin-plated can bodies and lids as well as some aluminum beverage cans. An initial visual examination showed that both the tin-plated cans and the aluminum cans had organic coatings at least on their interior surfaces, and maybe some on the exterior surfaces as well. The aluminum beverage cans had decorative paint on their outer surfaces. Pieces from samples B, C, and D were attached to an aluminum scanning electron microscope (SEM) stub with conductive copper tape and sputter coated with a thin layer of gold before examination in the SEM.

Pieces from samples C, D, E, F, and G were mounted on edge in filled epoxy hot pressed mounts. The mounts were ground through 600 grit silicon carbide paper. The samples were examined with direct and polarized light and selective photographs were made of the overall can wall configuration and of the coatings on the materials. The container thicknesses for the samples were measured using a calibrated eyepiece reticle. Some of the coatings were pigmented and active to polarized light, making them easily seen, while others were not. The coatings on the aluminum cans were difficult to see, and the actual coating boundaries could not be positively identified. The samples were further polished with 6 micron diamond slurry on a cotton cloth and reexamined. Finally, the samples were etched to reveal the can metal microstructure.

Representative photomicrographs were made. The mount was then given a thin gold coating and examined in the SEM.

The aluminum cans had organic coatings on the inside of the body and organic coatings on both the insides and outsides of the lids. Most of the paint was removed from the metal surface by light grinding with silicon carbide abrasive paper. The organic coatings and remaining paint were removed from the samples by heating them in the flame of a Meeker burner. Samples weighing about 0.2 g were then dissolved in 5 mL concentrated nitric acid (HNO_3), 5 mL of concentrated hydrochloric acid (HCl), and 5 mL of deionized water. The solutions were diluted to 100 mL with deionized water and analyzed using ion coupled plasma (ICP) spectroscopy.

Rectangular pieces of the tin-plated can material were cut from samples A, C, and D. The areas of the pieces were measured. The samples were immersed in concentrated hydrochloric acid to remove the organic coatings and tin plating. The samples were attacked by the acid at edges and defects in the organic coatings. After about an hour the organic coatings were undercut by the acid and floated free from the samples; the tin platings had been dissolved. The samples were removed from the acid solution and washed with deionized water. The hydrochloric acid solutions were analyzed for tin using the ICP spectrometer. Pieces of steel from what remained of the samples were used for chemical analysis. Samples for ICP analysis were weighed, then dissolved in a mixture of 2.5 mL of concentrated HNO_3, 2.5 mL of concentrated HCl, and 2.5 mL of deionized water. Solutions were diluted to 50.0 mL and then analyzed by ICP spectroscopy. Samples for carbon/sulfur analysis were weighed into crucibles and combusted in the carbon/sulfur analyzer.

9.3.2 Long Term Monitoring Results

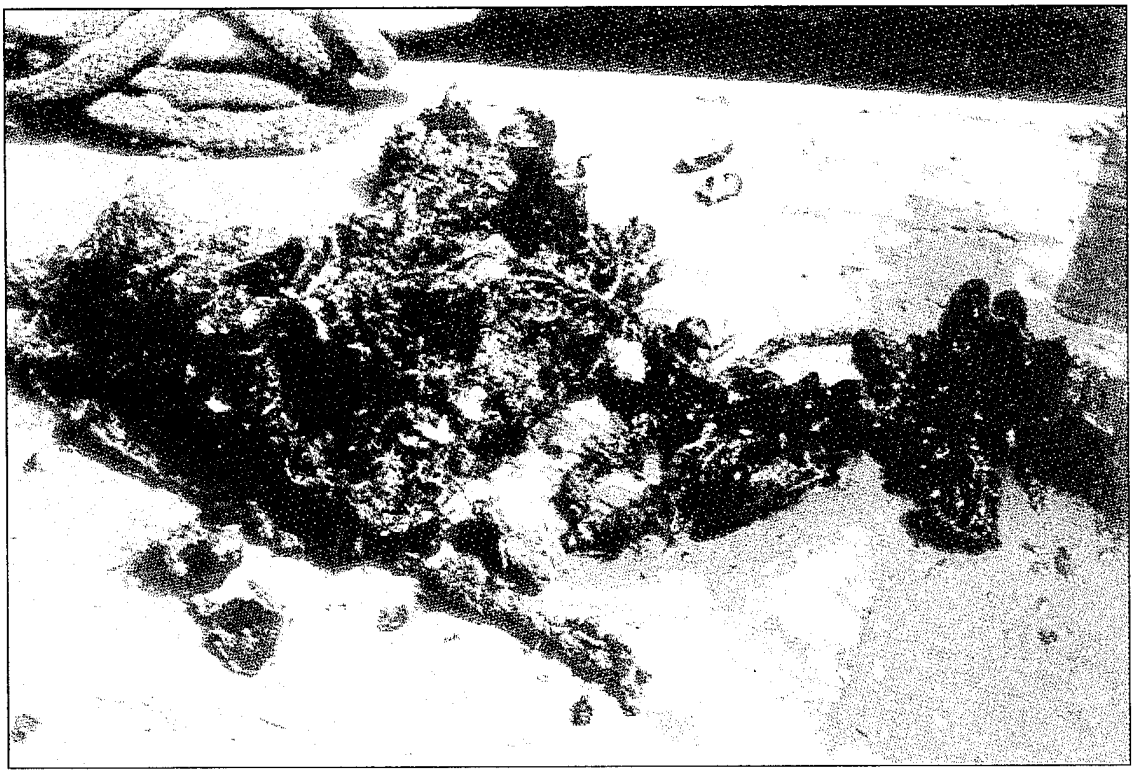

Figure 9-8. Shredded metal pieces coated heavily with marine life.

Long-Term Monitoring. The three bags placed onto the sediment surface in San Diego Bay were monitored for about a year. The bags were occasionally checked between 6 July 1994 and 30 May 1995. After about two months, while attempting to lift the bags, the burlap, weakened by degradation, broke, and the materials inside were deposited on the bottom. On 30 May, attempts to videotape the material on the sediment surface were made difficult because much of it had been silted over, or possibly because it could not be recognized as anything different from other items normally found on the bottom. However, when lifting up one of the lines previously attached to the burlap, a conglomeration of metal pieces heavily coated with marine life was found (see figure 9-8). This bundle was not recognizable as shredded metal without pulling organisms off (possibly the reason why the video was not useful). The amount and diversity of organisms was quite large, suggesting a healthy community. Metal pieces recovered at this time were sent on for corrosion analysis. The following is a list of some of the species observed:

Amphipods	Bryozoans	Limpids	Scallops
Annelids	Clams	Mussels	Shrimp
Barnacles	Crabs	Oysters	Sponges
Brittle Stars	Hydrozoans	Radiolarians	Tunicates

The high diversity of the community found attached to the shredder material suggests that, at a minimum, the material was not detrimental to the organisms found there. This does not, however, preclude any negative effects, particularly to highly sensitive species. The effects observed for

Gonyaulax in the bioassay tests might be considered indicative of a sensitive species. However, exclusion of species from the surface of the material can only be considered to be an adverse condition if the surface area of shredder material is sufficiently large relative to the areal extent of the normal habitat. Although discussed in detail later within the context of mass loading to Special Areas, it can be safely assumed here that the amount of surface area provided by the shredder material is likely to be insignificant.

9.3.3 Corrosion Results

Table 9-5. ICP chemical analysis results for shredded aluminum containers compared to standard aluminum alloys. Values are in weight percent of total; balance is aluminum.

Sample	Cr	Cu	Mg	Mn	Si	Ti	Zn	Fe
Sample E body	0.005	0.181	1.09	1.01	0.132	0.018	0.05	0.40
Sample F body	0.007	0.160	1.06	1.08	0.162	0.024	0.03	0.36
Sample E lid	0.019	0.028	4.01	0.288	0.030	0.009	0.01	0.19
Sample F lid	0.010	0.009	4.10	0.291	0.030	0.014	0.01	0.15
3004 Specification	-	0.25 max	0.8-1.3	1.0-1.5	0.30 max	-	0.25 max	0.7 max
5182 Specification	0.10 max	0.15 max	4.0-5.0	0.20-0.50	0.20 max	0.10 max	0.25 max	0.35 max

Aluminum Containers. The results of the ICP analysis for the aluminum containers are given in table 9-5. The chemistry of the body alloy is consistent with aluminum alloy type 3004 while the lid is consistent with type 5182. The dimensions of the aluminum containers measured by metallography are given in table 9-6.

Table 9-6. Coating and metal thickness of shredded aluminum containers.

Sample	Metal Thickness (in)	Coating thickness (in)
Sample G, side wall	0.0044	
Sample F, side wall	0.0043	0.0002
Sample F, upper side wall	0.0067	0.0002
Sample H, bottom	0.0128	
Sample H, lower side	0.0101	
Sample F, top	0.0096	
Sample F, pop top	0.0090	
Sample F, pull tab	0.0133	

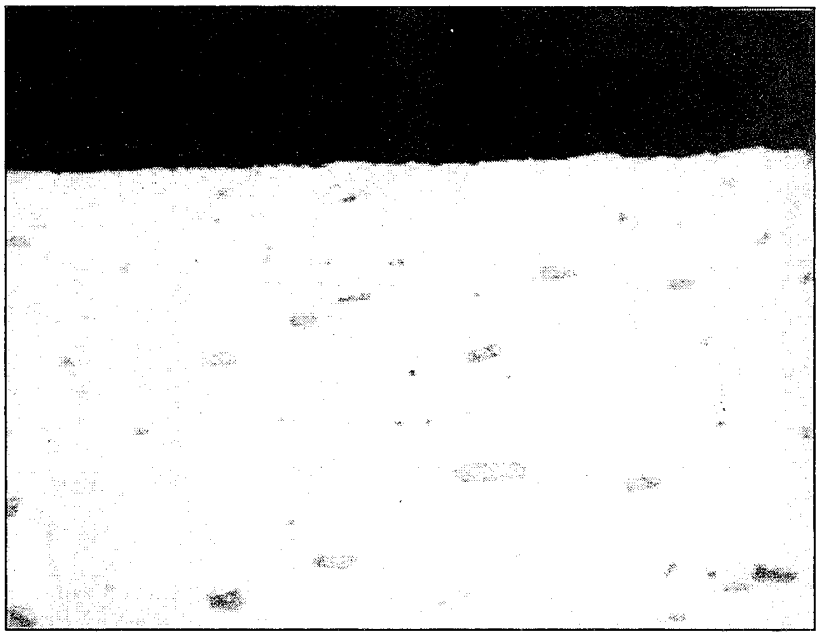

Figure 9-9. Micrograph of the aluminum side wall of sample F. The inner coating is just barely visible.

Figure 9-9 is a micrograph of the aluminum side wall of sample F. The inner coating is just barely visible. It is presumed that this is an organic coating of some type, but its exact nature is not known. Also visible in the microstructure of the aluminum are inclusions of aluminum-manganese intermetallic particles that are typical of this alloy type. Figure 9-10 is a micrograph of the top-to-side joint from sample F. Modern aluminum beverage cans are two piece cans that have joints only on the top lid. The bottom of the can is formed from the same piece of metal as the can side walls.

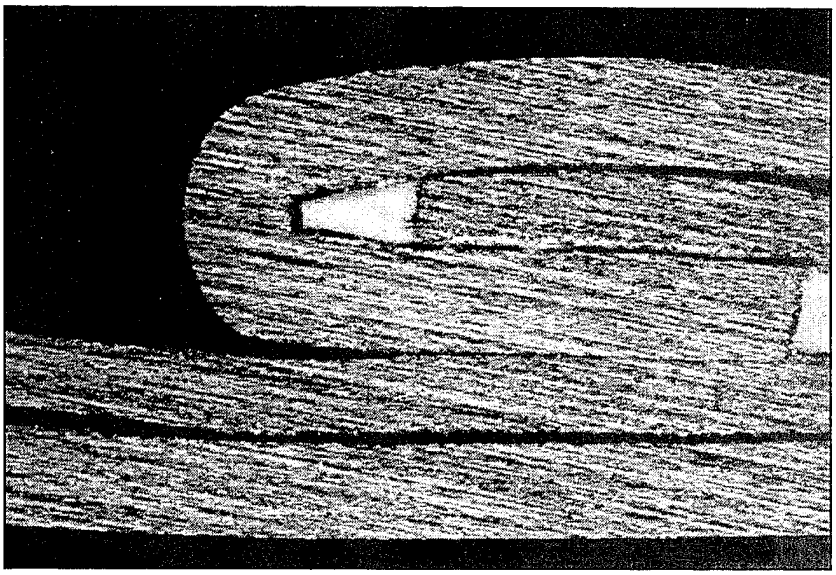

Figure 9-10. Micrograph of the top-to-side joint from sample F.

Table 9-7. Corrosion rates for type 3003-H14 aluminum under varying environmental conditions (Reinhart, 1976). Corrosion rates are reported for aluminum exposed in the water column and buried in the sediments in units of mpy.

Depth (ft)	O_2 Concentration (ml/l)	pH	Salinity (ppt)	Temperature °C	Exposure time (days)	Rate Exposed (mpy)	Rate Buried (mpy)
5	5.9	8.1	33.51	15	181	1.1	-
5	5.9	8.1	33.51	15	366	1.0	-
5	5.5	8.1	33.31	15	588	1.2	-
2340	0.4	7.5	34.36	5	197	1.2	1.6
2370	0.4	7.5	34.36	5	402	1.4	1.7
5640	1.3	7.6	34.51	2.3	123	0.5	1.9
5640	1.3	7.6	34.51	2.3	751	2.3	2.5
5300	1.2	7.5	34.51	2.6	1064	2.0	1.9
6780	1.6	7.7	34.40	2.2	403	3.9	3.7

Reinhart (1976) has no corrosion data for type 3004 aluminum. He does give data for type 3003-H14 (shown in table 9-7), which does not have the 1% magnesium that is present in type 3004. Since magnesium additions have been shown to not affect the pitting potential of aluminum alloys (Beavers et al., 1986), the performance of type 3003 would be similar to that of type 3004. The "H14" in the designation refers to some strain hardening to the alloy. The aluminum in beverage can bodies is severely strain hardened. These data appear somewhat scattered, but the corrosion rates are higher at the greatest depths. Similarly, there are no data for type 5182, but the data for most 5000 series aluminum alloys are very similar. The 5000 alloys

tend to be more corrosion resistant than the 3000 series alloys (table 9-8). The composition of type 5086 (4% Mg, 0.4% Mn) is not too different from the lid alloy 5182.

Table 9-8. Corrosion rates for type 5086 aluminum under varying environmental conditions (Reinhart, 1976). Corrosion rates are reported for aluminum exposed in the water column and buried in the sediments in units of mpy.

Depth (ft)	O_2 Concentration (ml/l)	pH	Salinity (ppt)	Temperature °C	Exposure time (days)	Rate Exposed (mpy)	Rate Buried (mpy)
5	5.9	8.1	33.51	15	181	1.2	-
5	5.9	8.1	33.51	15	366	0.8	-
5	5.5	8.1	33.31	15	588	1.6	-
2340	0.4	7.5	34.36	5	197	0.7	1.1
2370	0.4	7.5	34.36	5	402	0.6	1.3
5640	1.3	7.6	34.51	2.3	123	0.1	1.4
5640	1.3	7.6	34.51	2.3	751	2.0	-
5300	1.2	7.5	34.51	2.6	1064	0.9	1.2
6780	1.6	7.7	34.40	2.2	403	0.6	0.8

Electrochemical measurements of corrosion potentials and currents on aluminum by Dexter (1980) indicate that the apparent increase in corrosion rates of aluminum with depth is probably due to the effect of reduced pH. He found that when oxygen concentration and pH are varied together, the effect of pH dominates the corrosion rate. Lower pH increases both the pit initiation rate and the pit growth rate.

The above data show very little effect of temperature on the corrosion of aluminum. While one study does indicate that the corrosion rate of 3004 aluminum is a factor of two, higher at 25°C than 10°C, the corrosion rate of type 6061 alloy aluminum in tropical waters near the Panama Canal Zone is not significantly greater than the rate near Port Hueneme, California (Beavers et al., 1986). The passivity of the oxide films on aluminum may be diminished at higher temperatures, as the corrosion mechanism has been seen to change from pitting to uniform attack at higher temperatures (Beavers et al., 1986).

Table 9-9. Corrosion rates for type 5086 aluminum during a five-year shallow-water immersion study (Ailor, 1969). Rates are in units of mpy.

Exposure time	Rate mpy
1 year	0.25
2 years	0.17
5 years	0.15

Corrosion data for shallow-water immersion tests of 5086-H112 by Ailor (1969) are shown in table 9-9. These rates are about an order of magnitude smaller than those observed by Reinhart

(1976). Since exposure conditions are not given in Ailor's study it is difficult to comment critically on the reasons for the difference. It may be that some experimental factor such as the cleaning method is involved.

Tin-Plated Steel Containers. Figure 9-11 shows energy dispersive x-ray spectra from surfaces of the tin-plated steel material that was examined in the SEM. The outside "tin"surface of sample B showed both light and dark regions in the SEM. The dark regions were areas where a thick organic coating was present, as indicated by figure 9-10. The bright areas must have been locations where the organic coating was either very thin or missing altogether. The x-ray spectrum from the bright area (figure 9-11b) shows intense tin and iron lines. Most likely this is from a thin (less than 1 μm) coating of tin that is penetrated by the electron beam to cause x-ray emission from the iron below. The inside can surface of sample B, which had a "gold" appearance, was covered with an organic coating, as is shown from the x-ray spectrum in figure 9-11c. The x-ray spectrum from an area on the same side of sample B where the golden coating had been scraped away is shown in figure 9-11d. Tin is present beneath this coating as well. The tin to iron intensity ratios indicate that the thickness of the tin is probably larger on the "gold" side of sample B than the "tin" side. The x-ray spectra of sample D (figure 9-12) were very similar to sample B. Samples B and D appear to be tin plated on each side and have organic coatings on top of the tin plate. Sample C is tin plated on one side (figure 9-12a) and has a paint-like coating on the other side (figure 9-12b) that contains some titanium dioxide pigment.

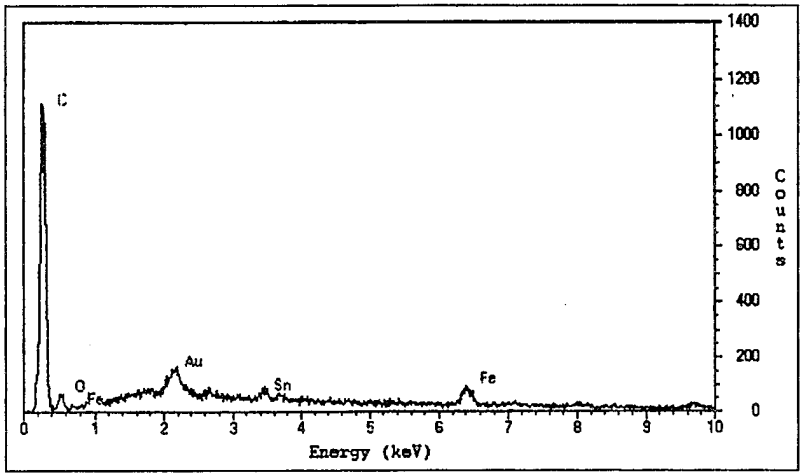

11-a. Organic coating of "tin" side of sample B.

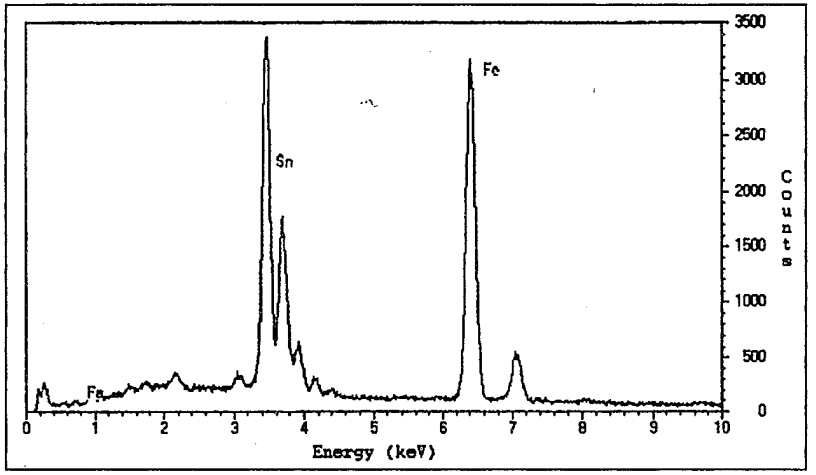

11-b. Tin plate over iron on "tin" side of sample B.

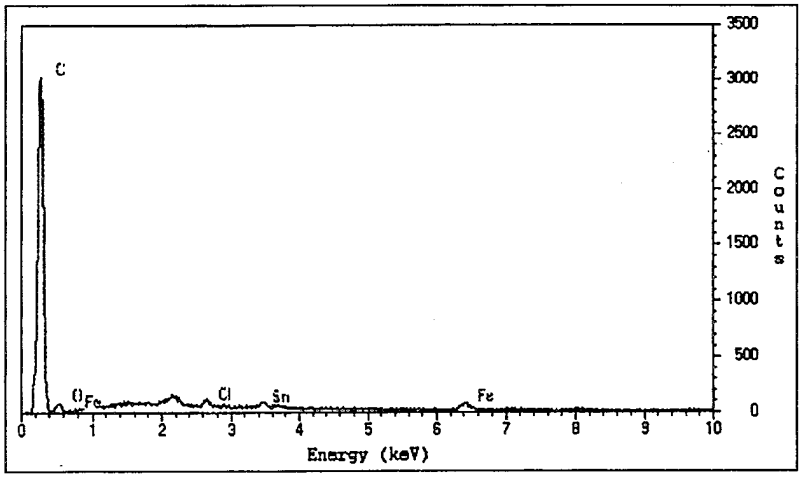

11-c. Organic coating on "gold" side of sample B.

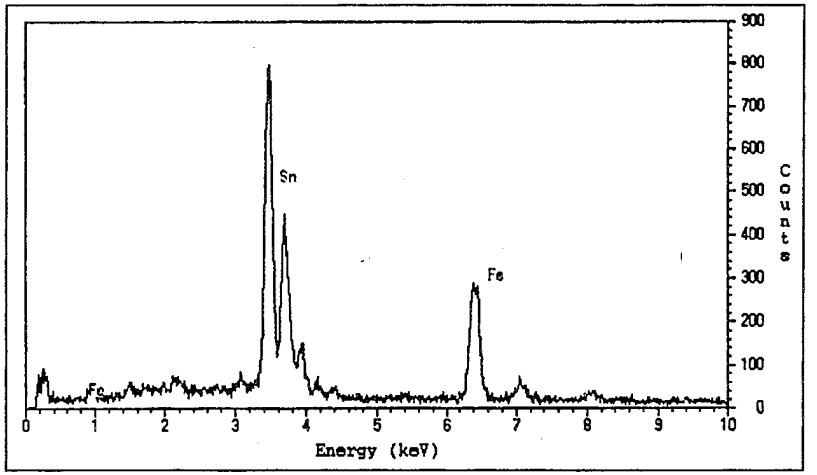

9-d. Thicker tin plate on "gold" side than "tin" side of sample B.

Figure 9-11. Energy dispersive x-ray spectra from surfaces of the tin-plated steel material examined in the SEM for sample B.

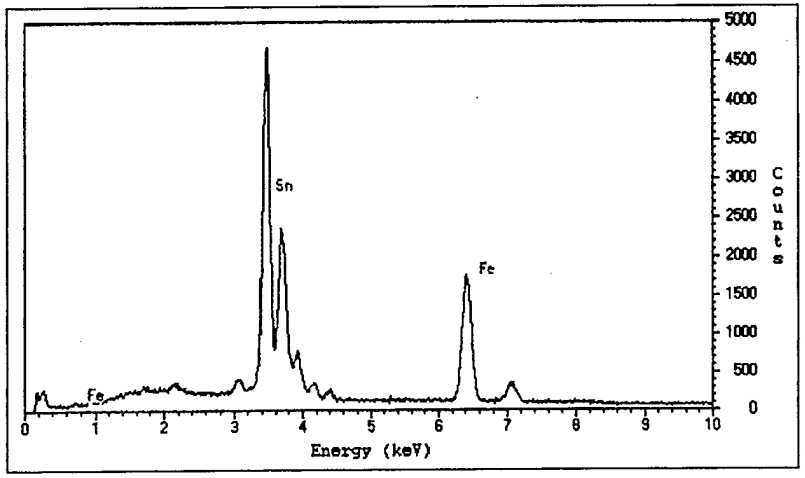

12-a. Tin plate over iron on "tin" side of sample C.

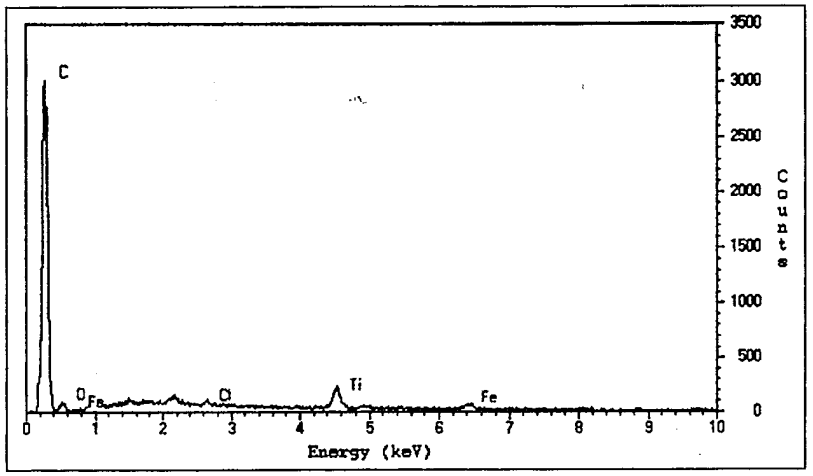

12-b. Paint-like coating on "white" side of sample C.

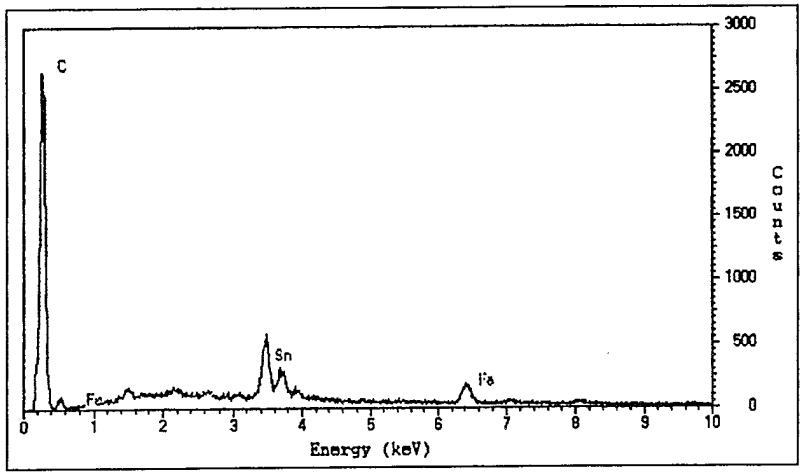

12-c. Tin plate under organic coating on sample D.

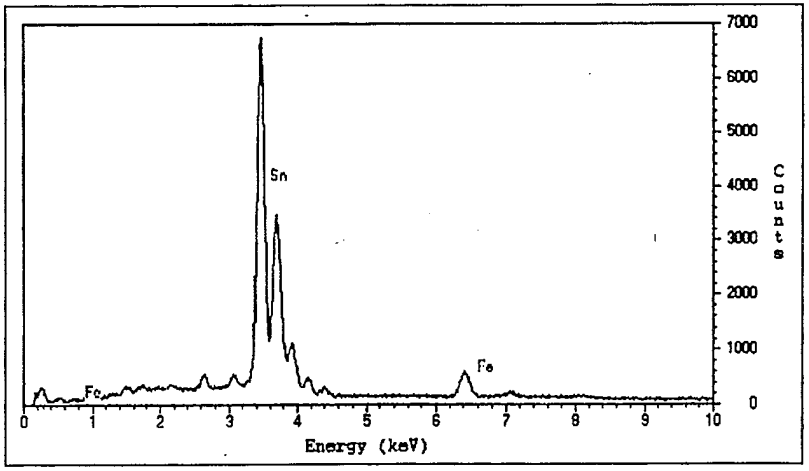

12-d. Scratch on the "gold" side of sample D showing tin plate.

Figure 9-12. Energy dispersive x-ray spectra from surfaces of the tin-plated steel material examined in the SEM for samples C and D.

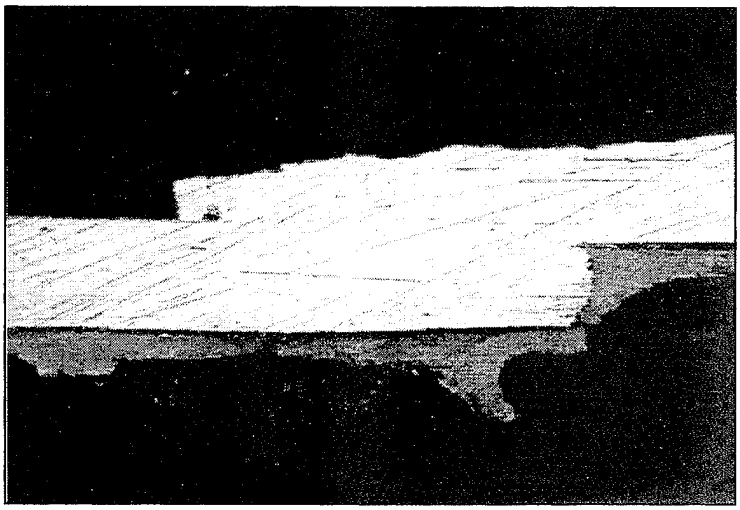

Figure 9-13. Optical micrograph of the bottom-to-side joint from sample C.

The chemical analysis results for the tin-plated steel containers are given in table 9-10. The steel meets the specifications for Type L steel (see ASTM A 623, 1984), a type commonly used for tin-plate food containers. This steel is a mild carbon steel that is very low in residual elements. Table 9-11 gives results of the thickness measurements for tin-plated steel containers. Figure 9-13 is an optical micrograph of the side wall seam from sample D. The seam appears to be a resistance weld. It does not have the bent geometry one would expect from a solder joint. Neither is there evidence of lead in the x-ray spectrum from the joint. A fair amount of an organic coating had been applied around the seam.

Table 9-10. Chemical analysis results for shredded steel can body and lid compared to type L steel specification. Values are in weight percent of total; balance is iron.

Sample	C	Al	Cr	Ni	Mn	Cu	Si	S	P	Mo	V	Co
D	0.110	0.052	0.016	0.018	0.51	0.014	0.010	0.007	0.013	0.000	0.003	0.001
A	0.109	0.022	0.041	0.021	0.43	0.014	0.003	0.009	0.004	0.001	0.002	0.002
Type L specification (maximum values)	0.13	-	0.06	0.04	0.60	0.06	0.020	0.05	0.015	0.05	0.02	0.02

Table 9-11. Coating and metal dimensions of shredded tin-plated steel containers.

Sample	Metal Thickness (in.)	Coating thickness (in.)
Sample C, side wall	0.0096	<0.005
Sample D, side wall	0.0113	0.003
Sample D, welded Seam	0.0131	0.0019
Sample D, near seam	0.0067	<0.005
Sample C, bottom lid	0.0087	0.0002

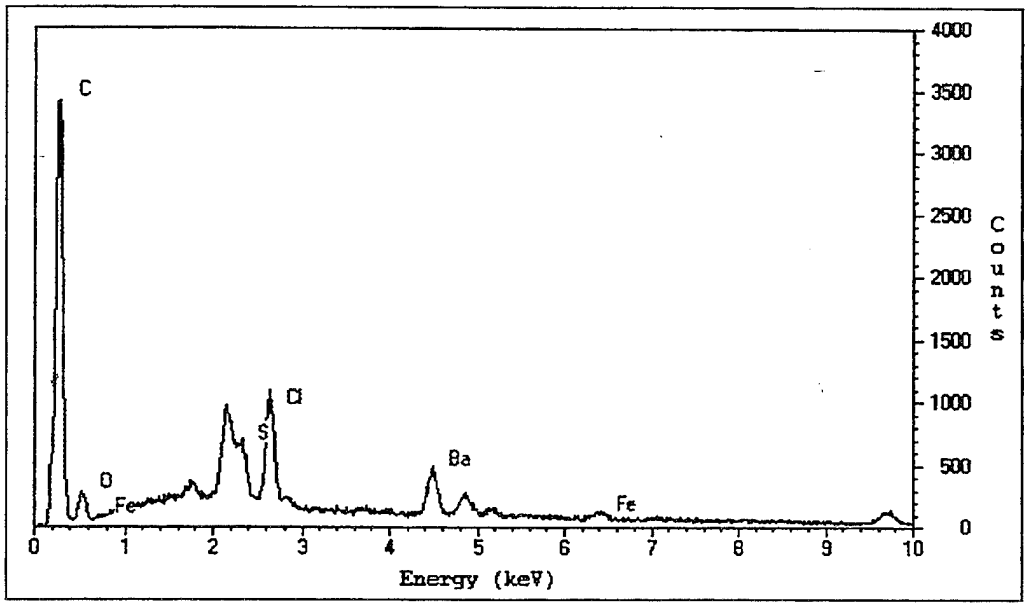

Figure 9-14. X-ray spectrum from the organic coating.

The x-ray spectrum from the coating is shown in figure 9-14. The coating appears to be a chlorinated organic material that is filled with barium sulfate. The barium sulfate may be present as an aid to automated x-ray inspection of the coating integrity.

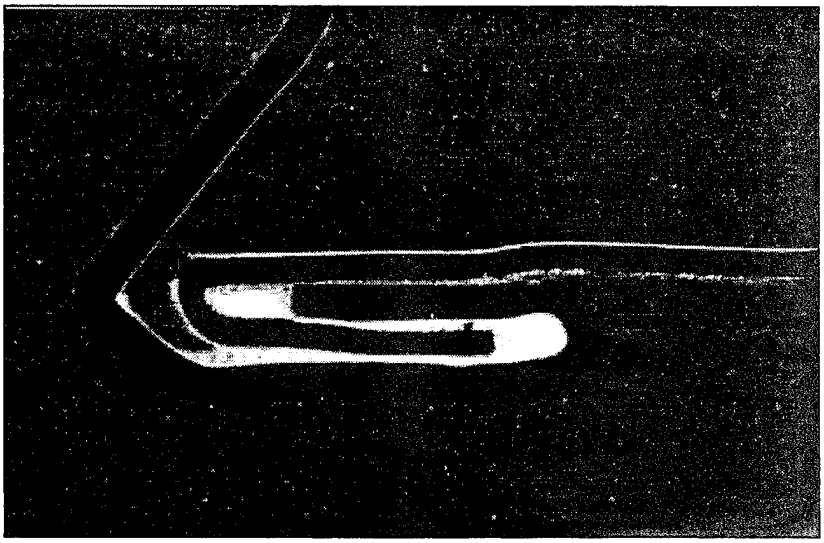

Figure 9-15. Optical micrograph of side joint of sample C.

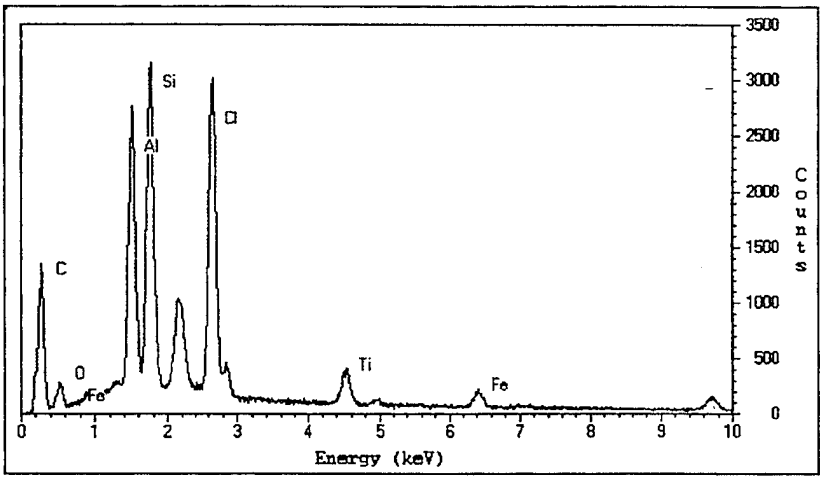

Figure 9-16. X-ray spectrum from joint sealant.

Figure 9-15 is an optical micrograph of the bottom-to-side joint from sample C. The sealant is a chlorinated organic compound, that in this case is filled with aluminum and silicon compounds, probably oxides (figure 9-16). It is also possible that silicon is present as embedded silicon carbide from the grinding media. Figure 9-17 is a micrograph of the sample C side wall that shows the white coating in cross-section. The coating is actually two layers. The layer closest to the steel appears to contain the most pigment. The x-ray spectrum of the layer closest to the steel is shown in figure 9-18. The layer actually looks like a paint that contains a significant amount of titanium dioxide pigment.

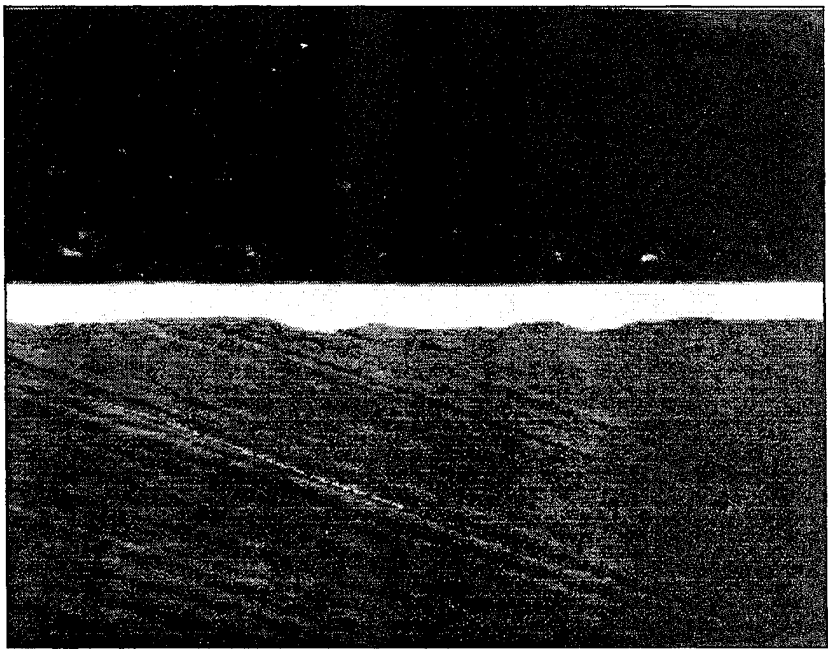

Figure 9-17. Optical micrograph of sample C side wall that shows the white coating in cross section.

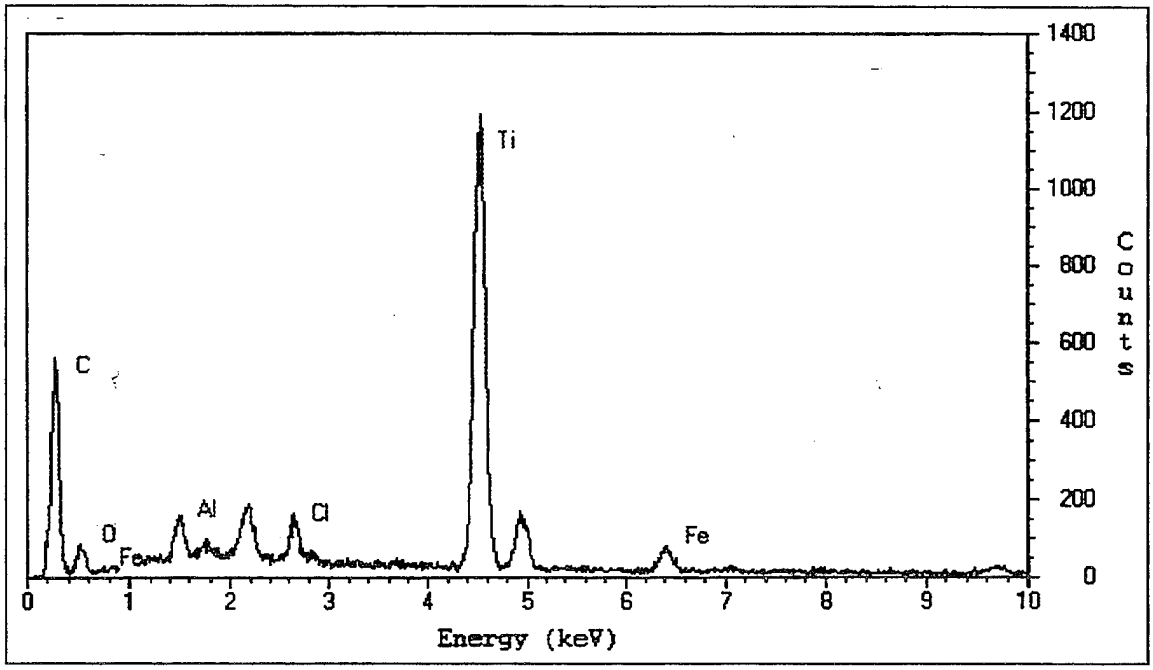

Figure 9-18. X-ray spectrum from the inner coating layer closest to the steel.

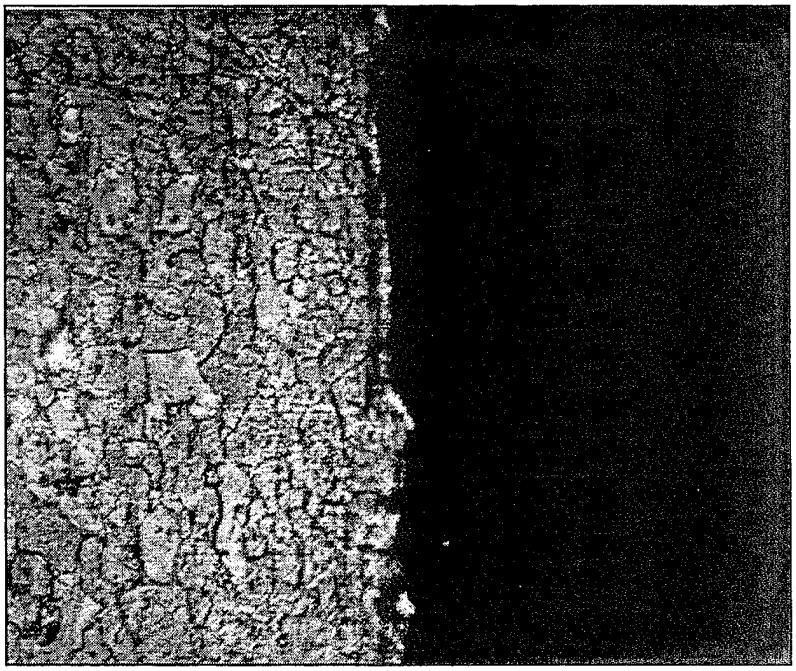

Figure 9-19. Optical micrograph of sample D showing the tin plating

Figure 9-19 barely shows the presence of the tin plating on the etched surface of sample D. The plating is too thin for its thickness to be measured optically. The measurement of tin plating thickness is usually done indirectly by stripping the tin from the sheet and using bulk chemical analysis to determine how much tin was present on a given surface area. Tin plating thicknesses were estimated from the ICP analysis of the solutions containing tin stripped from samples A, C, and D by:

$$t = \frac{m_{Sn}}{\rho_{Sn} A} \qquad \text{(Eq. 9-1)}$$

where t is the total plating thickness, m_{Sn} is the mass of the tin from the analysis, ρ_{Sn} is the density of tin, and A is the area of the sample. The total thicknesses for samples A., B, and C were 45, 10, and 73 micro inches, respectively. In the case of samples A and D, the total thickness includes coatings on both sides. The measurement for sample C is for only one side, as the acid did not attack the paint-like coating on the other side. Examinations in the SEM confirm the presence of a tin plating of around 30 micro inch adjacent to the paint surface on sample C.

Table 9-12. Common tin plating thickness (ASTM Standard A 624, 1984).

Designation	Tin Coating weight each surface (lb/base box)	Tin Thickness each side (micro inch)
10	0.05/0.05	06/0.06
20	0.10/0.10	12/12
25	0.125/0.125	15/15
35	0.175/0.175	22/22
50	0.25/0.25	30/30
75	0.375/0.375	45/45
100	0.50/0.50	60/60
D 50/25	0.25/0.125	30/15
D 75/25	0.375/0.125	45/15
D 100/25	0.50/0.125	60/15
D 100/50	0.50/0.25	60/30
D 135/25	0.675/0.125	82/15

While the samples that were examined are somewhat limited, some conclusions about the materials can be drawn. Food containers are made from a mild steel that has a low concentration of residual elements. The cans may or may not have tin platings. Some foods, such as tomatoes, are known to taste better if there is no organic coating on the inside of the can consequently, cans may or may not have organic coatings. Joints are sealed with organic sealants that can contain a variety of inorganic fillers. We observed no lead containing solders, but our sample was quite limited. The more corrosion resistant organic coatings (and the thicker tin plate) will usually be on the inside of the can. The measured thicknesses of the cans (with the exception of seam areas) ranged from about 0.009 inch to 0.013 inch. In the tin industry this is commonly referred to as 80 to 112 lb "plate." The samples that we examined had varying thickness of tin plating. Table 9-12 lists common tin-plating thickness.

The tin plating thickness measurement of sample D shown in table 9-11 is consistent with a D 100/25 differential coating. Sample A is consistent with a D 50/25 differential coating. Sample C is probably also from a D 50/25 differential coating. The thickness of the thin platings thus can vary from can to can (or between bodies and lids) and between the inside and outside. The thicker tin platings are usually on the inside of the can. A "base box" of tin-plated sheet, for the thicknesses common in food containers, will weigh around 100 pounds. Thus, less than 1% of the mass of a tin-plated steel food container is tin.

Table 9-13. Corrosion rates for AISI 1010 steel under varying environmental conditions (Reinhart, 1976). Corrosion rates are reported for aluminum exposed in the water column and buried in the sediments in units of mpy.

Depth	O_2 Concentration (ml/l)	pH	Salinity (ppt)	Temperature °C	Exposure time (days)	Rate Exposed (mpy)	Rate Buried (mpy)
5	5.9	8.1	33.51	15	181	9.1	-
5	5.9	8.1	33.51	15	366	8.0	-
5	5.5	8.1	33.31	15	588	8.9	-
2340	0.4	7.5	34.36	5	197	1.6	1.2
2370	0.4	7.5	34.36	5	402	1.1	1.1
5640	1.3	7.6	34.51	2.3	123	2.7	1.9
5640	1.3	7.6	34.51	2.3	751	0.8	0.6
5300	1.2	7.5	34.51	2.6	1064	1.0	0.7
6780	1.6	7.7	34.40	2.2	403	1.9	1.1

Table 9-14. Corrosion rates for JIS SS41 steel for varying depths, oxygen concentration, and pH conditions (Shimada, 1975). Corrosion rates are in units of mpy.

Depth (ft)	O_2 (mL/L)	pH	Exposure time (days)	Rate (mpy) Exposed
6.6	6.9	8.1	720	11
98	6.4		720	9
197	3.3		720	4
295	6.2		720	8

Corrosion rates for pure tin in seawater have been measured both at the surface and at depth (Reinhart, 1976). The rates range from 8 mpy at the surface to 0.5 mpy at 1665 m. The rates are somewhat correlated with the dissolved oxygen content. In seawater, tin is cathodic to (more noble than) iron, so one might expect iron in contact with tin to corrode preferentially. However, with the very thin tin platings present on our samples (0.015 to 0.060 mil), it seems likely that the tin plating (where not protected by organic coatings) would be rapidly undercut and spalled away from the can surface by iron oxide corrosion products. The tin plating should corrode away quite rapidly in seawater. Table 9-13 shows corrosion rate data for AISI type 1010 steel, a mild steel very similar in composition to the Type L steel used in tin-plated food cans. Table 9-14 shows

corrosion rate data for JIS SS41steel (equivalent to AISI 1020), a mild steel with around 0.2% carbon.

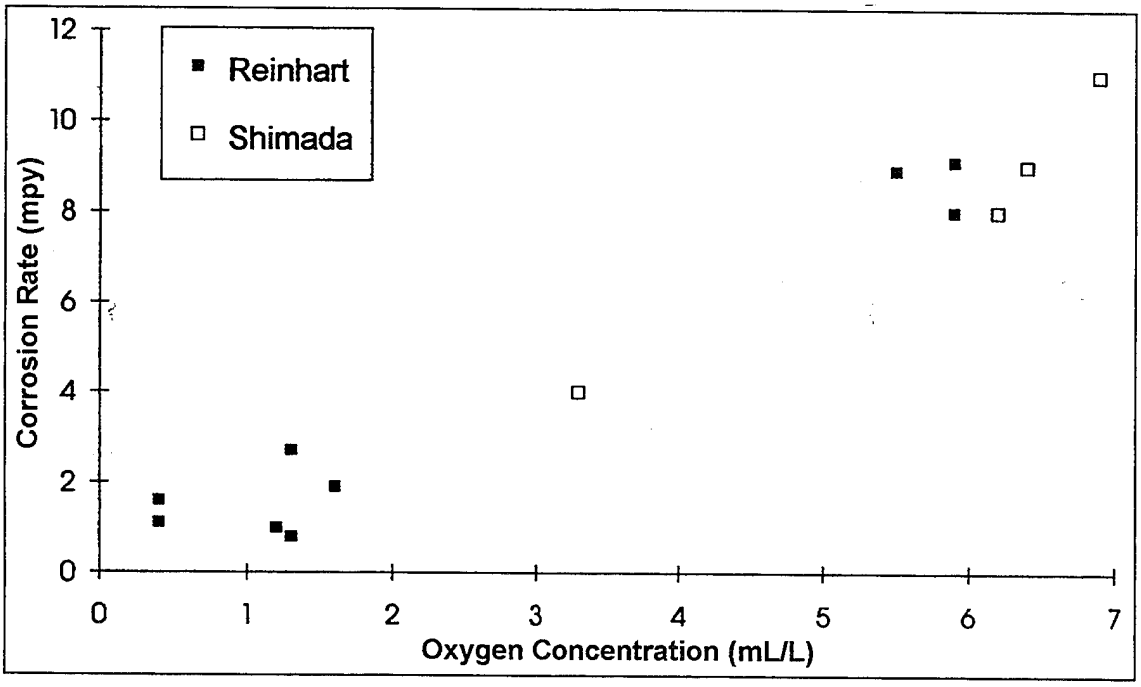

Figure 9-20. Corrosion rate of mild steel as a function of oxygen concentration.

The data from the Reinhart (1976) and Shimada et al. (1975) studies show remarkably good correlation between oxygen content and corrosion rate, as is shown in figure 9-20. However, the Shimada et al., (1975) study also examined corrosion rates in a polluted bay where the dissolved oxygen concentration was only 0.09 $mL \cdot L^{-1}$. The corrosion rate under those conditions was about 7.9 mpy, much larger than would be expected from the oxygen level. This may be due to the presence of sulfate reducing bacteria and the sulfide that they produce. The presence of sulfide generally increases the corrosion rate of steel in seawater. This may be due to catalytic effects that increase the rates of both the oxidation and reduction reactions at the steel surface, as well as stabilization of the corrosion products as insoluble sulfides (West, 1980).

Peterson and Lennox (1984) measured the corrosion rates of mild steel where the mean temperature was 25°C, the mean dissolved oxygen content was 8.6 $mL \cdot L^{-1}$, and the mean pH was 8.07. Samples were exposed in a laboratory cell at a low flow rate, from a pier with normal tidal flow, and in a flume at flow of 0.23 $m \cdot s^{-1}$. The corrosion rates were 2.3, 4.2, and 7.9 mpy, respectively. While these data show the effect of flow, the corrosion rates are somewhat less than might be expected from the oxygen concentration when compared with the data in figure 9-20. This is indicative of the variability in results that might be expected between different studies that use perhaps slightly different materials and methodologies at different locations. Other near-surface immersion studies (Beavers et al., 1986) with exposure conditions unknown give initial corrosion rates for carbon steel of about 4 to 5 mpy, which stabilize over the long term (many years) to around 3 mpy.

Controlled laboratory studies suggest that the corrosion of steel is accelerated by increasing temperature (Peterson and Lennox, 1984). However, in natural waters, the temperature has a significant effect on other factors such as the dissolved oxygen concentration and level of biological activity. For example, Shimada et al., (1975) found that in unpolluted seawater the corrosion rates were highest in winter months when oxygen concentrations were highest even though temperatures were lower. In polluted seawater (with very low oxygen levels) the corrosion rates were highest in summer months when biological activity was at its highest. Reinhart and Jenkins (1971) used linear multivariate regression analysis to give the following formula for the dependence of the corrosion rate of steel on oxygen concentration and temperature:

$$Corrosion\ Rate\left(\mu m \cdot yr^{-1}\right) = 21.3 + 25.4\left[0_2\left(mL \cdot L^{-1}\right)\right] + 0.356\left[T\left(^{\circ}C\right)\right] \qquad \text{(Eq. 9-2)}$$

At ocean oxygen concentrations that typically range from 1 to 7 $mL \cdot L^{-1}$, it is clear from equation 9-2 that oxygen concentration dominates the corrosion rate for steel in seawater.

The effect of biofouling on the corrosion rates of steel is open to some question. In theory, marine organism growth should slow uniform attack corrosion by restricting access of oxygen to the steel surface. Pitting and crevice corrosion should be increased by the creation of differential aeration cells at marine organism attachment sites. Comparison of corrosion rates between samples immersed in filtered and unfiltered seawater show no significant difference, either in the general corrosion rate or the depth of pits (Traverso et al., 1979). In another study (Shumacher, 1979), it was noted that under fouling conditions initial corrosion rates can be quite rapid (>13 mpy), proceeding until specimens are covered by marine organisms (after about 1.5 years). At that point, corrosion rates decrease until oxygen is excluded from the specimen surface and corrosion is controlled by sulfate reducing bacteria. The corrosion rates then stabilize at about 2 to 3 mpy.

10.0 DISPERSION AND FATE MODELING

10.1 Methods

As was previously discussed, the hydrodynamic processes responsible for the dispersion and fate of Naval shipboard paper/cardboard discharge were divided into two separate numerical model studies. One model (TBWAKE) was used to address mixing in the ship's wake over a period of minutes (an equivalent distance of around 10 boat lengths). The second model (SEDXPORT) was used to predict the subsequent ambient dilution over a period of several days. The discharge is considered, for both wake and ambient models, as an infinite line source, so there were no gradients in concentration along the ship's track.

Wake Model

Wake Model Selection. The choice of the wake model was based on its applicability to the U.S. Navy surface ships of interest. Whereas full-scale trials have led to semiempirical wake discharge models for barges (Ball and Reynolds, 1976; Csanady, 1981) and tankers (Delvigne, 1987; Lewis and Riddle, 1989), similar full-scale experiments with U.S. Navy surface ships have not been performed. However, there is an ongoing interest in numerical, as well as full and small-scale, modeling studies of U.S. Naval surface ship wakes. This effort is motivated to minimize the probability of detection of ship wakes, both by satellite (Vesecky and Stewart, 1982; Scully-Power, 1986; Griffin et al., 1992; Meadows et al., 1994) and through the acoustical back-scatter of entrained microbubbles (Hyman, 1990), and as an aid in efficient ship design (Hoekstra, 1991). The numerical models, which are evolving from these efforts, presently provide the best available description of the turbulent flow field in a wake of a surface vessel. One of the most sophisticated models, TBWAKE, was developed to study the evolution of microbubble populations in surface ship wakes. Microbubbles are introduced into the wake via hull boundary layer entrainment, bow and stern wave breaking, and propeller cavitation and ventilation. This numerical model has been verified with full-scale experiments on many classes of U.S. Naval surface craft under a wide range of oceanic conditions. These studies are documented in Hyman and Smith (1987), Hyman et al. (1987), and Hyman (1990,1992,1994). Because discharged particles would be subject to the same wake forces, Dr. Hyman of NCSS was tasked to modify the microbubble computer code for particles, and the microbubble wake model was chosen for the present study.

Overview. The numerical simulation is based on standard convective-diffusive modeling of continuous fluid fields. A considerable body of work in modeling surface ship wakes has accumulated over the last several years. The model to be applied is a parabolic Navier-Stokes solver in which the equations describing the instantaneous flow field are ensemble averaged. The result is a set of three dimensional differential equations which are elliptic in character. If the assumption is made that the streamwise pressure and stress gradients are negligible and that there is no flow reversal, then terms which render the equations elliptic either become zero or behave in a manner that allows one to treat them as parabolic. The price that is paid for this very useful character is that the simulation cannot be initiated very close to the ship, but rather at some distance downstream where the above assumptions are satisfied. At that location, all dependent variables must be specified, forming what will be termed the Initial Data Plane (IDP). The numerical algorithms then propagate this prescribed data downstream. The IDP for the present calculations was 70 m downstream of the vessel.

The methodology used in the simulations is well documented. Smith and Hyman (1987) outline a transport model for microbubble fields in ship wakes and Nyugen and Hyman (1988a,b) describe modeling the turbulent free sheer flows in wakes. Hyman (1988c) discusses results of comparing the numerical simulation of a naval ship with limited data taken from tow tank measurements. Hyman (1990) and Miner and Ramber (1988) discuss construction of the IDP. Additional considerations that must be made when including stratification as well as sea state are discussed in Hyman (1992), and in Stewart (1987). Estimation of the IDP is the weakest link in the simulation process. It is currently not possible to obtain full-scale wake flow data and there exist only a very few sets of tow tank data at useful downstream locations. In the near future, the IDP will be calculated via solution of the full Navier-Stokes equations around the ship's hull.

Table 10-1. Pulped paper setting velocity and cumulative mass fraction as a function of particle size (radius) used for modeling. Particle properties for each size bin were derived by polynomial interpolation/extrapolation of setting column results and microscopic analysis.

Radius (μ)	Terminal Velocity ($cm \cdot s^{-1}$)	Cumulative Mass Fraction
200	0.05	0.09
500	0.24	0.20
800	0.30	0.31
1000	0.40	0.37
1200	0.67	0.44
1400	1.2	0.50
1600	2.1	0.57
1800	3.0	0.63
3000	7.7	1.0

Shipboard discharge is modeled both as a passive scalar (i.e., a neutrally buoyant dye), and as paper/cardboard discharge in order to investigate how sensitive wake dilution is to the nature of the discharged material. The particles of pulped paper/cardboard were assumed to be from 100 to 3000 μm in radius (r), and with a density of 1.54 $gm \cdot cm^{-3}$. A continuous particle population (with units $N \cdot m^{-3} \cdot m^{-1}$), proportional to r^{-3}, was defined and discretized at 10 particle sizes. Particles were not allowed to change size (they neither coalesce nor shear apart nor decompose), and they were presumed to be always falling at their (size dependent) terminal velocity. Actual size distributions and terminal velocities of the particles were interpolated from microscopic analysis and water column tests (see table 10-1 for examples of discretized sizes, settling velocity and mass fraction).

The original algorithm was developed for simulating microbubble transport and employed a surface boundary condition of the zero gradient type. This allows bubbles to escape at the surface via buoyancy. While this condition remained appropriate for a passive scalar discharge simulation, particles tend to descend, and a gradient-free boundary condition at the surface leads to particles entering the domain there. Therefore, a zero flux condition was imposed to first order accuracy. Unfortunately this approximation resulted in a gradual production of mass at the

surface for about the first 3000 meters downstream of the vessel, resulting in a net increase in mass of about 8 to 25%, increasing with increasing ship speed. In this sense, the resulting concentration estimates will be conservative.

With the above assumptions made, the transport of dye and paper/cardboard particles can be approximated by a parabolic convective-diffusive equation in which the ensemble average scalar field is convected by the mean hydrodynamic flow and diffused by the turbulent flow. The only difference is that in the first case, the equation is solved once, and in the second case, it is solved once for each particle size (with the appropriate vertical terminal velocity accounted for). The hydrodynamic information required is provided by simulation of the flow field. This is achieved via solution of the ensemble averaged parabolic Navier-Stokes equations, together with a two equation model (k-e) for turbulent closure.

Simulation. A series of simulation sets were performed. Each set included dilution results for an aircraft carrier and a frigate, moving at speeds of 10, 20, and 25 kts (5.15, 10.3, and 12.875 $m \cdot s^{-1}$). These two ship scenarios were thought to be representative of relatively high and low wake-loadings. The ship speeds chosen span normal operating conditions. The amount and rate of paper/cardboard discharge were not the same for the different vessels but rather reflected what would be realistic estimates based on the crew complement and projected pulping output. For comparison purposes, one set of simulations was repeated for the carrier, using the same discharge parameters but with a passive scalar effluent. Relevant ship and discharge parameters are listed respectively in tables 10-2 and 10-3.

Model simulations were run for each vessel, for a variety of ambient conditions. The ambient conditions included: an unstratified case, a generic (relatively severe) stratified case, and several specifically chosen for the Special Areas. The domains on which the computations were performed varied with ship speed and type, but in general, the lateral dimension was between 0.4 and 0.7 ship lengths and the vertical dimension was between 0.12 and 0.2 ship lengths. The 200 (streamwise) by 91 (horizontal) by 41 (depth) grids were uniform in the lateral direction, but had a high density near the sea surface and the IDP. The total amount of mass flux through the IDP was determined by the shipboard discharge rate. A series of tests in which the location and size of the initial discharge area were moved within the IDP showed little effect on the final concentration fields measured 3000 to 5000 m downstream.

The output of the wake model for each case considered (comprised of a specific vessel, ship speed, and ambient condition) consisted of cross-sectional profiles at various downstream positions (70 m to 5000 m) of either the total effluent concentration (for the passive scalar case) or for several (10) discretized particle size concentrations for the case of the paper/cardboard discharge. At each downstream location total (summed over all particle sizes) peak and average effluent concentrations were calculated. Concentration contours of the lowest (0 to 1 μm radius; representative of passive scalar dispersion), mid (999 to 1000 μm radius), and highest (2999 to 3000 μm radius) size particles were separately plotted in order to investigate the behavior of the different size particles at successive downstream positions.

Ambient Model

The resulting concentration field data from the TBWAKE model were used as the initial conditions for the SEDXPORT ambient dispersion model. Several adaptations were made to make the linkage between the two models as "seamless" as possible. This included having the

models share compatible gridding, particle size bins, diffusivity and shear calculations, as well as "slaving" initialization of the ambient model to the output of the wake model. Illustrative environmental conditions from the Baltic and North Sea are used as input for the SEDXPORT model.

Ambient Model Selection. The long term dispersion of paper/cardboard ship discharge is determined by the ambient motion of the sea, which is driven by wave, current, wind force, and by the differences in the density of the particles and surrounding fluid. Ambient motion is expected to become important after about 10 ship lengths downstream from the point of paper/cardboard discharge (Hyman, 1992), when the effects of wake mixing subside. The choice of the ambient model was based on its ability to best incorporate both the ambient forces (e.g., wind, tidal, and waves) and the effect of density variations.

The commercially available software packages (STFATE, CORMIX, and MIKE21) were tested to predict ambient dispersion of shipboard waste and were found to be inappropriate for various reasons. For instance, none of these codes were able to include a vertical variation in density and/or velocity. Furthermore, the output from the initial wake dispersion calculation was not amenable for input to the STFATE (concentration was too dilute) and CORMIX (discharge must be liquid with no particles) models. Consequently, a research model, SEDXPORT, was chosen for this study.

The SEDXPORT model is a particle dispersion model for the ocean environment. It has evolved from a sediment transport model originally developed for noninteracting spherical particles in a field of gravity waves (Jenkins and Inman, 1985). It was subsequently expanded to include dispersion by current and waves, and was adapted for the State of California Water Resource Board to determine the fate of suspended solids in sewage discharged into the ocean (Jenkins, Nichols and Skelly, 1989). The model was further refined to include cohesive particle dynamics in problems of scour and erosion of muddy seabeds (Jenkins and Wasyl, 1990) and hindered settling dynamics as a result of particle to particle stress transfer in high concentration suspensions (Aijaz and Jenkins, 1994). Recently the model has been expanded to include vertical stratification of the water column due to river plumes and mixed layer dynamics. The model was used successfully in ocean optics field experiments (Jenkins and Wasyl, 1994) calculating features of hindered settling layers at the pycnocline interface and bottom turbid layers. In this most recent version, the model has been integrated into the Navy's Coastal Water Clarity Model and the Littoral Remote Sensing Simulator (Hammond et al., 1995) and has been partially validated. Validation for particles less than 30 mm in mid-to-inner shelf waters (Hammond et al., 1995; Schoonmaker et al., 1994) was shown by three independent methods: 1) direct measurement of particle numbers and particle size distribution by means of a laser particle sizer, 2) measurements of water column optical properties, and 3) comparison of computed particle dispersion patterns with LANDSAT imagery.

Dr. Jenkins, who developed SEDXPORT, is a research oceanographer and engineer at SIO and is modifying this ambient model to incorporate the specific characteristics of the pulped paper particles and the output of the wake dispersion model.

Overview. The SEDXPORT code is a time-stepped finite element model which solves the advection diffusion equations over a fully configurable three-dimensional grid. The vertical dimension is treated as a two-layer ocean with a homogeneous surface mixed layer and a homogeneous bottom layer separated by a pycnocline interface. The code accepts any arbitrary

density and velocity contrast between the mixed layer and bottom layer that satisfies the Richardson and Froude number stability criteria. The code does not time split advection and diffusion calculations, and will compute additional advective field effects arising from spatial gradients in eddy diffusivity, i.e., the so-called gradient eddy diffusivity velocities after Armi (1979). Eddy mass diffusivities are calculated from momentum diffusivities by means of a series of Peclet number corrections based upon particle size and mass and upon the mixing source. Peclet number corrections for the surface and bottom boundary layers are derived from the work of Nielsen (1979), Jonsson and Carlsen (1976), and Jenkins and Wasyl (1990). Peclet number correction for the wind-induced mixed layer diffusivities are calculated from algorithms developed by Martin and Meiburg (1994), while Peclet number corrections to the interfacial shear at the pycnocline are derived from Lazaro and Lasheras (1992a and 1992b). The momentum diffusivities to which these Peclet number corrections are applied are due to Thorade (1914), Schmidt (1992), Durst (1924), and Newman (1952) for the wind-induced mixed layer turbulence, and to List et al., (1990) for the current-induced turbulence.

Griding and Initialization. SEDXPORT was gridded in a 200 x 200 YZ-computational domain with 1.0 meter depth increments (Z-dimension) and 1.5 meter horizontal increments (Y-dimension). This allowed the cross-wake data plane of the initial particle distribution from the TBWAKE code to be nested inside the far field grid using compatible grid cell dimensions. The TBWAKE YZ-data plane was 99 x 41 in 1.5 x 1.0 meter grid cells, and was centered inside the SEDXPORT grid with the sea surface at Z = 0. The remaining portions of the 200 x 200 SEDXPORT grid not occupied by the TBWAKE grid were initialized with zero particles at time t = 0.

The particle size distribution output of TBWAKE was described by 9 particle size bins with the mass fraction and settling velocities as shown in table 10-1. The dry density of the paper/cardboard particles was assumed to be the same for all size bins, and was taken as the experimentally determined value of 1.54 $gm \cdot cm^{-3}$. SEDXPORT computes advection-mixing dynamics independently for each of the size fractions which make up the particulate distribution because each size fraction has a different Peclet number and corresponding diffusivity. Time step lengths varied depending upon the size of particulates and were chosen to ensure that particles moved only a few grid cells (less than 4) in a time step in order to maintain numerical stability. Because the larger particles advected vertically faster due to gravity, they require shorter time step intervals. For the 200, 1200, and 3000 μm radius particle bins results presented, the time step lengths were 7000, 194.4, and 31.1 seconds, respectively.

Typically, time step lengths would also be controlled by the mean currents, but because no information is available on the spatial structure of the current field for the particular sites, nor the orientation of the ship track relative to the currents, the currents are assumed to be normal to the computational plane, i.e., parallel to the axis of the wake. Similarly, the wave propagation is also assumed to be parallel to the ship track. Consequently, particle advection is exclusively due to settling and the only dynamic influence of the currents is to enhance diffusivities by interfacial shear at the pycnocline, or by current boundary layer turbulence at the bottom.

Table 10-2. Representative boundary conditions and input forcing used in modeling pulped paper dispersion in the Baltic and North Seas.

Ambient Conditions	Central Baltic (Winter)	Southern North Sea (Summer)
Depth	200 m	50 m
Swell Height	0 m	0 m
Swell Period	0 sec	0 sec
Wind Wave Height	2.0 m	0.5 m
Wind Wave Period	6.0 sec	6.0 sec
Winds	9 $m \cdot sec^{-1}$	5.0 $m \cdot sec^{-1}$
Mixed Layer Depth	50 m	50 m
Mixed Layer Density	6.0 sigma t	24.6 sigma t
Bottom Layer Density	12.0 sigma t	0 sigma t
Mixed Layer Current	0 $cm \cdot sec^{-1}$	10 $cm \cdot sec^{-1}$
Bottom Layer Current	0 $cm \cdot sec^{-1}$	0 $cm \cdot sec^{-1}$
Bottom Roughness	2.0 cm	10.0 cm

The environmental conditions for the Special Areas of interest, Baltic and North Seas, are specified according to characteristic "climate atlas" figures. SEDXPORT boundary conditions and forcing function inputs derived from these climate atlas figures are shown in table 10-2. In both the Baltic and North Sea simulations, no specific bathymetry was evaluated for effects on wave shoaling or current boundary layers; thus horizontal gradients in diffusivity were not included. The absence of such gradients ensures that the 2-dimensional YZ-computational plane remains adequate for representation of the problem. The bottom was treated as a flat plane boundary with random roughness as indicated in table 10-2.

10.2 Results

The modeling results are divided into wake and ambient subsections which respectively address the dispersion predictions of the TBWAKE and SEDXPORT models. The wake subsection is composed of series of computational simulations investigating how wake dilution is effected by the type of vessel (aircraft carrier verses frigate), nature of the discharge (neutrally buoyant dye verses paper/cardboard), the speed of the vessel (10, 20, and 25 knots), and ambient conditions (unstratified verses stratified, and several Special Area environments). The wake results are presented in several ways. First, the total concentration field (i.e., summed over all 3000 one μm radius particle bins) is used to calculate dilution as a function of downstream position. Secondly, a few examples of concentration contours for different particle size bins are presented to illustrate their different response to the wake. A more extensive set of concentration profiles of individual size particles, along with complementary flow field contours, can be found in appendix H.

The continuous density stratification chosen was taken during the summer off the coast of Southern California. The Brunt-Vaisaila period ($2\pi \cdot N^{-1}$) was about 500 s over the first 30 m of depth. The ambient conditions for the two Special Areas chosen (Baltic and North Sea) are listed in table 10-2 and are representative of relatively poor and good mixing conditions.

Near Field-Wake Modeling Results

Wake Dilution Estimates-Stratified verses Unstratified. Minimum dilutions were calculated by dividing the concentration of effluent at discharge and by the maximum concentration of effluent calculated in a cross section of the ship's wake. Likewise, average dilutions were calculated by dividing the concentration of effluent at discharge by the average concentration of effluent calculated in a cross section of the ship's wake. For these calculations, the concentration of each paper/cardboard particle size was added.

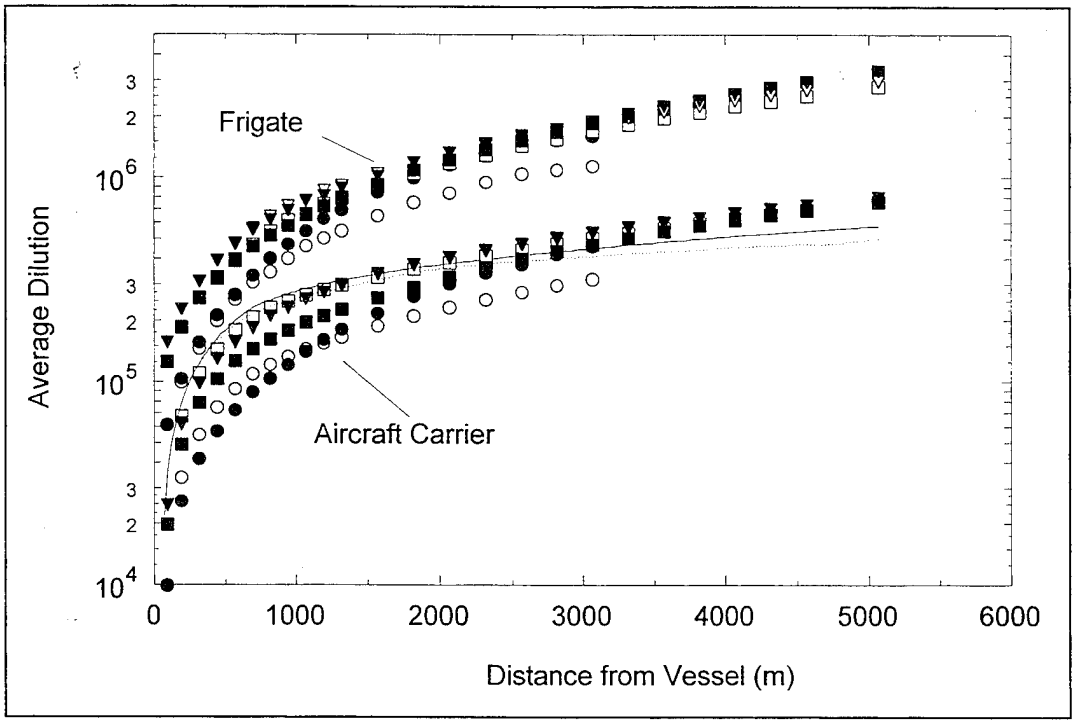

Figure 10-1. TBWAKE average dilution estimates as a function of distance from discharging vessel (frigate or aricraft carrier). Symbols represent pulped paper and cardboard discharge and lines represent dye discharge. Open symbols=unstratified, closed symbols=stratified, circle=10 kts, square=20 kts, triangle=25 kts. Solid line=20 kts unstratified, dotted line=20 kts stratified. Stratification was $2\pi \cdot N^{-1} \approx$ 500 s.

Average dilution estimates of paper/cardboard for the aircraft carrier and frigate, at 10, 20, and 25 knots (5.15, 10.3, and 12.875 $m \cdot s^{-1}$) and for unstratified and stratified ($2\pi \cdot N^{-1}$ = 500 s) ambient conditions are plotted in figure 10-1 as a function of downstream distance from the vessel. Also included, for the aircraft carrier, are the dye results for the 20 knot case. For all these cases, a relatively low background diffusivity of 10 $cm^2 \cdot s^{-1}$ was chosen so that the wake dynamics would be most prominent.

Several general features of the data in figure 10-1 are worthy of comment. Most evident are the large dilution factors provided by the mixing of the wake. Average dilution levels for the 20 and

25 knots carrier simulations for the paper/cardboard and dye were, respectively, between 7 to $8 \cdot 10^5$ and 5 to $7 \cdot 10^5$ at 5000 m behind the vessel (at 20 knots, 5000 m is equivalent to about 8 minutes after discharge). The reason for the higher dilutions for the particle discharge case at 20 and 25 knots appears to be attributed to the different settling velocities between particles of different size, which assists in spreading out the discharge.

There was essentially no difference (less than 1%) in average dilution, for the aircraft carrier at 20 and 25 knots, between the unstratified and stratified ($2\pi \cdot N^{-1} = 500$ s) simulations of paper/cardboard discharge. When dye was simulated as the carrier discharge at these same speeds, average dilutions were about 15% less under the same stratified conditions.

The numerical calculations for the 10 knot carrier simulations stopped at a downstream location of 2820 m because the larger particles were beginning to leave the computational domain. At the lower ship speeds, the wake was less energetic, and the larger particles will sink faster out of the wake. The stratified simulations ($2\pi \cdot N^{-1} = 500$ s) were found to result in greater average wake dilutions ($4.2 \cdot 10^5$) than for the unstratified case ($3.0 \cdot 10^5$) (figure 10-1). This difference in average wake dilution could result from the particle fall velocity being reduced by the stable stratification, thereby allowing the particles to remain in the wake longer. The corresponding simulation (carrier at 10 knots) predictions for the dye discharge predicted a 40% increase in average dilution when the ambient fluid was stratified. While this behavior is similar to the paper/cardboard simulation, i.e., greater dilution in stratified flow, the reasons must be different since, by definition, the dye has zero terminal velocity. When the accompanying velocity field is examined, one finds that the stratification has a very large effect, which is not clearly always detrimental towards mixing the dye.

The corresponding average dilution estimates for the frigate, for 20 and 25 knot ship speed, were between 2.8 and $3.3 \cdot 10^6$, about 4 times higher than for the carrier. This increase in dilution is due to the greater amount of energy (per unit area) in the frigate's wake as well as to the smaller flux of volume discharge. Average dilutions for the stratified case ($2\pi \cdot N^{-1} = 500$ s) were between 10% (25 knots) and 20% (20 knots) greater than the corresponding unstratified case. At 10 knots, average wake dilutions were $1.1 \cdot 10^6$ and $1.5 \cdot 10^6$ (~ 40% greater), respectively, for the unstratified and stratified frigate cases. Again, as in the case for the aircraft carrier, stratification actually helps the wake dilution process by slowing the descent of the paper/cardboard particles through the wake (where it is mixed most effectively).

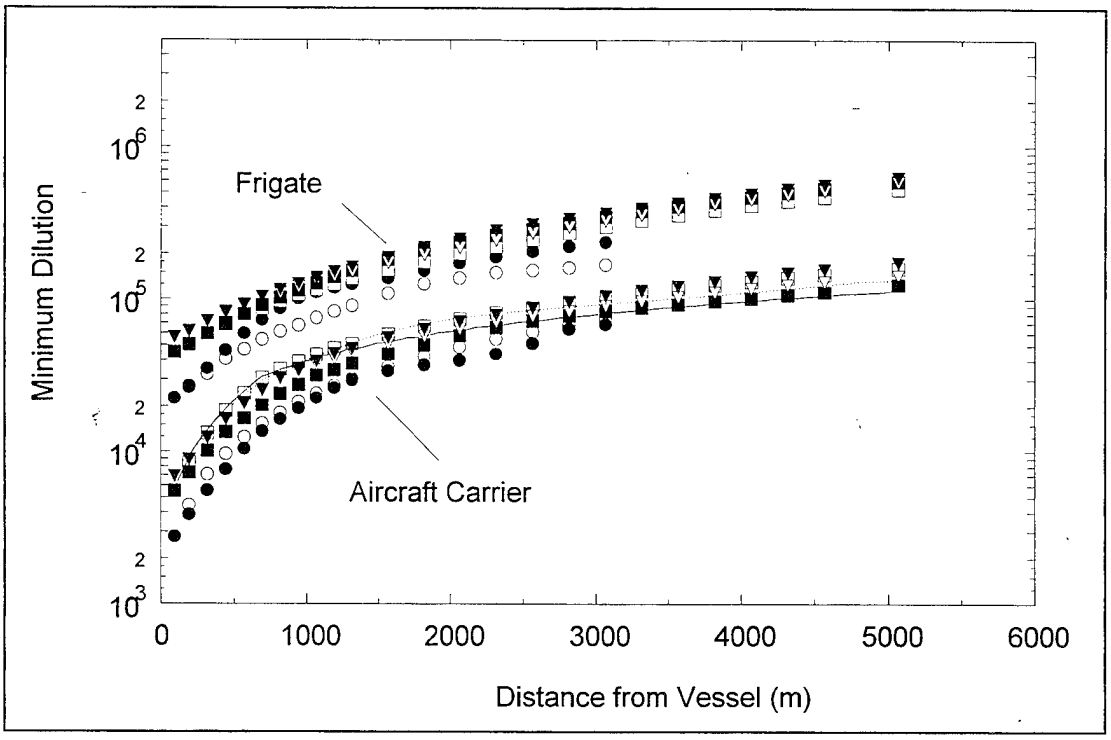

Figure 10-2. TBWAKE minimum dilution estimates as a function of distance from discharging vessel (frigate or aircraft carrier). Symbols represent pulped paper discharge and lines represent dye discharge. Open symbols=unstratified, closed symbols=stratified, circle=10 kts, square=20 kts, triangle=25 kts. Solid line=20 kts unstratified, dotted line=20 kts stratified. Stratification was $2\pi \cdot N^{-1} \approx 500$ s.

Similar plots for the minimum dilution calculations are shown in figure 10-2. Minimum dilutions (which depend on the maximum concentration calculated in the plane of interest) were about 20% of that calculated for average dilutions, regardless of vessel and speed. Because the governing equations were originally ensemble averaged, the maximum concentrations calculated will most likely be less than those found in any single realization. It has been estimated for bubble concentrations that the difference between maximum concentrations found for single realizations and ensemble averages are typically less than 50%. It is expected that a roughly similar relationship should hold for the present problem.

The effect of stratification on the model estimates of minimum dilution were usually less than 20%. However, it was not unusual to find cases (e.g., 10-knots paper/cardboard discharge) where stratification would increase the average dilution while decreasing the minimum dilution. Whether this is an artifact of the model or reflects some physical principals is not known. For the present order of magnitude analysis, these relatively small differences are beyond the scope of this work.

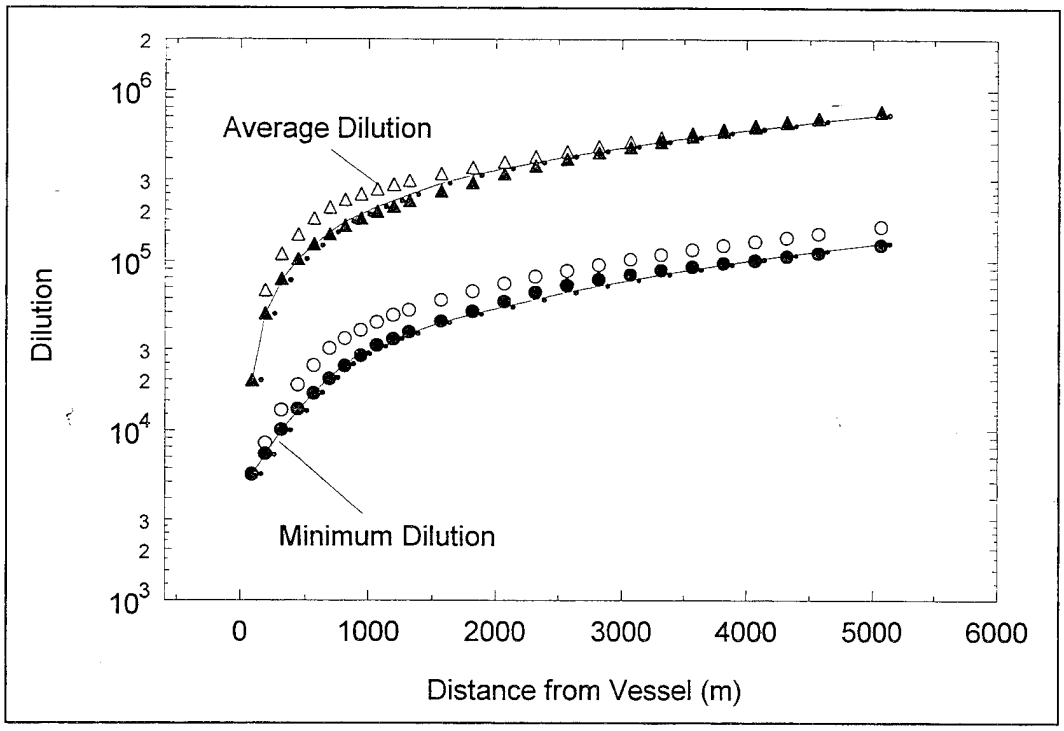

Figure 10-3. Comparison of TBWAKE dilution estimates of pulped paper discharge from an aircraft carrier moving at 20 kts (10.3 $m \cdot s^{-1}$) for different ambient conditions. Solid line=Baltic Sea, dotted line=North Sea, open symbols=unstratified, solid symbols=stratified ($2\pi \cdot N^{-1} \approx 500$ s).

Wake Dilution Estimates-Special Area Conditions. Ambient conditions for the Baltic and North Seas were also chosen as background for running TBWAKE. Depth dependent diffusivities were provided by SEDXPORT, which calculated mass diffusivities based on various environmental parameters such as wind, wave, and the density differences across the mixed layer. Background momentum diffusivities were about an order of magnitude higher than those used in the previous figures (figures 10-1 and 10-2). Nevertheless, the dilutions (average and minimum) calculated from TBWAKE did not significantly differ from those shown. Wake dilution results for paper/cardboard discharged from a carrier moving at 20 knots for the Baltic and North Sea conditions specified (see table 10-2) are shown in figure 10-3. Paper/particle dilution curves for the Baltic and North Sea cases were essentially indistinguishable. The corresponding results for the paper/particle dilutions were included in figure 10-3 for the stratified ($2\pi \cdot N^{-1} = 500$ s) and unstratified ambient conditions previously considered. All data show reasonable agreement, thereby suggesting that to first order the environment is unlikely to significantly influence initial wake dilutions.

Wake Particle Concentration Field. While the principle focus of this work is to estimate the dilution of paper/cardboard discharge, it is also of interest to consider the spatial distribution of the different size paper/cardboard particles. Contours of the particle concentration field reveal flow features which can not be seen in the previous dilution data. Particle concentration contours for the aircraft carrier simulations at 20 knots, for both unstratified and stratified ($2\pi \cdot N^{-1} =$

500 s) conditions, are presented next. These results were chosen because they were generally representative of other cases.

The IDP contains several principal flow features; propeller momentum excess and swirl, hull momentum defect, and a set of outward turning hull vortices. There is a turbulent energy field associated with each component. Since these components are overlaid or very near one another, they do not evolve independently. Nevertheless, wake evolution under nonstratified conditions is characterized by the monotonic decay of these structures as they exist at the IDP. Decay rate depends on the location of components with respect to each other.

Under stratified conditions, however, the decay is often not monotonic. Simulations with stratification are conducted under the assumption that, at the IDP, the density field is fully mixed within the ship wake. Subsequent wake dynamics are, in large part, the fluid response to that mixing. There is a certain amount of potential energy at the IDP due to the assumption of a fully mixed density field within the ship's wake. Subsequent exchange of this energy into mean and turbulence kinetic energy and back into potential energy yields a nonmonotonic decay. Most important in this process is the formation of a set of mid-depth vortices near the wake edge. These vortices vary in strength as they exchange energy with the density field. All the above phenomena serve to transport the scalar fields.

In figures 10-4a through 10-4c are plotted paper/cardboard particle density contours of 1, 1000, and 3000 μm radius for the nonstratified 20 knot carrier case 5 km from the point of discharge. The 1 μm size particles simulate the dye's behavior. The 3000 μm radius particles are representative of the largest paper/cardboard particles, and consequently have the greatest terminal velocity. Figure 10-4d shows the corresponding total distribution of mass. The mass distribution is calculated by integrating the mass over the entire particle size range at each point in space.

These data show that after about 8 minutes in the wake of the carrier, the port and starboard plumes of 1000 μm radius particles have begun to merge together, while the 1 μm particles have too low a descent velocity to appreciably carry them down in depth. For all the particles, the highest concentration tends to be at the outer region of the plume where they are convected by the propeller and hull vortices. The rate of transport diminishes with the decay of these vortices. This tends to be a more effective transport mechanism than dispersion due to fluid turbulence. On the other hand, the large and heavy 3000 μm particles descend fairly rapidly and are influenced by other regions of the flow field. Their downward velocity is augmented by being on the other (downward) side of the hull and propeller vortices. Overall mass distribution in figure 10-4d shows that the overall mass has also begun to descend (due to the large mass contribution from big particles) but at a lateral location more aligned with the smaller particles.

Figures 10-4e through 10-4h show the same particle sizes at the same downstream location but for the stratified case. The structure of the particle plumes is now quite different, retaining greater cohesiveness, and showing a greater tendency of downward drift. This is due to the formation of the additional vortices noted above and to a more rapid decay of turbulence. The new vortices at mid-depth serve also to convect discharged particles there outward and faster than at the surface. In appendix H, additional plots (which include the accompanying velocity fields) for both the carrier and frigate, at different downstream positions, can be found.

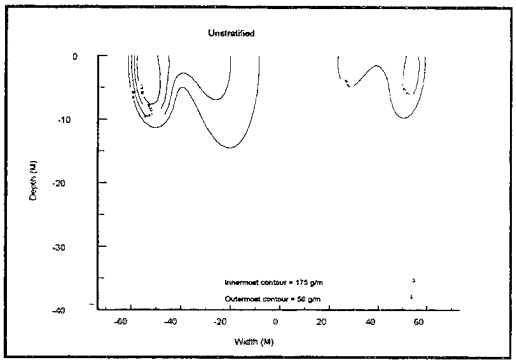

a 1 Micron Radius

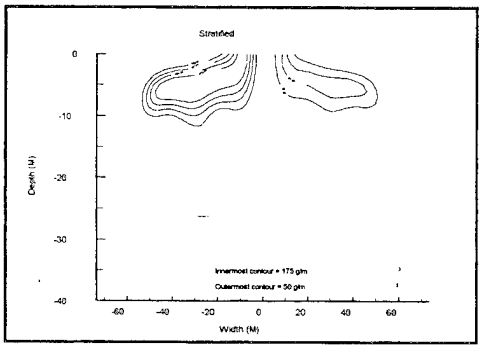

e. 1 Micron Radius

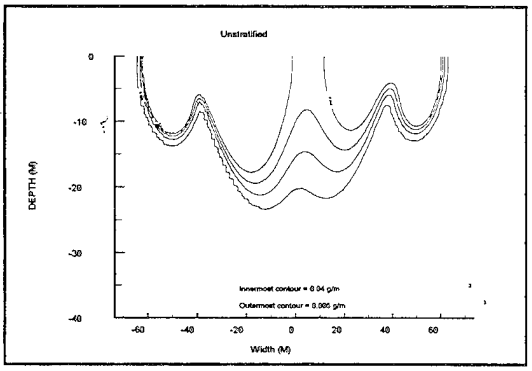

b. 1000 Micron Radius

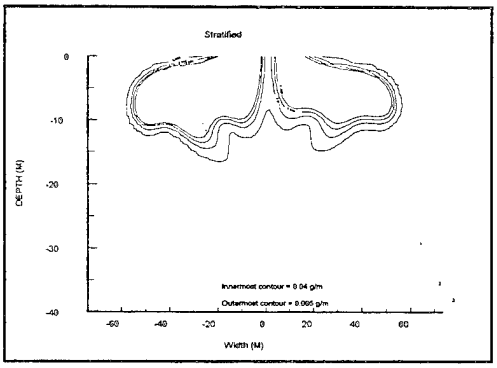

f. 1000 Micron Radius

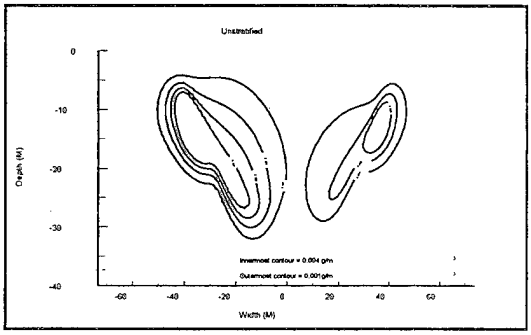

c. 3000 Micron Radius

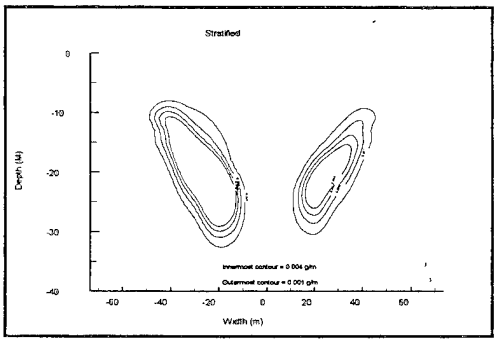

g. 3000 Micron Radius

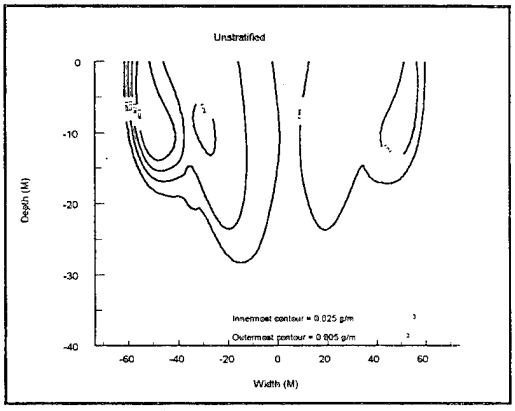

d. Total Pulped Paper

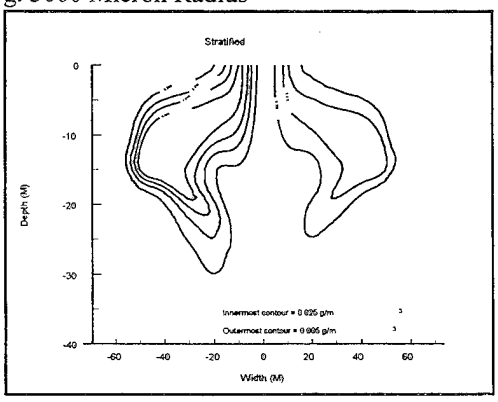

h. Total Pulped Paper

Figure 10-4. TBWAKE simulations of pulped paper particle concentration cross wake sections 5 km downstream of an aircraft carrier moving at 20 kts in unstratified (a-d) and stratified (e-h) conditions. Concentrations (gm^{-3}) are shown for 1, 1000, and 3000 μm (radius) particles and total particle load.

Far Field-Ambient Modeling Results

The ambient conditions considered for the far field dispersion of shipboard discharge are shown in table 10-2. Plots of cross wake particle dispersion simulations from SEDXPORT are shown in appendix I for the winter time Baltic Sea conditions and for the summer time North Sea conditions. Dispersion plots are given for three separate particle size bins spanning the particle size distribution shown in table 10-1. These bins are centered around 200 (0 to 350), 1200 (1100 to 1300) and 3000 (>2400) μm radii particles, each with a specific gravity of 1.54. Each particle size dispersion pattern begins from the initial far field distribution from TBWAKE at time t = 0 (which for the cases studied is less than 10 minutes after discharge occurred).

All plots have depth on the vertical axis with the surface appearing at the top of the plot at Z = 0.0. For the Baltic case, the full vertical scale is from 0 to 200 m while for the North Sea case, the full range vertical scale is from 0 to 50 m. The horizontal scale for both cases is in terms of grid cell number (1.5 m wide) across the wake from port to starboard. Thus the full range horizontal scale is from 0 m on port to 300 m on starboard, with the ship wake centered at grid cell number 100, or at Y = 150 m. Thus all dispersion plots have a vertical exaggeration, which was 1.8 to 1 for the Baltic and 7.2 to 1 for the North Sea. All dispersion plots have been dynamically scaled in terms of particle number concentrations.

The Baltic case, in appendix I, results in the worst-case scenario in terms of arrival time at the sea floor but the best-case scenario for minimum dilution. This is due to the greater depths, higher sea states, and stronger winds of the Baltic relative to the North Sea.

There are several features common to all particle concentration profiles which are remnants of the wake flow field and method of discharge. For example, the initial concentration distribution will reflect the number of screws; hence, the four distinct "blobs" of particle concentration are initially apparent for each particle size bin. Also, the concentration of paper/cardboard was initially much greater on the port side due to the discharge locations. This feature generally persists throughout the subsequent ambient simulations. It is interesting how the 200 μm size particles in the Baltic conditions begin merging of the port and starboard blobs as they pass through the hindered settling regime at the 50 m depth pycnocline. Below the pycnocline, the port and starboard blobs become fully merged with an asymmetric center of mass displaced to the port side of the wake. The larger size particles, which fall faster, have smaller diffusivities. They are less well-mixed, and the dispersion patterns continue to show distinct port and starboard blobs throughout the residence time in the water column.

In the Baltic, the concentration of the 0 to 350 μm size particles start with about $2 \cdot 10^4$ particles$\cdot m^{-3}$ at the surface at time zero and dilute about 20 to 1 while passing through the mixed layer. They begin arriving at the bottom after about 78 hours while the center of mass of the dispersion pattern has reached depths of about 120 m and has diluted to about 500 particles$\cdot m^{-3}$ or 40 to 1 minimum dilution. The center of mass of the 0 to 350 μm size particles reaches the bottom after about 117 hours and has diluted to about 250 particles$\cdot m^{-3}$, or a minimum dilution of 80 to 1. By contrast, the larger particles have much shorter bottom arrival times and less dilution. The center of mass of the 1100 to 1300 μm particles reach the bottom in 10.8 hours with a minimum dilution of 20 to 1. The largest size (>1800 μm radius) paper/cardboard particles, which account for 37% of the total mass, reach the bottom in 41 minutes with a minimum dilution of only 10 to 1.

In the shallower depths and calmer conditions of the North Sea in summer, there is much less ambient mixing and correspondingly less dilution. Inspection of the dispersion plots in appendix I reveals much less merging of blobs and less lateral dispersion (although the vertical exaggeration is also greater in these plots). Here the center of mass of the 0 to 200 μm size particles reaches the bottom in about 29 hours with a minimum dilution of 20 to 1. The 1000-1200 μm size particles reach the bottom in 97 minutes at 7 to 1 dilution, while the largest (>1800 μm radius) particles reach the bottom in only 10 minutes at 5 to 1 dilution.

Model and Measurement Comparisons

Tow Tank (Wake Growth) Comparison. A flow visualization experiment was performed at CDNSWC/AD on a subscale model of a naval surface ship, using a laser light sheet and a fluorescing dye. A 100 milliwatt argon-ion laser was used to form a thin sheet of blue-green light in a plane normal to the track of the model. The sheet was formed using an oscillating mirror controlled by a signal generator and a second stationary mirror which redirected the light sheet across the basin.

A compact charge-couple device (CCD) camera was suspended two feet beneath the surface in a waterproof housing and was offset from the basin centerline by two feet, allowing the model to pass freely by the camera and its supporting mount. The camera was aimed at the transverse light sheet so that the trajectory of the lateral edge of the wake could be recorded. Dye was introduced into the wake through plastic tubes originating at the propeller hubs.

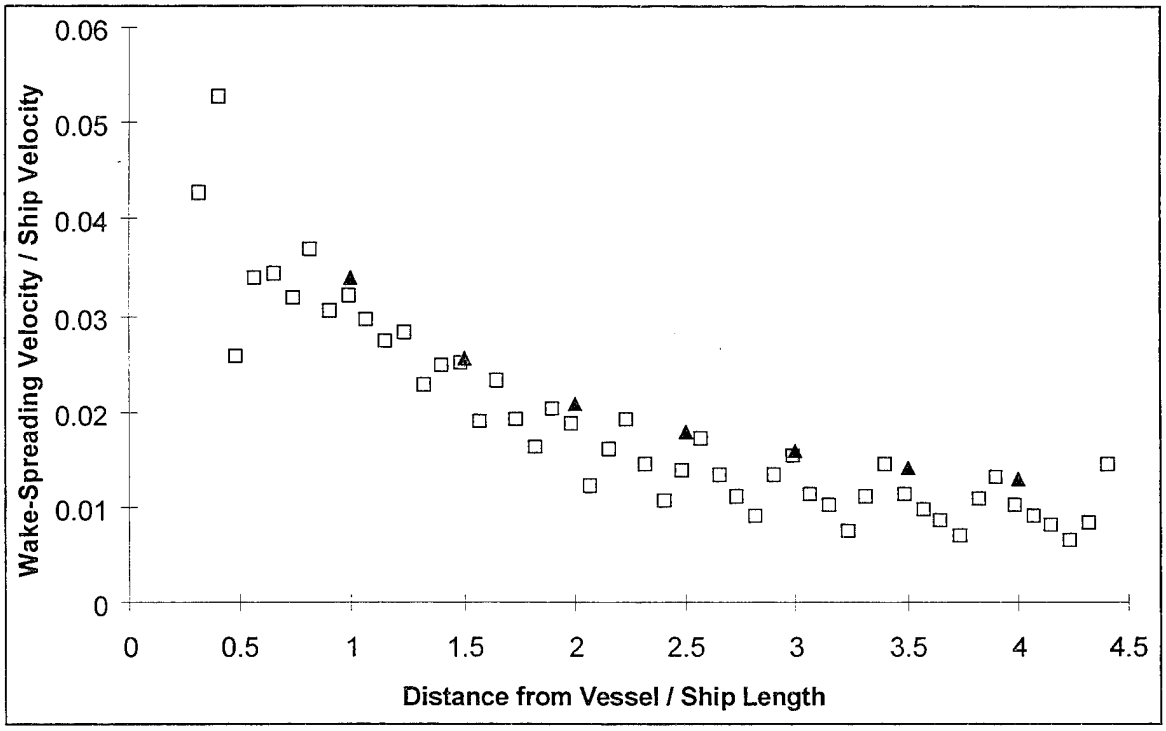

Figure 10-5. TBWAKE comparison of modeled and laboratory lateral wake-spreading rates. Closed symbols=tow tank measurements (Hyman et al., 1995), open symbols=TBWAKE numerical predictions.

Analysis of the small-scale model wake at subsequent downstream locations indicated that its width could be approximated by $2Y/B \sim 1.75(X/L)^{0.3}$, where Y is the width of the wake, X is the location downstream, B is the beam of the vessel, and L is its length. From this relationship the lateral growth of the wake could be determined. Figure 10-5 compares the laboratory model and the numerical simulation results for nondimensional wake growth as a function of nondimensional downstream distance. Wake growth is nondimensionalized by the beam of the ship, and downstream distance is nondimensionalized by the length of the ship. Overall the wake comparison is good, with the numerical model somewhat underestimating its lateral growth.

In the numerical model output, the scalar field growth has what appears to be a periodic component. This is somewhat deceptive. The flow at the IDP is composed of the hull induced momentum defect wake, the propeller induced momentum excess wake, and several vortices on either side of the ship. As a result, when the scalar field grows in width, it gets "bumped" outward when it reaches a vortex. This occurs at discreet athwartship distances and produces a growth rate that appears periodic.

Laboratory Stratification (Merritt, 1972) Comparison. The TBWAKE model is capable of simulating wake development under continuously stratified conditions. Density stratification resulting from both temperature and salinity variations in the water column can significantly affect the wake hydrodynamics, and consequently the dispersion of shipboard effluent. A previous laboratory study by Merritt (1972), investigating the effects of stable stratification on the simulated momentumless wake of a submerged, self-propelled vehicle, provides another opportunity for comparison with the numerical model.

Laboratory tests found that the initial round wake would, because of the stratification, eventually "collapse" into an elliptical patch, and measurements of the horizontal and vertical evolution of the wake had been made (Merritt, 1972). A correction was made to the wake halfwidths used in the numerical simulations such that they agreed with Merritt's data at the initial data plane (see Hyman, 1990 for details). Good agreement between experimentally determined wake growths and the simulations were found.

Barge/Tanker Wake Dilution Comparison. Measurements of industrial waste discharged into the wake of a barge suggest that the cross section of the wake is about 2.5 times the beam (B) and 3 times deeper than the draught (D) of the vessel, unless limited by the depth of the thermocline (Csanady, 1981). The volume of wake generated per second is then about $8 \cdot B \cdot D \cdot U$, where U is the ship's velocity. If W represents the volume flux of discharged material ($m^3 \cdot s^{-1}$), and if the shipboard discharge is assumed to be uniformly distributed throughout the wake, then the average wake dilution, $D_{Csanady}$, can be approximated as:

$$D_{Csanady} = \frac{8BDU}{W} \qquad \text{(Eq. 10-1)}$$

Initial wake dilutions behind a barge appear to range from 5000 to 10000 (Csanady, 1981; Devine, 1987).

The following formula relating initial dilution in the wake of a tanker to the discharge rate, vessel dimensions, and speed has also evolved:

$$D_{IMO} = C_1 \frac{UL^2}{W} \cdot \frac{(Ut)^{0.4}}{L} \qquad \text{(Eq. 10-2)}$$

Here D_{IMO} is a minimum dilution, defined as the ratio of the waste concentration at discharge to the maximum concentration of the waste in a cross section of the ship's wake. The coefficient C_1 is equal to 0.003 for single discharge and 0.0045 for multiple discharge, L is the length of the vessel, and t is the time after the ship's passage. The range of applicability of equation (10-2) is $3<U \cdot t/L<40$, where t must be >300 seconds. This formula, upheld by the International Maritime Organization (IMO, 1975), is based on field (Dahl & Tollan, 1972; Dahl et al., 1973; 1975) and laboratory (Mercier et al., 1973; Delft Hydraulics Laboratory, 1975) experiments. The relationship between minimum dilution and time, $D_{min} \alpha t^{0.4}$, is derived from an analysis of the growth of a momentumless wake (Birkhoff & Zarantonello, 1957; Tennekes & Lumley, 1972). Measured wake dilutions (minimum) behind tankers have ranged between 10^4 and 10^5 (Delvigne, 1987).

Table 10-3. Aircraft carrier and frigate waterline geometry used for modeling.

Ship	Length (m)	Beam (m)	Draft (m)	Disp. (tons)	Number Propellers	Propeller Diameter
Carrier	332.5	40.2	11	91000	4	6.4
Frigate	131.4	12.8	4.6	3600	1	4.3

Table 10-4. Pulper discharge configuration, rates, and concentrations for carrier and frigate installations.

	Large Pulper Starboard Port		Small Pulper Starboard Port		Slurry Discharge Rate ($m^3 \cdot s^{-1}$)	Discharge Conc. ($gm \cdot m^{-3}$)
Carrier	1	2	0	1	0.0372	5420
Frigate	0	0	1	0	0.00315	4000

Initial wake dilution estimates using equations 10-1 and 10-2 with the appropriate ship dimensions (table 10-3) and discharge rates (table 10-4) are shown in figures 10-6 through 10-8 for the aircraft carrier moving at 10, 20, and 25 knots (5.2, 10.3, and 12.9 $m \cdot s^{-1}$), respectively. Csanady's predictions, based on equation 10.1, were plotted at the furthest downstream position evaluated. Included in these figures are the previous results for the unstratified and stratified ($2\pi \cdot N^{-1} \approx 500$ s) simulations for the dye and paper/cardboard discharge. Figures 10-9 through 10-11 contain the corresponding calculations for the frigate case moving at 10, 20, and 25 knots, respectively. The numerical values for the various dilution estimates (at their furthest downstream position calculated), and comparisons made between them, are listed in tables 10-5 through 10-8.

Table 10-5. TBWAKE predicted dilutions of pulped paper in the wake of an aircraft carrier compared to the dilution formulas of IMO and Csanady. Predictions are for varying ship speed (u) and stratification conditions.

	U(kts.)	X (m)	Average Dilution	Minimum Dilution	Avg. Dil. Min. Dil.	IMO Prediction	CSANADY Prediction	IMO Min. Dil.	IMO Avg. Dil.	CSANADY Avg. Dil.
Unstratified	10	2820	296175	67694	4.38	161614	488777	2.39	0.546	1.65
Stratified	10	2820	420155	64020	6.56					
Unstratified	20	5070	755928	159059	4.75	408787	977554	2.57	0.541	1.29
Stratified	20	5070	760168	124530	6.1					
Unstratified	25	5070	798233	141862	5.63	510882	1,221943	3.6	0.64	1.53
Stratified	25	5070	794721	173008	4.59					
Average					5.3 ± 0.9			2.9 ± 0.7	0.58 ± 0.1	1.5 ± 0.2

Table 10-6. Aircraft carrier dye discharge. Ambient: completely mixed verses stratified ($2\pi \cdot N^{-1} \approx 500$ s).

	U(kts.)	X (m)	Average Dilution	Minimum Dilution	Avg. Dil. Min. Dil.	IMO Prediction	CSANADY Prediction	IMO Min. Dil.	IMO Avg. Dil.	CSANADY Avg. Dil.
Unstratified	10	2820	189909	40633	4.67	161614	488777	3.98	0.851	2.57
Stratified	10	2820	265947	45917	5.79					
Unstratified	20	5070	575372	113793	5.06	408787	977554	3.59	0.710	1.7
Stratified	20	5070	500000	133827	3.74					
Unstratified	25	5070	736413	146684	5.02	510882	1221943	3.48	0.694	1.66
Stratified	25	5070	620137	156874	3.95					
Average					4.7 ± 0.8			3.7 ± 0.3	0.75 ± 0.1	2.0 ± 0.5

Table 10-7. Frigate pulped paper discharge. Ambient: completely mixed verses $2\pi \cdot N^{-1} \approx 500$ s.

	U(kts.)	X (m)	Average Dilution	Minimum Dilution	Avg. Dil. Min. Dil.	IMO Prediction	CSANADY Prediction	IMO Min. Dil.	IMO Avg. Dil.	CSANADY Avg. Dil.
Unstratified	10	2820	1088987	160174	6.8	288664	765090	1.80	.265	.703
Stratified	10	2820	1519349	221877	6.85					
Unstratified	20	5070	2792169	523064	5.34	730008	1530181	1.40	.261	.548
Stratified	20	5070	3280380	587988	5.58					
Unstratified	25	5070	2970397	583760	5.09	912531	1912726	1.56	.307	.644
Stratified	25	5070	3333067	625086	5.33					
Average					5.8 ± 0.8			1.6 ± 0.2	.28 ± .03	.63 ± 0.1

Table 10-8. Aircraft carrier pulped paper discharge. Ambient: Special Areas. Predictions are for ship speed of 20 kts in conditions representative of the Baltic and North Sea.

	U(kts.)	X (m)	Average Dilution	Minimum Dilution	Avg. Dil. Min. Dil.	IMO Prediction	CSANADY Prediction	IMO Min. Dil.	IMO Avg. Dil.	CSANADY Avg. Dil.
Baltic	20	5070	721778	127141	5.68	408787	977554	3.22	0.566	1.35
North Sea	20	5070	721450	127060	5.68	408787	977554	3.22	0.567	1.35

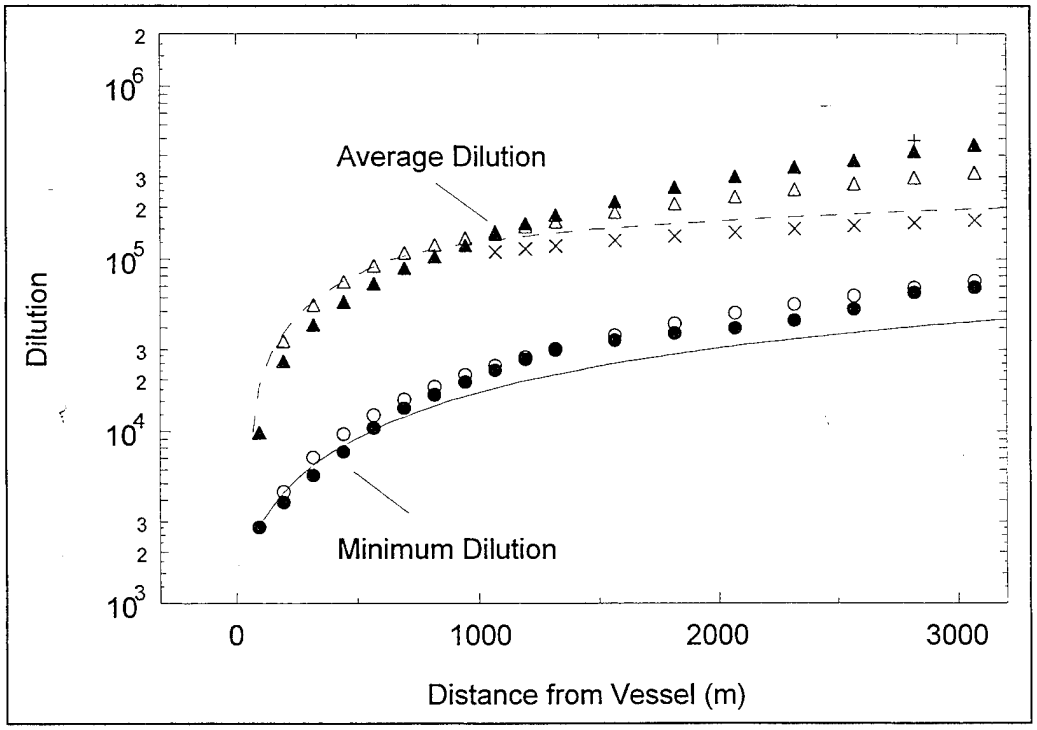

Figure 10-6. TBWAKE comparison of wake dilution estimates of pulped paper discharge from an aircraft carrier moving at 10 kts (5.15 $m \cdot s^{-1}$). Computational simulation: circles=minimum dilution, triangles=average dilution, +=Csanady's 1981 estimation, x=IMO's (Delvigne, 1987) estimation. Open symbols=unstratified, solid symbols=stratified ($2\pi \cdot N^{-1} \approx 500$ s).

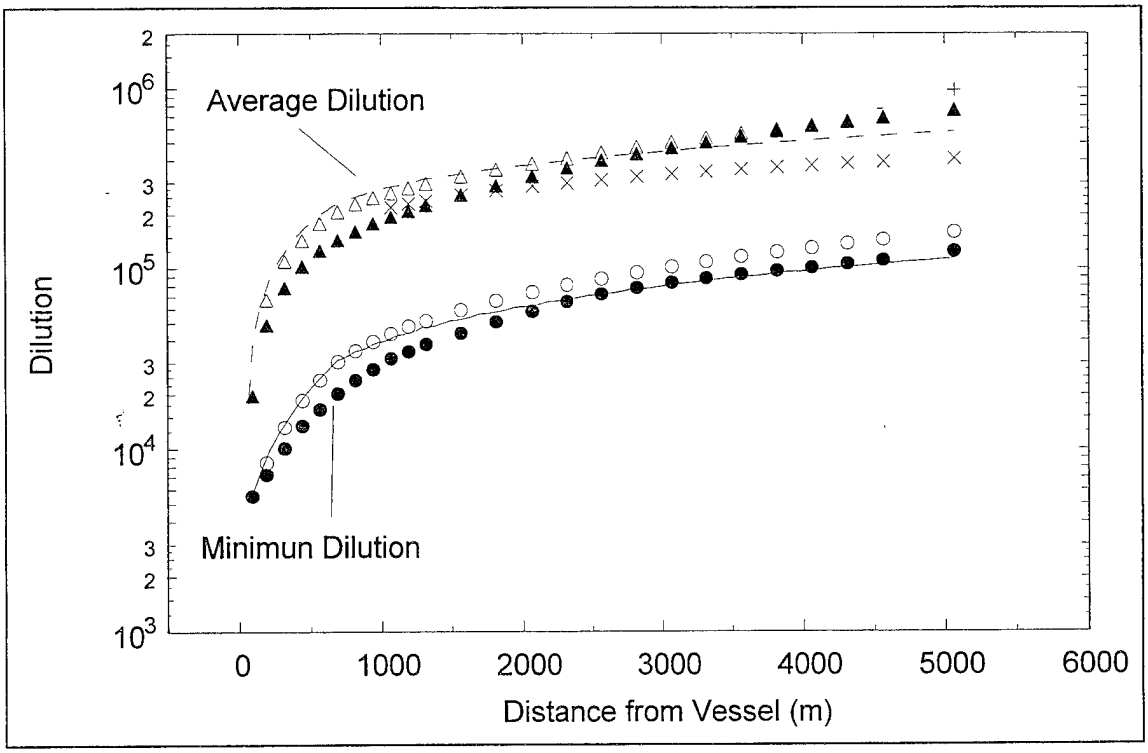

Figure 10-7. TBWAKE comparison of wake dilution estimates of pulped paper discharge from an aircraft carrier moving at 20 kts (10.3 $m \cdot s^{-1}$). Computational simulation: circles=minimum dilution, triangles=average dilution, +=Csanady's 1981 estimation, x=IMO's (Delvigne, 1987) estimation. Open symbols=unstratified, solid symbols=stratified ($2\pi \cdot N^{-1} \approx 500$ s).

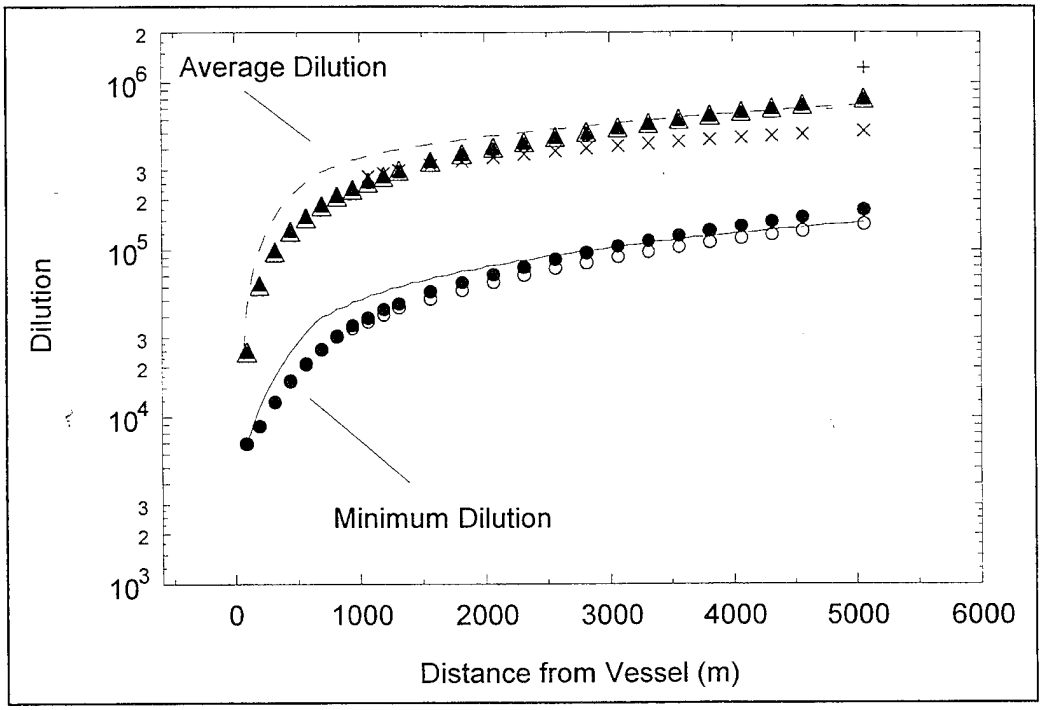

Figure 10-8. TBWAKE comparison of wake dilution estimates of pulped paper discharge from an aircraft carrier moving at 25 kts (12.875 $m \cdot s^{-1}$). Computational simulation: circles=minimum dilution, triangles=average dilution, +=Csanady's 1981 estimation, x=IMO's (Delvigne, 1987) estimation. Open symbols=unstratified, solid symbols=stratified ($2\pi \cdot N^{-1} \approx 500$ s).

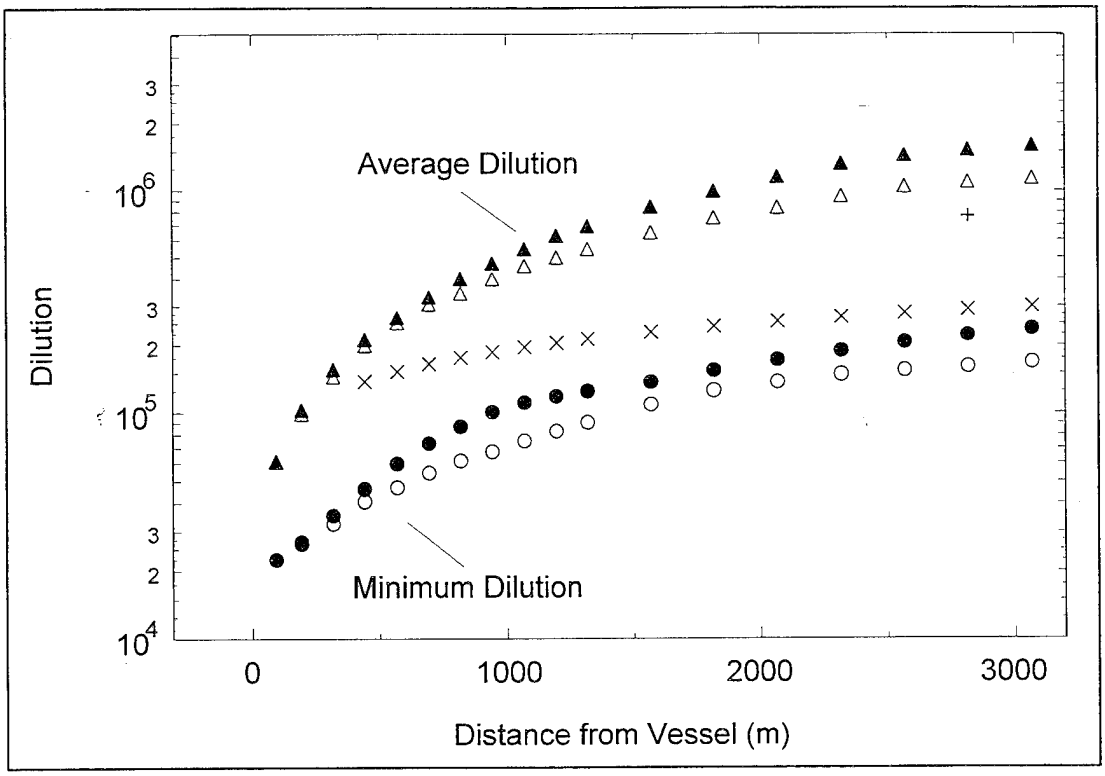

Figure 10-9. TBWAKE comparison of wake dilution estimates of pulped paper discharge from a frigate moving at 10 kts (5.15 $m \cdot s^{-1}$). Computational simulation: circles=minimum dilution, triangles=average dilution, +=Csanady's 1981 estimation, x=IMO's (Delvigne, 1987) estimation. Open symbols=unstratified, solid symbols=stratified ($2\pi \cdot N^{-1} \approx 500$ s).

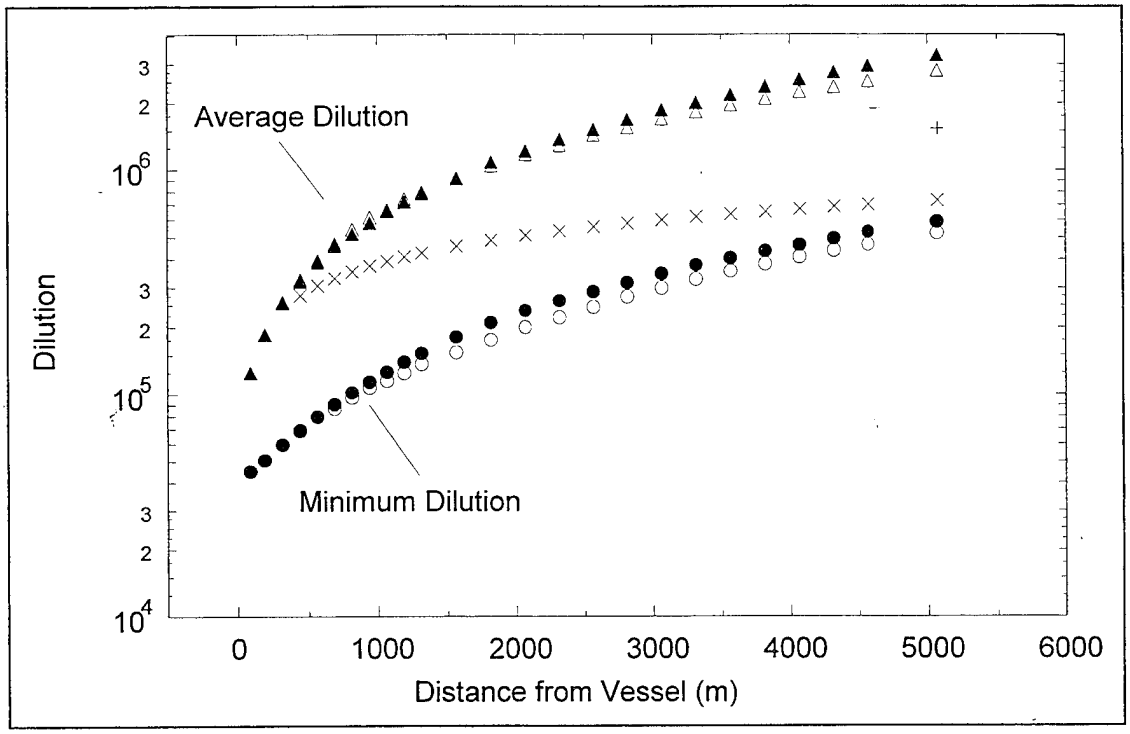

Figure 10-10. TBWAKE comparison of wake dilution estimates of pulped paper discharge from a frigate moving at 20 kts (10.3 $m \cdot s^{-1}$). Computational simulation: circles=minimum dilution, triangles=average dilution, +=Csanady's 1981 estimation, x=IMO's (Delvigne, 1987) estimation. Open symbols=unstratified, solid symbols=stratified ($2\pi \cdot N^{-1} \approx 500$ s).

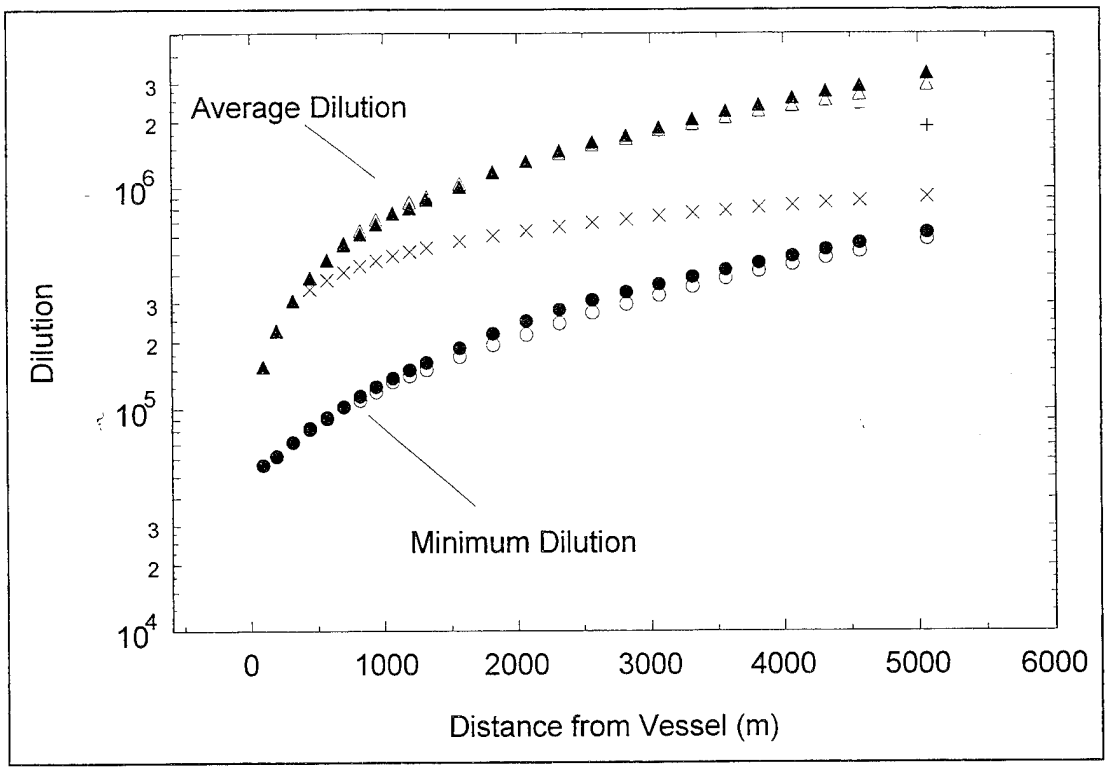

Figure 10-11. TBWAKE comparison of wake dilution estimates of pulped paper discharge from a frigate moving at 25 kts (12.875 $m \cdot s^{-1}$). Computational simulation: circles=minimum dilution, triangles=average dilution, +=Csanady's 1981 estimation, x=IMO's (Delvigne, 1987) estimation. Open symbols=unstratified, solid symbols=stratified ($2\pi \cdot N^{-1} \approx 500$ s).

Overall, considering the different wake conditions from which these models evolved, there is a remarkable similarity (i.e., often significantly better than order of magnitude agreement) between the numerical and semi-empirical predictions. Csanady's extrapolated aircraft carrier estimates of the average dilution, for both the dye and paper/cardboard discharge cases, and for the unstratified ambient case, were from 1.3 to 2.6 times greater than the model predictions, throughout the ship speeds compared (tables 10-5 and 10-6). The corresponding IMO, estimates for minimum dilution (Equation 10-2) ranged from 0.5 to 0.9 of the numerical model predictions for average dilutions, and from 2.4 and 4.0 times the numerical model estimates for minimum dilutions (tables 10-5 and 10-6).

Considering the frigate case, Csanady's estimates of average dilution throughout the same ship speed range and for paper/cardboard discharge were between 0.6 and 0.7 times those predicted by the numerical model (table 10-7). The corresponding IMO minimum dilution estimates for the frigate were between 1.4 and 1.8 times those predicted by the numerical model (table 10-7). Finally, the ratio of frigate to carrier dilution levels increased by a factor of 1.6 for Csanady's predictions, 1.8 for the IMO, predictions and about 3.7 (throughout the range of ship speeds studied and for both average and minimum dilutions) for the numerical model predictions. Similar agreement between the Special Area (Baltic and North Sea) model predictions and the

barge and tanker extrapolations (via equations 10-1 and 10-2) can be found in table 10-8.

11.0 FIELD MEASUREMENTS

11.1 Methods

An at-sea test was conducted on 27 January 1995 to determine the wake dispersion characteristics of pulped cellulose after a simulated pulper discharge into the wake of a moving ship. A mixture of pulped cellulose material, fluorescent dye, and seawater was pumped directly into the wake of the RV *Acoustic Explorer*. Before and after the discharge, chemical and physical characteristics of the seawater were measured using the RV *Ecos* and a 21' skiff, while a helicopter was used to photograph the discharge dye plume. The experiment was scaled to simulate the discharge of a pulper system from an aircraft carrier. The experiment scaling considerations and survey test plan are included in the Solid Waste Field Sampling Plan, and a summary of the data acquired is included in the Marine Environmental Survey Capability (MESC) Survey Data Acquisition Report (appendix J).

The test was performed approximately 3.2 km offshore of San Diego in approximately 21 m of water. Prior to discharge, the RV *Ecos* was used to place a current meter/temperature array at the center point of a predetermined discharge line. The RV *Ecos* was then used to map a variety of chemical and physical seawater parameters along a prescribed track, while the 21' skiff was used to perform vertical plankton net tows at random locations in the vicinity of the discharge line. After the discharge from the RV *Acoustic Explorer*, the RV *Ecos* was used to map the time variation of a wake cross-section by transiting back and forth perpendicular to the major axis of the wake. Thus it was possible to resample a single growing cross-section over time. The center point of the wake cross-section was determined using the dye and a surface current drogue as indicators. The 21' skiff more or less followed the cruise track of the RV *Ecos* during this time continuing with its vertical plankton net tow sampling.

The mixture discharged from the RV *Acoustic Explorer* was as follows: 61 L of 20% rhodamine WT, 27.7 kg (wet weight) of dewatered pulped paper obtained from CDNSWC/AD (@ 6.3 kg wet per kg dry), and 2 kg NaCl mixed to a total volume of 231 L in seawater. This mixture provided starting concentrations of 53 $g \cdot kg^{-1}$ (~5%) dye and 19 $g \cdot L^{-1}$ pulped paper (~2%). The salt was added to bring the salinity up to background, ~33 psu. The mixture was pumped out of a large vat using a Jabsco pump directly into the ship's wake @ 59 $L \cdot min^{-1}$. The mixture was discharged for 3.3 minutes while the vessel transited at 10 kts, creating a line source of material 1 km in length.

The RV *Ecos* was equipped with its MESC, a real-time data acquisition and processing system (Lieberman et al., 1989; Chadwick and Salazar, 1991; and Katz et al., 1991). The MESC was used to measure salinity, temperature, sample depth, bottom depth, pH, dissolved oxygen, light transmission, oil, chlorophyll *a*, rhodamine dye fluorescence, and wind and water current velocities, all as a function of position, which was determined using a differential global positioning system (DGPS). The hydrographic data were acquired at a 2-second interval, while fluorescence, wind velocity, and position data were collected at a 1-second interval, providing a nominal spatial resolution of $\leq$ 10 m for all data throughout the survey. Current velocity, however, was averaged over spatial scales between 150 and 300 m.

The RV *Ecos* was configured to obtain rhodamine fluorescence and light transmission data simultaneously from multiple depths throughout the survey. Prior to discharge, these data were collected at the surface (1.7 m) using a hull mounted pump and from the standard MESC tow

system which was used to profile from the surface to 10 m during portions of the pre-discharge mapping survey. Throughout the post-discharge survey, a third set of rhodamine fluorescence and light transmission data were simultaneously collected at a depth of 3 m. The fluorometric measurements were all made using seawater flow-through systems. A multiwavelength transmissometer installed on the hull pump system was also used in flow-through mode.

A Tracor Acoustic Profiling System (TAPS) was also attached to the MESC towed sensor package during this survey which autonomously collected acoustic data at multiple frequencies to determine volume scattering (particles) information. The acoustic data collection and initial processing were provided by Tracor Corporation.

Discrete water samples were obtained from either the MESC surface or towed flow-through systems. The discrete samples were later analyzed for BOD_5, TSS, Chlorophyll *a* (Chl-*a*), Nutrients, and TOC. Samples were collected at random times throughout the survey. The first 8 sets of samples were obtained during the pre-discharge mapping, while the remaining 22 sets were obtained after the discharge. Not all sample types were collected during each sampling. The discrete data were used for calibrating the MESC Chl-*a* fluorometer and transmissometers and provided discrete data on those parameters not measured by the MESC. The discrete samples analyzed for BOD_5 and TOC were delivered immediately to ATI for analysis, while those measured in-house were stored frozen until analyzed. Five samples were also analyzed by ATI for TSS and Nutrients as a way of cross-checking analyses.

The vertical plankton net tows performed on the 21' skiff utilized a 29 cm diameter, 20 μm mesh plankton net, with a 30 μm filtering cod. The net was lowered to a depth of approximately 15 to 20 m and retrieved manually at a rate of 0.5 $m \cdot s^{-1}$. Five net tows were taken randomly prior to the discharge of material, and 26 tows were made after the discharge. The post-discharge sampling was carried out along each of the RV *Ecos'* transects, and was designed to collect data outside, on the edge of, and inside the visible dye patch. Particles adhering to the sides of the plankton net were recovered in the cod by rinsing the net from the outside using a hose. A squirt bottle was used to rinse out the sample from the filter cod into 250 mL polyethylene bottles. The samples were placed into a -19°C freezer upon return until they were analyzed.

11.2 Results

The small-scale field experiment conducted in the coastal waters off San Diego, California, on 27 January 1995 served two primary purposes. The first objective was to provide a direct measure of the dilution of the pulped paper waste stream due to wake and ambient mixing. The second objective was to test a range of plume tracking equipment and methods prior to attempting a large-scale field test.

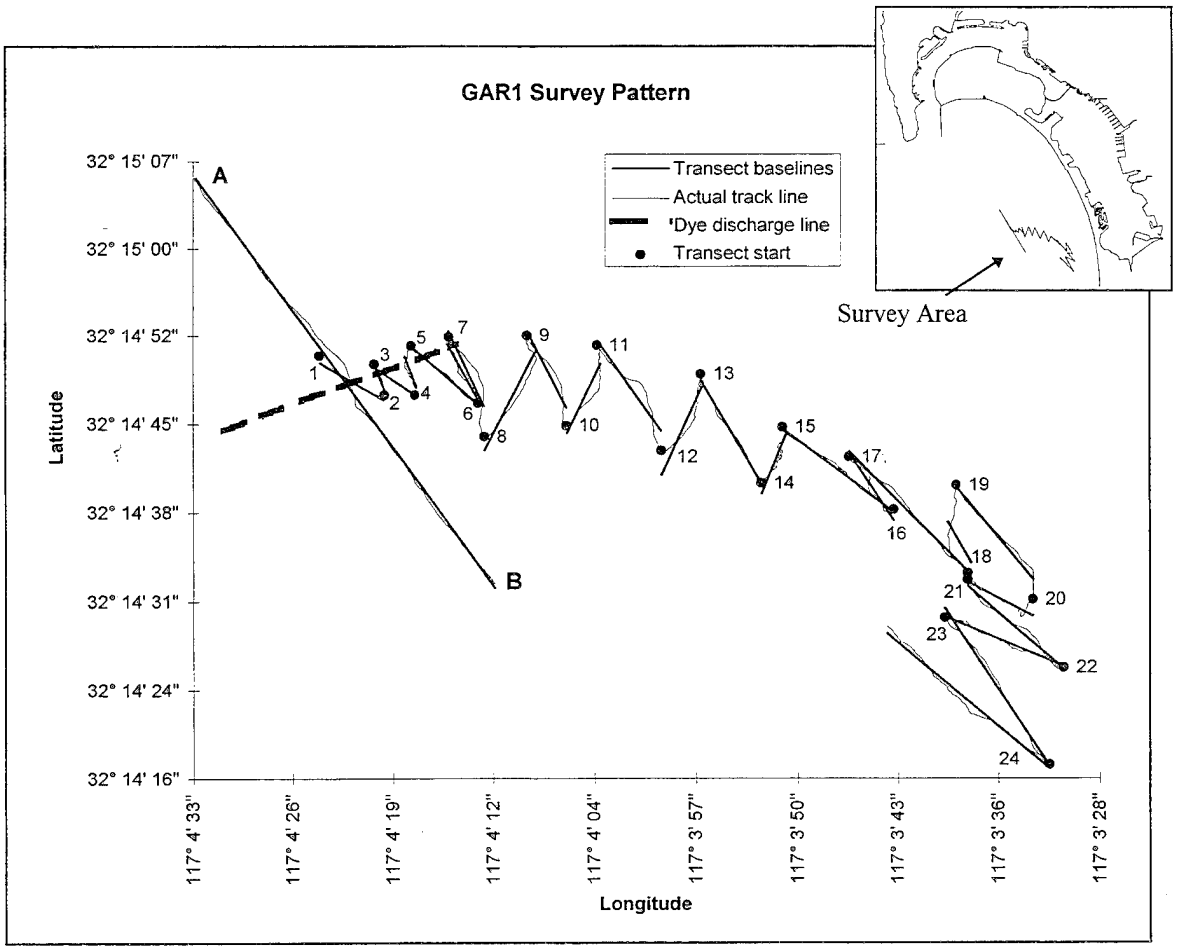

Figure 11-1. ECOS wake dispersion field survey track. Thick solid straight lines are the transect lines based on a linear regression of the actual track line. Rhodamine dye was discharged by the RV *Acoustic Explorer* along line represented by the thick dashed line.

Pre-Discharge Survey. The track followed during the test and the location of the transects utilized for analysis are shown in figure 11-1. A background transect performed prior to the discharge revealed a low salinity (32.6 psu) surface layer to a depth of about 5 m, below which the salinity was somewhat higher (33.2 psu) and uniform to the bottom at a depth of about 21 m. Water temperature was fairly uniform throughout the study area at about 14.5°C. The resulting ambient density structure was thus primarily a function of salinity and showed a strong pycnocline at a depth of about 5 m. A high-background particulate load was associated with the low-density surface layer, apparently due to stormwater runoff from the Tijuana River located to the southeast of the study area. TSS levels in the surface layer reached 9 $mg \cdot L^{-1}$ and dropped to 3 $mg \cdot L^{-1}$ in the subpycnocline water (figure 11-2). This background loading made it difficult to distinguish the pulped paper particles during the discharge operation.

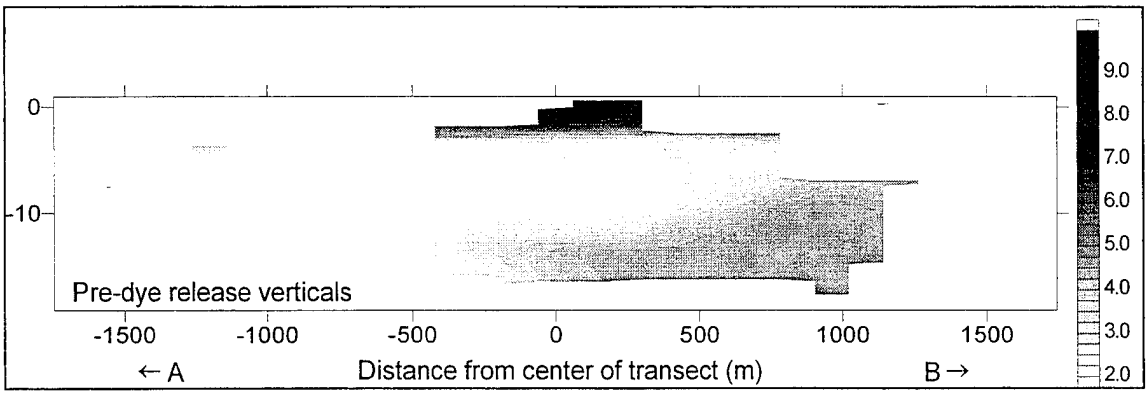

Figure 11-2. Cross-section of wake dispersion field survey area before rhodamine dye release showing total suspended solids based on transmissometer data.

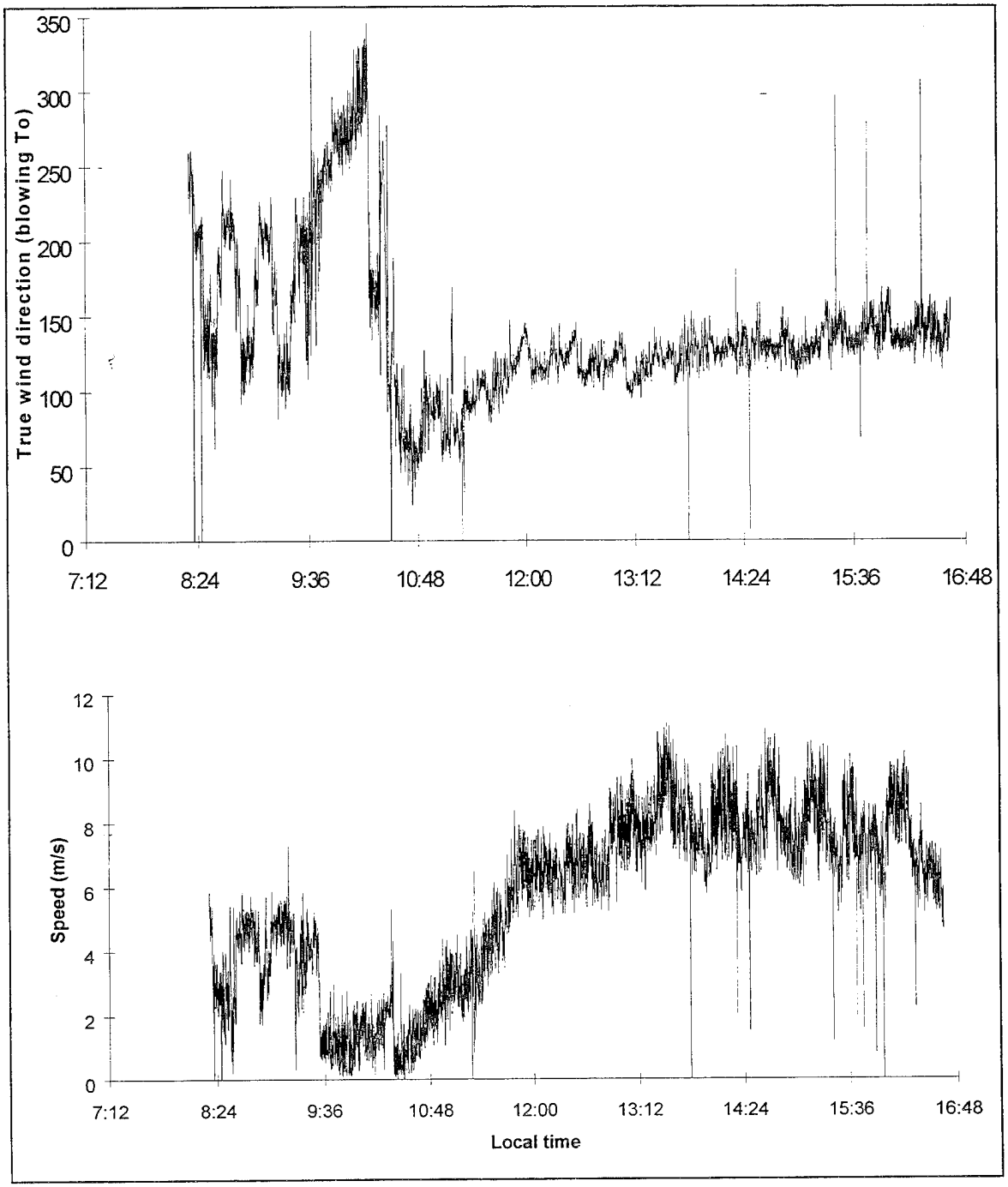

Figure 11-3. Unfiltered wind direction and speed during the wake dispersion field survey. Note that the wind direction indicated is the direction the wind is blowing.

A mooring at the center of the study region recorded currents at 5 and 10 m depths, and temperatures at 1, 5, and 10 m. Variations in temperature were insignificant. Currents at the surface ranged from 5 to 15 $cm \cdot s^{-1}$. Surface currents prior to the discharge were eastward at 10-12 $cm \cdot s^{-1}$. Following the discharge, large oscillations (5-8 $cm \cdot s^{-1}$) were observed in the surface currents indicating possible internal waves or shear instabilities on the density interface.

Average surface currents remained eastward at about 10 $cm \cdot s^{-1}$ during the wake tracking. Surface currents appear to have been influenced by surface wind stress. Winds during the study were light during the morning hours and increased to 8 $m \cdot s^{-1}$ from the west (figure 11-3). A surface drifter released at the mooring was also observed to drift to the east over the course of the experiment. Currents at the 10 m depth ranged from 1 to 8 $cm \cdot s^{-1}$ and showed an oscillation at the semidiurnal tidal period (figure 11-4). Prior to the discharge, the deep currents were southward at about 8 $cm \cdot s^{-1}$ and decreased to 2 $cm \cdot s^{-1}$ just prior to the release. Following the discharge, the currents slowly changed to northward and increased during the tracking to 6 to 8 $cm \cdot s^{-1}$.

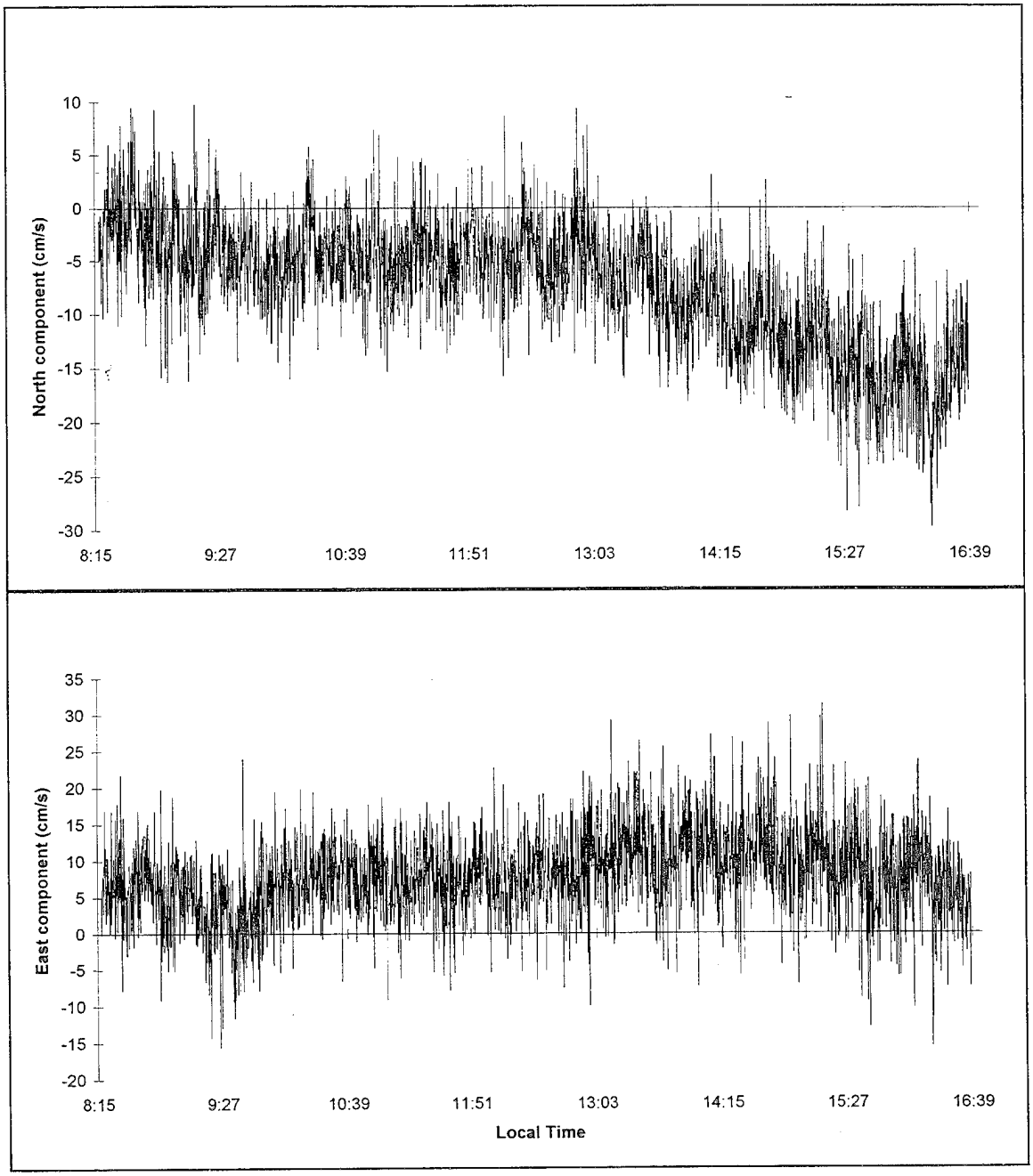

Figure 11-4. Unfiltered water current velocity at a depth of 2.7 m (separated into north and east components) during the wake dispersion field survey measured by an acoustic Doppler current profiler (ADCP).

Post-Discharge Survey. Between 1029 and 1033 hours, the RV *Acoustic Explorer* transited through the study area discharging a mixture of pulped paper and rhodamine dye. The initial pulp and dye concentrations were ~5% and ~2%, respectively. A total of 231 L of the mixed material was discharged along a 1 km transect at a speed of 10 knots. After the ship passed the midpoint of the transect, the RV *Ecos* began a series of transects across the wake.

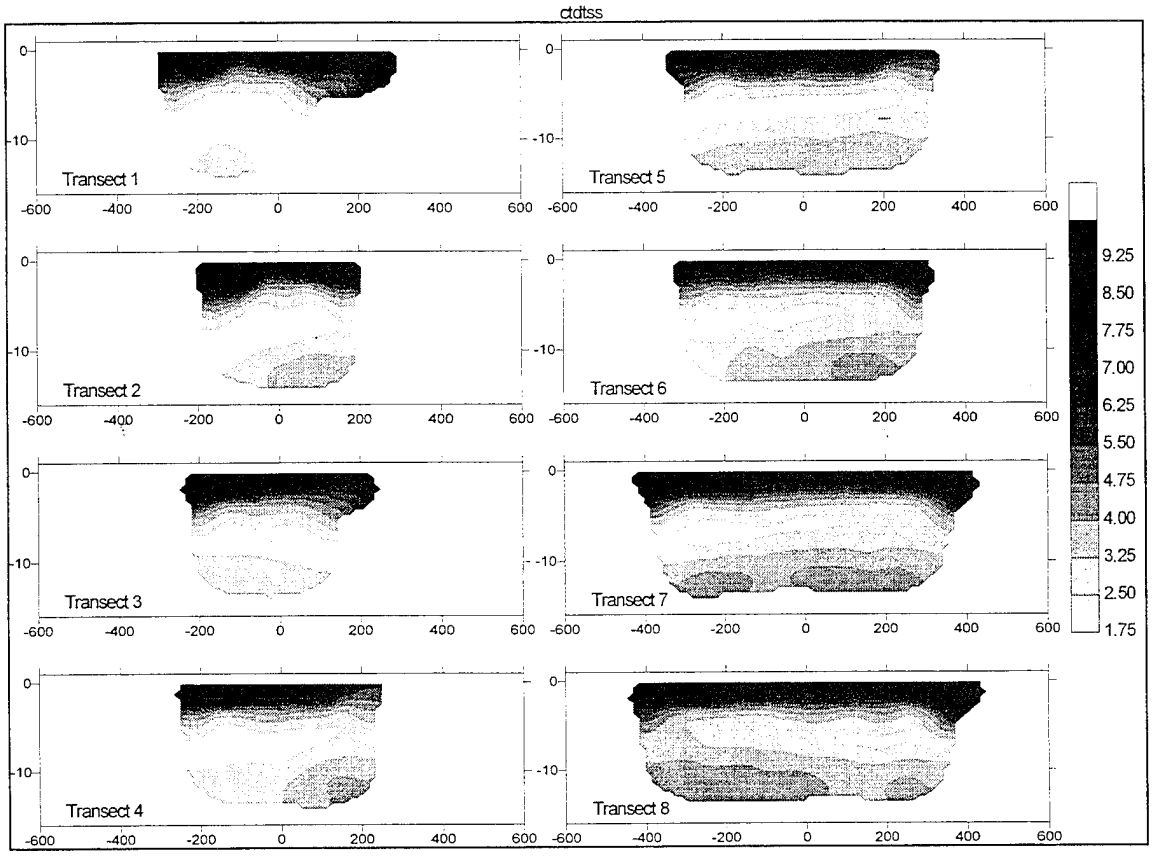

Figure 11-5. Total suspended solids in units of $mg \cdot L^{-1}$ for transects 1 through 8 of the wake dispersion field survey. White indicates no data. Vertical axis shows water depth in meters and horizontal axis is in meters from center of transect.

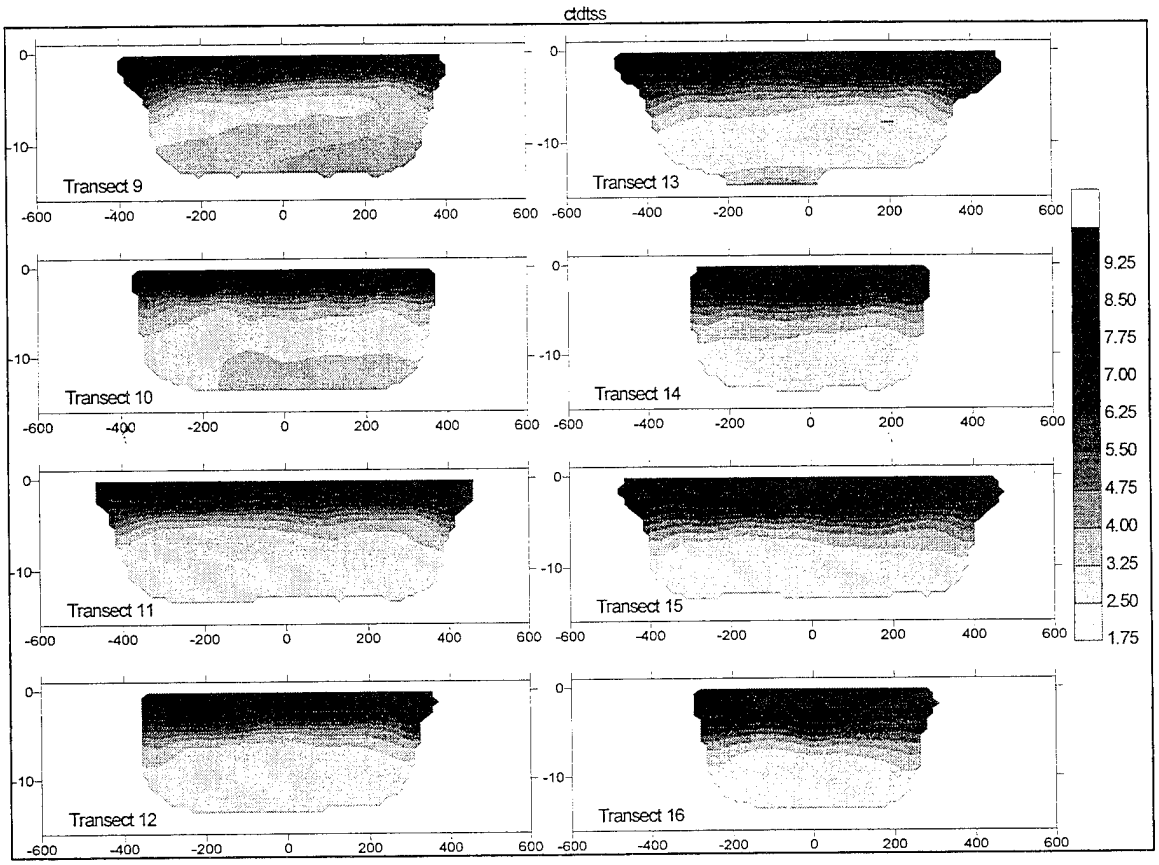

Figure 11-6. Total suspended solids in units of $mg \cdot L^{-1}$ for transects 9 through 16 of the wake dispersion field survey. White indicates no data. Vertical axis shows water depth in meters and horizontal axis is in meters from center of transect.

The TSS distribution was dominated by the background signal in the surface layer which was observed to diffuse downward over the course of the study, probably due to wind-driven mixing (figures 11-5 through 11-7). No obvious signal from the pulped paper was resolved by either the optical or acoustic particle tracking instruments. In fact, low TSS levels in transects 1 to 3 were observed in the wake of the discharge vessel, apparently due to the mixing of low-background, subpycnocline water into the surface layer by the action of the wake. This effect was also apparent in the helicopter photos which showed the RV *Acoustic Explorer* parting the turbid surface layer during its transect (figure 11-8).

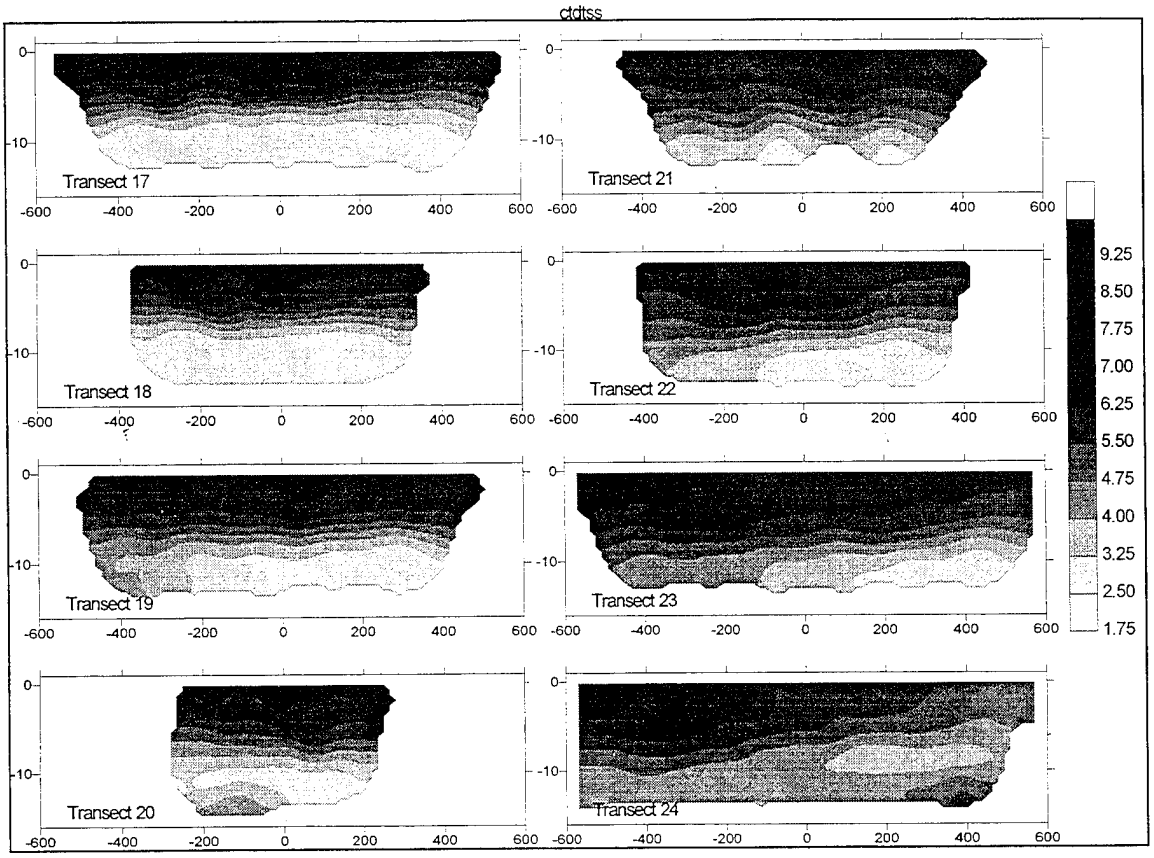

Figure 11-7. Total suspended solids in units of $mg \cdot L^{-1}$ for transects 17 through 24 of the dye release survey. White indicates no data. Vertical axis shows water depth in meters and horizontal axis is in meters from center of transect.

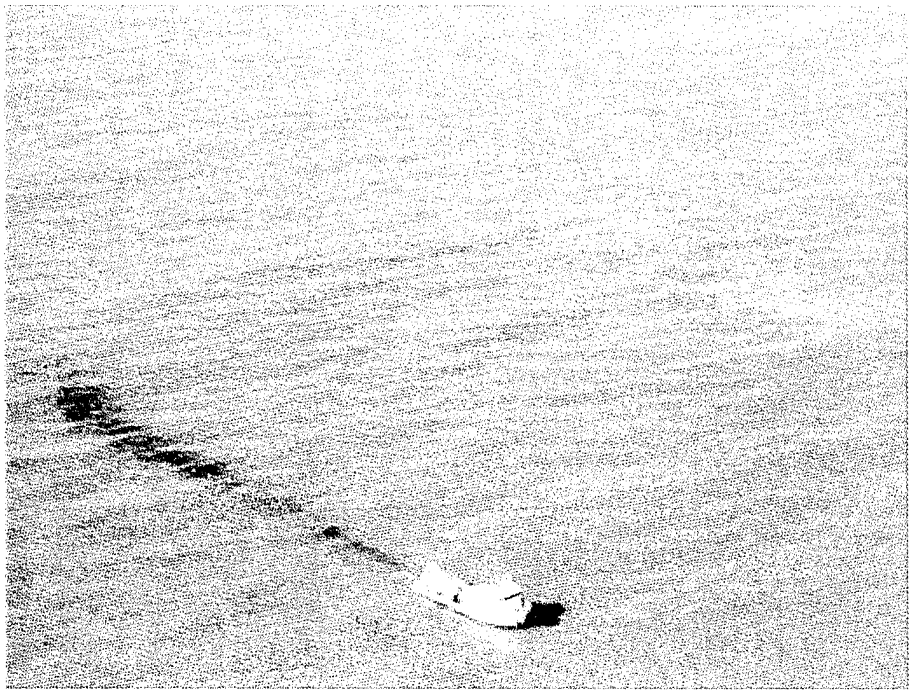

Figure 11-8. Photo showing wake from RV *Acoustic Explorer* parting the turbid surface layer revealing the wake dispersion field below.

The low background for rhodamine made tracking the dye significantly more effective than the pulped paper. The disadvantage of the dye is that is does not sink in the same manner as the larger particles of the pulped material are expected to do. The dye data are still useful in that they provide insight into (1) the effectiveness of the initial wake mixing when gravity effects on the particles are negligible, (2) the dilution of the elutriate or liquid-phase ejected as part of the waste stream, and (3) the dilution of the small, slowly sinking particles which would generally be of most concern for longer term exposure.

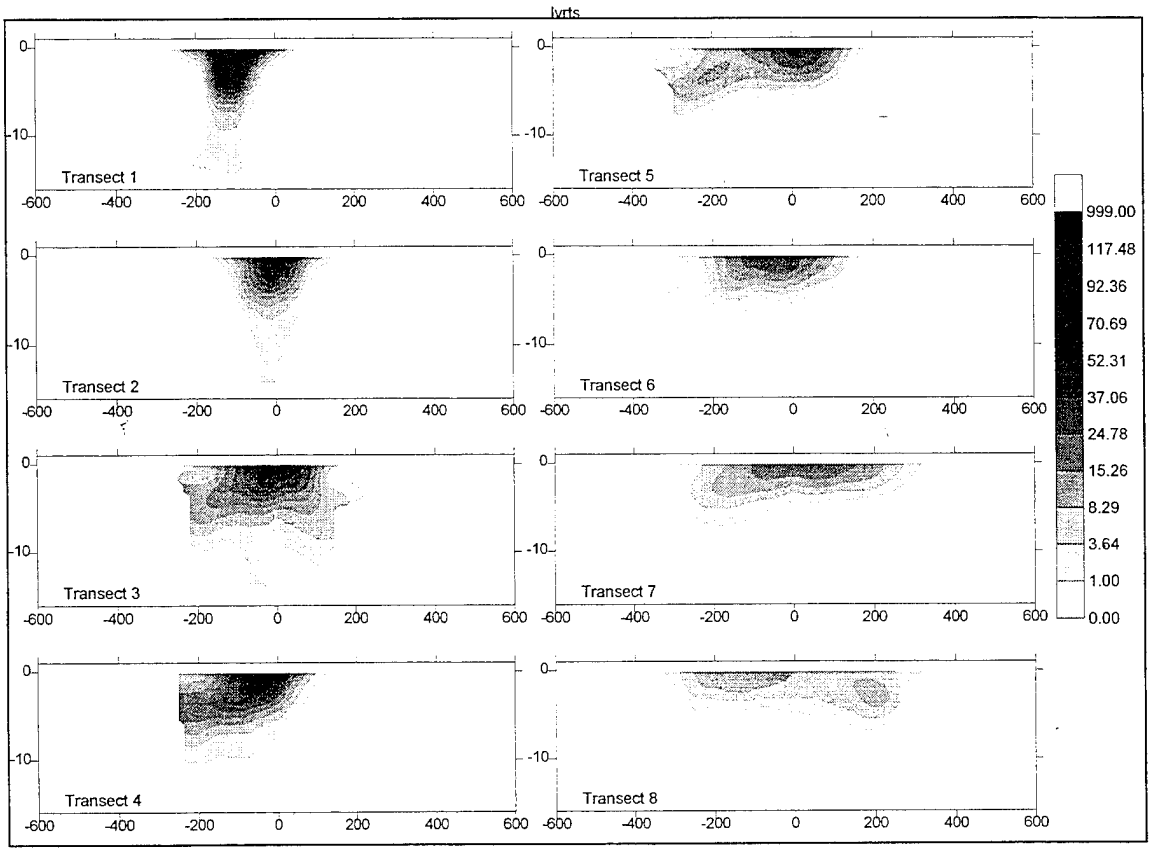

Figure 11-9. Rhodamine dye concentrations for transects 1 through 8 of the wake dispersion field survey. White indicates not detected or no data. Dye concentrations are in $\mu g \cdot L^{-1}$. Vertical axis shows water depth in meters and horizontal axis is in meters from center of transect.

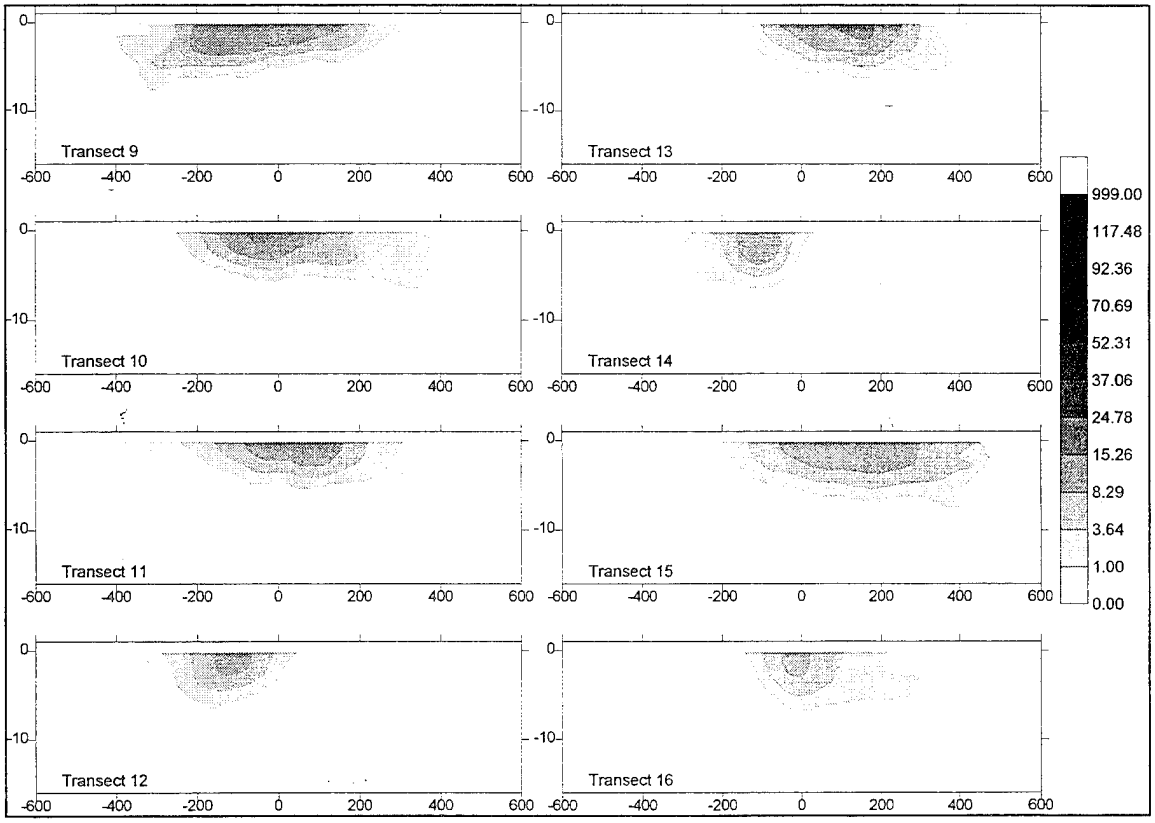

Figure 11-10. Rhodamine dye concentrations for transects 9 through 16 of the wake dispersion field survey. White indicates not detected or no data. Dye concentrations are in $\mu g \cdot L^{-1}$. Vertical axis shows water depth in meters and horizontal axis is in meters from center of transect.

The dye sections (figures 11-9 through 11-11) show that the initial discharge was rapidly mixed over a region extending ~200 m in width and 5 to 10 m in depth. There is some indication of elevated concentrations extending to depths >10 to 12 m in sections 1 through possibly due to dye carried on the large, rapidly sinking particles. Subsequent mixing of the dye is primarily in the horizontal plane. The contour maps of dye were integrated to determine if the measurements accounted for the amount of dye released. Based on the discharge scenario described above, it was estimated that ~0.0055 $kg \cdot m^{-1}$ of dye was discharged into the wake. Comparing this value to the integrated contours, the measurements and the discharge estimate agree within a factor of ~3, with the measurements overestimating in the early stages of the experiment (figure 11-12). Csanady (1981) suggests that a mass balance within one order of magnitude should still provide reasonable likelihood of observing peak dye levels and estimating the effects of oceanic mixing. It appears that the overestimate of total dye during the early transects may be an artifact of the contouring process because the spacing between tow-yo was large compared to the length scale of the dye gradient. It can also be attributed to nonperpendicular wake crossing.

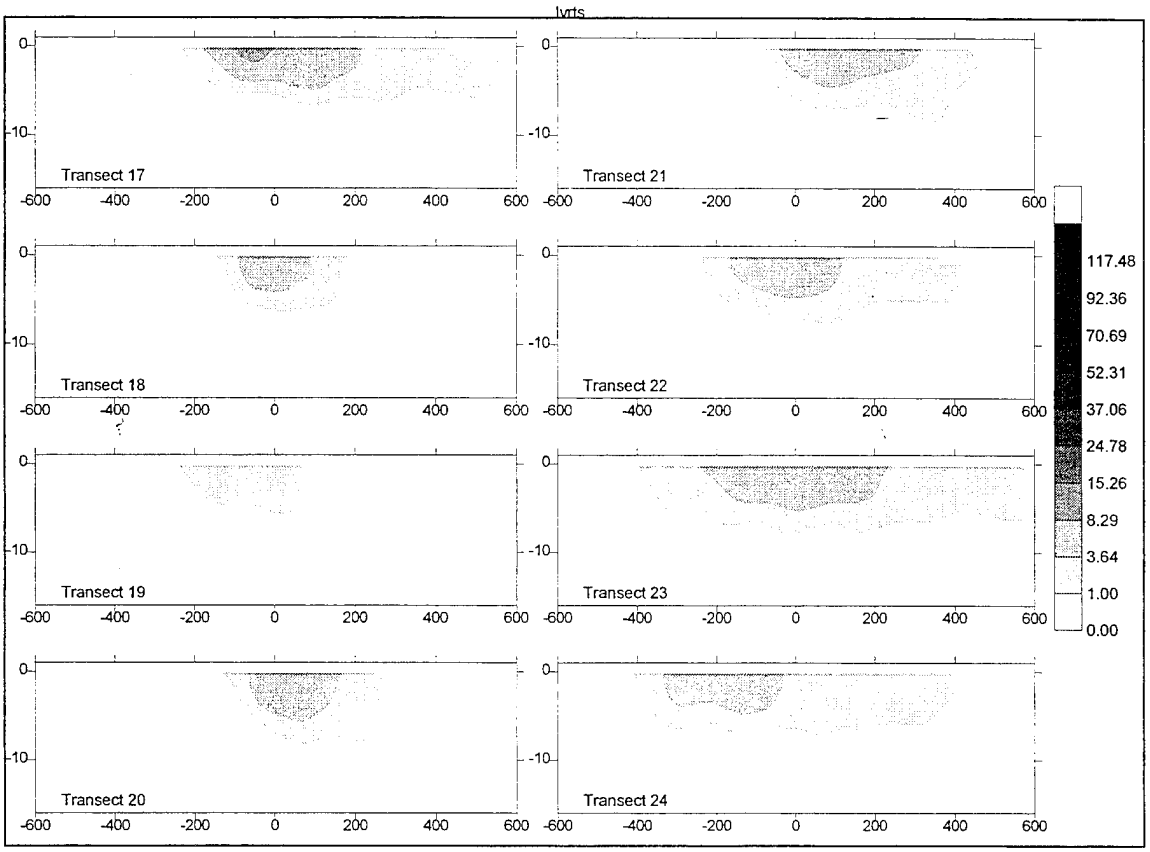

Figure 11-11. Rhodamine dye concentrations for transects 17 through 24 of the wake dispersion field survey. White indicates not detected or no data. Dye concentrations are in $\mu g \cdot L^{-1}$. Vertical axis shows water depth in meters and horizontal axis is in meters from center of transect.

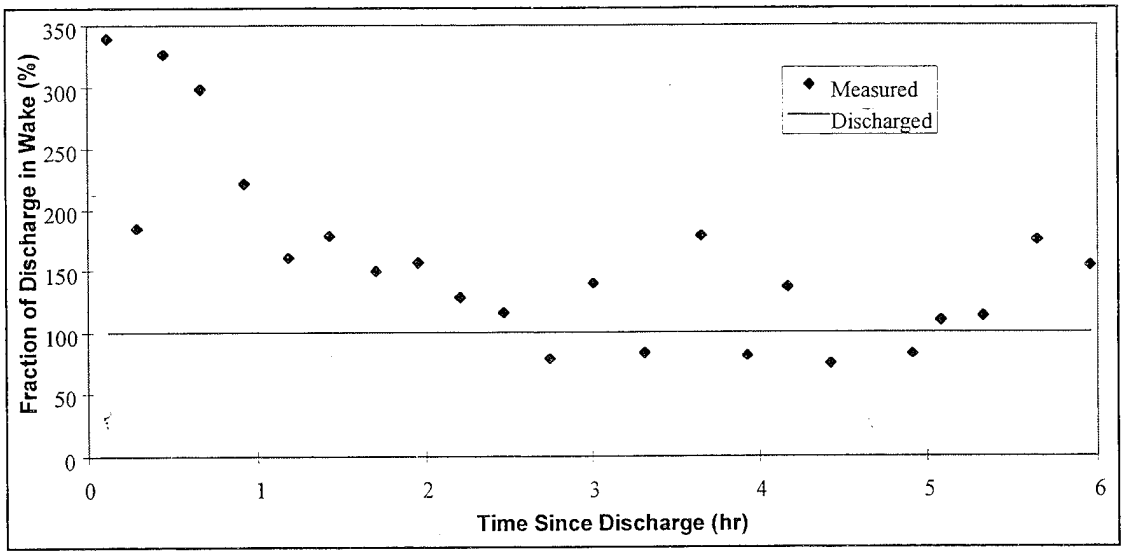

Figure 11-12. Comparison of integrated cross-sectional dye loading per unit length and estimated discharge loading per unit length over time.

The cross-sectional plots show that the plume width grew from ~200 m width on transect 1, just after discharge, to a maximum width of ~1200 m on transect 24 performed about 6 hours after the discharge. Using 4.3 times the horizontal standard deviation (90% level) of the dye plume as an indicator of the observable plume width (Csanady, 1981), the measured width is plotted in figure 11-13. Assuming the plume width satisfies a constant diffusion velocity model, e.g.,

$$\sigma_y = \omega t \qquad \text{(Eq. 11-1)}$$

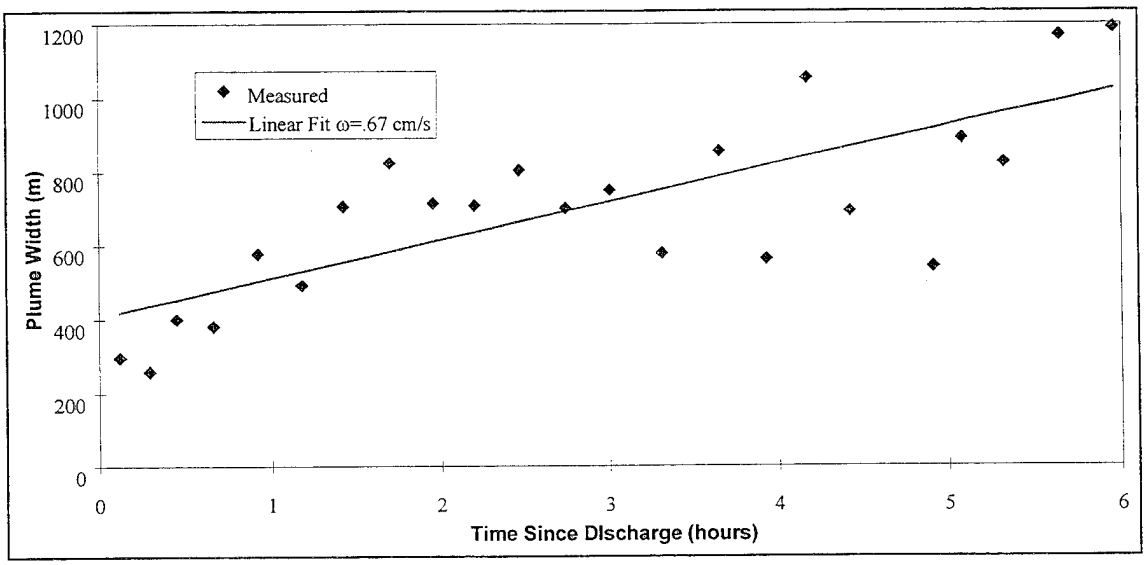

Figure 11-13. Linear fit using wake spreading velocity of ω =0.67 cm·s^{-1}. Width of dye plume over time measured in field experiment survey.

where σ_y is the standard deviation of the plume, ω is the diffusion velocity, and t is time, the diffusion velocity was found to be about 0.67 $cm \cdot s^{-1}$. This value is in reasonable agreement with the range of 0.2 to 2.0 $cm \cdot s^{-1}$ reported by previous investigators (Csanady, 1966, 1973; Okubo, 1971; Pritchard and Okubo, 1969) where 0.2 corresponds to quiescent conditions, and 2.0 corresponds to strongly mixed conditions.

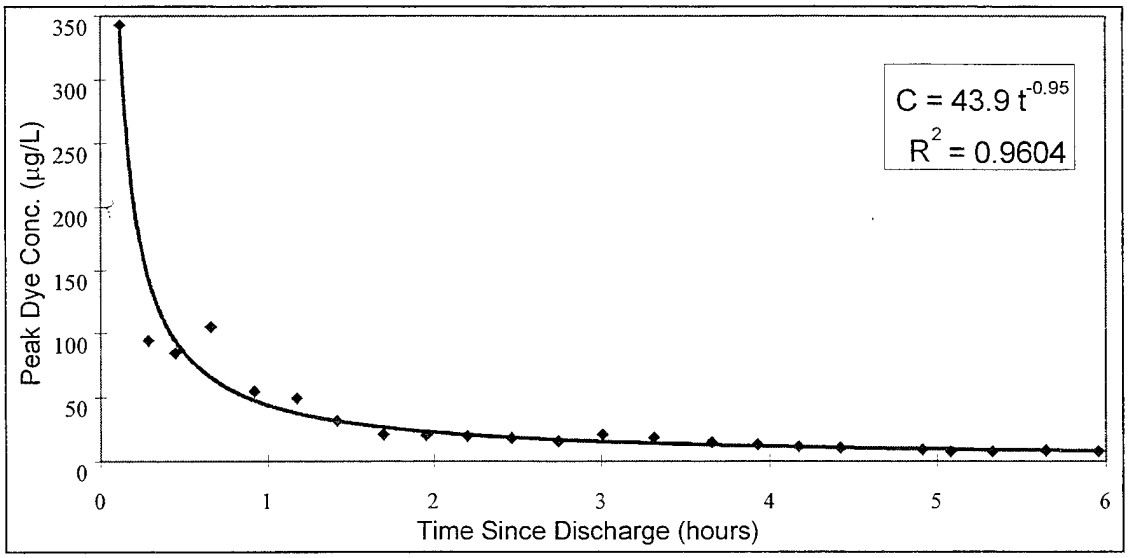

Figure 11-14. Peak dye concentrations over time measured during field survey experiment. A power-law regression to the data is represented by the solid line.

The peak concentration in the plume was extracted from each transect and plotted as a function of time since discharge (figure 11-14). The plot indicates that the peak dye level dropped rapidly from its highest level of about 350 $\mu g \cdot L^{-1}$ on transect 1 to about 50 $\mu g \cdot L^{-1}$ at 1 hour after discharge. The concentration then dropped more gradually over the remaining 5 hours of the study. A best fit to the data indicates a relationship of the form

$$C_{max} \propto t^{-0.95} \qquad \text{(Eq. 11-2)}$$

which is consistent with the constant diffusion velocity model ($C_{max} \propto t^{-1}$). Based on the known initial concentration of the dye (~5%), the initial dilution in the wake, and the subsequent dilution rate by the ambient ocean, mixing can be estimated (figure 11-15). Based on the peak concentration of transect 1, the dilution due to wake mixing was about $1.5 \cdot 10^5$. As a check on this value, Csanady (1981) provides a scaling for the wake mixing base on empirical data of the form:

$$D = \frac{8BDL}{V} \qquad \text{(Eq. 11-3)}$$

where B is the ship breadth, D is the draft, L is the length of the discharge, and V is the volume of the discharge. For the RV *Acoustic Explorer*, B≅8 m and D≅3 m. For this experiment, L≅1000 m and V≅12 L. This gives an expected initial wake dilution of $\sim 8 \cdot 10^5$, somewhat higher than the measured dilution on transect 1 but within reasonable agreement of dilution rates observed within the first hour following the discharge. The subsequent ambient dilution was found to satisfy the relation:

$$D \propto 10^6 t \qquad \text{(Eq. 11-4)}$$

where t is in hours, so that after 1 hour, $D \sim 1 \cdot 10^6$, and after 6 hours, $D \sim 6 \cdot 10^6$. Thus the field results indicate a fairly high initial dilution within ~1 hour due to the wake mixing, followed by a more gradual dilution process associated with the ambient ocean mixing.

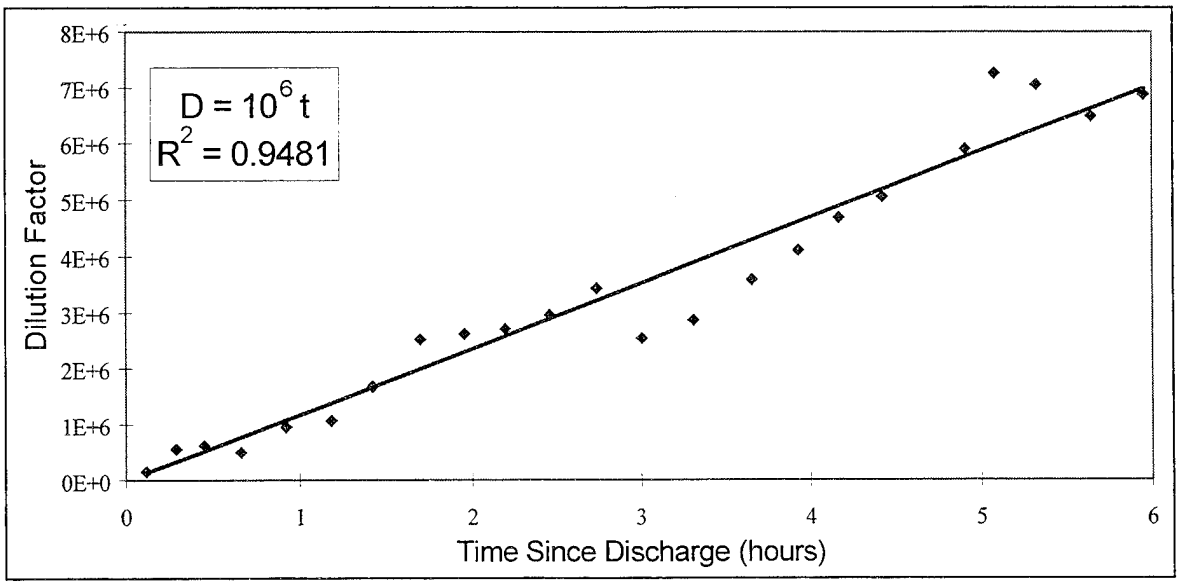

Figure 11-15. Measured dilution of dye based on peak concentrations observed in the wake during the wake dispersion field survey.

12.0 ANALYSIS

12.1 Fate and Effects of Pulped Paper Waste Stream

The discussion presented in this section is organized into three areas: (1) a general discussion of the fate and effects from a typical ship discharge operation, (2) an analysis of the potential effects of hypothetical multiship operational scenarios in each of the Special Areas, and (3) an analysis of basin scale mass loading issues based on historical operational data from specific MARPOL Special Areas. This section summarizes the discharge conditions, effluent characteristics, and water column and sea floor processes which determine the fate and potential effects of the pulped paper waste stream.

Discharge Conditions

Rate. Discharge conditions determine the amount of material that enters the environment, the rate at which it enters, and the initial condition for subsequent environmental processes. For a given ship, the discharge rate for the pulped paper is established by the processing rate of the pulpers, the number of pulpers installed on the ship, and the number of pulpers operated at a given time. The small and large pulpers have processing rates for paper/cardboard of 45 and 226 $kg \cdot hr^{-1}$, respectively (NAVSEA, 1993). The number of pulpers installed ranges from one small pulper on smaller ship classes (e.g., DDG 51 through 67, FFG 7), to three large pulpers on the CV and CVN class ships. This gives a maximum possible range for discharge rates of 45 to 678 $kg \cdot hr^{-1}$. During the pulping process, the paper is mixed with water in an initial ratio of about 1:50 (2% by weight). The mixture is then discharged by eduction with seawater resulting in typical water/solids ratio at the discharge point of about 1:100 (1% by weight). Thus for every pound of paper discharged, approximately 100 pounds of water are discharged. This water will have been vigorously mixed with the solid phase and thus may contain soluble fractions of the waste stream.

Duration. The discharge period will be determined by the waste stream generation rate and the operational practices of the ship. The waste stream generation rate for paper/cardboard has been estimated at 0.50 $kg \cdot person^{-1} \cdot d^{-1}$, and the ship complements ranges from about 50 persons on the MHC 51 class ship to about 6286 persons for the CVN 68 (NAVSEA, 1993). Thus the total solid waste stream generation rate ranges from 25 to 3200 $kg \cdot d^{-1}$. Based on a solids content of 1%, an additional 2500 to 320000 $kg \cdot d^{-1}$ of liquid phase would also be discharged. So for the CVN 68, the total discharge period could range from about 4.6 $hr \cdot d^{-1}$ with all three pulpers running to about 14 $hr \cdot d^{-1}$ with only one pulper running. The number of pulpers run at a given time and the manner in which the discharge period is distributed through the day will vary from ship to ship and depend on operational constraints.

Area of Impact. Together with the discharge period, the discharge speed determines the overall length of the discharge plume. Operating speeds for Navy ships range from 10 to 30 knots (9 to 56 $km \cdot hr^{-1}$) with typical transit speeds of about 15 knots (28 $km \cdot hr^{-1}$). Thus, based on the estimated discharge period for the CVN 68, and assuming continuous discharge with no interruptions, the length of the discharge plume could range from between 130 to 400 km with a solids loading of about $2.4 \cdot 10^{-4}$ $kg \cdot m^{-1}$. In either case, the initial plume would be extremely long and narrow. Assuming the initial plume width to be approximately three ship breadths (Csanady, 1987), the CVN 68 would have a plume width of ~100 m. The aspect ratio (length:width) of the plume would thus range from about 1300:1 to 4000:1.

Discharge Location. Discharge location on the ship will vary from ship to ship, but in general will be located somewhat above the waterline along the side of the ship. Previous studies have reached conflicting conclusions regarding the effect of discharge location on the ship. Delvigne (1980) studied the dispersion of acid waste in the wakes of tankers and found no significant difference in wake dilution between a discharge 0.2 ship lengths forward of the stern and a discharge directly into the propeller wake. Model studies of tankers conducted by Mercier et al. (1973) showed variations in wake dilution dependent on discharge location with maximum mixing occurring for a discharge point 0.2 ship lengths forward of the stern and just below the turn of the bilge. Sea tests of sewage and dye mixing in the wake of an LCU by Alig (1974) indicated that material discharged off the side of the ship was substantially mixed across the wake. Results from model simulations for this study also showed little sensitivity to the initial athwartship location of the discharge. In general, it appears that the material will be mixed into the wake in most discharge configurations, while it may be best to keep the discharge point near the stern of the ship and underwater for optimum mixing. Clarification of this issue would require further study.

To summarize, the pulped waste stream discharge will vary significantly depending on generation rates, number of pulpers, pulper processing rates, operational practices, ship speed, ship class, and discharge location. In general, the resulting initial discharge plume will consist of a solids portion consisting of the pulped paper and a liquid portion containing soluble fractions of the waste stream which have partitioned during the pulping process. A typical plume will extend over an area of up to several hundreds of kilometers in length, several to hundreds of meters in width, and several of meters in depth. The material is likely to be significantly diluted by wake action of the ship independent of exact discharge location, however, the actual degree of dilution may have some dependence on the location of the overboard discharge port.

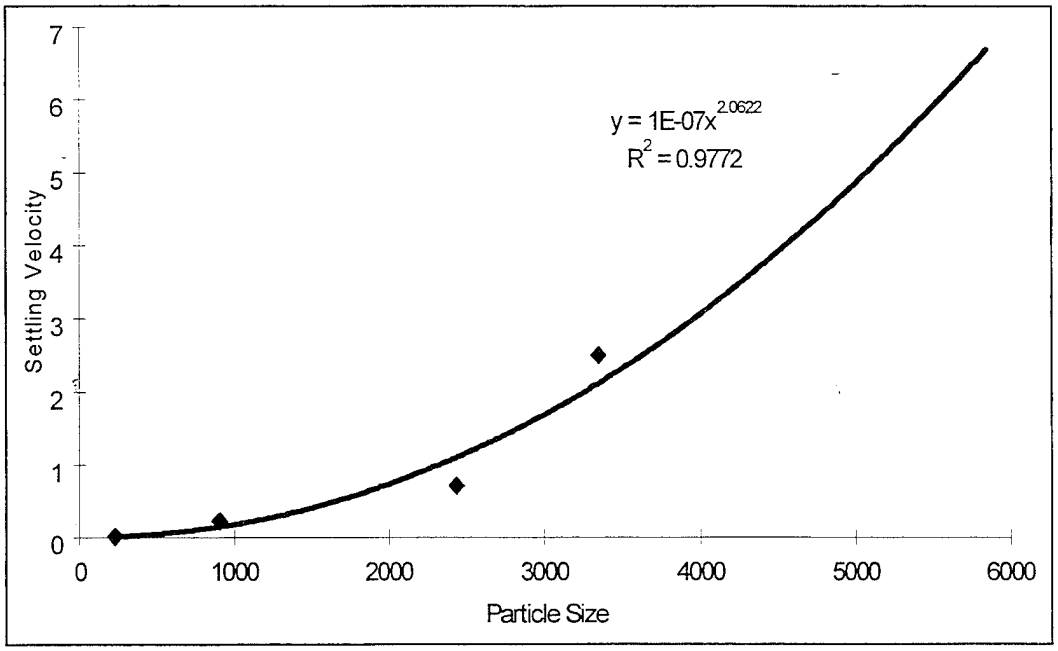

Figure 12-1. Particle size verses settling velocity. The relationship between particle size and settling velocity was estimated indirectly by combining the microscopic size verses mass fraction results with the settling column size verses settling velocity results.

Waste Stream Characteristics

Bulk Composition & Physical Characteristics. The pulped paper waste stream consists primarily of white paper and cardboard with a small fraction of other paper types. Paper is generally made up of cellulose fibers combined with a small fraction of additives including fillers, dyes, and inks. Test results indicate that typical samples contain about 92% organic matter, suggesting that a maximum of about 8% of the waste stream might consist of inorganic fillers and other additives. Settling column, sieve, and microscopic analysis of the pulped paper indicate that the solids fraction of the pulped waste stream is composed of a range of particle sizes from about 16 to about 6000 μm. The particles are typically composed of either single paper fibers, or some combination of fibers, which are bundled together or interlaced in matrix form. Individual fibers are roughly cylindrical with diameters of about 20 μm and aspect ratios of >5:1. The fibrous nature of the particles results in a high surface area to volume ratio. For instance, a typical matrix particle made up of ten fibers each 20 μm in diameter by 200 μm long would have a surface area of $1.26 \cdot 10^5$ μm^2 and a volume of $6.28 \cdot 10^5$ μm^3 giving a surface area to volume ratio of about 0.2. A spherical particle of the same volume would have a diameter of 106 μm and a surface area to volume ratio of about 0.06, or about 36% of the matrix. Although there are large numbers of small fibers, they only make up <5% of the waste stream by mass, while about 95% is contained in larger fibers, bundles, and matrices (figures 8-1 and 8-2). The density of the material was found to be fairly uniform across the various size fractions: with a mean density of 1.52 $g \cdot cm^{-3}$. This high density and the large fraction of the mass contained in the larger particle sizes indicates that much of the solid phase will sink rapidly. This was confirmed by settling tests which indicated average overall sinking rates of about 700 $m \cdot d^{-1}$. The settling

tests suggest that the material can be roughly divided into three fractions, a rapidly sinking (820 $m \cdot d^{-1}$) large particle fraction which contains about 85% of the solid phase by weight, a slowly sinking (6 $m \cdot d^{-1}$) midsize particle fraction which contains about 12% of the solid phase, and a smaller nonsinking fraction which contains about 3%. The relationship between particle size and settling velocity was estimated indirectly by combining the microscopic size verses mass fraction results with the settling column size verses settling velocity results (figure 12-1). Based on this analysis, the size of the rapidly sinking particles is generally >1000 μm, the slowly sinking particles from about 200 to 1000 μm, and the smallest particles from about 15 to 200 μm.

Chemical Characteristics. The chemical analysis confirmed that the bulk of the solid phase consists of organic cellulostic material. Average background-corrected water quality of the paper waste stream directly out of the pulper were 214 $mg \cdot L^{-1}$ BOD_5, 417 $mg \cdot L^{-1}$ COD, 0.15 $mg \cdot L^{-1}$ PO_4, 1.29 $mg \cdot L^{-1}$ N, 3158 $mg \cdot L^{-1}$ TSS, and 0.2% TOC. The total solids fraction of ~0.3% indicates that previous estimates of 1% solids in the pulper waste stream are fairly accurate. Consistent with the chemical composition of cellulose $(C_6H_{10}O_5)_n$, the pulped material is mainly composed of organic carbon with very little nitrogen or phosphorous. The ratio of C:N:P (by weight) in the solid phase of the pulped material is roughly 2000:1.3:0.15 compared to average values for naturally occurring marine organic matter which have C:N:P ratios of roughly 41:7.2:1 (Redfield, 1934), 17:7.5:1 for treated municipal sewage (Wastewater Chemistry Laboratory, 1994), and 56:6 for C:N in marine sediments (Sverdrup et al., 1942). This result has two primary implications. First, it implies that the nutrient loading from the pulper effluent will be low relative to other sources of particulate organic material in the ocean. This suggests that productivity should not be significantly enhanced by the waste stream and thus eutrophication should not be a major impact. The second implication is that because of its low nutrient content, the material would not be the best source of carbon to marine bacteria. This suggests that microbial degradation would likely be hindered where nutrient conditions were limiting such as occurs in the surface waters of many of the Special Areas.

The refractory nature of the pulper waste stream is also reflected in the BOD_5 and COD values. The BOD_5 value, when corrected for dilution (0.3%), is about 0.07 $g \cdot g^{-1}$, consistent with published values for cellulose of 0.08 $g \cdot g^{-1}$ BOD_5 (Furness, et al., 1990). However, the dilution corrected COD level of 0.14 $g \cdot g^{-1}$ is considerably lower than the theoretical total oxygen demand (TOD) value of 1.18 $g \cdot g^{-1}$ required for complete oxidation of cellulose. This may be due to incomplete oxidation in the COD test as suggested by Pitter and Chudoba (1990). The BOD_5 and COD levels are also relatively lower than those found in sewage treatment plant influents (Wastewater Chemistry Laboratory, 1994) or in discharge effluent not subjected to primary treatment (Pyewipe, 1992-1994). The amount of organic carbon and high surface area of the particles generated in the pulping process is sufficient to generate these levels. It should be noted that although cellulose has the same basic molecular makeup as starch, the BOD_5 of starch is 7 times greater at 0.62 $g \cdot g^{-1}$ (Pitter et al., 1990). This suggests a substantially lower degradability of the cellulose relative to starch as a result of structural differences. Results from the water quality characterization are compared to typical sewage treatment levels and representative ocean discharge standards in figure 12-2.

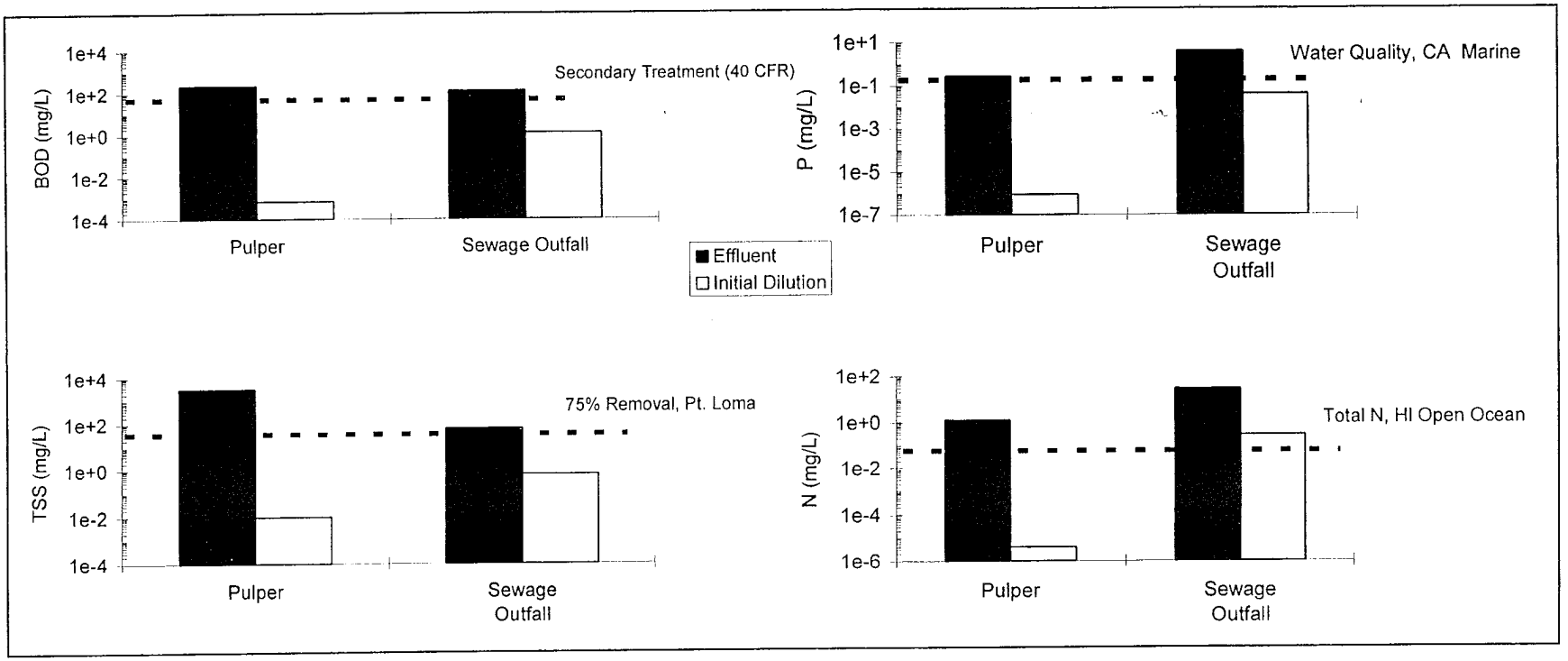

Figure 12-2. Chemical characterization of pulper effluent. The two bars on the left of each plot are for pulped paper constituents. The two bars on the right of each plot represent similar values for a typical sewage discharge effluent. Initial dilution (unfilled bars) represent wake dilution of 10^5 for pulper and 10^2 for a typical sewage diffuses. The dotted lines are various criteria which have been published for the control of waste water discharge.

The results of the priority pollutant scans showed no pollutants at levels which would be expected to produce impacts. All 126 compounds were below the detection limit of the analyses performed except for zinc at 5.6 $mg \cdot kg^{-1}$, acetone at 1.8 $mg \cdot kg^{-1}$, and a few aliphatic hydrocarbons between C_{16} and C_{20} at 6 $mg \cdot kg^{-1}$ (all on a dry weight basis). The presence of zinc at 6 $mg \cdot kg^{-1}$ dry weight is a factor of 25 below the Effects Range Low (ERL) threshold for zinc in sediments (150 $mg \cdot kg^{-1}$, Long et al., 1995), a guideline for concentrations representing minimal toxicity effects. It is also well below the 960 $mg \cdot kg^{-1}$ screening level guideline for sediments, using Puget Sound Sediment Management Standards, 1991, one of the only sources for sediment quality guidelines. The presence of aliphatic hydrocarbons at the low levels observed are indicative of background values that would naturally be present in the marine environment, and as such, do not constitute a contaminant. There are no water or sediment quality criteria for acetone. The only hazard criterion available to compare with is the Material Safety Data Sheet value for an oral rat toxicity at 9750 $mg \cdot kg^{-1}$ (LD_{50}). It is unclear whether the acetone was a degradation product of bacteria associated with the paper, or a constituent of the waste stream itself. For all of the priority pollutant measurements, it must be kept in mind that the compounds measured may potentially be a result of their presence in the river water used for pulping the material at CDNSWC/AD rather than from the pulped material (remembering that the paper was well saturated).

Table 12-1. Mass loading estimates for the daily discharge of pulped paper constituents from various Navy ship classes. All values are in $kg \cdot d^{-1}$.

	Ship Class				
Constituent	CVN 68	CG 47	AOE 1	DD 963	FFG 7
TSS	3176	412	362	199	111
BOD_5	213	28	24	13	7
COD	417	54	48	26	15
TOC	2010	261	229	126	70
PO_4	0.1	0.013	0.011	0.006	0.003
N	1.3	0.17	0.15	0.08	0.05
Zn	5.4	0.70	0.62	0.34	0.19

The expected waste loading for a typical ship discharge can be estimated for the constituents analyzed using the discharge data summarized above. Based on an inputs from 111 to 3176 $kg \cdot d^{-1}$ for a range of ship classes, the waste loading for a typical one-day discharge was estimated and summarized in table 12-1. The table shows that daily constituent inputs may vary by more than an order of magnitude, depending on ship class, and that the waste input will be primarily organic carbon in the form of cellulose.

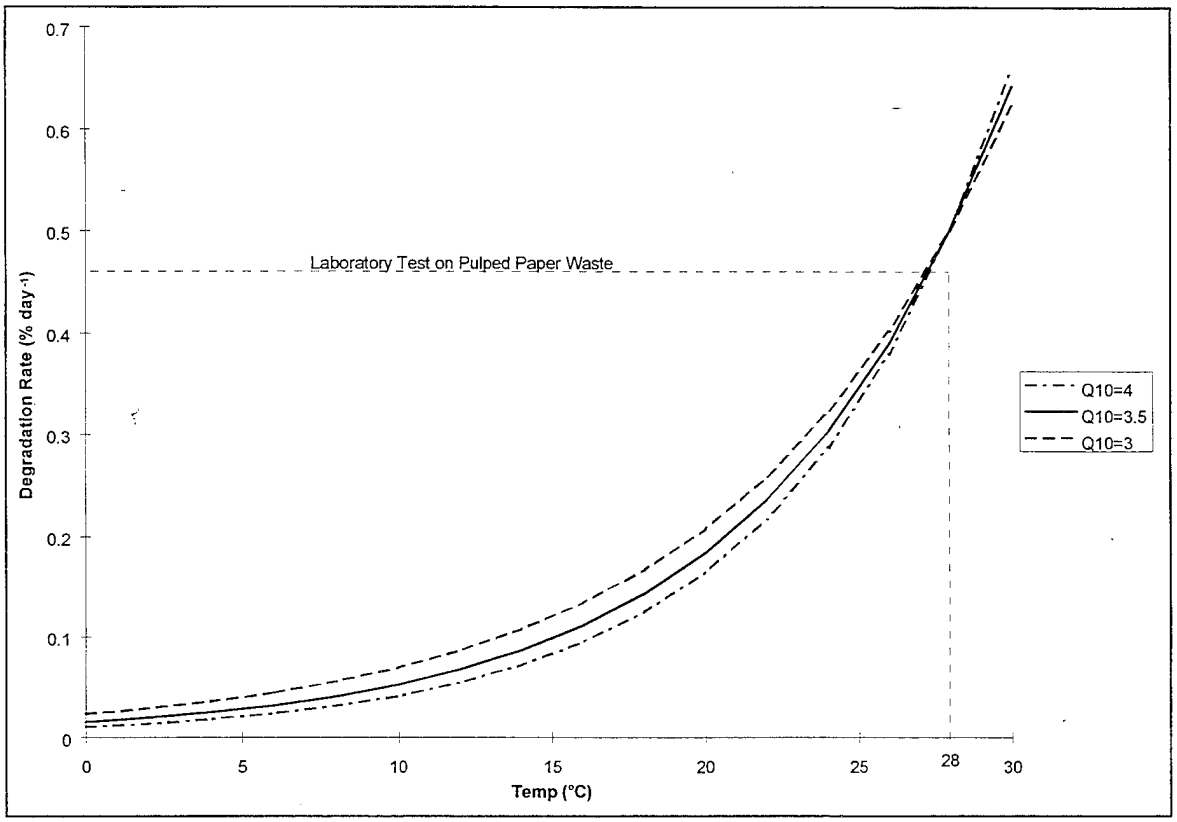

Figure 12-3. Degradation rate of pulped paper waste as a function of water temperature. The degradation rate at 28° is based on lab measurements on pulped paper. The extrapulation to other temperatures is based on the range of Q10 values reported by Benner, et al., 1986.

Degradability. The long term fate of much of the solid phase may be controlled by the rate of microbial degradation either in the water column or on the sea floor. Relatively little is currently known about the biological fate of cellulostic material in the open ocean or the cellulolytic abilities of natural oceanic bacterial assemblages primarily because cellulose is not naturally abundant in such environments. Factors which may regulate microbial degradation of the pulped paper include background abundance of cellulolytic organisms, particle size and structure, temperature, pressure, and redox conditions experienced by the attached bacterial community. Previous studies have shown rates of mineralization of plant polysaccharides (cellulose and hemicellulose from wood and grasses) range from 0.2 to 2.0%·d^{-1} (for particles <500 mm in diameter under aerobic conditions) in tropical and subtropical coastal marshes and mangrove swamps (Benner et al., 1984, 1985; Benner and Hodson, 1985). Initial laboratory tests of the solid phase pulper material indicate first order degradation rates of about 0.5 %·d^{-1} as an upper limit to degradation in seawater when temperature is optimal (28°C) and inorganic nutrients are available in excess. Previous studies have shown that cellulose decomposition rates increased by 3 to 4-fold (Q10) when incubation temperatures were increased from 10° to 20 °C (Benner et al., 1986). Using the degradation rates from this study and the Q10 value of Benner et al., (1986), a rough estimate of degradation can be obtained as a function of temperature (figure 12-3). This suggests that degradation rates in the Special Areas could vary from about 0.01%·d^{-1} in the cold bottom waters of the Caribbean, to 0.6%·d^{-1} in the warm surface waters of the Mediterranean.

Additional effects might be expected based on changes in pressure as the material sinks to the bottom.

Biological Effects Levels. Biological tests on the pulper effluent were performed on both the solid phase and elutriates of the solid phase. Particle exposure tests using zooplankton and fish showed no detectable effects for concentrations below 1 $mg \cdot L^{-1}$. At concentrations above ~160 $mg \cdot L^{-1}$, feeding interference was observed in the zooplankton species *Calanus pacificus* and *Acartia spp*. Evidence of blockage by particle pellets was observed in the digestive tracks of sardines exposed to concentrations of ~1 $mg \cdot L^{-1}$, while feeding interference was observed at concentrations of about 1 $mg \cdot L^{-1}$. Particle exposure to benthic invertebrates, including the amphipod *Grandidierella japonica* and the polychaete *Neanthes arenaceodentata,* showed no effects at any of the test exposures. The exposures corresponded to layers of 0.01, 0.1, and 1.0 mm thick, evenly distributed along the sea floor.

Elutriate tests were performed on a wide range of organisms including the luminescent bacteria *Photobacterium phosphoreum*, the marine chain diatom *Skeletonema costatum,* the bioluminescent dinoflagellate *Gonyaulax polyedra*, the benthic shrimp *Mysidopsis bahia*, and the saltwater minnow *Menidia beryllina.* The elutriate tests provide a direct indicator of the effects of the liquid phase of the waste stream and an indirect measure of the potential effects of the solid phase. Elutriates prepared with 5% pulp concentration provide a conservative (~2 to 5 times) model of the liquid phase as it exits the ship (typically ~1%). This assumes that the mixing in the pipe is similar to the mixing in the lab preparation which is also conservative since the laboratory mixing time was somewhat longer than the pulper retention time. Based on this model and the test results, no effects would be expected for the liquid phase as long as the material is initially diluted by at least 15 times the original concentration. For lower dilutions, a range of responses to the elutriate were observed, including a decrease in biomass for *Skeletonema costatum* (IC_{50}=12.5-50%), reduced stimuable light output in *Gonyaulax polyedra* (IC_{50}=27%), and mortality in the mysids (LC_{50}=22-32%). The elutriate tests can also be interpreted based on the assumption that the liquid phase is formed during mixing with the ambient water following discharge. In this case, the assays run on the 0.01% (100 $mg \cdot L^{-1}$) pulp indicate that no effects would be expected so long as the initial dilution of the solid phase exceeds ~100. Typically, immediate dilutions are on the order of 10^5 if discharged directly into the wake.

To summarize, the pulped paper waste stream is composed primarily of organic material in the form of cellulose. The majority of the mass is contained in relatively few large particles which tend to sink rapidly. The nutrient loading from the waste stream is low compared to other natural and anthropogenic sources of organic material. No toxic chemicals were detected in the waste stream at levels which would be expected to induce effects in marine organisms. The cellulostic material in the waste stream is refractory as indicated by the low BOD_5 levels and the low degradation rates. Conservative estimates suggest that biological effects should be negligible for concentrations less than about 1 $mg \cdot L^{-1}$. Higher concentrations may cause deleterious effects if sustained for periods of hours to days (based on the testing period). It is also likely that sublethal effects such as feeding inhibition would only be of transient nature as demonstrated by zooplankton and sardine recovery tests.

Water Column Processes

Initial Dilution. Discharge of pulped paper waste is expected to occur primarily during underway operations. Discussions with Navy officers indicate that static discharge scenarios were unlikely and would, in general, be avoided (personal communication, Commander Lane Wilson). Thus while static discharges could occur under unusual circumstances, initial dilution in the water column is expected to generally be controlled by mixing in the wake of the ship. This is an important distinction because dilution rates associated with static discharge tend to be several orders of magnitude lower than for wake mixing. Observations near the discharge of shipboard oil/water separators under static conditions showed initial dilutions ranging from 10 to 1000 fold (NRaD unpublished data). These values can be expected to vary significantly based on ambient conditions. Assuming 100 fold dilution for the static case, the initial concentration of the solid phase near the discharge point could be expected to reach levels of 100 $mg \cdot kg^{-1}$. If discharge were sustained for several hours in a region of poor circulation, higher concentrations might be expected. Comparing this to biological effects thresholds suggests effects on fish feeding in the upper water column would only be potentially experienced under static discharge conditions.

The results of this study and previous studies (Csanady, 1979; IMO, 1992) indicate that much higher rates of initial dilution can be expected in the wake of the ship. Scaling analysis of waste volume to wake volume ratios indicate that aircraft carriers and frigates are representative of the high and low end of the wake-loading spectrum (figure 12-4). Detailed numerical modeling studies of these two ship classes showed that the aircraft carrier represents a worst-case wake-loading scenario. Modeling results for the aircraft carrier over a range of speed and ambient stratification gave ranges of minimum dilution (based on peak concentration in the wake) from between $6.4 \cdot 10^4$, and $1.7 \cdot 10^5$ within 5 to 10 minutes of discharge. The lowest dilution rate of about $6.4 \cdot 10^4$ was observed at low speeds (10 kts) with strong stratification for the aircraft carrier. Dilution of the liquid phase was shown to be reasonably similar to the solid phase so that it can be assumed that the initial dilution of both phases in the wake is similar. Assuming an initial discharge concentration of 1% and a worst-case dilution in the wake of $6 \cdot 10^4$ the resulting peak concentration in the wake immediately following discharge would be about 0.17 $mg \cdot L^{-1}$. This represents the worst-case exposure in the water column, as differential particle settling, advection, and mixing will tend to reduce concentrations further. Comparing this to threshold levels for biological effects indicates that no effects would be expected in any of the organisms tested in this study because the concentration was about five times lower than the lowest concentration for observed feeding effects on clupeoid fish. The high dilution in the wake under a range of operating and ambient conditions is important because it suggests that initial exposure levels and potential effects can be minimized independent of the geographic location where the discharge occurs.

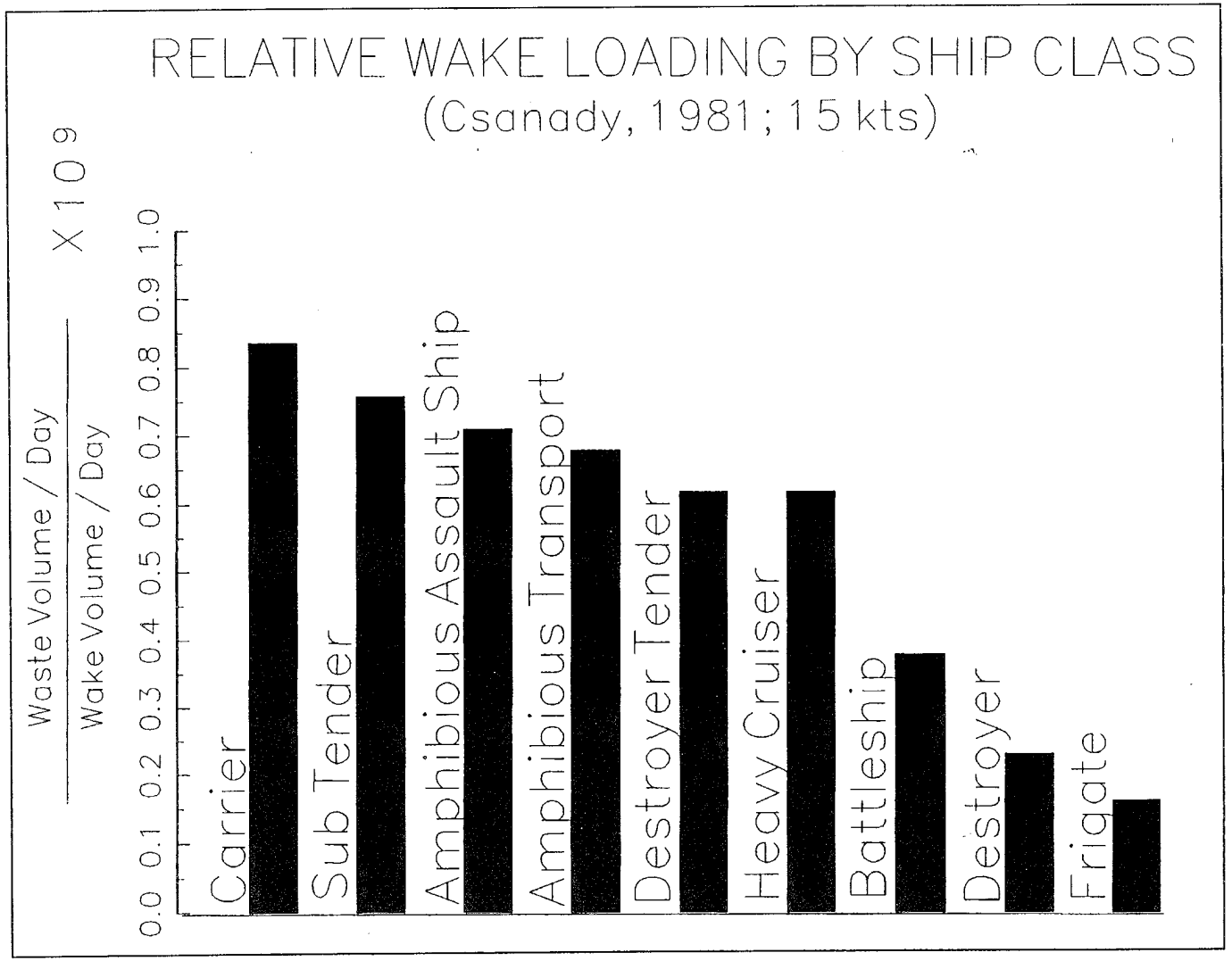

Figure 12-4. Relative pulped paper wake-loading by ship class. The waste volume is based on the waste generation rate for each ship class, while the wake volume is scaled based on the estimate of Csanady (1981). All estimates are for a speed of 15 kts.

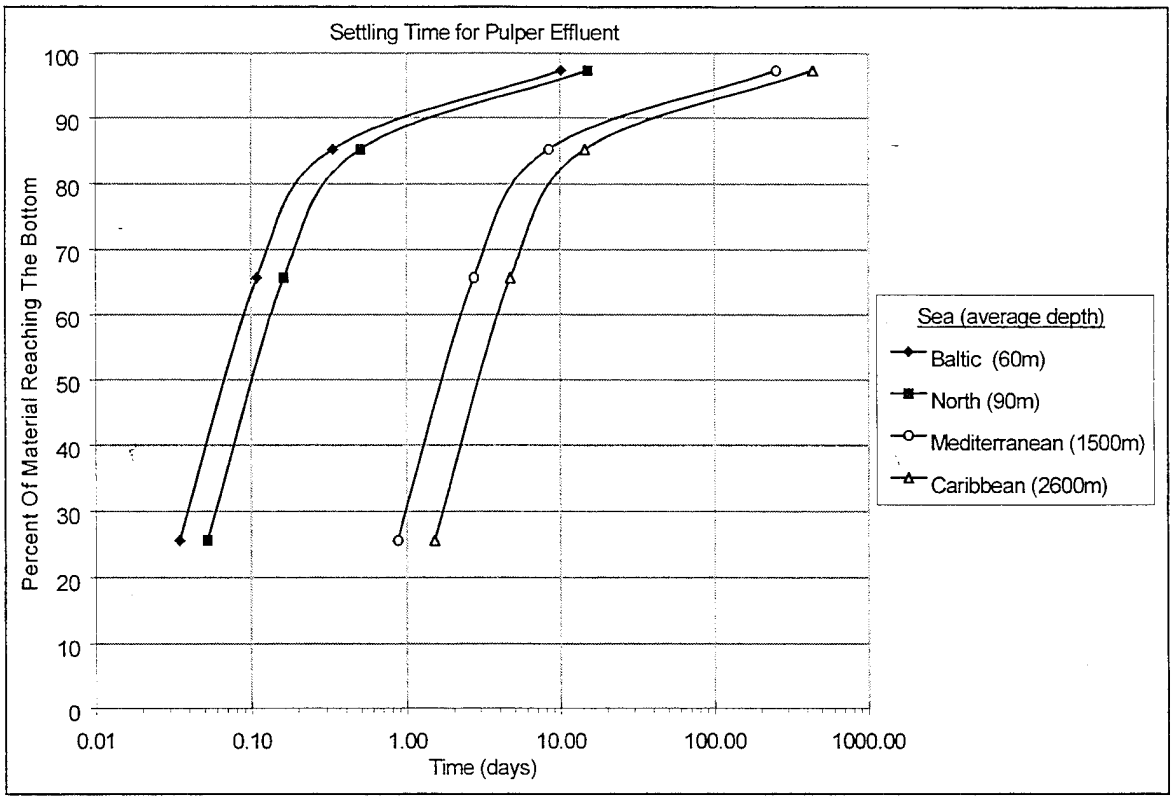

Figure 12-5. Settling time of pulper effluent for each of the Special Areas assuming no degradation. Settling times are based on the average depths for the Special Areas. Approximately 85% of the material (by weight) settles rapidly within a time range of about 1-10 days. A slower settling fraction representing about 12% of the material settles in about 10-300 days. The remaining ~ 3% remains in suspension indefinitely.

Ambient Dilution and Transport. Following discharge and mixing in the wake, the dominant mechanisms which influences the fate of the waste stream include gravitational settling, lateral transport, and ambient mixing. Some fraction of the waste stream may partition to the surface microlayer or be consumed by water column particle feeders as well. Column settling experiments suggest that about 85% (by weight) of the solid phase is composed of large particles which will settle rapidly at an average rate of about 1 $cm \cdot s^{-1}$. A smaller size fraction composing about 12% of the solid phase settles more slowly at an average rate of about 0.007 $cm \cdot s^{-1}$. The remaining ~3% will probably remain in suspension and subject to water column degradation. Average depths for the Special Areas range from a low of about 60 m for the Baltic to a high of about 2600 m for the Caribbean. Assuming no degradation, this implies that ~85% of the pulped waste will reach the bottom in times ranging from a few hours for the Baltic to about 10 days for the Caribbean (figure 12-5). The remaining ~12% will reach the bottom in about 10 days for the Baltic and 100 days for the Caribbean.

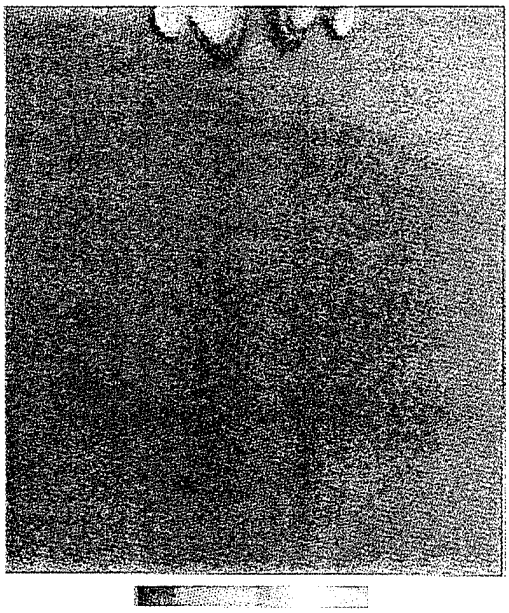

Figure 12-6a. Far field particle dispersion: Baltic Sea, January, 0.12 cm particles, t=0. Vertical axis is depth from 0 to 200 m, horizontal axis is distance port/starboard from 0 to 300 m. Color scale is 0 (purple) to 5 (red) particles·m^{-3}.

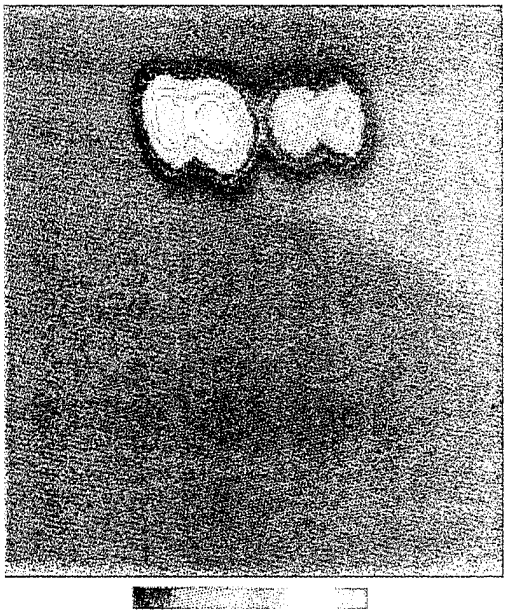

Figure 12-6b. Far field particle dispersion: Baltic Sea, January, 0.12 cm particles, t=1.8 hours. Vertical axis is depth from 0 to 200 m, horizontal axis is port/starboard 0 to 300 m. Color scale is 0 (purple) to 5 (red) particles·m^{-3}.

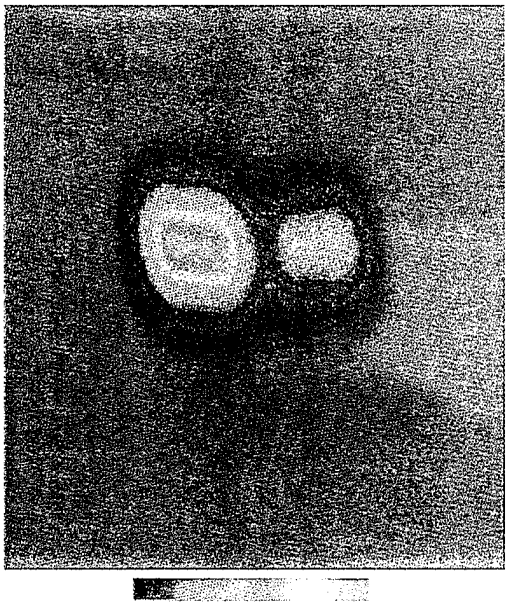

Figure 12-6c. Far field particle dispersion: Baltic Sea, January, 0.12 cm particles, t=4.3 hours. Vertical axis is depth from 0 to 200 m, horizontal axis is port/starboard 0 to 300 m. Color scale is 0 (purple) to 5 (red) particles·m^{-3}.

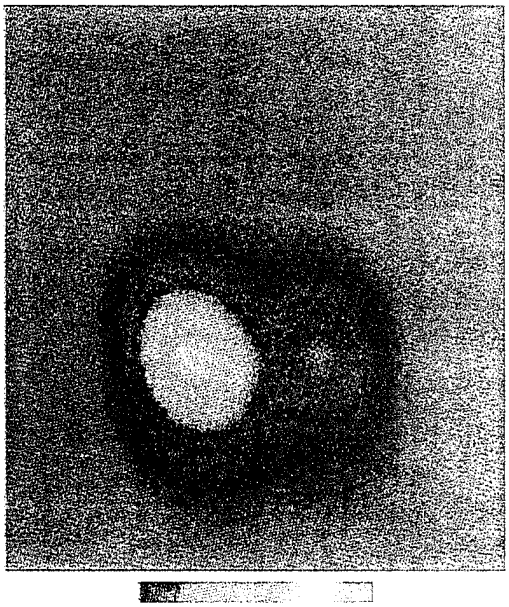

Figure 12-6d. Far field particle dispersion: Baltic Sea, January, 0.12 cm particles, t=6.5 hours. Vertical axis is depth from 0 to 200 m, horizontal axis is port/starboard 0 to 300 m. Color scale is 0 (purple) to 5 (red) particles·m^{-3}.

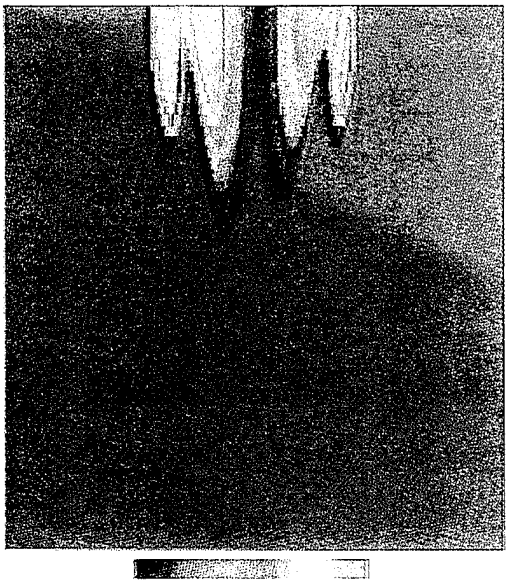

Figure 12-7a. Far field particle dispersion: North Sea, July, 0.12 cm particles, t=0. Vertical axis is depth from 0 to 50 m, horizontal axis is port/starboard 0 to 300 m. Color scale is 0 (purple) to 20 (red) particles·m^{-3}.

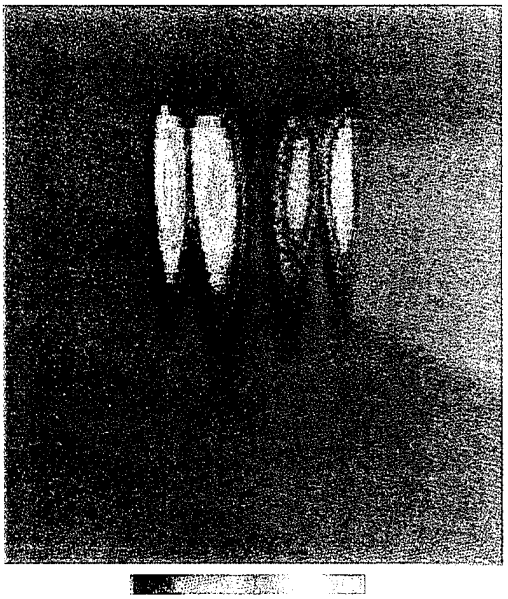

Figure 12-7b. Far field particle dispersion: North Sea, July, 0.12 cm particles, t=32.4 min. Vertical axis is depth from 0 to 50 m, horizontal axis is port/starboard 0 to 300 m. Color scale is 0 (purple) to 20 (red) particles·m^{-3}.

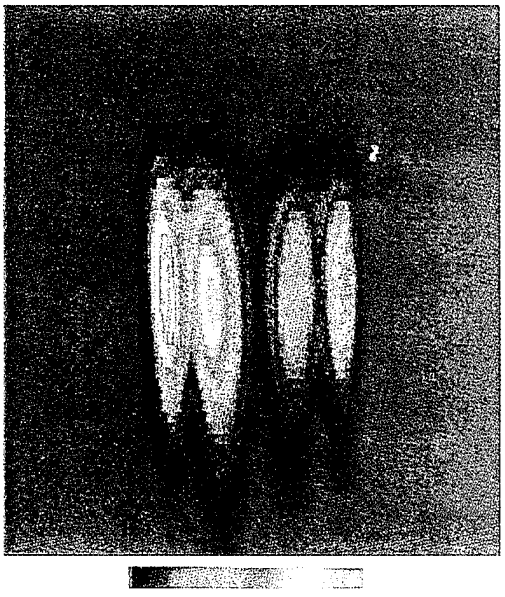

Figure 12-7c. Far field particle dispersion: North Sea, July, 0.12 cm particles, t=64.8 min. Vertical axis is depth from 0 to 50 m, horizontal axis is port/starboard 0 to 300 m. Color scale is 0 (purple) to 10 (red) particles·m^{-3}.

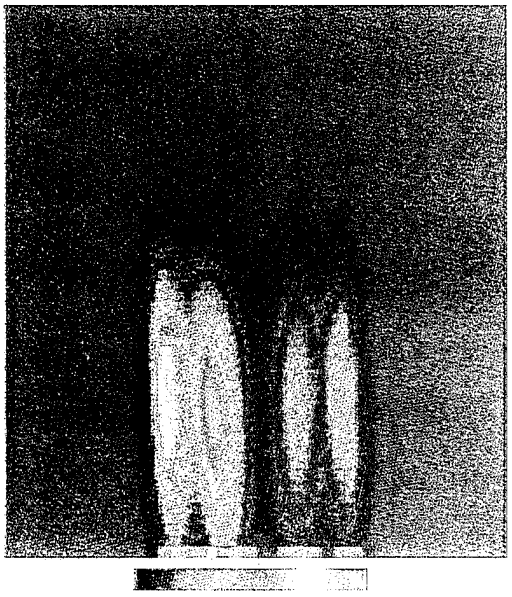

Figure 12-7d. Far field particle dispersion: North Sea, July, 0.12 cm particles, t=97.2 min. Vertical axis is depth from 0 to 50 m, horizontal axis is port/starboard 0 to 300 m. Color scale is 0 (purple) to 10 (red) particles·m^{-3}.

The rapid settling of the majority of the pulped waste is confirmed by numerical simulations for the Baltic and the North Sea (figures 12-6a-d, 12-7a-d). For the Baltic site, a depth of 200 m and a strong pycnocline at 50 m depth were used to simulate winter conditions for the central Baltic. The simulations show the size fractions of ~1100 to 1300 μm arriving at the bottom within about 10 hours and the smaller size particle fraction (<350 μm) arriving within about 5 days. For particle fractions arriving at the bottom in the Baltic case, dilution factors range from 10 to 80 for the large and small particles, respectively. A depth of 50 m with no stratification was used to simulate the southern North Sea in summer. The model results show that the larger fractions reach the bottom in about 2 hours while the smaller size fraction arrives within about a 1 to 2 days. Dilution factors for the ambient mixing in the North Sea case range from 5 to 20 for the large particles and the small particles, respectively. The modeled dilution rates are in reasonable agreement with the results from the small scale field test which showed dilution by a factor of about 10 below the wake concentration within the first hour after discharge and subsequent dilution proceeding linearly proportional to elapsed time (see figure 11-14). Assuming that most of the mass resides in the large particle fraction, and assuming the worst-case dilution based on the North Sea simulation, the concentration of the pulp material when it arrives at the bottom would reduced by a factor of about 5 from the wake concentration to a value of about 0.033 $mg \cdot L^{-1}$. The corresponding value for the Baltic case would be about 0.017 $mg \cdot L^{-1}$. For deeper basins, such as the Mediterranean and the Caribbean, dilution during this transport period could be substantially higher. In general it appears that the relatively high density of the pulped material combined with the large fraction of the mass associated with the large particles tend to make most of the material sink rapidly independent of ambient conditions.

The lateral advection of the pulped material is important with regard to shoreward transport and the potential littering of beaches and shorelines. This aspect of the transport could not be readily treated in the numerical simulation because of grid size limitations. Some analysis of this problem is considered here based on the measured settling rates, simplified bottom topography, current speed, and discharge distance from shore. Discharge distance from shore was considered for two possible limits of 3 and 12 nautical miles (5.6 and 22.2 km). A review of Special Area bathymetric charts indicates typical depths at the 3 to 12 mile limit range from about 20 to 200 m. The bottom topography is assumed to slope linearly from the discharge limit depth to a depth of 0 m at the shore. The range of depths from 20 to 200 m gives shelf slopes ranging from 0.1% to about 0.9% which is similar to the average value reported by Sverdrup et al., (1942) of 0.2%. Assuming again that the majority of the material is contained in the large size particle fraction, a typical settling rate of about 1 $cm \cdot s^{-1}$ is applied. The predicted depositional depth and depositional distance from shore was then determined for onshore current velocities ranging from 0 to 1 $m \cdot s^{-1}$ (figure 12-8a-b). The results show that for a typical current speed of about 0.5 $m \cdot s^{-1}$, the depositional depth for the 12 nmi limit ranges from about 20 to 150 m and the depositional distance from shore ranges from about 16 to 22 km. At the highest onshore velocity examined (1 $m \cdot s^{-1}$), the depositional depth ranged from about 20 to 120 m and the depositional distance from about 12 to 21 km. For the 3 nmi limit and 0.5 $m \cdot s^{-1}$ current speed, the depositional depth decreases to 20 to 80 m and the depostional distance moves inshore to about 2 to 5 km.

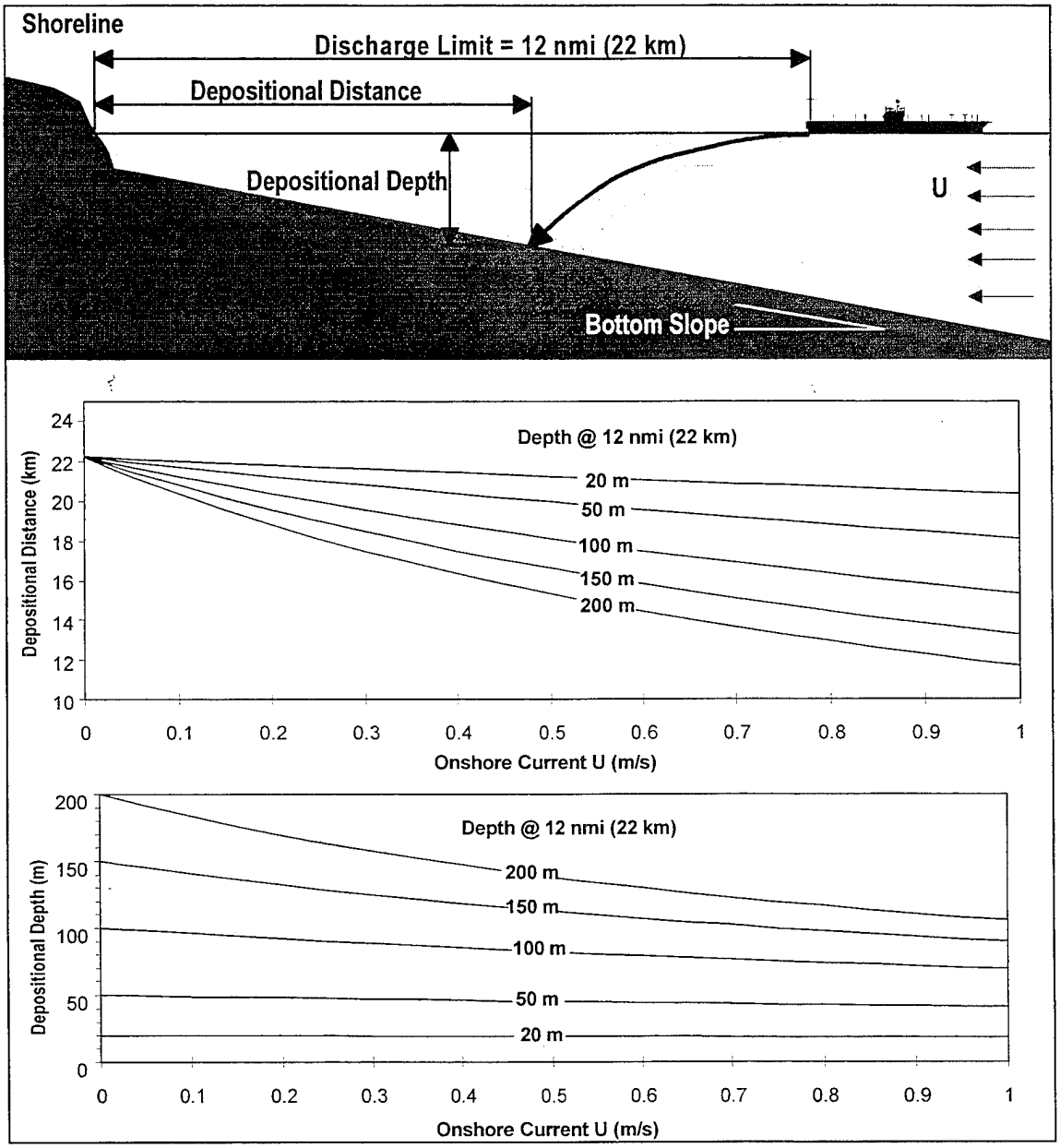

Figure 12-8a. Pattern of pulper discharge deposition at various depths and distancesfor the 22 km discharge case. Shown are depths and distances from shore of pulper discharge deposition under a range of onshore velocities (u) and bottom slopes.

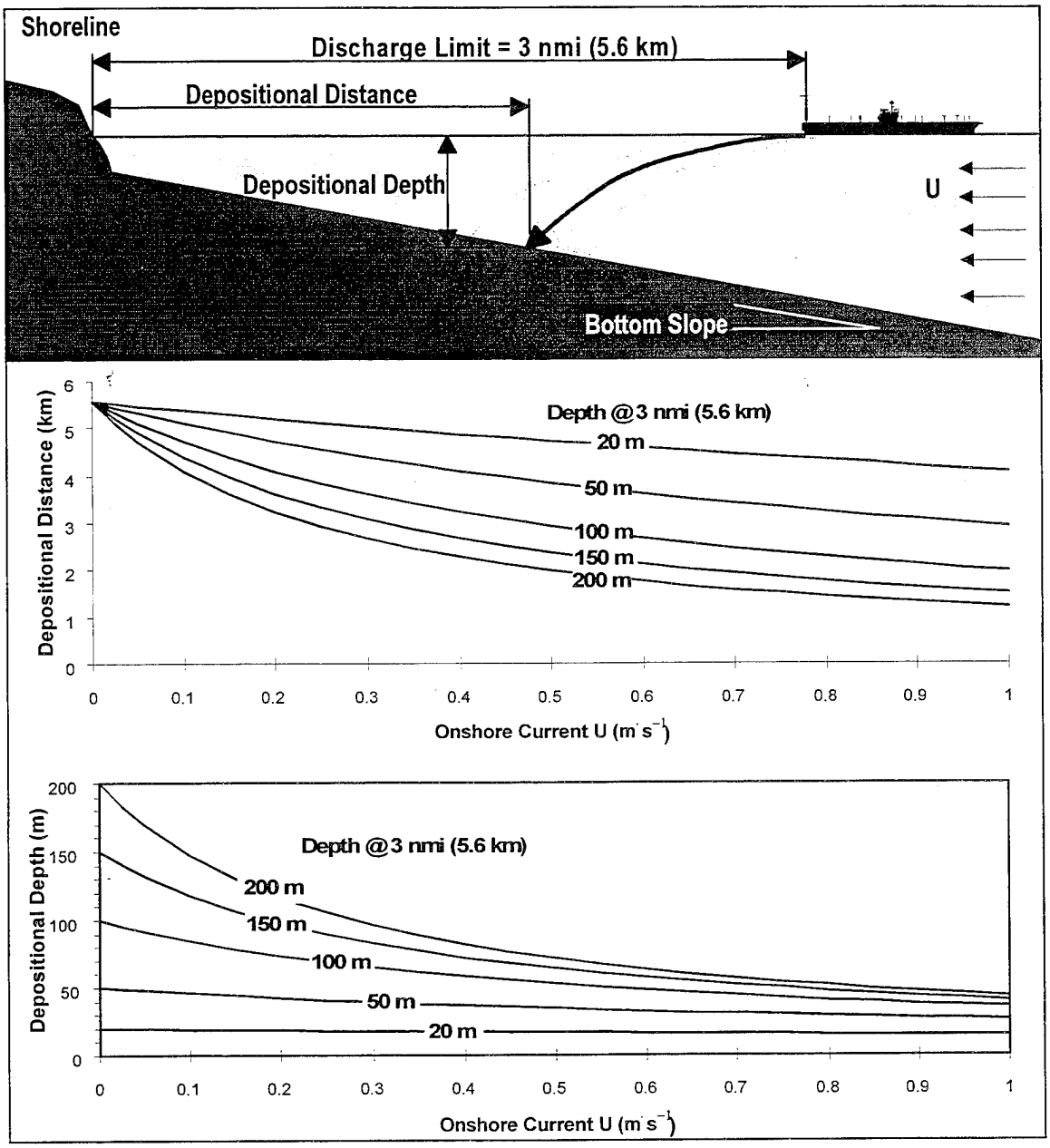

Figure 12-8b. Pattern of pulper discharge deposition at various depths and distances for the 5.6 km discharge case. Shown are depths and distances from shore of pulper discharge deposition under a range of onshore velocities (u) and bottom slopes.

The steeper bottom slope of the deeper basins, such as the Caribbean and the Mediterranean, would generally lead to greater depositional depths but smaller distances from shore, while more gently sloping shallow basins such as the North Sea, would have shallower deposition depths and larger depositional distances. The transport time for the 0.5 $m \cdot s^{-1}$ case ranges from about 1 to 3 hours. Assuming dilution rates similar to those from the numerical and field results, a conservative dilution of 10 could be expected during the transport period resulting in concentrations at the deposition area of about 0.017 $mg \cdot L^{-1}$. As an example, consider a region

such as the Caribbean where coral reefs exist to depths of 100 to 150 m (Dubinsky, 1990). Assuming a typical bottom slope of about 0.02 and onshore velocity of 0.5 $m \cdot s^{-1}$, depositional depths for the 3 and 12 nmi discharge scenarios would be 130 and 300 m, respectively. These results suggest that exposure to the paper pulp would be minimal since the dilution prior to exposure would be high, and the majority of material should settle at depths greater than the deepest portions of a reef community.

Surface Microlayer. No direct testing of partitioning or effects to the surface microlayer was attempted in this study. However, because the waste stream is discharged above the waterline and is mixed vigorously with surface waters within the wake, there is potential for some fraction of the waste stream to partition into the surface microlayer. The surface microlayer consists of a thin layer at the surface of the ocean where enrichment of hydrophobic dissolved and particulate materials are found. The surface microlayer is known to concentrate some toxic materials at levels significantly higher than within the bulk phase of the water column (MacIntyre, 1974; Liss, 1975; Carlson, 1982; Lion, 1982; Hardy, 1985). This has raised concerns regarding exposure to egg and larval stages of some species which reside in the microlayer during portions of their lifecycle. In addition, the microlayer is thought to exert control over the surface exchange of gases and heat. Various studies and models suggest that the upper portion of the microlayer consists of a mixture of dissolved and particulate materials including proteins, polysaccharides, lipids, and humics with an overall thickness ranging from about 0.1 to 10 μm. Previous studies of the microlayer in an estuarine salt marsh have shown that particle size distribution in the microlayer is similar to that in the bulk phase. Positive enrichment of particulate organic carbon in the surface microlayer has been measured at ratios ranging from 2.2 to 9.6 above the bulk phase under a range of coastal and oceanic conditions (Williams et al., 1986). In the wakes of ships, evidence suggests that the microlayer may be further enriched due to the scavenging of surfactants from the water column by bubbles entrained in the wake. A theoretical analysis by Davis et al., (1986) estimated enrichment ratios of 1 to 10 above background microlayer levels could occur over scavenging periods of 30 to 45 minutes.

This description of the microlayer suggests that the pulped paper waste consisting primarily of particulate cellulose would contribute to the polysaccharide fraction of the microlayer. Assuming that the larger particle fractions would sink rapidly and be unavailable to the microlayer, ~3% of the waste stream would be available for scavenging in the wake. Taking worst-case dilution rates as described above, the concentration of the small particle fraction in the wake would be about 0.005 $mg \cdot L^{-1}$. If the background microlayer enrichment is by a factor of 10 above water column levels, and the wake produces an additional factor of 10 enrichment above the background microlayer, then a conservative upper bound for the microlayer concentration in the wake would be 100 times the wake concentration or about 0.5 $mg \cdot L^{-1}$. This concentration range is below the level at which biological effects were observed for any of the test organisms. Using the standard molecular formula for cellulose $(C_6H_{10}O_5)_n$ and the results from the CHN analysis indicates a carbon content of about 40% by weight. Then the contribution of POC to the microlayer would be about 0.2 $mg \cdot L^{-1}$ in the region of the wake. This falls within the range of microlayer POC concentrations reported by Williams (1984) of about 0.03-1 $mg \cdot L^{-1}$ suggesting that localized enrichment would not be significantly above background levels.

Table 12-2. Estimated fate of a typical one day discharge of pulped paper from a CVN 68 class ship under a range of conditions representing four MARPOL Special Areas.

Special Area		Caribbean	Mediterranean	North Sea	Baltic Sea
Surface Layer	Depth (m)	100	75	50	40
	Temp (deg C)	28	26	10	10
	Deg Rate %·day^{-1}	0.50	0.39	0.05	0.05
Bottom Layer	Depth (m)	2500	1500	n/a	150
	Temp (deg C)	4	14	n/a	5
	Deg Rate %·day^{-1}	0.025	0.087	n/a	0.028
Mass Fraction	Small (kg)	95	95	95	95
	Med (kg)	381	381	381	381
	Large (kg)	2700	2700	2700	2700
Settling Rate	Small (m·day^{-1})	0	0	0	0
	Med (m·day^{-1})	6	6	6	6
	Large (m·day^{-1})	864	864	864	864
Wake	Width (m)	90	90	90	90
	Length (km)	130	130	130	130
Microlayer	Thickness (um)	10	10	10	10
	Concentration (mg·L^{-1})	0.50	0.50	0.50	0.50
Total Mass		3176	3176	3176	3176
Microlayer (kg)		0.06	0.06	0.06	0.06
Degradation	Surface Layer (kg)	127	114	97	97
	Bottom Layer (kg)	36	75	n/a	3
	Total (kg)	164	189	97	99
Deposition (kg)		3012	2987	3079	3077

Water Column Fate. The degradation of the pulped material in the water column can be estimated based on residence time and temperature. First order kinetics suggest that degradation would proceed as

$$m_i \approx m_{oi} e^{-kt_{res}} \qquad \text{(Eq. 12-1)}$$

where m_i is the i^{th} mass fraction at time t_{res}, m_{oi} is the initial mass of the i^{th} mass fraction, $k = k(T)$ is the degradation rate as a function of temperature (figure 12-3), and t_{res} is the water column residence time. The residence time depends on the settling rate and the depth as $t_{res}=h/w_i$ where h is the water depth and w_i is the settling velocity of the i^{th} mass fraction. Using this model for the degradation, the settling rates, and the microlayer partitioning described above, a simple model was developed to describe the fate of the pulped material in the water column. The model is simplified to include only the effects of settling, degradation, and microlayer partitioning, and is thus very qualitative in nature. It is also possible that some fraction of the material could also be digested or repackaged as fecal pellets by water column particle feeders or have other alternate fates. These effects are ignored in this analysis. Based on typical conditions selected from the four Special Areas, the model predicts the percent of the material that will partition to the microlayer, the percent that will be degraded, and the percent that will settle to the bottom (figure 12-9). The temperature structure in each area was simplified to a two or one-layer profile to

simplify the analysis. The degradation rate for each layer was determined from figure 12-3 assuming a midrange Q10 value of 3.5. The results are shown in table 12-2 and indicate that ~95% of the material can be expected to settle to the sea floor, ~5% of the material will be degraded in the water column, and <0.001% of the material will partition to the microlayer. These results suggest that exposure and degradation processes in the water column will be limited by the rapid settling rate of most of the pulped paper material.

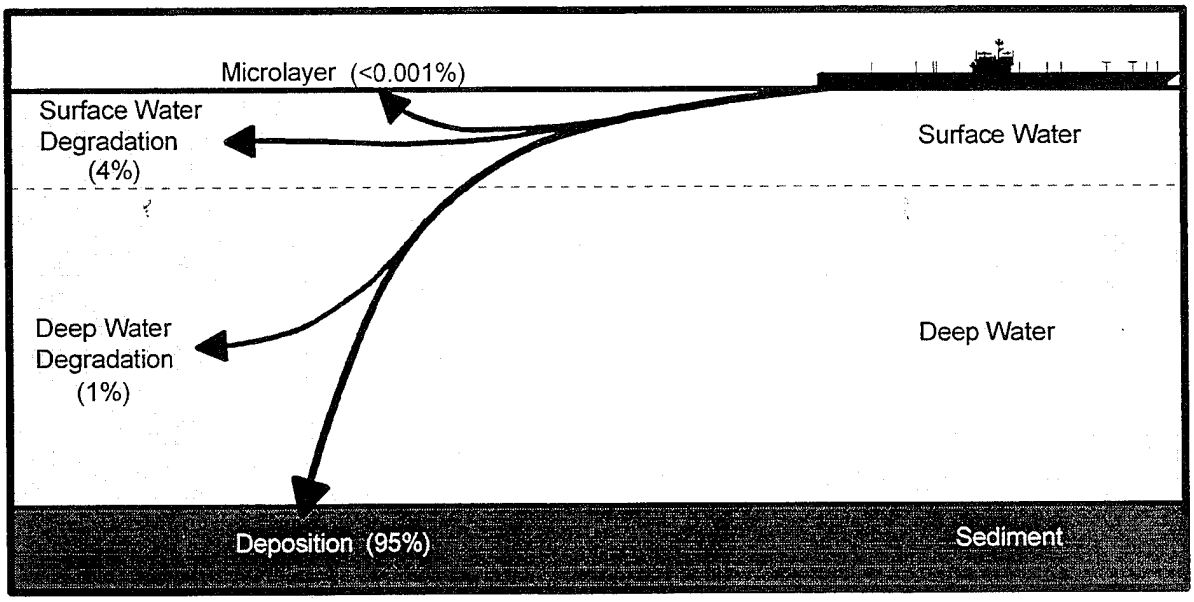

Figure 12-9. Estimated portioning of pulped paper discharged to Special Areas based on a simplified water column fate model.

Water Column Exposure and Effects. It has been shown above that the discharge for the CVN 68 represents a worst-case scenario for potential water column exposure to pulped paper. Following discharge, the exposure is regulated by three primary factors: wake mixing, ambient mixing, and settling. Modeling and field results for both the wake and ambient mixing suggest that a reasonable estimate of the dilution can be obtained from a simple diffusion velocity model of the form

$$D(t) \approx 10^6 t + 1 \qquad \text{(Eq. 12-2)}$$

which results in a predicted peak concentration that satisfies

$$C(t) \approx \frac{C_o}{10^6 t + 1} \qquad \text{(Eq. 12-3)}$$

where t is the time following discharge in hours and C_o is the concentration entering the environment. The dilution in the wake varies slightly depending on ship speed and stratification, while the ambient mixing can also be expected to vary depending on local conditions.

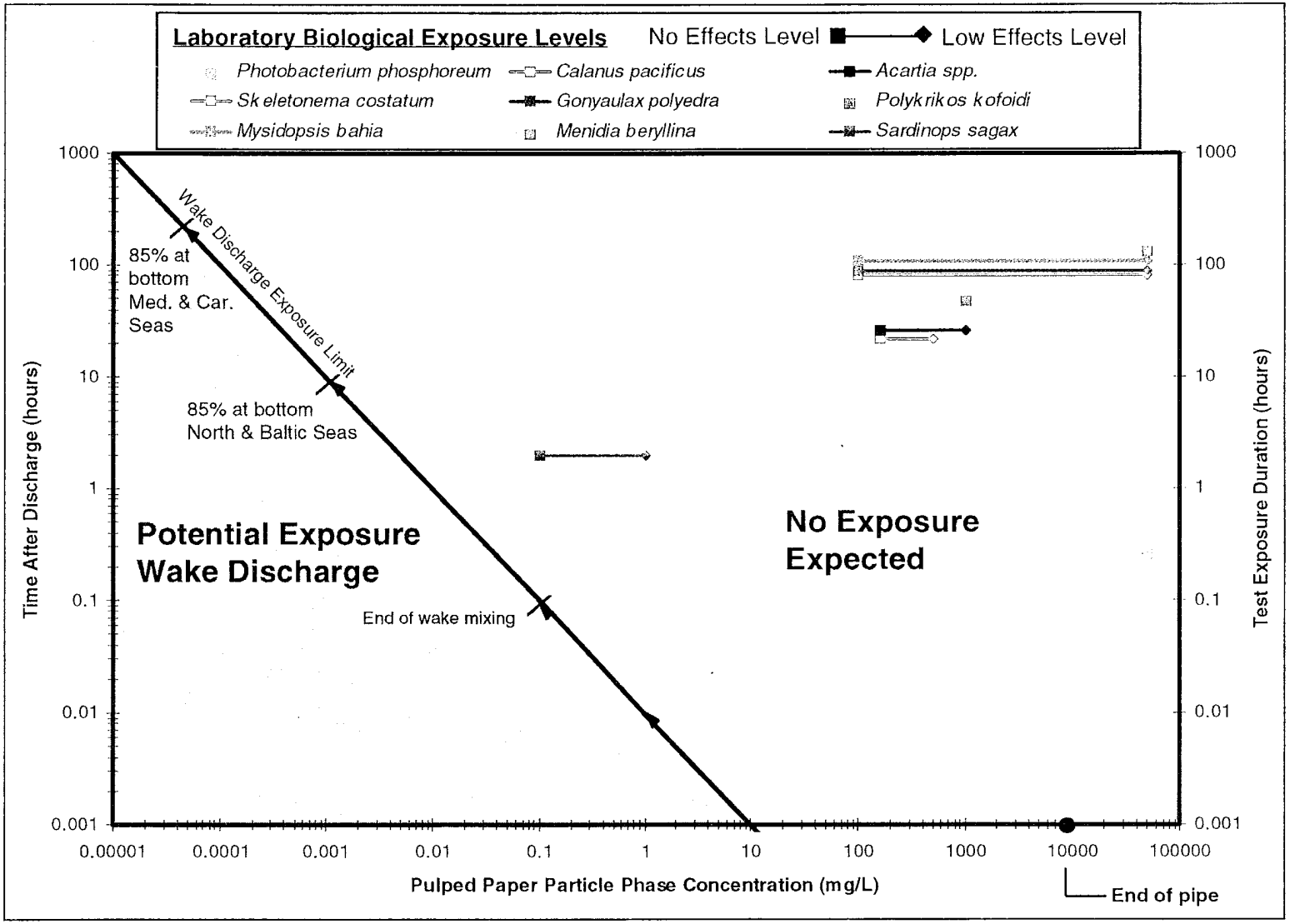

Figure 12-10. Estimated water column exposure limits compared to biological response levels for the pulped paper particle phase.

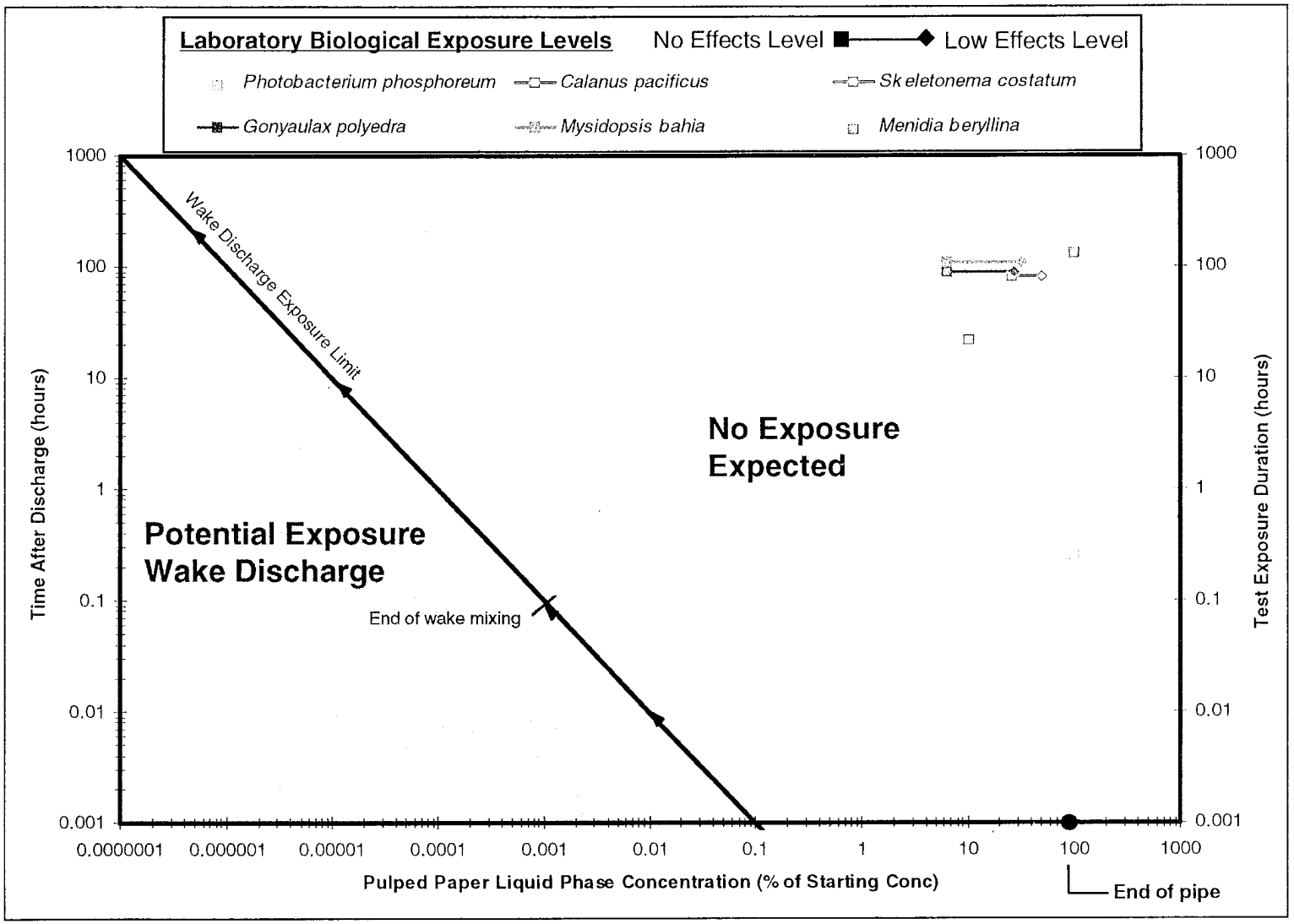

Figure 12-11. Estimated wake column exposure limits compared to biological response levels for the pulped paper liquid phase

This exposure limit is plotted on figures 12-10 and 12-11 for the particle phase and liquid phase exposures, respectively. The limit represents a reasonable upper bound for the expected exposure under wake discharge scenarios. The region on the plot below this line can be interpreted as the exposure range, which can be expected in the environment, where exposure is defined as a given concentration over a given period of time.

The potential for effects on organisms residing in the water column is also a function of exposure. Results from the broad range of test species were used to identify the potential range of effects based on exposure concentration and test duration. Results from these tests are plotted on figures 12-10 and 12-11 including the concentration at which no effects were observed and the lowest concentration at which effects were observed. In some cases, no effects were observed at any of the test exposures. For the tests where a no-effects and low-effects level are shown, the actual effects threshold lies somewhere on the line between the two points. The exposure duration for all of the tests was taken to be the bioassay testing period. In some cases (e.g., *Gonyaulax polyedra*, *Skelotonema costatum*) effects were observed over shorter times than the overall testing period.

Analysis of figures 12-10 and 12-11 indicates that for ships discharging into wake while underway, environmental exposure levels will generally be significantly below the exposure levels required to cause effects in the organisms tested. The most sensitive test organism for the particle phase, *Sardinops sagax* or sardines, showed some signs of impaired feeding ability at exposure concentrations and a duration approximately 10 times higher than the exposure level based on wake discharge. Recovery tests also showed that feeding impairment did not continue after the pulped paper was removed. Effects of the particle or liquid phase on other organisms were only found at exposure concentrations and a duration many orders of magnitude above the wake discharge exposure levels. Because the majority of the material sinks quite rapidly (~1 $cm \cdot s^{-1}$), about 85% of the particulate phase should be below 50 m within about 1 to 2 hours and exposure to the surface feeding sardines should be minimized.

Nutrients contained at low levels within the waste stream provide a mechanism for enhancing primary production on the local scale which could lead to increased potential for eutrophication. This potential is substantially reduced by the high C:N:P ratio for the waste stream and the probability that the majority of the material will sink to depths below the euphotic zone where primary productivity occurs. In shallow seas, such as the North Sea and the Baltic, even material which sinks to the bottom may be available for utilization by primary producers. Thus a crude estimate of the localized contribution to productivity by a typical daily discharge could be estimated by assuming that all of the nutrient inputs are converted to phytoplankton biomass within the region of discharge. Given a typical daily discharge from the CVN 68 of about 3176 $kg \cdot day^{-1}$ with a nitrogen content of about 408 $mg \cdot kg^{-1}$ gives a daily nitrogen loading of about 1.2 $kg \cdot day^{-1}$. Applying the average C:N ratio for phytoplankton and using a wake area of 100 m wide by 130 km long gives an estimated productivity rate of about 0.0005 $gC \cdot m^{-2} \cdot d^{-1}$. This can be compared to typical values for the Mediterranean of about 1.4 $gC \cdot m^{-2} \cdot d^{-1}$ (table 6-3). Thus the local increase of productivity due to the nutrient loading of the waste stream would represent about 0.4% of the background level.

To summarize, an analysis of water column processes suggests that the primary fate of pulped paper waste entering the water will be deposition to the sea floor. Of the particulate phase material entering the water column, ~95% can be expected to reach the bottom, while ~5% could be degraded in the water column, and a small fraction (<0.001%) could partition to the microlayer. Highest exposures will be found in the wake just after discharge, and modeling

results indicate worst-case peak concentrations of about 0.17 $mg \cdot L^{-1}$. This concentration is below the level at which biological effects were observed in any of the wide range of test organisms. No effects would be expected from the liquid phase generated during the pulping process. Effects levels for the liquid phase were above the wake discharge exposure levels. Localized increases in productivity that might contribute to eutrophication appear to be several orders of magnitude below background levels. Lateral transport of the material towards shore should also be minimized by the rapid settling of the majority of the waste stream. The results show that for a typical current speed of about 0.5 $m \cdot s^{-1}$, the depositional depth for the 12 nmi (22 km) limit ranges from about 20 to 150 m and the depositional distance from shore ranges from about 16 to 22 km, depending on bottom topography. For the 3 nmi limit and 0.5 $m \cdot s^{-1}$ current speed, the depositional depth decreases to 20 to 80 m and the depositional distance moves inshore to about 2 to 5 km.

Sea Floor Processes

The results of this study indicate that a large fraction of the particulate associated with the pulper discharge will settle rapidly to the sea floor. Processes which will regulate the fate and effects of the material on the sea floor are summarized in figure 2-2 and include deposition, resuspension, transport, burial, degradation, and biological interactions. The accumulation of materials on the sea floor can be expected to vary depending on the balance of these source and sink terms. Direct dilution of material on the sea floor may take place through resuspension and redistribution, vertical mixing due to physical or biological turbation, or sedimentation of background materials. Primary processes which could be anticipated to influence the fate of pulped paper on the sea floor are discussed below. Based on these processes, estimates of sea floor exposure levels are developed and compared to biological testing results.

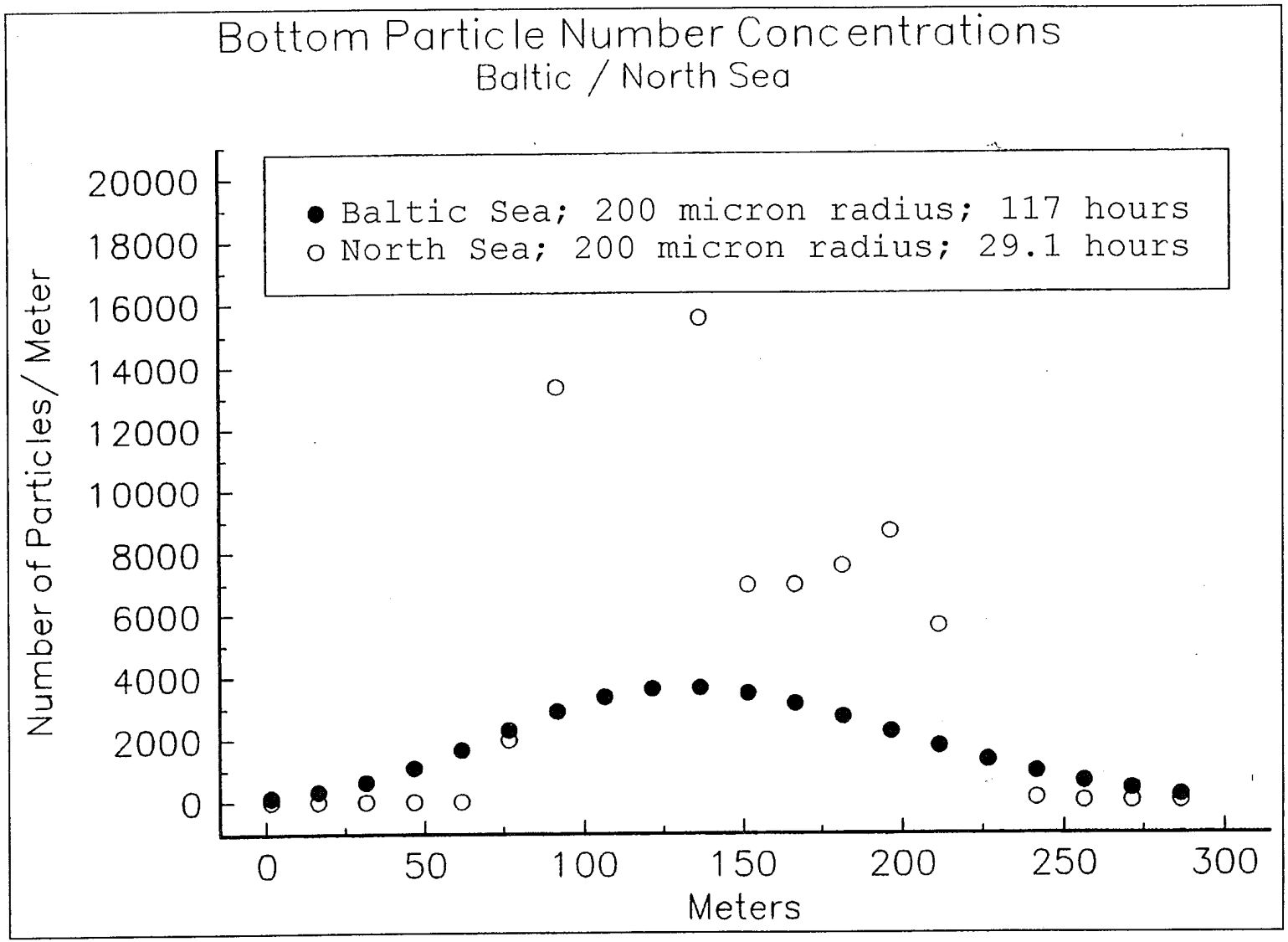

Figure 12-12. Nonuniform deposition in the Baltic and North Seas. Nonuniform depositional distribution of the 200 μm particle fraction in the Baltic and North Seas according to SEDXPORT.

Deposition. The deposition of pulped paper to the sea floor is controlled by processes in the water column as described previously. Analysis of these processes indicated that ~95% of the material discharged should reach the sea floor within a period of about 10 to 500 days depending on the depth of the Special Area. For a typical ship discharge operation, the amount of material deposited at a given location depends on the amount of material discharged (m_o), and the area (A) over which it is spread such that the mass per unit area of sea floor is given approximately by

$$d \approx \frac{m_o}{A} \qquad \text{(Eq. 12-6)}$$

assuming that the material is evenly distributed. This need not be the case, especially in shallower regions such as the North Sea or Baltic where deposition of the nonuniform water column distribution leads to a peaked distribution of the material on the bottom as seen in the numerical dispersion simulations (figure 12-12). Differing size fractions may also be separated in the water column by horizontal current shear because of their varying settling rates. Using the above equation, a reasonable upper bound for deposition can be obtained by taking a shallow water case, such as the North Sea, and assuming negligible ambient mixing. For the case of the CVN 68 traveling at 10 knots, the amount of material discharged per unit length of wake is about 37 $g \cdot m^{-1}$, and the width following wake mixing only is ~100 m. Assuming all the material reaches the sea floor, this gives a deposition of ~0.4 $g \cdot m^{-2}$. Taking a wet:dry weight ratio of about 6 for the pulped paper, and assuming a density of 1 for seawater and 1.5 for pulped paper, the layer thickness of the discharge would be about $4 \cdot 10^{-4}$ mm. From the numerical simulations it appears that peak concentrations on the bottom could exceed mean values by a factor of 2 to 3, so a conservative upper bound for the depositional layer thickness for a single ship discharge would be about $1 \cdot 10^{-3}$ mm. This is significantly thinner than the average particle size of ~20 μm, which implies that for a single ship discharge, the particle density would be insufficient to cover the bottom. Using the average particle thickness of ~20 μm and neglecting pore water volume gives a relative coverage area for the pulped paper of about 1.3%.

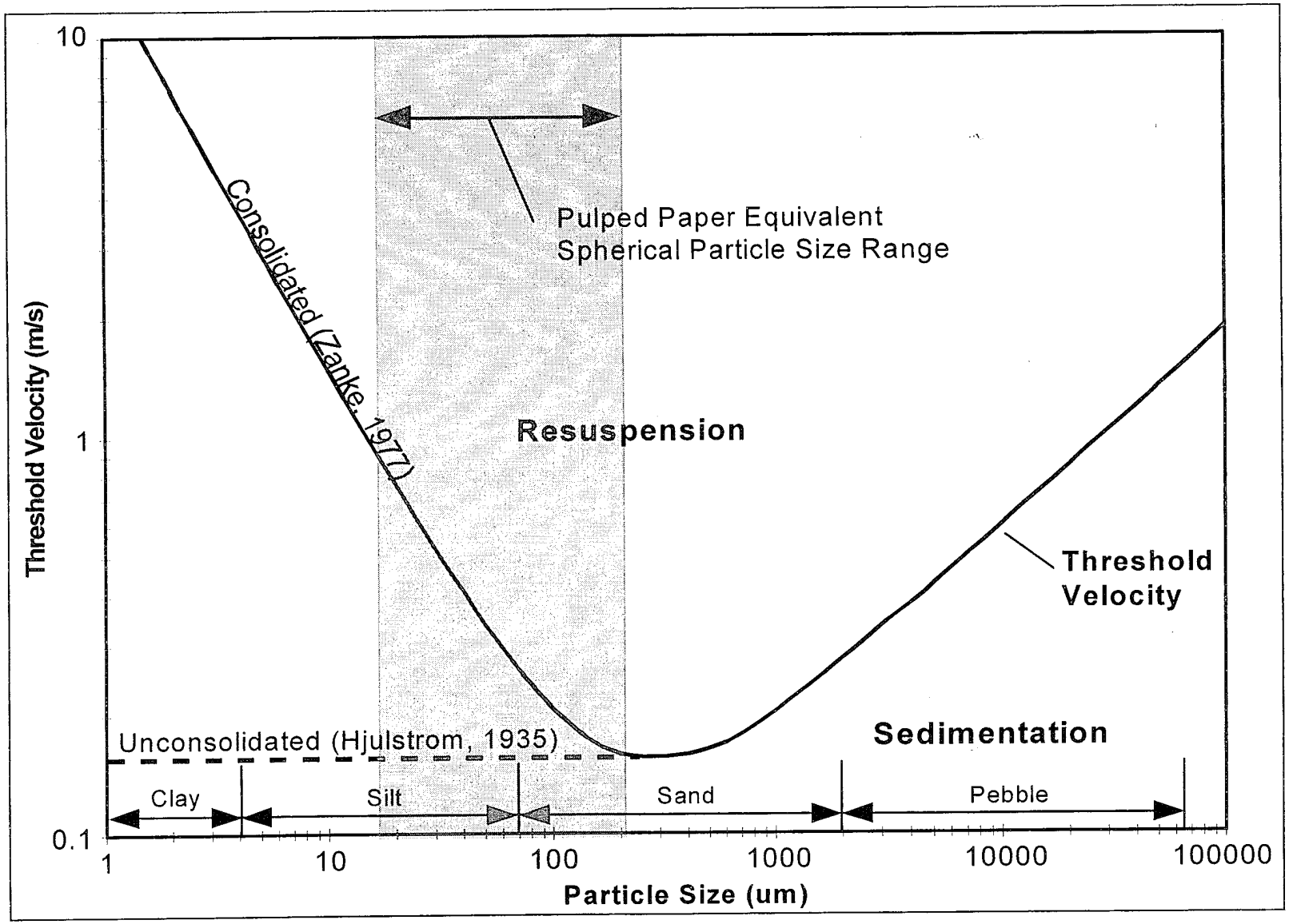

Figure 12-13. Theoretical relationship between particle size and resuspension threshold velocity for the pulped paper particles.

Resuspension, Transport, and Burial. Resuspension of particles is primarily governed by particle size and water velocity. Pulped material which settles to the bottom may be subject to resuspension and transport depending on the strength of the bottom currents in the region where deposition takes place. In general, strong bottom currents and subsequent resuspension will be found in shallower regions where the effects of wind and tides are more pronounced, and the deeper areas of restricted circulation may be characterized by low resuspension activity. A variety of relationships have been proposed to describe the relationship between particle size and resuspension threshold velocity (Raudkivi, 1990). In general, it is found that for sand grains of uniform shape, the threshold velocity obtains a minimum value of about 0.2 $m \cdot s^{-1}$ at a particle size of about 200 to 300 μm. For particles smaller than this size, bed smoothness and particle cohesion effects usually lead to higher threshold velocities, while for larger particles the increased hydrodynamic drag required to lift the particles also requires higher threshold velocities. If the sediments are unconsolidated, the threshold velocity for the finer grains may be reduced (e.g., Hjulstrom, 1939). A typical model for this relationship is that proposed by Zanke (1977) which takes the form

$$U_c = 2.8(g' d)^{\frac{1}{2}} + 14.7\frac{vc}{d} \qquad \text{(Eq. 12-7)}$$

where U_c is the threshold resuspension velocity, g' is the reduced gravity based on particle density, d is the grain diameter, ν is the kinematic viscosity, and c is a cohesion coefficient taken as 1 for noncohesive sediments. This curve is plotted in figure 12-13 along with the range of equivalent spherical particle sizes for the pulped paper. The range of equivalent spherical particle sizes for the pulped paper particles was estimated from Stokes Law settling (Raudkivi, 1990) using the measured settling rates for the large size particle fraction (w@1 $cm \cdot s^{-1}$) and the smaller particle fraction (w@0.007 $cm \cdot s^{-1}$). This gives an equivalent spherical particle size range of about 15 to 200 μm. Assuming that paper particles behave similarly to unconsolidated spherical grains with respect to resuspension, the figure suggests that threshold velocities would be about 0.2 $m \cdot s^{-1}$. These are velocities which are likely to be encountered in moderate to high energy coastal environments, while in deeper basins velocities exceeding 0.1 $m \cdot s^{-1}$ will be unlikely. In general, the majority of the pulped paper (~85%) has an equivalent particle size range that is centered near the minimum of the threshold velocity curve. This indicates that paper particles would be included among the more mobile fraction of the particle distribution on the sea floor. The actual resuspension behavior of pulped paper particles may be significantly different than that predicted for uniform spherical grains.

Burial of the pulped paper could proceed by two processes: burial by naturally occurring sedimentation, or by vertical migration within the sediment column by physical mixing or bioturbation (Aller, 1980). These are all processes that vary widely across the spectrum of conditions that would be encountered in MARPOL Special Areas. Natural sedimentation rates represent the long term difference between deposition and erosion which typically vary from about 1 to 20 $mm \cdot 1000\ y^{-1}$ in the deep sea, to 40 to 200 $mm \cdot 1000\ y^{-1}$ on the continental slopes, and >1000 $mm \cdot 1000\ y^{-1}$ on the shelf and coastal regions (Seibold and Berger, 1982; Kennett, 1982). Representative sedimentation rates in some of the Special Areas are listed in tables 6-1 to 6-4 and typically show values similar to shelf rates in the range of 1-10 $mm \cdot y^{-1}$ or 0.003-0.03 $mm \cdot d^{-1}$. In a localized region then, the discharge from a single ship at $\sim 1 \cdot 10^{-3}$ mm would represent about 3 to 30% of the average daily influx. Thus pulped paper arriving at the sea floor might be expected to be diluted with natural sedimentary particles by a factor of about 3 to 30.

Further dilution of the pulped paper material could be expected due to vertical mixing at the sediment water interface. This is achieved under natural conditions by a combination of physical

redistribution by currents and bioturbation by benthic organisms. Typical vertical mixing depths for coastal and shelf sediments have been reported as several centimeters. For example, Peng et al., (1986) reported mixed layer depths based on carbon-14 dating of 7 to 8 cm in the western equatorial Pacific, and Seibold and Berger (1982) report a value of 6 cm for the North Atlantic based on the vertical distribution of volcanic ash. Typical mixing rates due to bioturbation indicate a range of biodiffusion coefficients for particles from $0.02 \cdot 10^{-12}$ to $12 \cdot 10^{-12}$ $cm^2 \cdot s^{-1}$ for deep sea sediments to $200 \cdot 10^{-12}$ to $1200 \cdot 10^{-12}$ $cm^2 \cdot s^{-1}$ for near shore sediments (Berner, 1980). The dilution of pulped paper with bottom sediment due to bioturbation can then be estimated from diffusion theory as

$$D \sim \frac{\sqrt{D_B t}}{h_o} \qquad \text{(Eq. 12-8)}$$

where D is the dilution, t is time, h_o is the initial layer thickness assumed to be the nominal particle thickness of ~20 μm, and D_B is the biodiffusion coefficient. The dilution based on this estimate is plotted as figure 12-14 and shows that dilution of the particle phase over a period of 1 to 10 days for a single ship discharge could be expected to range from 10^3 for deep basin environments to 10^6 for near shore sediments. Over this short time then, the resulting concentration of the pulped paper in the bulk sediment phase could be expected to range from about 1 to 1000 $mg \cdot kg^{-1}$. No data on bioturbation rates in anoxic sediments was found, however it can be expected that bioturbation would be significantly reduced in the absence of oxygen, and thus, dilution by this process would be much less efficient.

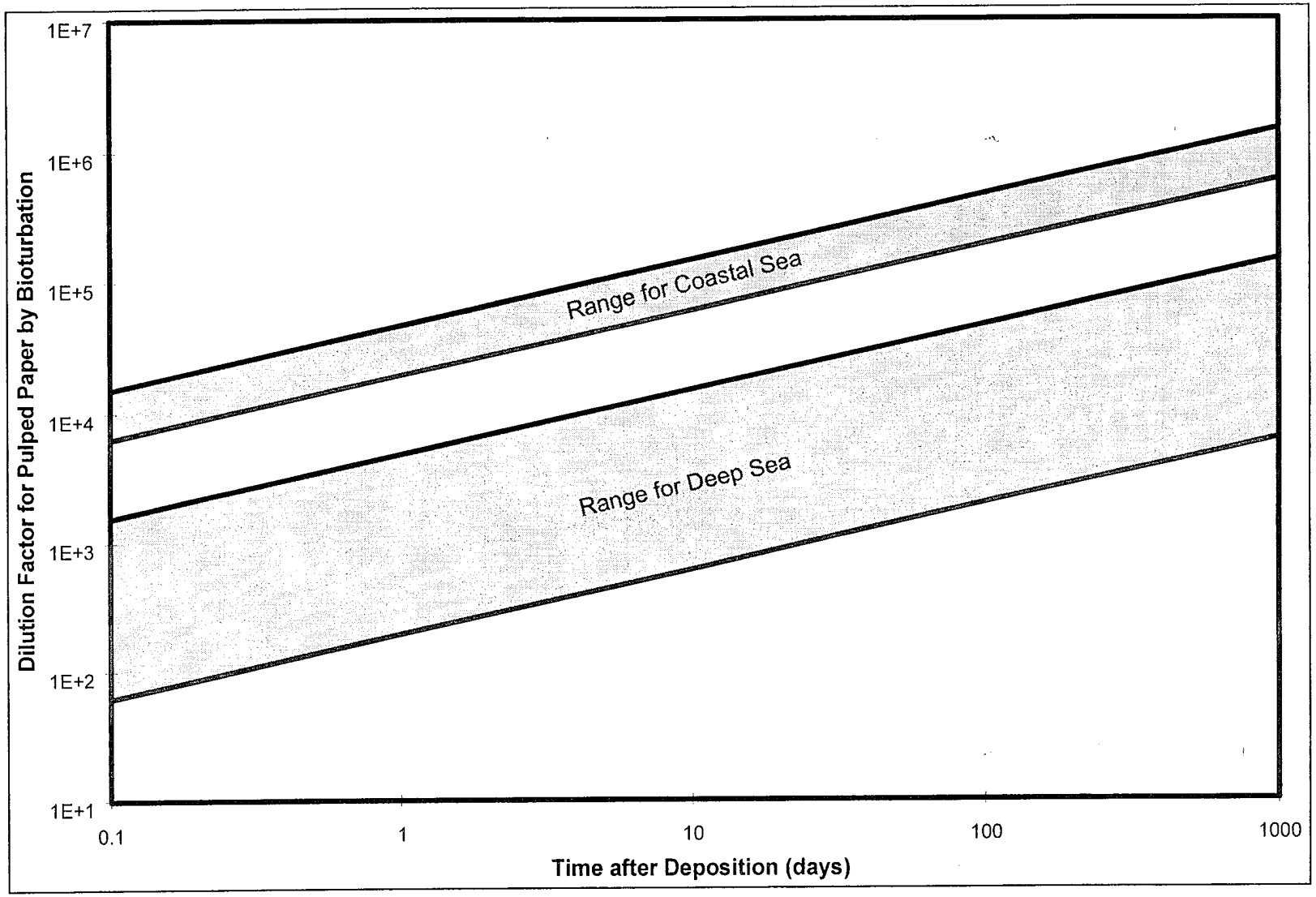

Figure 12-14. Dilution of pulped paper with bottom sediment from bioturbation for the ranges of deep sea and coastal biodiffusion coefficients reported by Berner (1980).

Degradation. No tests were performed on the degradation of pulped paper in sediment during this study. However, degradation in the sediment can be expected to be controlled by many of the same factors which control degradation in the water column including particle characteristics, microbial community structure, temperature, nutrient availability, and pressure. In addition, oxygen levels may often be limiting, especially in near shore sediments where high organic carbon levels often lead to anaerobic conditions at some depth within the sediment column. Assuming that oxygen is not limiting, degradation rates in sediments might be expected to be similar to those found in the laboratory studies in seawater solutions. Based on the estimated range of degradation rates (figure 12-3) and bottom temperatures in the Special Areas, the half life of the pulped paper material due to microbial degradation ranges from about 1000 days in the warm, saline deep waters of the Mediterranean to about 3000 days in the cold bottom waters of the Caribbean basins.

Fate on the Sea Floor. The high organic content of the pulped paper waste stream suggests that the long term fate of the fraction of the material that reaches the sea floor would be remineralization via microbial degradation. It is also possible that a significant fraction of the material could be consumed by particle feeders, although no reasonable approach for estimating this amount was found. During the degradation process, the material will continue to be redistributed by the physical and biological transport processes described above. For a given discharge, the long term concentration in the sediment will thus be a function of the dilution due to redistribution and the removal due to degradation and consumption by particle feeders. A rough estimate of the concentration as a function of time could thus be obtained as

$$C(t) \approx \frac{h_{pulp} e^{-kt}}{\sqrt{D_B t} + St + h_o} \qquad \text{(Eq. 12-9)}$$

where C(t) is the concentration of pulped paper in the sediment, S is the sedimentation rate, k is the first order degradation rate constant, h_{pulp} is the layer thickness of the pulped paper if it were spread evenly over the sea floor, and the other variables are as defined previously. Resuspension and consumption by particle feeders are neglected. Predicted concentrations based on this model are plotted in figure 12-15 for the range of Special Area conditions located in tables 6-1 to 6-4. The pulped paper layer thickness, h_{pulp}, was estimated by applying the water column dilution rate (e.g., figure 12-10) to the maximum layer thickness estimated above ($\sim 1 \cdot 10^{-3}$ mm), assuming that the layer thickness would be reduced due to dilution during settling. Biodiffusion coefficients were estimated roughly on the basis of depth of the Special Area compared to biodiffusion coefficients for coastal and deep sea areas. Assuming first order degradation, the amount of pulped paper remaining on the bottom is estimated as a function of time and plotted in figure 12-16. These analyses suggest that the concentration of the pulp in the sediment for a typical discharge will be controlled primarily by bioturbation initially with concentrations at day 10 ranging about 20 to 100 $mg \cdot kg^{-1}$. Short term concentrations depend primarily on the amount of dilution in the water column and the degree of benthic bioturbation activity. The effect of sedimentation appears to be small since the time scale for sedimentation to cause the same dilution as bioturbation is about 30 years. The effects of degradation are not apparent until times greater than about 100 days. Up until that time, the concentration decreases as $C \propto t^{-1/2}$, consistent with bioturbation.

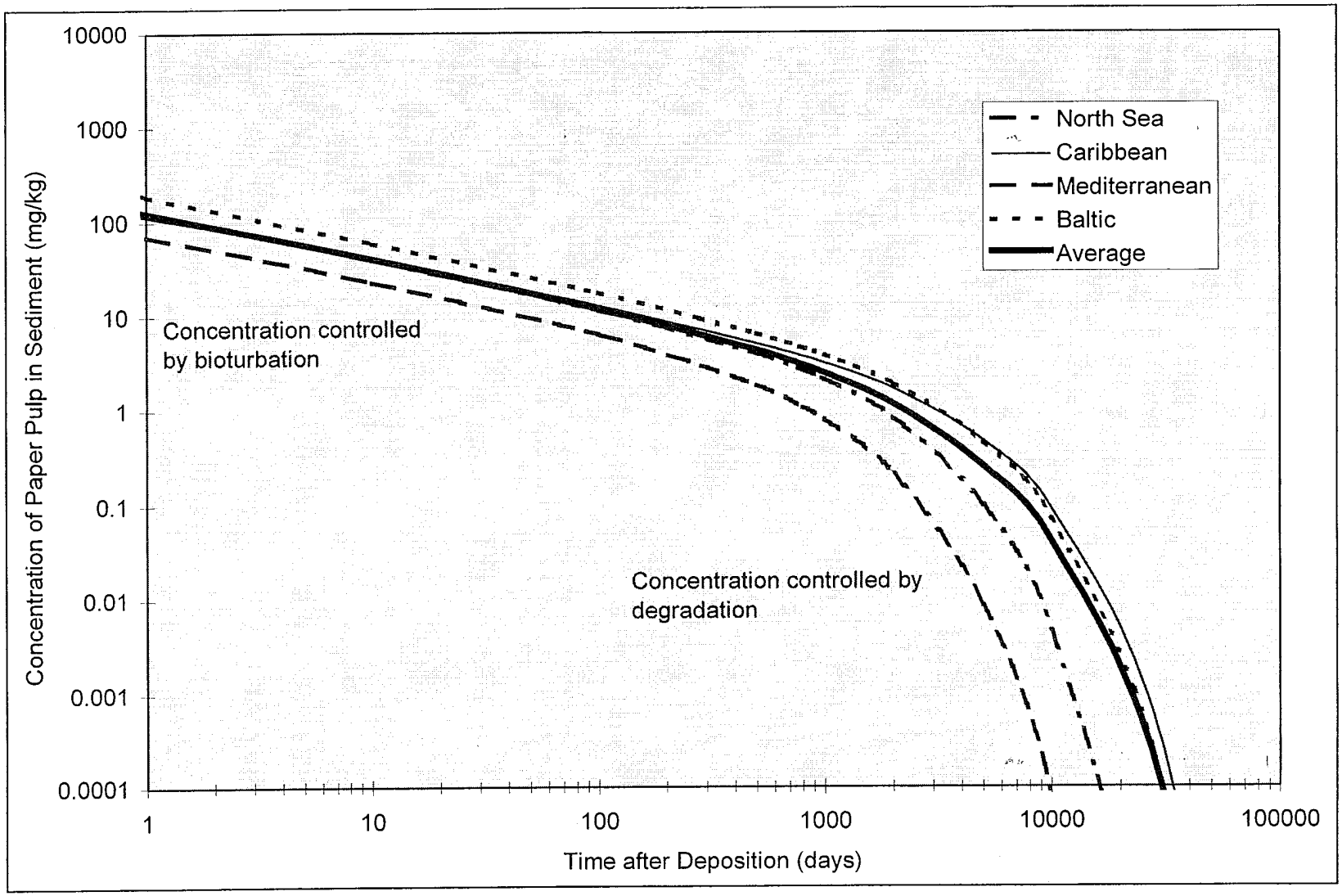

Figure 12-15. Predicted concentration of paper pulp in sediment as a function of time based on estimated rates of vertical mixing, burial, and degradation. Resuspension and consumption by particle feeders are neglected.

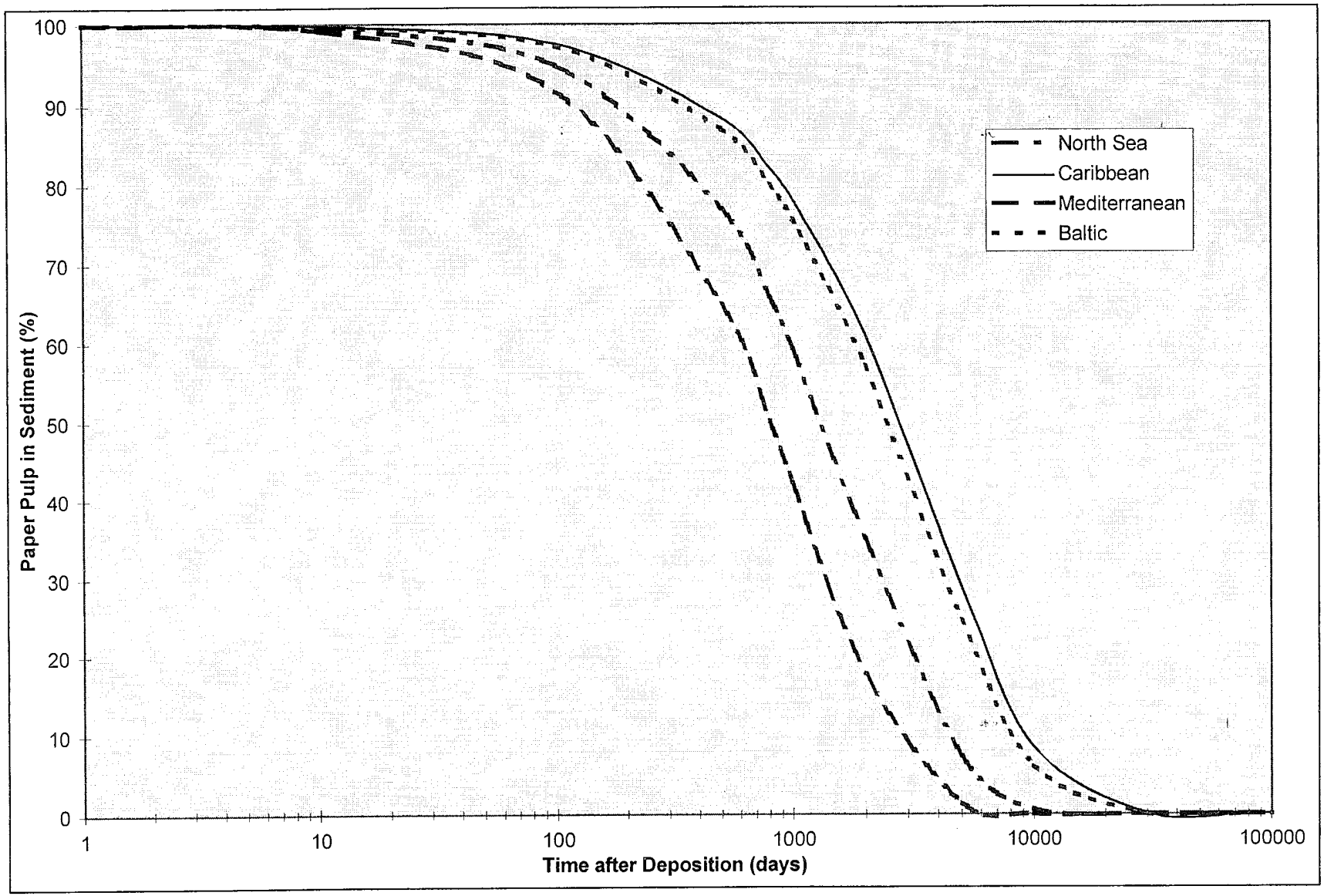

Figure 12-16. Fraction of pulped paper remaining in sediment over time based on estimated removal rates due to biodegradation.

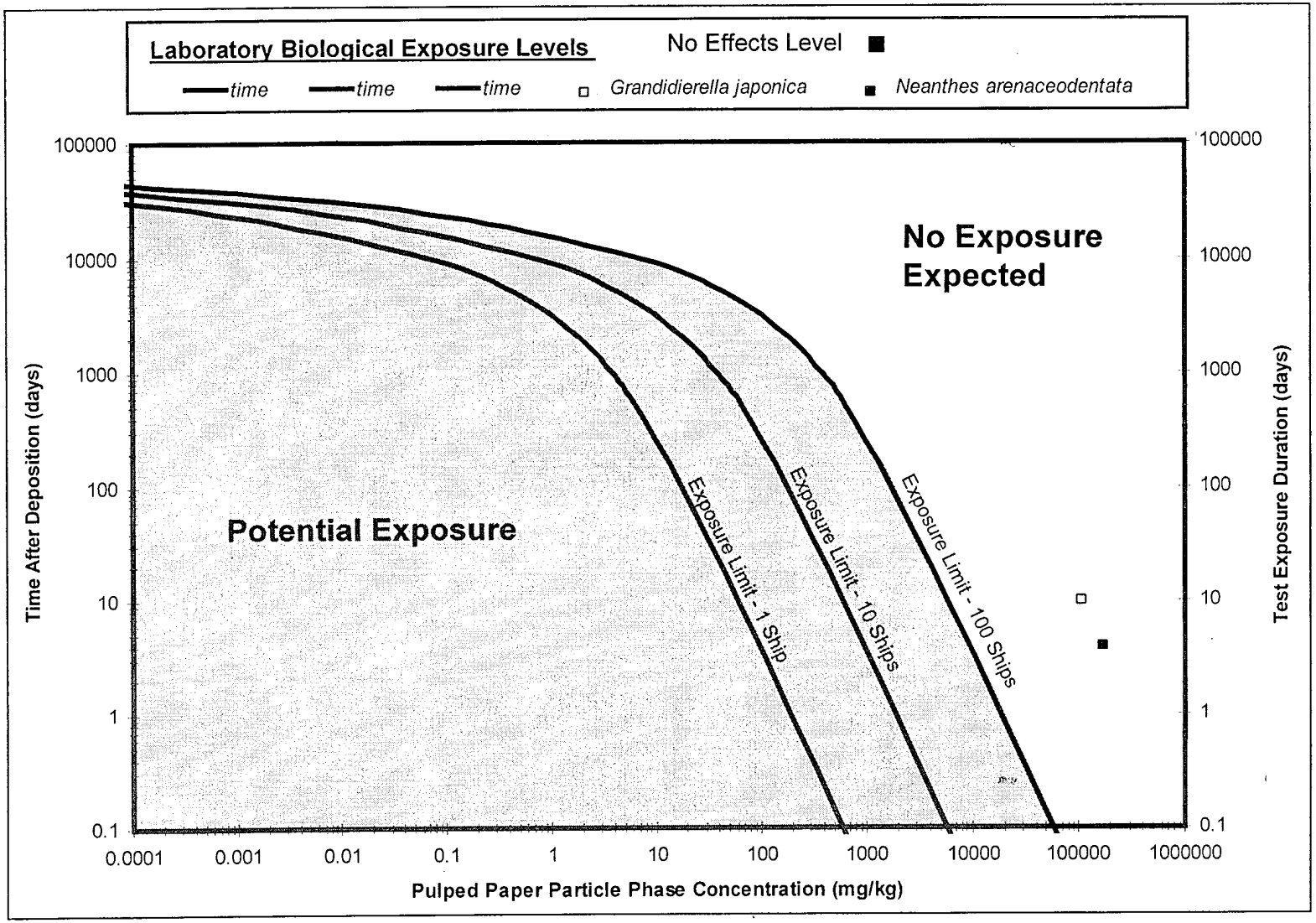

Figure 12-17. Estimated sea floor exposure limits compared to biological response levels for the combined pulped paper discharge of 1, 10, and 100 ships in the Baltic Sea.

Exposure and Effects on the Sea Floor. Based on the analysis above, it is possible to make a rough estimate of the potential exposure to pulped paper on the sea floor. Because of the long residence time of the pulped paper on the sea floor, it is likely that more than a single discharge could contribute to the mass loading at a specific site. Exposures related to hypothetical multiship operations are described in the following section. In this section, the potential exposure is simply estimated as a function of the number of ships which have discharged over the same area by assuming that their contributions to the overall sediment load is additive. Using the concentration model described above, the worst-case Special Area conditions for the Baltic Sea, and a range from 1 to 100 ship crossings over the same site, a range of potential exposures was calculated as a function of time after deposition (figure 12-17). Since the bottom coverage from a single ship is about 1%, 100 ship crossings corresponds to the amount of material required to cover 100% of the area beneath the ship with a single layer of particles. The plot indicates that maximum short term exposures (1 to 10 days) would be in the range of 100 to 10000 $mg \cdot kg^{-1}$ although these exposures would be limited to a very thin layer of sediment. These values are also averaged in the sense that they assume the mixing to be homogenous whereas, in general, the processes of burrowing and irrigation by benthic organisms leads to heterogeneous distributions.

Only limited effects data were developed for pulped paper in sediment. These consisted of a range of exposures to two benthic invertebrates, the amphipod species *Grandidierella japonica,* and the polychaete species *Neanthes arenaceodentata.* Tests were run for exposures approximately equivalent to pulped paper bottom layer thickness from 0.01 to 1 mm. No effects were found in either of the organisms at any of the test exposures. The no effects level was thus taken to be 1 mm thickness, and no low effects threshold could be determined without higher exposures. Using the relation between initial thickness and exposure concentration developed above, the no effects level concentration for the two tests was determined based on test duration and plotted on figure 12-17. This analysis suggests that no effects would be expected on representative benthic organisms for as many as 100 to 1000 discharges deposited in the same location. Based on the natural variability in ship tracks and ambient conditions, it seems unlikely that this number of repeated deposition events would occur at the same location. In addition, much of the material is likely to be redistributed by currents, an effect not accounted for in the analysis above.

To summarize, processes which will influence the fate of the pulped material on the sea floor are expected to include deposition rates, resuspension, transport, burial, degradation, and biological interactions. The analysis above suggests that deposition rates will be controlled primarily by the number of discharge events at a given location, and the depth dependent ambient mixing of the material. Based on particle characteristics, lateral redistribution of the material due to resuspension and transport appears to be likely in moderate to high energy environments such as coastal and shelf regions, and less likely in deep basins and quiescent regions where bottom currents are less than ~20 $cm \cdot s^{-1}$. Vertical mixing and burial of the pulped material will be determined by rates of natural sedimentation and bioturbation, with bioturbation being the primary controlling mechanisms except in regions near large sources of particulate input such as river mouths. Long term loss of pulped material may occur through microbial degradation over periods of 1000 to 3000 days assuming aerobic conditions prevail. In anoxic basins such as exist in the Baltic, degradation rates may be reduced, and vertical mixing rates due to bioturbation may also be limited. Peak exposure levels in the sediment should not exceed levels shown to be innocuous to representative benthic organisms even assuming deposition from 100 to 1000 ships at the same location.

Operational Scenarios

In this section, the potential effects of a hypothetical, multiship operational scenario is analyzed. This analysis is important because Navy ships often operate in groups and these groups may operate in restricted regions. This implies that pulped paper waste discharged from these ships may build up within areas where extended operations of the ship groups take place.

Table 12-3. Estimated mass loading of pulped paper from the combined input of typical ships comprising a BG and an ARG.

Ship Group	Ship	Number of Ships	Large Pulpers	Small Pulpers	Complement	Loading ($kg \cdot man^{-1} \cdot day^{-1}$)	Pulp Input ($kg \cdot day^{-1}$)
BG	CV/CVN	1	3	0	6,200	0.50	3123
	CG 47	2	1	0	409	0.50	412
	DD 963	1	1	0	396	0.50	199
	AOE 1	1	1	0	719	0.50	362
	FFG 7	1	0	1	220	0.50	111
						Total Input Rate =	4207
ARG	LHD 1	1	1	0	3,151	0.50	1587
	LSD	1	1	0	852	0.50	429
	LPD 4	1	1	0	1,487	0.50	749
	FFG 7	1	0	1	220	0.50	111
	AOE 1	1	1	0	719	0.50	362
						Total Input Rate =	3238

The number and type of ships, the area of operation, and the duration of the operation are the primary factors that will influence the concentrations and exposures that result form a multiship deployment. These factors vary greatly from operation to operation. Analysis of historical operations suggest that a reasonable operational profile might include one Battle Group (BG) and one Amphibious Ready Group (ARG). Ships included in the BG and ARG and their estimated daily pulper discharge rates are summarized in table 12-3. A typical mission duration might extend from 2 weeks to about 6 months, so that a 6 month duration could be chosen as a conservative estimate. The operational area can vary significantly, but a reasonable lower bound can be established by using an estimated operational radius for the CVN during flight operations of about 100 nmi.

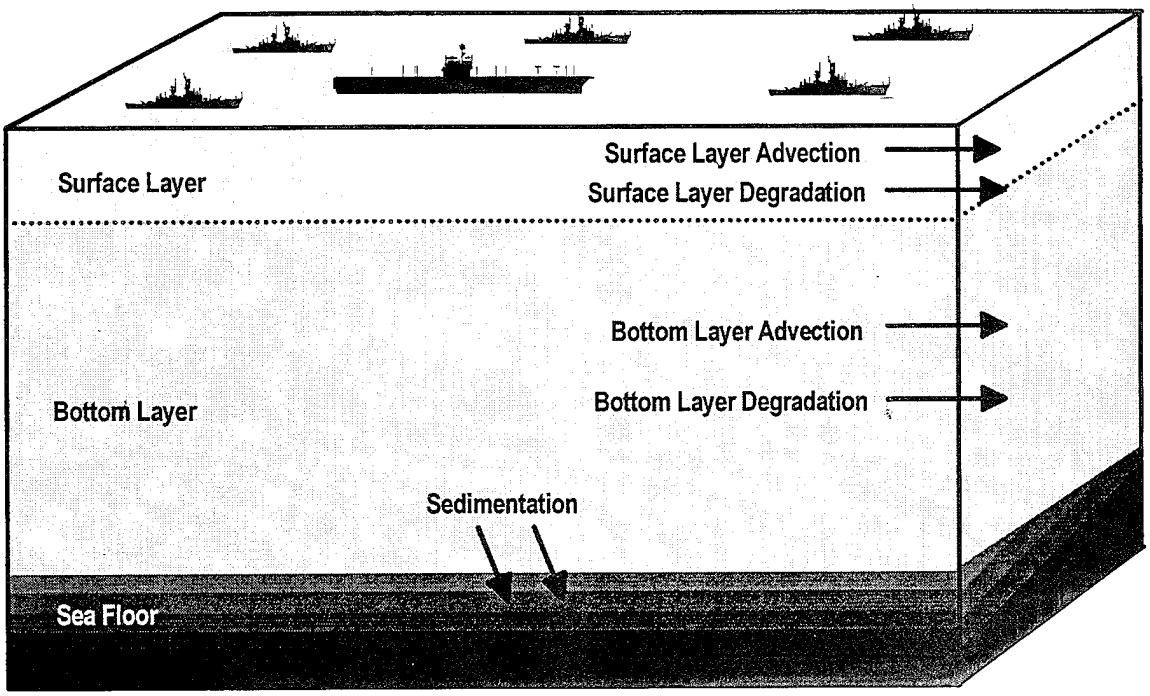

Figure 12-18. Schematic of the simple box model used to represent hypothetical operational scenarios in Special Areas.

The potential effects within Special Area regions was evaluated using this hypothetical operational scenario. This was done using the simple box model shown schematically in figure 12-18. The input rate of pulped paper was taken to be the average daily combined discharge from all of the ships operating in the region. The input was assumed to be spread evenly throughout the operational area. The water column was divided into one or two layers to simulate conditions of the Special Area in question. Processes accounted for in the water column include degradation, settling, and advection out of the operational area by currents. It was further assumed that the 6 month operation duration was sufficient to reach a steady state balance within the water column. Thus the mass balance for the surface layer is between input, advection, degradation, and settling, and the balance for the deep layer (where applicable) is between settling, advection, degradation, and sedimentation. These can be written as

$$\textit{Surface Layer}: \quad I = U_s h_s L C_s + k_s A_o h_s C_s + w A_o C_s \qquad \text{(Eq. 2-10)}$$

$$\textit{Bottom Layer}: \quad w A_o C_s = U_b h_b L C_b + k_b A_o h_b C_b + w A_o C_b$$

Where I is the pulped paper input rate from all ships, U_s and U_b are the surface and bottom velocities, h_s and h_b are the surface and bottom layer depths, C_s and C_b are the steady state surface and bottom water pulp concentrations, L is the length of the operational area, k_s and k_b are the surface and bottom water degradation rates, A_o is the operational area, and w is the average settling velocity for the pulped paper.

Table 12-4. Estimated steady-state exposure levels and fate in four MARPOL Special Areas from the combined pulped paper discharge of one BG and one ARG within a 10000 nmi^2 (32400 km^2) operational area.

Special Area		Caribbean Sea	Mediterranean Sea	North Sea	Baltic Sea	Average %
Operational	# of BGs	1	1	1	1	
	# of ARGs	1	1	1	1	
	Area (km·10^2)	32400	32400	32400	32400	
	Duration (months)	6	6	6	6	
	Total Input Rate (kg·day^{-1})	7443	7443	7443	7443	
Surface Layer	Depth (m)	100	75	50	40	
	Temp (deg C)	28	26	10	10	
	Deg Rate %·day^{-1}	0.500	0.389	0.052	0.052	
	Velocity (m·s^{-1})	0.75	1.5	0.5	0.05	
Bottom Layer	Depth (m)	2500	1500	n/a	150	
	Temp (deg C)	4	14	n/a	5	
	Deg Rate %·day^{-1}	0.025	0.087	n/a	0.028	
	Velocity (m·s^{-1})	0.5	0.5	n/a	0.02	
Mass Fraction	Small (kg·day^{-1})	223	223	223	223	
	Med (kg·day^{-1})	893	893	893	893	
	Large (kg·day^{-1})	6327	6327	6327	6327	
Settling Rate	Small (m·day^{-1})	0	0	0	0	
	Med (m·day^{-1})	6	6	6	6	
	Large (m·day^{-1})	864	864	864	864	
Surface Layer	Concentration (mg·L^{-1})	$1.05 \cdot 10^{-6}$	$7.97 \cdot 10^{-7}$	$2.33 \cdot 10^{-6}$	$1.12 \cdot 10^{-5}$	
	Mass in Layer (kg)	3416	1936	3767	14515	
	Advection (kg·day^{-1})	1230	1394	904	348	13.0
	Degradation (kg·day^{-1})	17	8	2	8	0.1
	Settling (kg·day^{-1})	6196	6041	6537	7087	86.9
Bottom Layer	Concentration (mg·L^{-1})	$1.34 \cdot 10^{-7}$	$1.57 \cdot 10^{-7}$	n/a	$3.39 \cdot 10^{-6}$	
	Mass in Layer (kg)	10881	7650	n/a	16485	
	Advection (kg·day^{-1})	2611	1836	n/a	158	15.5
	Degradation (kg·day^{-1})	3	7	n/a	5	0.0
	Sedimentation (kg·day^{-1})	3582	4199	6537	6924	71.3

Based on these relationships, it is possible to solve for the steady state concentrations of the small, medium, and large size fractions and then determine the total layer concentration and the magnitude of each of the mass balance terms. These results are summarized for each of the Special Areas in table 12-4. The combination of one BG and one ARG results in an average input rate of about 7400 kg d^{-1}. Solving for C_s and C_b above for a range of Special Area conditions results in steady state concentrations ranging from about 0.8 to 11 ng·L^{-1} in the surface layer and 0.1 to 3 ng·L^{-1} in the bottom layer. The highest concentrations are generally found where the currents are assumed to be weak (e.g., Baltic) since this reduces the advective loss of material from the region. As with the single ship case, most of the material is found to settle through both layers and on to the bottom with an average of ~87% of the material settling

through the surface layer and ~71% reaching the bottom. In areas where the currents are strong, a substantial fraction of the material will be advected out of the operational area. The average advective loss for the four cases was ~13% for the surface layer and ~16% for the bottom layer, for a total of ~29%. Loss by degradation within the operational area is generally small (<1%) because advection tends to remove the material from the area before it can degrade. The material that is swept out of the area by currents will still be subject to settling and degradation but will not contribute to the water column loading of the operational area.

The water column concentrations that result from this model suggest that long term elevation of pulped paper levels in large areas during fleet operations is not a limiting case. The concentrations are orders of magnitude below measured laboratory effects levels and significantly below background levels of oceanic POC. The amount of material reaching the bottom is substantial, ranging from 3.6 to 6.9 $mt \cdot d^{-1}$. Over the 6-month duration this gives a total input to the sea floor of about 645 to 1246 mt. Assuming this material is spread evenly over the sea floor in the operational area, the thickness of the bottom layer would be 0.08 to 0.15 μm. This is 6 to 12 times less than the local exposure scenario described previously, suggesting that sea floor exposure would not be severely increased by a concentrated operation so long as the material were reasonably evenly distributed over the operational area. These results could be altered if discharge conditions or natural forces acted to concentrate the discharges into particular areas that are significantly smaller than the operational area. This is unlikely for the water column since most of the material sinks rapidly. Depending on bottom topography and currents, it is common for sedimentation to be concentrated in certain depositional areas (Seibold and Berger, 1982). The potential for concentrated deposition also exists in regions near major Navy ports where ships may be likely to discharge after leaving port or prior to returning. However, biological tests indicate that even for layers of ~1 mm (5 orders of magnitude greater than the average layer thickness), no effects were found on benthic organisms.

To summarize, hypothetical operational profiles for four Special Areas were investigated using a simple steady-state box model. The overall partitioning of the material was controlled primarily by settling and advection. Of the total material input into the area, about 71% could be expected to settle to the sea floor within the same area, while the remaining ~29% would be advected out of the operational area. The results suggest that the operation of multiple ships within a limited area should not produce concentrations of pulped paper in the water column or on the sea floor which are greater than local exposures due to a single ship. Thus, significant biological effects would not be expected under operational scenarios such as those described above.

Basin-Scale Scenarios

The analysis above describes some possible outcomes from the discharge of pulped paper waste for a single ship, or for several ships operating within a limited region. In this section, the largest scale of the problem is considered in which the total input of pulped paper within a Special Area is considered (figure 2-4). For a normal point source discharge, this type of analysis would be inappropriate since the region of impact is expected to be localized. For the case of Navy discharges, however, the input is naturally diffused due to the mobile nature of the discharge source. Thus the input of pulped paper can be expected to be delivered to random locations over a wide spatial area. The purpose of this analysis is to determine the overall contribution of pulped paper discharges to the constituent budgets of the Special Areas. The objective is to determine if the input of pulped paper from ships constitutes a distributed source which is large

enough to produce significant changes in the overall budgets and processes within the Special Areas.

To determine the overall input of pulped paper to the Special Areas, the CNO EMPSKD database was reviewed. Based on 10 years of ship movement data from 1984 through 1993, and typical ship complements for ships present, average man-days per year were estimated for each Special Area. From this, the total yearly mass loading of pulped paper for each Special Area was determined. The combined average man-days in the four Special Areas analyzed ranged from a high of ~3.4 million man-days·y^{-1} in the Mediterranean, to a low of about 23,000 man-days·$year^{-1}$ in the Baltic. The input of pulped paper per man is about 0.5 kg·d^{-1}. This gives an overall range of mass loading from about 173 mt·y^{-1} in the Mediterranean to about 12 mt·y^{-1} in the Baltic. The loading to the North Sea is similar to the Baltic at about 16 mt·y^{-1} while the loading to the Caribbean is closer to that of the Mediterranean at 128 mt·y^{-1}.

Table 12-5. Annual basin-wide constituent loading from U.S. Navy ships into four MARPOL Special Areas (kg·yr^{-1}) based on estimated pulped paper discharges and results from chemical analysis.

Special Area	North Sea	Baltic Sea	Mediterranean Sea	Caribbean Sea
TSS	16264	11568	1730681	1284068
BOD_5	1107	787	117752	87365
P	1	1	148	110
COD	1981	1409	210858	156445
N	6	5	685	508
TOC	10293	7321	1095368	812701
Zn	0.10	0.07	10	8

Pulped paper represents a source of particulate material which contributes to the overall suspended load of the water column. Chemical analysis of the pulped paper indicates that it is primarily organic matter in the form of cellulose, so the waste stream can be expected to add to the background levels of particulate organic matter. Associated with the decomposition of the pulped paper are values of BOD_5 and COD which reflect roughly the expected oxygen requirement and the maximum possible oxygen requirement. Low levels of the nutrients nitrogen and phosphorus and the trace metal zinc were also present in the waste stream. The mass loading of the major constituents, the oxygen demand, and the minor constituents was estimated from the chemical analysis and the estimated overall loading to the Special Areas. These results are summarized in table 12-5.

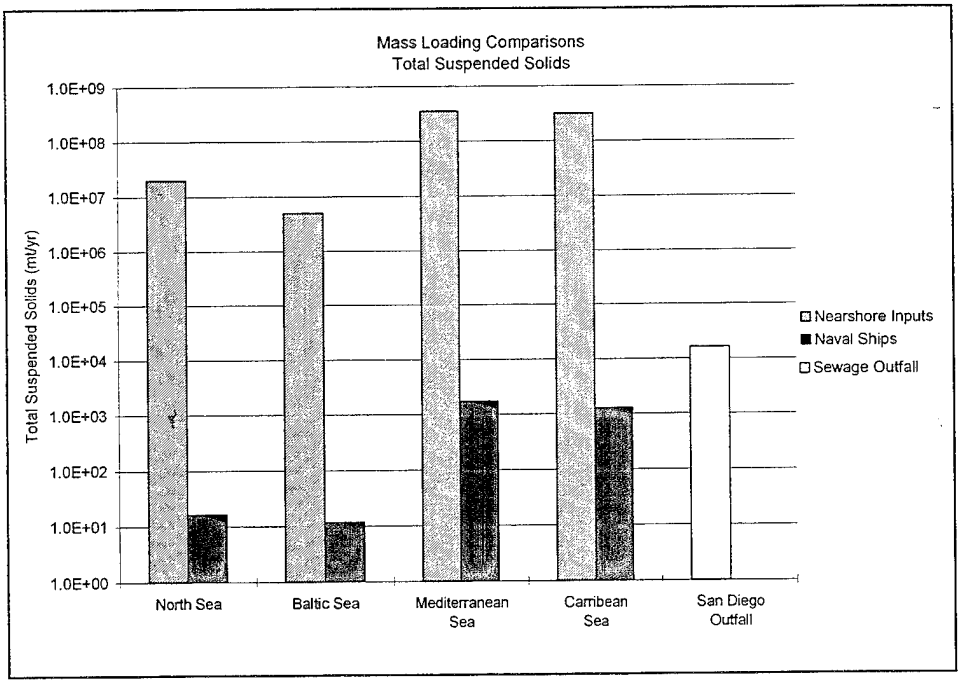

Figure 12-19a. Comparison of estimated TSS mass loading from pulped paper discharges by U.S. Navy ships with near shore inputs in four Special Areas and the San Diego municipal sewer outfall.

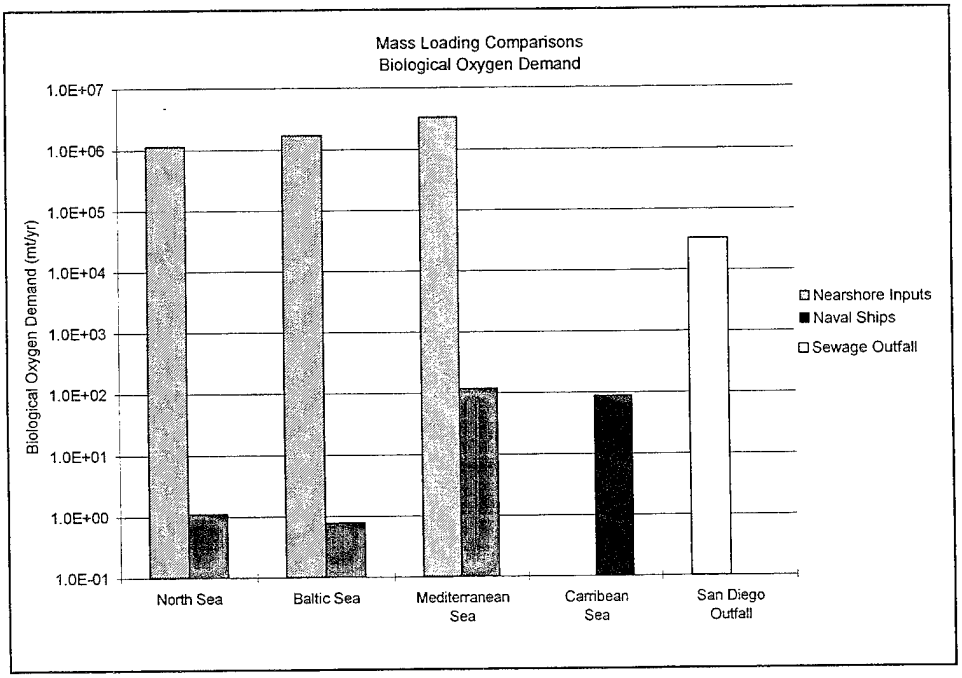

Figure 12-19b. Comparison of estimated BOD from pulped paper discharges by U.S. Navy ships with near shore inputs in four Special Areas and the San Diego municipal sewer outfall.

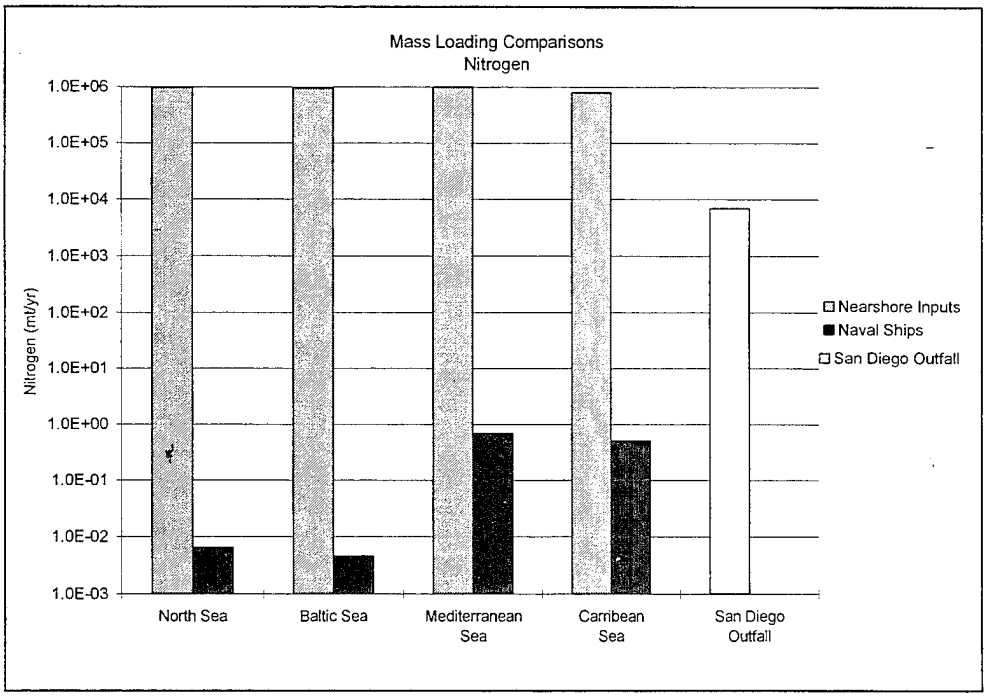

Figure 12-19c. Comparison of estimated nitrogen mass loading from pulped paper discharges by U.S. Navy ships with near shore inputs in four Special Areas and the San Diego municipal sewer outfall.

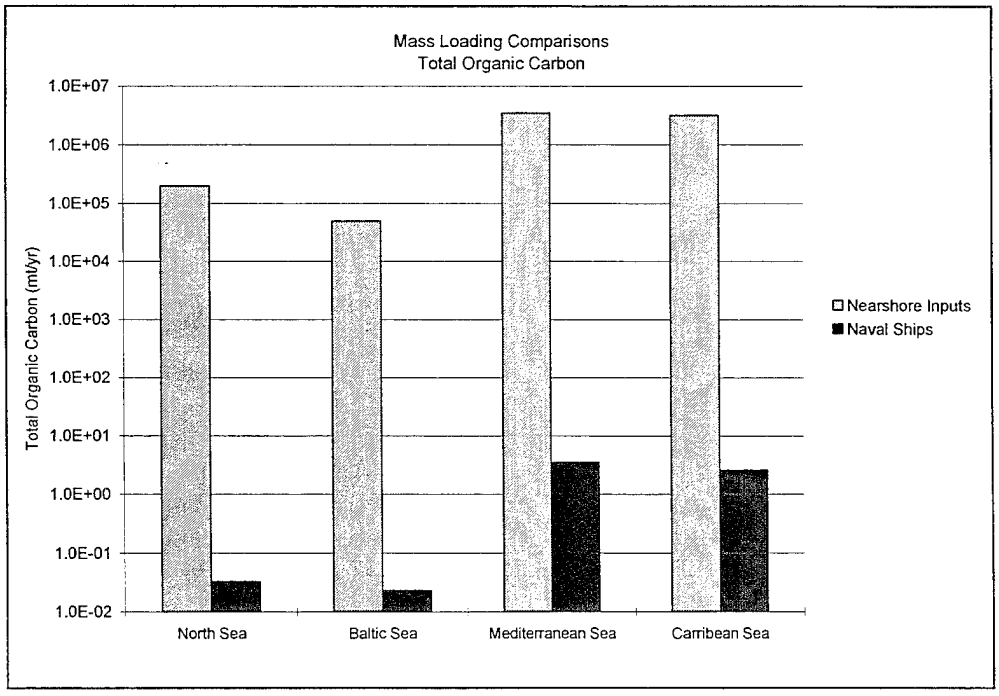

Figure 12-19d. Comparison of estimated TOC mass loading from pulped paper discharges by U.S. Navy ships with near shore inputs in four Special Areas.

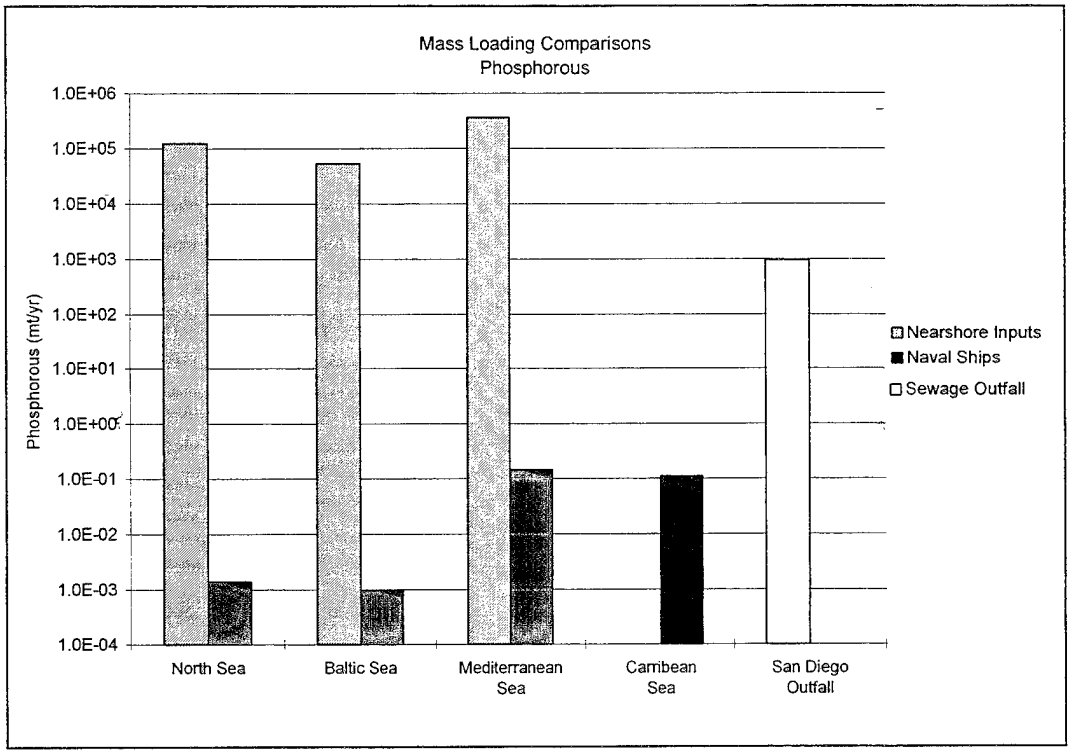

Figure 12-19e. Comparison of estimated phosphorous mass loading from pulped paper discharges by U.S. Navy ships with near shore inputs in four Special Areas and the San Diego municipal sewer outfall.

To determine the relative contribution from ship discharges to the material budgets of the Special Areas, estimates of basin-wide and regional inputs were obtained from the Special Area literature review and direct contact with environmental managers and municipal treatment plants in the Special Areas. The comparison between the literature values for basin-wide inputs and the estimated ship loadings are shown in figures 12-19a-e. The result of this analysis indicate that pulped paper discharges from all the ships within Special Areas represents a small fraction of the total inputs. The majority of particulate matter entering the Special Areas originates from rivers, primary production, and treated and untreated municipal sewage (table 6-1 to 6-4). For TSS, the particulate fraction discharged by ships ranges from about 16 to128 $mt \cdot y^{-1}$, while the background inputs to Special Areas range from about $5 \cdot 10^6$ $mt \cdot y^{-1}$ to $320 \cdot 10^6$ $mt \cdot y^{-1}$, so that the contribution from Navy ships would represents between about 0.00008 to 0.0005% of the annual budget for the Special Areas studied. Inputs of TOC range from about 7.3 to 1100 $mt \cdot y^{-1}$ representing about 0.005 to 0.03%. Annual inputs of BOD_5 by Navy ships range from about 0.8 $mt \cdot y^{-1}$, to about 118 $mt \cdot y^{-1}$ while background inputs to the Special Areas have been estimated to range from $1.7 \cdot 10^6$ $mt \cdot y^{-1}$ to $3.3 \cdot 10^6$ $mt \cdot y^{-1}$. The BOD_5 input from ships based on these estimates would range from about 0.0001 to 0.003% for the Baltic and Mediterranean, respectively. Similar analysis for nitrogen and phosphorus give ranges of 0.0000007 to 0.00007% and 0.000001 to 0.00004% for their fractional contribution to the Baltic and Mediterranean. The lower percentages for these nutrients reflects their relatively low presence in the waste stream. The total input of zinc is estimated to range from a low of $6.6 \cdot 10^{-5}$ $mt \cdot yr^{-1}$ in the Baltic to a high of about $9.5 \cdot 10^{-4}$ $mt \cdot yr^{-1}$ in the Mediterranean. This compares with a basin-wide input of zinc to the Baltic estimated at $1 \cdot 10^4$ $mt \cdot yr^{-1}$ (Somer, 1977) and to the Mediterranean at $2.5 \cdot 10^4$ $mt \cdot yr^{-1}$ (UNEP, 1989).

From the above analysis it is clear that from a basin-wide perspective, the input of pulped paper by Navy ships will not contribute significantly to the overall constituent budgets of the Special Areas. For instance, assuming the total mass loading of pulped paper sinks to the bottom with no degradation, the average sedimentation rate across the Mediterranean can be estimated. For an overall input yearly of 128 mt·y^{-1}, a density of 1.5 g·cm^{-3}, and a solids content of ~15%, the estimated sedimentation rate for pulped paper over the $2.5 \cdot 10^6$ km^2 area of the Mediterranean would be about $3.4 \cdot 10^{-8}$ mm·y^{-1}. Given a typical sedimentation rate for the Mediterranean of 1 mm·y^{-1}, this represents an increase above background of about 0.000003%. Similarly, taking the worst-case scenario for the Mediterranean, the basin-wide oxygen depletion based on a yearly input of pulped paper from Navy ships can be estimated. Assuming all the pulped material is degraded with a theoretical TOD value of 1.18 g·g^{-1}, then the total oxygen consumed in the Mediterranean in one year would be about 1.18·128 mt = 151 mt. Given the volume of the Mediterranean at about $3.7 \cdot 10^6$ km^3, and an average oxygen content of 5 mL·L^{-1}, the standing stock of oxygen in the Mediterranean is about $2.6 \cdot 10^{10}$ mt. Thus the oxygen utilization per year of discharge represents about 5 billionths of the standing stock. Eutrophication effects on a basin-wide scale can be estimated by assuming a worst-case scenario in which 100% of the nutrients input with the pulped paper are converted to biomass via primary production. Assuming a C:N ratio for phytoplankton of 41:7 by weight, the maximum possible phytoplankton biomass that could be generated in the Mediterranean would be about 0.00000001% of the estimated $3.6 \cdot 10^{13}$ kgC·y^{-1} primary production rate for the Mediterranean.

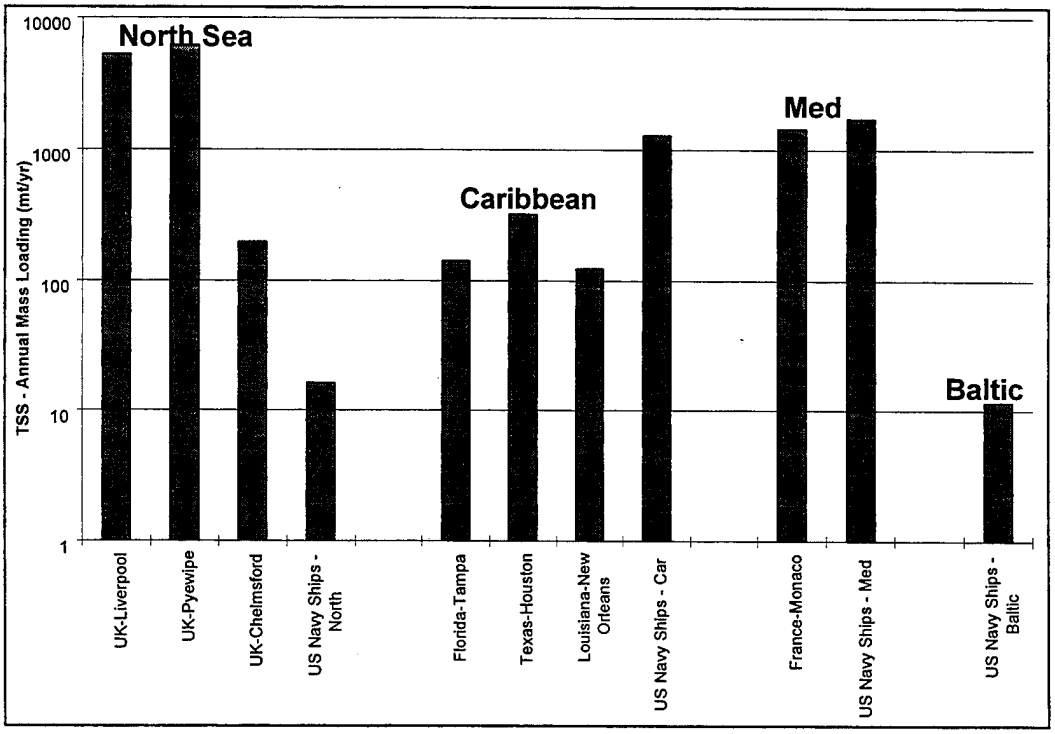

Figure 12-20a. Annual TSS mass loading from typical sewage treatment plants compared to estimated inputs from pulped paper discharges by U.S. Navy ships in four Special Areas.

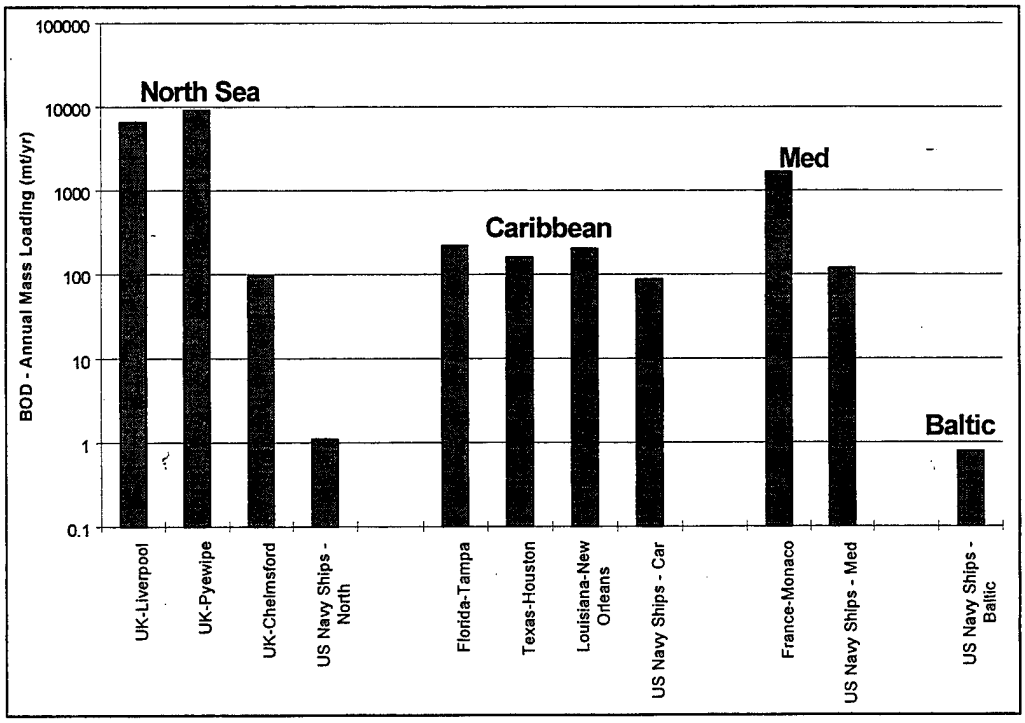

Figure 12-20b. Annual BOD mass loading from typical sewage treatment plants compared to estimated inputs from pulped paper discharges by U.S. Navy ships in four Special Areas.

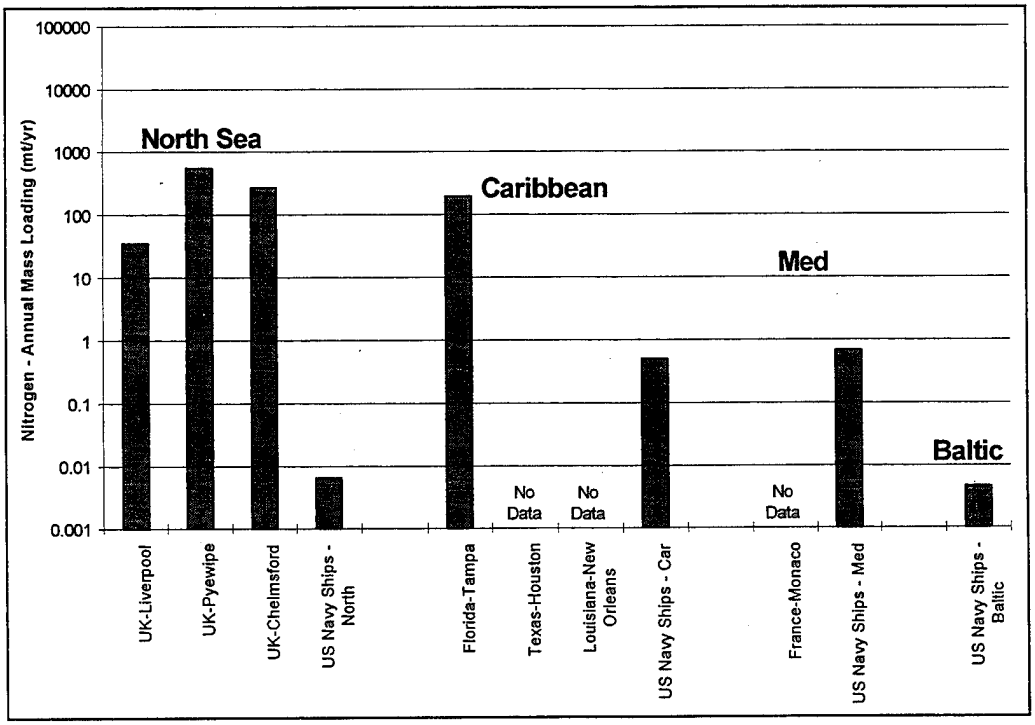

Figure 12-20c. Annual nitrogen mass loading from typical sewage treatment plants compared to estimated inputs from pulped paper discharges by U.S. Navy ships in four Special Areas.

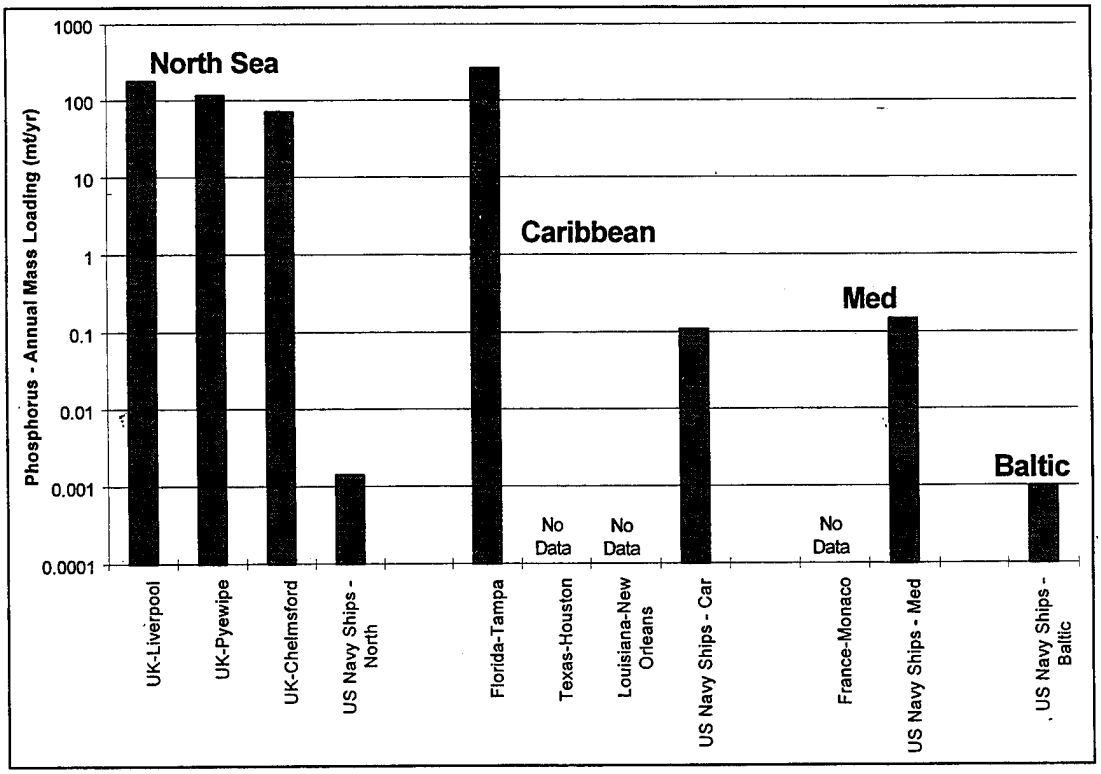

Figure 12-20d. Annual phosphorus mass loading from typical sewage treatment plants compared to estimated inputs from pulped paper discharges by U.S. Navy ships in four Special Areas.

To give additional perspective to the magnitude of pulped paper input, figures 12-20a-d show the comparative input of all ships with localized inputs from typical sewage treatment plants in the Special Areas. The purpose of this comparison is to provide a baseline for interpreting the potential relative impact of pulped paper discharges by ships which are currently restricted to allowed levels of discharge for municipal waste which are restricted to levels which would minimize impacts. It should be stressed that the inputs from Navy ship discharges would be significantly more diffuse than those from point source discharges such as sewage treatment plants. This comparison shows that inputs of total solids from pulped paper discharges by all ships represent from about 0.1 to 200% of the annual discharge from individual sewage treatment plants which are currently discharging into the Special Areas. The input of BOD_5 from all ships in each Special Area represents a range of about 0.01 to 50% of the annual input of individual treatment plants. The input of nitrogen from all ships constitutes about 0.001 to 1%, and input of phosphorus represents about 0.0001 to 10% of the input from individual treatment plants. These comparisons suggest that the highly diffuse discharge from ships, much of which will occur in the open sea, represents at most the equivalent input of typical municipal treatment plants which discharge routinely into the coastal waters of the Special Areas.

To summarize, an analysis of basin-wide inputs of pulped paper from U.S. Navy ships suggests that this source is insignificant in the overall constituent budgets of the Special Areas. Estimated inputs from ships of TSS, BOD_5, nitrogen, and phosphorus represent much less than 1% of the Special Area annual budgets. Thus, potential broad scale effects such as eutrophication due to nutrient inputs or oxygen depletion due to organic loading do not appear to be an issue on the

basis of this source alone. In areas where these problems already exist, these inputs will probably not contribute to the existing imbalance to a measurable extent. Comparative data suggest that total annual input of pulped paper from all ships within a Special Area is roughly equivalent to spreading the entire discharge from a single sewage treatment plant over the entire Special Area.

12.2 Fate and Effects of Shredded Metal and Glass Waste Stream

Discharge Conditions

The fate and effect of the shredded metal and glass waste stream as outlined in the conceptual model (figure 2-2) are discussed in this section. The discharge conditions for this waste stream are a bit simpler than that of the pulped paper waste stream because once the material is shredded, it is bagged in burlap and manually tossed over the side of the ship. This means that individual components of the waste stream are unlikely to be dispersed over large areas, although individual bags will. The number of bags discharged over a given time and the manner in which the discharge period is distributed through the day will vary from ship to ship, thus typical operational conditions will be applied in the following discussion.

Rate. For a given ship, the general discharge rate of metal and glass is established by the processing rate of the shredder and the number of shredders operated at a given time. However, temporary storage of bags after shredding and prior to dumping could result in episodic rates that can be somewhat higher than those predicted by the processing time alone. The nature of these operations would be highly variable and unpredictable; therefore, the rates discussed here will be based strictly on shredder processing operational conditions. The shredders have processing rates for metal/glass of 275 $kg \cdot hr^{-1}$ (NAVSEA, 1993). Except for CV and CVN class ships, which have 2 shredders installed, all other ships, will have only one shredder. This gives a maximum possible range for discharge rates of 275 to 550 $kg \cdot hr^{-1}$. Based on results of this study, a typical full bag weight is 4.8 kg. Thus, the discharge rate translates into 57 to 115 $bags \cdot hr^{-1}$.

Duration. The discharge period will be determined by the waste stream generation rate and the operational practices of the ship. The waste stream generation rate for metal/glass has been estimated at 0.25 $kg \cdot person^{-1} \cdot d^{-1}$ (NAVSEA, 1993). Ship complements range from about 50 persons on the MHC 51 class ship to about 6300 persons for the CVN 68 (NAVSEA, 1993). Thus, the total solid waste stream generation rate ranges from 12 to 1575 $kg \cdot d^{-1}$. In terms of number of bags, the discharge is 3 to 328 $bags \cdot d^{-1}$. This result simply quantifies the obvious fact that carriers with their huge complement will be the largest single ship source of this waste stream. The shredder processing and generation rates for a CVN 68 translate into a discharge period ranging from about 2.9 to 5.8 $hr \cdot d^{-1}$ depending on whether one or two shredders are running.

Discharge Density. An estimate of the likely sea floor area covered from the daily discharge of a single CVN class ship can be computed using typical operational ship speeds and discharge rates. Operating speeds for a CVN class ship range from 18 to 55 $km \cdot hr^{-1}$ with typical transit speeds of about 28 $km \cdot hr^{-1}$. As noted previously, discharge rates vary from 275 to 550 $kg \cdot hr^{-1}$ or 57 to 115 $bags \cdot hr^{-1}$. A maximum density of bags along the track of a carrier computes as 30 $kg \cdot km^{-1}$ or 7 $bags \cdot km^{-1}$ using minimum transit speeds and maximum discharge rates. Conversely, using maximum transit speeds and minimum discharge rates produces a minimum density of 5 $kg \cdot km^{-1}$ or 1 $bag \cdot km^{-1}$. Thus, the density of bags on the sea floor along the ship's track will range from 5 to 30 $kg \cdot km^{-1}$ or 1 to 7 $bags \cdot km^{-1}$. At a typical cruising speed of 28 $km \cdot hr^{-1}$ and using the lower discharge rate, the density of bags computes as 10 $kg \cdot km^{-1}$ or 2 $bags \cdot km^{-1}$.

Based on an estimated discharge period of either 2.9 to 5.7 $hour \cdot d^{-1}$ for the CVN 68, and assuming a continuous discharge with no interruptions, the length of the discharge line source for one day ranges from between 52 to 313 km. At typical transit speeds, the daily line source would

be 80 to 160 km, depending on the number of shredders used. These line source numbers are conservative from the point of view that the discharges are likely to be spread out over the full day and will thus be spread out further than calculated here. As an example, a CVN class ship transiting for 24 hours at 28 $km \cdot hr^{-1}$ would have potential discharge line source that was 672 km in length. The average density of bags along a daily line source would therefore be 1 bag every 2 km rather than the 1 to 7 $bags \cdot km^{-1}$ calculated above under continuous discharge.

Using the line source for a continuous discharge scenario from a CVN (80 to 160 km) and a swath width equivalent to the ship's beam of 40 m, the area of sea floor covered would range from 3.2 to 6.4 km^2. Assuming that all 328 bags reach the bottom directly below the ship's track, the sea floor covered by bags daily is 66 m^2 (each bag has a frontal area of 0.2 m^2). This represents a coverage ratio of 1 to $2 \cdot 10^{-5}$ (10-20 parts per million). At this rate the ship would have to transit back and forth along the same route for at least 50,000 days (137 years) to cover the full swath with bags.

Discharge Location. Discharge location on the ship will vary from ship to ship, but in general is expected be located above the waterline. Operations observed aboard the USS *George Washington* showed that bags were thrown down a chute from the second hangar deck roughly 7 m above the water line (Sean Gill, personal communication). Although the location of discharge along the length of a ship is not a concern for this waste stream, the height above the water might be important from the standpoint of bag breakage. Although no tests were performed in this study to determine the probability of bag breakage as a function of discharge height, data collected by CDNSWC/AD led to the choice of the burlap bag packaging because of its durability and sinking characteristics (Sean Gill, personal communication). The effect of breaking open a bag would be to distribute the material more evenly over a given area and possibly slow the overall settling of the material. The introduction of loose materials into the water column would potentially increase the chances that they would attract and be swallowed by large fish, particularly when pulped food wastes are simultaneously present in the water column.

To summarize, the shredded metal and glass waste stream discharge will vary mainly as a function of ship class, the ship's generation rate, and its operational practices. Maximum daily discharges of 1575 kg or 328 bags are expected from CVN class ships with rates up to 115 $bags \cdot hr^{-1}$. Variations in ship speed, discharge rate, and duration will of course affect the area over which the bags are dispersed although a typical daily line source from a CVN will likely extend roughly 300 kilometers. The area of sea floor covered by a daily discharge from a single CVN will be 10 to 20 parts per million.

Waste Stream Characteristics

Sinkability. The three bags tested in this study all readily sank. The shredding process appears to minimize the likelihood that significant amounts of trapped air space are produced and there is good reason to believe that any bags produced in this manner would always sink readily. Measured settling velocities of 0.51 to 0.59 $m \cdot s^{-1}$ indicate that the bags fall quickly through the water column. The time it takes to reach the bottom in water depths of 60, 1500, and 2600 m, average depths found in the Baltic, Mediterranean, and Caribbean Seas, respectively, are 1.8, 46.3, and 80.2 minutes, respectively, using an average sink rate of 0.54 $m \cdot s^{-1}$. This suggests that water column processes are likely to play a minimal part in the fate and effects of this waste stream whereas sea floor processes will be important.

The fast sink rates found for shredder bags are in distinct contrast to the results obtained for bags generated by Type II Horizontal Trash Compactors which showed that 60% did not sink (Olson et al., 1989). The addition of metal weights was still insufficient to sink 17% of them. This suggests that the shredder system is significantly more effective in creating a sinkable waste stream, undoubtedly a result of minimizing air pockets within the material.

Chemical Composition. The components making up the shredded metal and glass waste stream were shown to be primarily tin-plated steel cans, glass, and organics (food wastes associated with the containers). These were found at 71%, 13%, and 6% by weight, respectively. Minor components included aluminum cans and paper labels each making up about 2% by weight. The burlap bag containing these materials was another 8%, by weight, of the total waste stream. For the following analysis, the organic food wastes, paper labels, and burlap are not considered further.

The percentages of steel cans and glass materials found in this study are similar to those found by Manzi (1994). In that study, ferrous and glass materials were found to be 66% and 14%, respectively, by weight. However, the aluminum fraction measured by Manzi (1994) was 20% by weight which was substantially higher than the 2% average and the 5% maximum observed in this study. Variations in the waste stream mass fractions should be expected given the discrete nature of the samples. Because the primary source of aluminum in the waste stream is in the form of beverage containers, it is possible that recycling of aluminum cans aboard the USS *George Washington* could account for the significant reduction observed relative to Manzi (1994).

Table 12-6. Elemental makeup of the shredded metal and glass waste stream. Included are comparison values for elemental composition found in average ocean sediments derived from Chester, 1990. Except for Si, Na, and Ca, the values are based on elemental concentrations found in deep sea clays. In the case of Si, Na, and Ca, the vlaues are based on percentages of their oxides. The final column in the table is the ratio of elements found in the waste stream to those found in typical ocean sediments.

Element	Waste Stream	Deep Sea Clays	Waste/Sediments
Fe	70%	6%	12
Si (oxide)	10%	55%	0.2
Na (oxide)	2%	1.5%	1.3
Al	0.9%	10%	0.09
Sn	0.7%	0.0002%	3500
Ca (oxide)	0.6%	0.9%	0.7
Mn	0.4%	0.6%	0.7
Mg	0.04%	2%	0.02

Based on the elemental analysis, the tin-plated steel and aluminum cans can be broken down into their major constituents. For steel cans these are (by weight): iron (98%), tin (1%), and manganese (0.5%). For aluminum cans these are: aluminum (94%), magnesium (4% max), and manganese (1% max). These materials all form oxides in seawater as part of the corrosion process. The major components of glass bottles include oxides of silicon, sodium, and calcium in typical percentages of 75%, 14%, and 5%, respectively, although the percentages can vary

with glass type (Rayotek Scientific, personal communication). The compositional makeup of elements as a percentage of the total waste stream (by weight), are summarized in table 12-6. A comparison of these percentages with those found in average ocean sediments (Chester, 1990) shows that only Fe and Sn are significantly enriched relative to background sedimentary material by factors of 12 and 3500, respectively.

Degradability. Corrosion rates were not directly measured in this study. Rather, the metal portion of the waste stream was characterized in terms of material types and amounts in order to estimate a likely range of expected corrosion times using literature rates. Although the materials were characterized fairly well, corrosion rates are highly dependent on the receiving environment, particularly on ocean parameters such as oxygen, pH, temperature, pressure, and biofouling. Because the receiving environments of Special Areas span the full range of possible conditions found in the sea, corrosion rates will span a large range. Likely ranges in rates as identified in the corrosion study were 0.6 to 11 mpy for steel cans and 0.1 to 3.9 mpy for aluminum cans. Measured thicknesses were 0.0067 to 0.00131 inch for steel cans and 0.0043 to 0.133 inches for aluminum cans. Given the range in thicknesses and corrosion rates, the full range expected for complete corrosion would be 0.6 to 22 years for steel cans and 1 to 130 years for aluminum cans. Using midrange thicknesses of 0.01 inch for both types of cans and rates of 4 and 1 mpy produces complete corrosion of the steel and aluminum cans in 2.5 and 10 years, respectively. Because of the thinness of the Sn coatings (< 0.00006 inch), even at low measured rates of 0.5 mpy, complete corrosion of Sn will likely occur in about a year.

Regardless of rates, corrosion of shredder materials is not truly a removal process. It is a mechanism by which the chemical constituents of the cans are redistributed mainly through transition from metal shreds to smaller particles and some dissolution. It also is a mechanism for changing the aesthetic nature of the waste stream from one which is clearly a component of anthropogenic litter to one which may not be recognizable as anything different from typical sedimentary materials. Although variable, the time scale for this to occur will be on the order of years.

Typical oxidation processes for the shredded metal will utilize oxygen in stoichiometries shown in equations 2-8 of appendix G. A gross estimate for the amount of oxygen utilized to completely oxidize the metal cans would be 0.75 mole O_2 per mole Fe. With roughly 3.4 kg of Fe (56 $g \cdot mole^{-1}$) the amount of O_2 used would be approximately 45 moles $O_2 \cdot bag^{-1}$. The effect of oxygen demand from corrosion will be considered later under basin-wide scenarios.

Degradation of the glass waste stream will occur mainly through the dissolution of its constituent oxides. The susceptibility of glass to fatigue fracture under static loading may also lead to physical degradation as well as an enhanced solubilization of silica within the fractures (Glass products and production, 1974), particularly at greater depths. Dissolution of glass, mainly SiO_2, will occur because the world's oceans, including Special Areas, are undersaturated with respect to silica. The time constants for these reactions, although poorly known, are exceptionally long which can be attested to by the fact that the there are large silicon-rich deposits distributed throughout much of the world's oceans when theoretically, there should be no Si present. In general Si-rich sediments are found underlying regions of high primary productivity where the flux of siliceous material to the sea floor is high and where burial rates are high. This suggests that the kinetics of reaction are sufficiently slow enough, relative to burial rates, to allow the material to become incorporated into the sea floor. It is therefore likely

that any input of glass from the waste stream will be incorporated into the sea floor in a state not much different than its original form.

Biological Effects Levels. Biological effects tests of the metal and glass waste stream were conducted on test solutions that were made by soaking shredder material in seawater for 1.5 hr. The tests were based on dilutions of leachate concentrations of 25% and/or 5% (metal/seawater by weight) although the full matrix of tests has not yet been completed (see table 9-3). Only one of the two phytoplankton species showed a dose-response at the 5% leachate level while shrimp, fish, and bacterial test organisms showed no response (i.e., EC_{50}, IC_{50}, or LC_{50} values were greater than 100% of the test solution). *G. polyedra* showed a dose-response with an IC_{50} of 19%. At the 25% test concentration, both phytoplankton species showed a dose-response with *S. costatum* showing an IC_{50} of 59% and *G. polyedra* showing an IC_{50} of 19%. An NOEC for the 25% elutriate test was 25% for *S. costatum* and 6.25% for *G. polyedra*. Fish and shrimp were not tested at the 25% level.

The results here indicate that there can be acute effects from the metal and glass waste stream at concentrations equivalent to roughly 5% (waste/water) by weight. These effects disappear below about 1% (waste/water) by weight. The organisms showed these effects when exposed over a time period of 1 to 4 days. Although the cause of the biological effects were not determined, sensitivity of the test organisms to metals leaching into the water is likely. It is highly improbable the organisms will be exposed to these concentration levels during the time it takes a bag to sink through the water column. Even when sinking to a maximum depth of 7700 m as is found in the Caribbean, the expected exposure time in the water column is less than 5 hours. Thus, organisms in the water column will not be exposed sufficiently to cause effect. Once the bags reach the bottom, the duration of exposure should be sufficient to consider dose-response effects. These will be addressed later under sea floor processes.

Another qualitative assessment of biological effects can be obtained from the long-term monitoring study performed in San Diego Bay. The observation that the solid metal material was highly colonized (figure 9-8) and that the species diversity was also quite high suggests that the material acts as a good substrate for many organisms and may not actually be harmful to them. This suggests that while the metal/glass waste stream may have some negative effects under certain laboratory conditions, these might not be reached under natural conditions.

In summary, the rates at which the shredder bags sink through the water column suggests that sea floor processes will be dominant in controlling their fate and effects. The process of shredding appears to be superior to that of compacting from a sinkability standpoint. The dominant component of the waste stream is tin-coated steel cans. Glass was next abundant while aluminum made up only a small fraction of the total. Corrosion of the metal is likely to occur over a period of several years, although the rates can be highly variable. However, corrosion is not a removal process, but rather is a mechanism for changing the aesthetic nature of the waste stream from a component of litter to a component more typical of sedimentary materials. Seawater leaching of the metal/glass was shown to cause some effects under laboratory conditions. Effects in the water column are unlikely because of the limited time of exposure in the water column. However, these effects need to be considered for the longer exposures expected at the sea floor. The diversity and abundance of organisms that colonized the metal/glass material on the bottom of San Diego Bay suggests that conditions that caused negative effects in laboratory tests may not occur under natural conditions.

Water Column Processes, Fate, and Effects

Because shredder bags sink quickly through the water column, processes in the water column will be quite limited, ranging from seconds to several hours. The processes likely to be important in the water column are therefore confined to lateral transport and the potential for the materials to impact the coastal zone as shore litter. Unless the bags break open, the exposure time to organisms in the water column are likely too short to be of consequence. The following discussion thus focuses on lateral transport, its consequence on the distribution of bags reaching the bottom, and the potential for reaching the shore.

Lateral Transport. Lateral transport of the bags during descent is strictly a function of water current speed and water depth because estimates of the hydrodynamic drag on the bag suggest that it becomes fully entrained in the current flow almost immediately. Also, any momentum imparted by the foreword motion of the ship would be quickly dissipated when the bag hits the water. Using the average sink rate of 0.54 $m \cdot s^{-1}$ and a nominal current condition of 0.5 $m \cdot s^{-1}$, the lateral displacement of the bags in water depths of 50 to 5000 m, which are average depths found in the North Sea and Antarctic for example, would be 46 to 4680 m from the drop point. These numbers would obviously change under differing flow conditions. Higher flows of up to 1.5 $m \cdot s^{-1}$ kts may be found in near-surface waters as a result of wind-driven conditions, such as those found in the Baltic Sea, or in constricted regions with tidal current flows up to 4 kts, such as those found within narrow straits of the Mediterranean (Defense Mapping Agency, 1988 and 1990). Maximum displacement in the Baltic under these flow conditions would be about 1.3 km using a maximum depth of 460 m. In the Mediterranean case, the high flows tend to occur in locations that are typically less than 500 m in depth and thus the displacement would be roughly 2 km. In both cases, the lateral transports are still reasonably small because the transport occurs over a short time interval. Although lateral transports are higher in these high flow areas, their likelihood of occurrence is much lower because of their limited spatial and temporal distribution.

Areal Distribution. The effect of lateral transport increases the potential areal distribution of bags impacting the bottom. Estimates made previously for the discharge area were based on no lateral transport of bags away from the ship track. The dispersal of bags away from a ship's trackline would increase the area potentially impacted by the bags. However, this would also serve to minimize the density of the impact and reduce the surface area ratio by effectively increasing the swath width. Thus, the most conservative estimates of surface area coverage were already made using a no lateral transport scenario.

Coastline Impacts. Another aspect of transport is whether or not the bags are likely to reach the shoreline during discharge and become a potential litter issue. Using the same parameters as discussed previously for the potential of onshore flow of pulper material, i.e., slope of 0.2% and onshore flows up to 1 $m \cdot s^{-1}$, it can be seen from figure 12-21a that bags discharged 22 km (12 nmi limit) from shore will not reach any closer than 21.8 km from the shore. The bags will be deposited at water depths very similar to those at which they are discharged e.g., if bags are discharged in water depths of 200 m, they will be deposited in a water depth of roughly 195 m (figure 12-21a). From this analysis it can be safely assumed that the bags, if discharged at distances greater than 22 km from shore under typical shelf flow conditions, will not likely be a source of coastal litter. When considering this same issue for discharge at 5.6 km (3 nmi limit), the closest point of deposition will be about 5.2 km from shore, again at depths similar to those of discharge (figure 12-21b). Again the shredder bags appear to be unlikely to reach shore and become a source of litter.

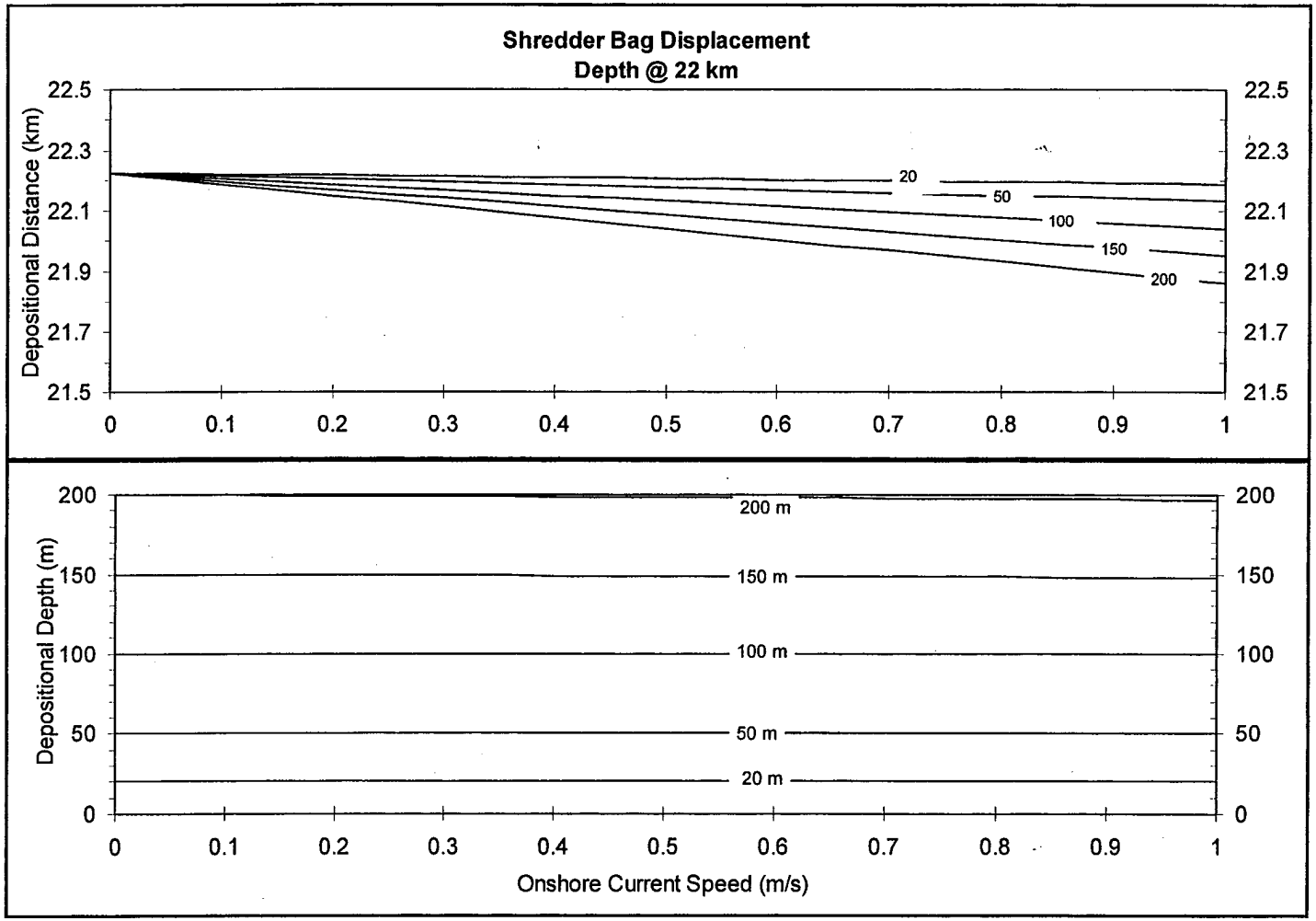

Figure 12-21a. Pattern of shredder bag discharge deposition at various depths and distances for the 22 km discharge case. Shown are the depths and distances from shore of shredder discharge deposited under a range of onshore velocities (u) and bottom slopes.

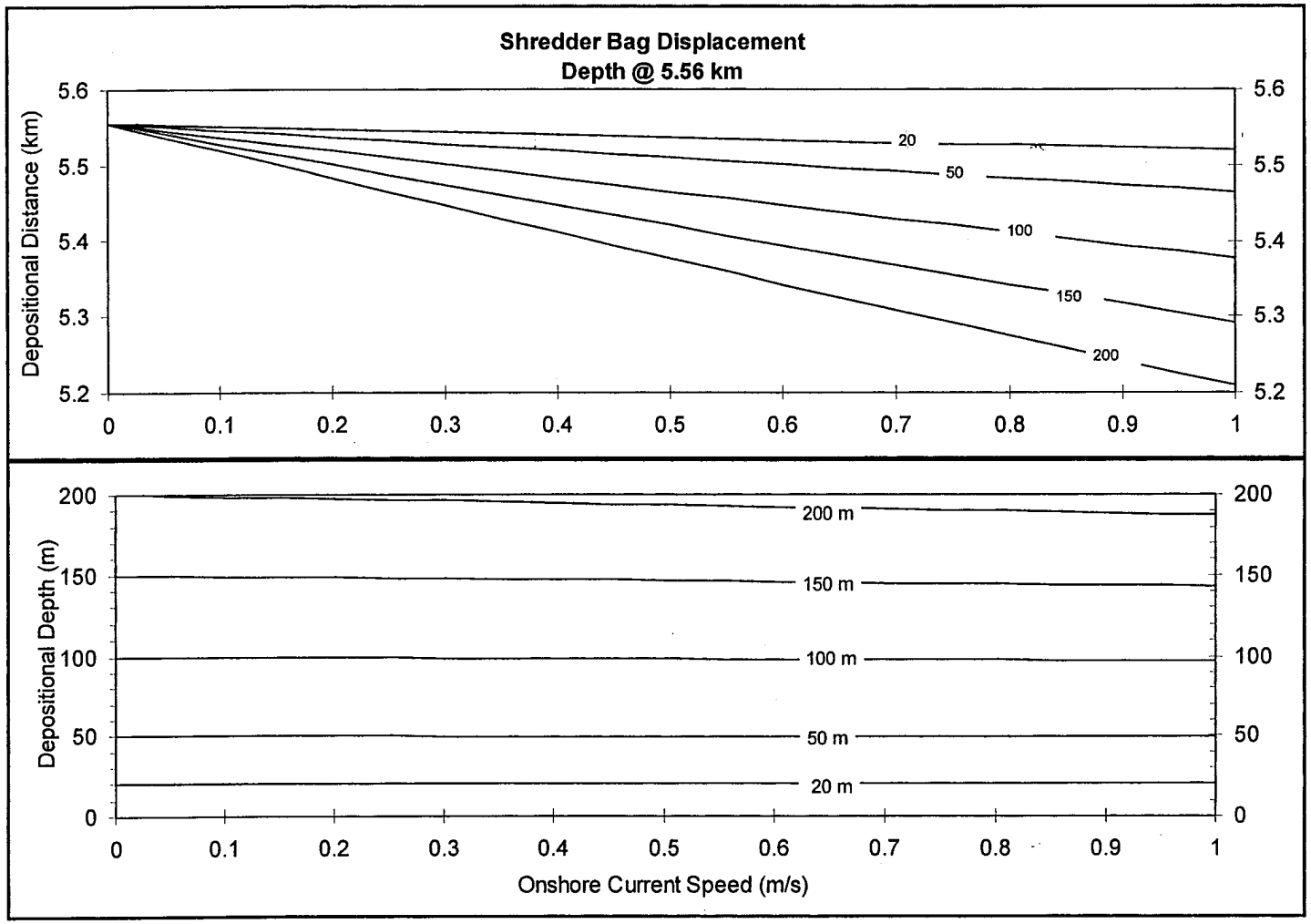

Figure 12-21b. Pattern of shredder bag discharge deposition at various depths and distances for the 5.6 km discharge case. Shown are depths and distances from shore of shredder discharge deposited under a range of onshore velocities (u) and bottom slopes.

In summary, the fate and effects of the metal/glass waste stream will not be important in the water column. The high sinking velocity minimizes the time bags spend in the water column, thus lateral transport will be somewhat limited and will mainly be dependent on water depths. Discharge of the metal/glass waste stream outside the 22 or 5.6 km limits should preclude this waste stream from being a source of coastal litter.

Sea Floor Processes

Based on this study, the shredded metal and glass waste stream components will settle rapidly to the sea floor. The deposition of these materials onto the sea floor will be unevenly distributed because of the discrete nature of the discharge. However, the material will be subject to processes that will lead to its redistribution over time. These include burial through vertical mixing and natural sedimentation, corrosion, resuspension, and transport. The redistribution will result in a dilution of these materials with naturally occurring sedimentary materials thereby reducing the impact from both a biological effects and aesthetics point of view. The following is a discussion of the important processes that will control the fate and effects of the shredded material once it reaches the sea floor.

Redistribution on the Sea floor. Burial of the bag material and vertical mixing by either physical, chemical, or biologically mediated processes will serve to redistribute and dilute it within the vertical sediment column over time. Although the material starts out as large particles contained within a bag, the bag will eventually degrade and break open as was observed in the long-term monitoring study. Individual pieces will eventually integrate into the sediment column through sedimentation and vertical mixing, although the initial size of the material may limit the effects of vertical mixing.

As seen previously in table 12-6, the two elemental constituents of the waste stream that are significantly enriched over typical oceanic sedimentary values are Fe and Sn. Therefore, except for Fe and Sn, the impact of the bags does not significantly alter the general chemistry of surficial sediments. While not necessarily pleasing from an aesthetic point of view, the shredded metal and glass waste stream is composed of materials that are not dramatically different from those occurring naturally on the sea floor. Thus, it is dilution of the Fe and Sn with background sedimentary materials that needs to be considered.

The time scale for vertical mixing of sedimentary materials is relatively long. Even using maximum biodiffusion coefficients for particle mixing rates due to bioturbation of 0.038 $cm^2 \cdot yr^{-1}$ for near shore sediments (Berner, 1980), the time to vertically mix down a few centimeters is over 300 years. This implies that the concentration of Fe and Sn based will be diluted very slowly in the vertical sediment column through vertical mixing. However, an additional way in which the metal and glass material will be integrated within the sediment column will be through natural sedimentation.

As mentioned previously, natural sedimentation rates typically vary from about 1 to 20 $mm \cdot 1000\ y^{-1}$ in the deep sea to >1000 $mm \cdot 1000\ y^{-1}$ on the shelf and coastal regions (Seibold and Berger, 1982; Kennett, 1982). Using a value of 1 $mm \cdot y^{-1}$ as might be found in the Baltic Sea (Voipio, 1981) and a metal can wall thickness of 0.025 mm, burial would take only a couple of weeks. But the material in the bags does not consist of thin flat surfaces. Rather, they are twisted and bent into shapes having overall thicknesses more on the order of a few centimeters. The time scale to completely bury pieces of metal of these dimensions at this sedimentation rate

would take roughly 30 years. A realistic time scale for burial rates in Special Areas would include a range of 1 to 300 years using common values for shelf sedimentation rates of 0.1 to 10 $mm \cdot y^{-1}$ (Seibold and Berger, 1982).

As stated earlier, corrosion is not a removal process but is one which transforms the metal from its original size and shape into smaller particles that make it less distinguishable from background sediment. The time scale for complete degradation of the material is on the order of years to tens of years depending on the conditions of deposition. This transformation will proceed once the material is deposited and all the while it is being buried and vertically mixed into the sediment column. The transformation to smaller and smaller particles will serve to enhance the integration of the material into the sediment column. The degradation of the materials into smaller particle sizes also has a potential impact on resuspension and transport.

It is expected that resuspension and transport is likely to be important in redistributing these materials only after there is sufficient time for degradation to minimize particle sizes. Other than in conditions of exceptionally high flow, such as those that might occur during storm surge or in constrictions with strong tidal currents, it is unlikely that the material would be moved over significant distances. Quantifying this effect is difficult because of the inability to the determine a reasonable hydrodynamic size to use in the estimation. Once the material has corroded into particle size fractions more closely resembling the rest of the sediment, the material can be expected to be resuspended and transported under similar criteria as shown in figure 12-13. Preliminary laboratory flume test results suggest relatively high current velocities (0.3 $m \cdot s^{-1}$ measured at the seabed) would be required to move these materials along the sea floor. These initial tests will be fully investigated in future studies.

Exposure and Effects on the Sea Floor. As discussed previously, the laboratory bioassay results are useful in understanding the potential effects on organisms in the field only when actual exposure (magnitude and duration) levels in the field are determined. In the case of the shredder bag waste stream, the bags are likely to settle onto the bottom without producing any effects within the water column. Once deposited on the bottom any solubilized material that would cause effects would be quickly diluted by the surrounding water. A conservative approach to determine the maximum potential exposure concentration is to consider that the metal/glass material is a constant point source of soluble "elutriate" within a fixed volume of water. Using a half-sphere to estimate a volume envelope, an equivalent elutriate concentration can be computed as a function of distance out from the bag center assuming a confined volume and an internal bag volume of 60 L. The results of this calculation are shown in figure12-22.

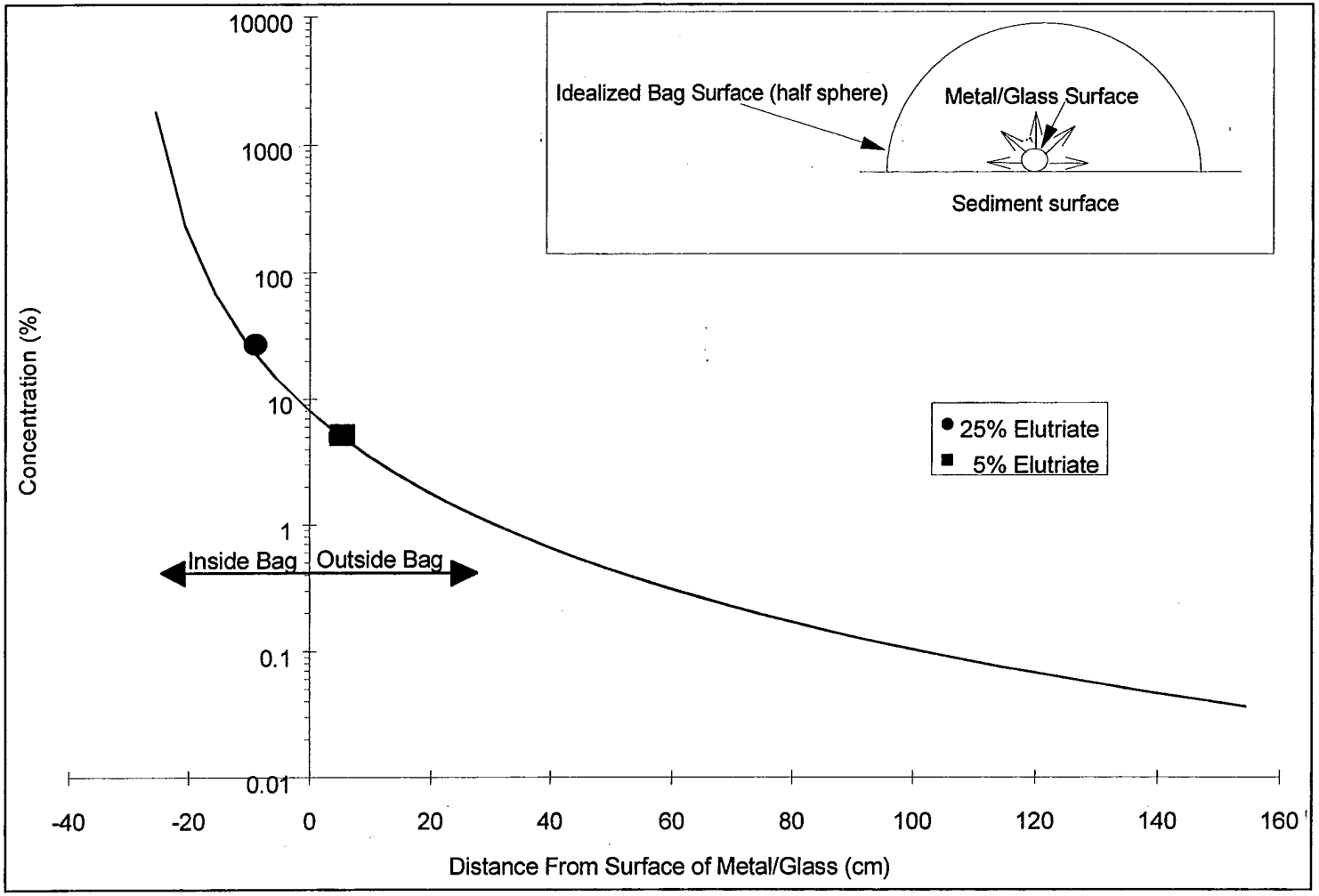

Figure 12-22. Concentration (mass of shredded material/mass of water) computed as a function of distance out from the center of the bag assuming a confined volume presuming a half-spherical bag shape.

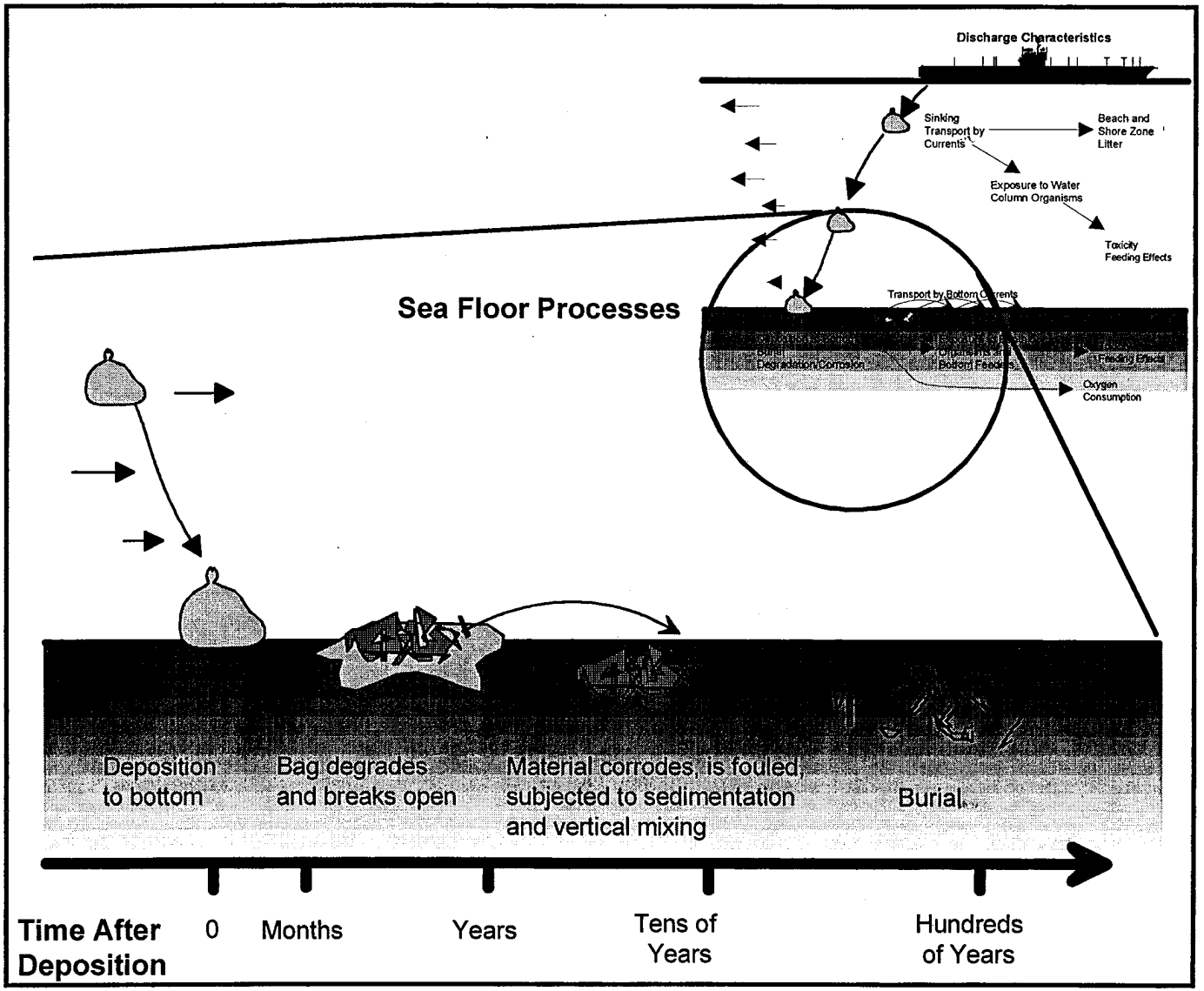

Figure 12-23. Primary processes and estimated time scales for the fate of shredder bags and contents.

As can be seen in figure 12-22, the concentration level at the idealized surface of the bag is equivalent to an 8% shredder/water mixture. The 25% elutriate concentration level tested in the biological interactions portion of this study would be confined to the internal volume of the bag, while the 5% test solution would be found just outside the bag volume. All tests, except for those of *G. Polyedra,* showed a NOEC below that which would be found at the surface of the bag. The results for *G. Polyedra* showing a NOEC of 6% (25% test solution) would be reached less than 5 cm from the outside surface of the bag. Based on laboratory tests and a conservative estimation of exposure concentration, effects would only be potentially observed within or near the bag surface.

The high degree of biofouling of the shredded metal and glass surfaces indicates, qualitatively, that the material was benign to a wide range of organisms. Biofouling can also have effects on the redistribution of the material. First, biofouling can affect the rate of degradation by altering the surface conditions, although whether this increases or decreases the rate will be dependent on a variety of depositional conditions. Secondly, the growth serves to increase the effective size and surface area of the material, and processes such as vertical mixing, resuspension, and burial become less quantifiable.

Fate on the Sea Floor. Once discharged from a ship, the metal and glass are, in essence, deposited and accumulated on the sea floor forever. Although degradation changes its form, the material remains. Thus, the main consideration of the sea floor are the rates at which these transformations occur and the time frame and spatial scales for which biological effects are important. These processes and time scales are shown schematically in figure 12-23.

Because of the high sinking velocity of the bags, deposition to the bottom depends mostly on the rate and area of discharge. Once on the bottom, physical and chemical degradation of the materials begin, and natural sedimentation will begin to cover the bag. Biological colonization will likely also begin shortly after deposition, although the burlap bag probably impedes this process at first. Eventually, on the order of months to years, the bag will break apart and the individual components within will be subjected to burial by sedimentation of natural materials, vertical migration through the upper sediment as a result of bioturbation, and biofouling. Further corrosion will result in a change in size and shape of the materials as will biofouling. These processes will likely be important over time scales of years to tens of years. Eventually sedimentation and bioturbation will effectively bury the material within the sediment column both diluting and removing the material from sight. These processes are expected to occur on time scales of ten to hundreds of years particularly in areas of low sedimentation and in zones of low biological activity such as anoxic environments.

In summary, the shredded metal and glass waste stream components deposited on the sea floor will be unevenly distributed because of the discrete nature of the discharge. The material will be subject to processes that will lead to its redistribution and burial over time. The compositional makeup of single bags are enriched with Fe and Sn relative to background sedimentary materials. This enrichment can be minimized by redistributing the material over a larger area than that of the bag. The processes that impact the fate of the material on the sea floor include burial, degradation, vertical mixing in the sediment column, resuspension, and lateral transport. The time scales for these processes can be relatively long, ranging from months to hundreds of years for complete burial and degradation. The exposure levels that were observed to cause a biological response in laboratory tests would be contained only within the volume of the bag, although the fact that biofouling occurs on the metal/glass surfaces qualitatively suggests that the material may be benign to a wide range of organisms.

Operational Scenarios

Table 12-7. Summary of estimated daily shredder waste discharge rates of the various ships making up a Battle Group and Amphibious Ready Group.

Ship Group	Ship	Number of Ships	Complement	Loading ($kg \cdot man^{-1} \cdot day^{-1}$)	Metal and Glass Input ($kg \cdot day^{-1}$)	($bags \cdot day^{-1}$)
BG	CV/CVN	1	6200	0.25	1550	323
	CG 47	2	409	0.25	205	43
	DD 963	1	396	0.25	99	21
	AOE 1	1	719	0.25	180	38
	FFG 7	1	220	0.25	55	12
			Total Daily Input Rate =		2088	437
ARG	LHD 1	1	3151	0.25	788	164
	LSD	1	852	0.25	213	44
	LPD 4	1	1487	0.25	372	78
	FFG 7	1	220	0.25	55	12
	AOE 1	1	719	0.25	180	38
			Total Daily Input Rate =		1607	336
			Combined Total Daily Input Rate =		3695	773

BG = Battle Group
ARG = Amphibious Ready Group

Although it appears that the important spatial scale of the shredded metal and glass waste stream is the size of the bag, the impact of multiple inputs over longer than daily time scales needs to be considered as well. In this section, the potential effects of a hypothetical, multiship operational scenario is analyzed using the same operational conditions that were used for the pulped paper waste stream. The scenario uses both the BG and ARG operational profiles on 6-month deployment within an operational area of $3.43 \cdot 10^4 km^2$ (100 by 100 nmi area). Ships included in the BG and ARG and their estimated daily shredded waste discharge rates are summarized in table 12-7. Differences in the conceptual model for the shredder from that of the pulper exist because of the lack of impacts in the water column and the fact that the bags are deposited quickly on the bottom.

The input rate of metal and glass was taken to be the average daily combined discharge from all of the ships operating in the region. The input was assumed to be spread evenly throughout the operational area and that lateral transport does not move the bags outside the operational area. The combination of one BG and one ARG results in an average input rate of about 3700 $kg \cdot d^{-1}$ or about 775 $bags \cdot d^{-1}$. Over a 6-month duration the amount deposited on the bottom is 675 mt or $1.4 \cdot 10^5$ bags. This number of bags has a surface area of $2.8 \cdot 10^4 m^2$ using a 2000 cm^2 bag frontal area. Over a deployment area of $3.43 \cdot 10^4 km^2$ the bags will cover $8.8 \cdot 10^{-7}$ (nearly 100 parts per million) of the bottom surface area. This can be compared to the daily discharge coverage computed earlier for a single ship discharge scenario which gave a bag surface area to bottom surface ratio of 10 to 20 parts per million. At this rate, the operation would need to carry on for roughly 5000 years in order to completely cover the sea floor with bags.

The effect of operating a large number of ships in a limited region as described above does not load the sea floor with bags at a significantly higher per unit area rate than already described for a single swath discharge. Any biological effects would therefore still related to any that would be found within or near a single bag. These results could be altered if operational practices acted to concentrate the discharges in particular areas that are significantly smaller than an operational area. This suggests that operational discharge practices should be minimized in areas that are constantly traveled such as before and after leaving Navy ports.

Basin-Scale Scenarios

In this section the total yearly input of metal and glass from all Navy shipboard operations is considered for each Special Area. The purpose of this analysis is to determine the contribution of this waste stream relative to other sources in each Special Area and to look at how this might impact each region as a whole. Annual discharges are considered as well as estimates of loadings that would occur under near-steady-state conditions.

Table 12-8. Annual mass loading estimates of the shredded metal/glass waste stream and Fe and Sn components into Special Areas by U.S. Navy ships. The inputs of the Fe and Sn are compared to river inputs to Special Areas using particulate loadings (tables 6-1 to 6-4) and concentration estimates of Chester, 1990.

	Baltic	North	Caribbean	Mediterranean
Total Waste Stream Loading (mt)	5.8	8.1	638	859
Total Waste Stream Loading (bags)	1200	1700	$1.3 \cdot 10^5$	$1.8 \cdot 10^5$
Waste Stream Fe Loading (mt)	4.1	5.7	446	601
Waste Stream Sn Loading (mt)	0.04	0.06	4.5	6.0
Riverine Fe Loading (mt)	$2.4 \cdot 10^5$	$9.6 \cdot 10^5$	$1.5 \cdot 10^7$	$1.7 \cdot 10^7$
Riverine Sn Loading (mt)	10	40	625	708
U.S. Navy/Riverine Ratio (ppm)	17	6	30	35
U.S. Navy/Riverine Ratio (%)	0.4	0.2	0.7	0.8

As was done previously, the CNO EMPSKD database was reviewed to determine the overall input of shredded metal and glass in each Special Area. Ship type, complement, and number of ships present were summarized for 10 years of ship movement data from 1984-1993 to compute average man-days per year in each Special Area (table 7-1). From this summary and estimated generation rates of 0.25 $kg \cdot d^{-1} \cdot person^{-1}$ (NAVSEA, 1993) the mass loading of shredded metal and glass in each Special Area ranges from 5.8 mt in the Baltic Sea to 859 mt in the Mediterranean (table 12-8). The number of bags dumped in each area on a yearly basis would thus range from 1200 to $1.8 \cdot 10^5$ (table 12-8). Based on a waste stream composition of Fe that is 70% of the total shredder waste stream input (Fe is 98% of the steel cans which are 71% of the total waste stream) and Sn which is 0.7% (Sn is 1% of steel cans which are 71% of the total waste stream) of the total, the annual loading of these components in Special Areas ranges from 4.1 to 601 mt (table 12-8).

Other significant sources of metal and glass components to Special Areas would include rivers, atmospheric fallout, industrial/sewage outfalls, and hydrothermal vents. For the most part, many of the components that make up the metal and glass waste stream are found as both dissolved and

particulate phases in river water and industrial effluents, as particulates in the atmosphere, and as dissolved constituents of hydrothermal vents. On a basin-wide basis, rivers are probably the dominant source of these materials in Special Areas even though some industrial and/or sewage inputs might be more important locally. Although hydrothermal waters have concentration levels as great or greater than those found in rivers, the source magnitudes are poorly known.

No literature values were found for riverine influx of Fe and Sn to Special Areas, the two elements in the shredder waste stream significantly enriched relative to typical sediments. However, Chester, 1990 has estimates for typical Fe and Sn concentrations measured in the particulate and dissolved phases of rivers as well as for crustal and sediments. Considering only the particulate phase of rivers, a typical concentration of Fe is 48 $mg \cdot g^{-1}$. Although Chester, 1990 gives no typical value for Sn in river particulates, crustal and sedimentary concentrations are about 2 $ug \cdot g^{-1}$. Using the value for suspended matter inputs from the major rivers of the Special Areas (tables 6-1 to 6-4), the annual input of Fe from these sources ranges from $2.4 \cdot 10^5$ mt in the Baltic Sea to $1.7 \cdot 10^7$ mt in the Mediterranean Sea (table 12-8). For Sn, the numbers range from 10 to 708 mt, respectively (table 12-8).

A comparison of the annual discharges of Fe and Sn from the shredded metal/glass waste stream from U.S. Navy ships into Special Areas with those amounts entering naturally from rivers indicates that the waste stream inputs are small fractions of the natural inputs. For Fe the ratio of waste stream to riverine inputs is in the range of 17 to 35 parts per million while for Sn these numbers range from 0.4 to 0.9% (table 12-8). In other words, it would take about 30,000 years of shredder bag inputs to match the annual discharge of Fe from natural sources into these areas and about 100 years to match it for Sn.

The annual loadings can also be compared to inputs from industrial sources where available. Based on the work of Lithner (1974), the annual discharge from a single metal works at Rönnskär on the Bothnian Bay was 3 to 500 mt·Fe·yr-1 and 1 mt·Sn·yr-1. These compare to annual loadings from all Navy ships of 4 mt·Fe·yr-1 and 0.04 mt·Sn·yr-1. This suggests that the shredder loading from all Navy vessels is on par or less than the loading from a single industrial source in the Baltic.

All the material will be deposited onto the sea floor. To determine how much of the sea floor would be covered on a regional basis, the number of bags discharged annually along with their frontal surface area are compared to the surface area available in each Special Area (tables 6-1 to 6-4). The ratio of total bag coverage to total sea floor area computes as follows: Baltic Sea $6 \cdot 10^{-10}$ (0.6 parts per billion), North Sea $6 \cdot 10^{-10}$ (0.6 parts per billion), Caribbean Sea $1 \cdot 10^{-9}$ (1 part per billion), and Mediterranean Sea $1.4 \cdot 10^{-9}$ (1.4 parts per billion). In other words, it would take nearly a billion years of dumping to completely cover the sea floors of these Special Areas with bags.

Another way to look at sea floor coverage is to consider the material as if it were evenly distributed over the sea floor rather than locked up in discrete bags. Using an average container thickness of 0.0254 cm, a density of 6 $g \cdot cm^{-3}$, the input rates discussed above, and the sea floor areas from tables 6-1 to 6-4, the ratio of area covered to total area measured this way is: Baltic Sea $1 \cdot 10^{-8}$ (10 parts per billion), North Sea $9 \cdot 10^{-9}$ (9 parts per billion), Caribbean Sea $1 \cdot 10^{-7}$ (100 parts per billion), and Mediterranean Sea $2 \cdot 10^{-7}$ (200 parts per billion). These numbers indicate that even if the material was spread out evenly over the sea floor, it would still take nearly 5 million years to cover the sea floor.

Table 12-9. Estimate oxygen utilization for the complete corrosion of the annual shredded metal waste stream into each Special Area. The estimates are based on annual inputs and general stiochiometry for oxidation. The standing stock of oxygen in each area is based on a seawater oxygen concentration of 5 $mL \cdot L^{-1}$.

	Baltic Sea	North Sea	Caribbean Sea	Mediterranean Sea
Total oxygen utilization (mt)	1.7	2.4	187	256
Oxygen standing stock (mt)	$1.5 \cdot 10^{8}$	$3.6 \cdot 10^{8}$	$4.4 \cdot 10^{10}$	$3.6 \cdot 10^{10}$

As discussed previously, corrosion of the metal material will result in oxygen utilization in a stoichiometry that will be roughly 45 moles $O_2 \cdot bag^{-1}$. The total oxygen utilization that can be expected to occur on a basin-wide basis would therefore range between 1.7 mt found in the Baltic Sea and 256 mt in the Mediterranean Sea (table 12-9). The standing stock of oxygen in each of the Special Areas, estimated using a typical oxygen value of 5 $mL \cdot L^{-1}$, ranges from $1.5 \cdot 10^{8}$ in the Baltic Sea to $2.5 \cdot 10^{10}$ in the Mediterranean Sea (table 12-9). There is at least a billion times more oxygen available in each of the seas than would be required to completely oxidize all the metal discharged annually. It is therefore highly improbable that the discharge of shredded metals by U.S. Navy operations will have any impact on the oxygen budget of Special Areas. Localized effects however, cannot be ruled out. This is particularly true given the relatively long time it takes for corrosion of the metals to reach completion.

Another question to consider for basin-wide effects is how much of the inputs of shredded material in the U.S. Navy waste stream will accumulate in each basin over time. This can be done using the concept of steady state in which the inputs will be balanced by removal processes. Comparing estimated input rates for U.S. Navy discharges of shredded metal to each area with corrosion rates will provide an estimate of the assimilation of the material into the sea floor. As such, this will be an appraisal of how much of the material is ostensibly altered from being a component of litter to being integrated into the sea floor similarly to other sedimentary material. Under steady-state conditions, the removal process balances the inputs according to:

$$M = \frac{I}{D}(1 - e^{-Dt}) \qquad \text{(Eq. 12-11)}$$

Where:
M = accumulated mass on the sea floor
I = mass input rate
D = corrosion rate (removal rate)
t = time

This condition cannot truly be reached because the amount corroded is a fixed fraction of the amount available and as inputs increase so do the losses (i.e., time would have to be infinite). Thus, steady state can be estimated as it is approached over time e.g., at times equivalent to 1/e (63%), $1/e^2$ (85%), or $1/e^3$ (95%).

Table 12-10. Steady state loading estimates of Fe and Sn in Special Areas. Estimates are made using equation 12-11 for amount of time to reach 95% of steady state which for Fe is 7.5 years and for Sn is 0.18 years. All values are in metric tons.

	Baltic Sea	North Sea	Caribbean Sea	Mediterranean Sea
Fe				
U.S. Navy Annual Input	4.1	5.7	446	601
Steady State Accumulation	9.7	13.5	1060	1427
Sn				
U.S. Navy Annual Input	0.04	0.06	4.5	6.0
Steady State Accumulation	0.002	0.003	0.26	0.34

Considering this equation for Fe and Sn for nominal conditions of inputs and corrosion rates for each area (table 12-10), the amount accumulated in each area for a time equivalent to 95% of steady state will range from 6.5 mt Fe in the Baltic Sea to 950 mt Fe in the Mediterranean, while for Sn the range is 0.04 mt to 6.3 mt, respectively (table 12-10). The time to reach these conditions for Fe is 7.5 years and is 0.18 years for Sn. These results suggest that the accumulation of metal materials, as litter, will be less than three times the annual rate and still a very small fraction of the total inputs of these components from natural sources.

In summary, the annual input of the shredded metal/glass waste stream from U.S. Navy ships operating in Special Areas constitutes a tiny fraction of basin-wide inputs. It is estimated that it would take hundreds to billions of years of U.S. Navy discharges to match a single year discharge from other basin sources such as rivers or industrial discharges. The amount of material discharged annually by U.S. Navy ships would cover only a tiny fraction (billionths) of the sea floor. Based on a steady-state analysis of the inputs and corrosion rates, the amount accumulated on the sea floor as a litter component would be roughly equivalent to about three years of discharges. From a basin-wide perspective, there is at least a billion times more oxygen available in Special Areas than is needed to completely oxidize the annual discharge of metal components of the waste stream implying that it is improbable that the discharges will have any impact on the oxygen budget of any of the seas.

13.0 CONCLUSIONS

The following conclusions are drawn from the pulped and shredded waste stream fate and effects analyses. The overall environmental impact of the pulped and shredded waste streams appears to be benign to minimal. Input levels are at or below background levels and exposure levels are far below those found to cause effects in the laboratory. The techniques of pulping and shredding are an improvement over existing methods. The size fractions inherent in the pulper are beneficial for rapid descent of the material to the benthos. Likewise, the shredded material packaged in burlap bags is optimized for rapid descent. In each case the sea floor processes are the dominant ones, and there is no evidence that exposure levels of either waste stream in the benthos will cause a negative environmental effect. In addition, the pulped waste stream has the added advantage of being discharged into the wake, which will greatly increase the dilution of the material. Since wake dilution is far dominant to ambient dilution, and is independent of Special Area conditions, it can easily be controlled by vessel operations.

Pulped Waste Stream

Discharge Conditions. The pulped waste stream discharge will vary significantly depending on generation rates, number of pulpers, pulper processing rates, operational practices, ship speed, ship class, and discharge location. In general, the resulting initial discharge plume will include a solids phase consisting of the pulped paper and a liquid phase containing soluble fractions of the waste stream which have partitioned during the pulping process. The percentage of solids in this slurry is estimated to be less than 1% by weight maximum, and more likely to be 0.3 to 0.5% operationally. A typical plume will extend over an area of up to several hundreds of kilometers in length, several to hundreds of meters in width, and several of meters in depth. The material is likely to be significantly diluted by wake action of the ship independent of exact discharge location, however the actual degree of dilution may have some dependence on the location of the overboard discharge port.

Waste Stream Characteristics. The pulped paper waste stream is primarily composed of organic material in the form of cellulose (~92%) with possibly an 8% fraction of additives including fillers, dyes, and inks. The majority of the mass is contained in relatively few large particles which tend to sink rapidly (~85% by weight will sink at ~820 m d^{-1}, ~12% will sink at ~6 m·d^{-1}, and the remaining fraction of ~3% will be subject to extended water column degradation and surface microlayer accumulation). Of the sinking fraction, some degradation of the material will also occur in the water column. The nutrient loading from the waste stream is low compared to other natural and anthropogenic sources of organic material. No toxic chemicals were detected in the waste stream at levels which would be expected to induce effects in marine organisms. The cellulose material in the waste stream is refractory as indicated by the low BOD_5 levels and the low degradation rates. Conservative estimates suggest that biological effects should be negligible for concentrations less than about 1 mg·L^{-1}. Higher concentrations may cause deleterious effects if sustained for periods of hours to days (based on the testing period). It is also likely that sublethal effects such as feeding inhibition would only be of transient nature as demonstrated by zooplankton and sardine recovery tests.

Water Column Processes. Processes which will influence the fate of the pulped material in the water column are expected to include wake dilution, ambient dilution, settling, transport or lateral advection, limited surface microlayer accumulation, degradation, and biological interaction. An analysis of water column processes suggests that the primary fate of pulped

paper waste entering the water will be deposition on the sea floor. Of the particulate phase material entering the water column, ~95% can be expected to reach the bottom while ~5% could be degraded in the water column, and a small fraction <0.001% could partition to the microlayer. Highest exposures will be found in the wake just after discharge, and modeling results indicate worst-case peak concentrations of about 0.17 $mg \cdot L^{-1}$ (based on a dilution of 10^{-5} in the wake within seconds after discharge). This concentration is below the level at which biological effects were observed in any of the wide range of test organismsins. In the unlikely event of a static discharge of the particulate phase from stationary ships could cause transient effects on the feeding success of surface feeding bait fish such as the sardines tested in this study. The duration of this impairment would not be expected to exceed about 2 hours based on the rapid settling of the material, and laboratory tests indicate that feeding success returns to normal after removal of the pulped paper. No effects would be expected from the liquid phase generated during the pulping process. Effect levels for the liquid phase were above both the wake and static discharge exposure levels. Localized increases in productivity that might contribute to eutrophication appear to be several orders of magnitude below background levels. Lateral transport of the material towards the shore should also be minimized by the rapid settling of the majority of the waste stream. Under strong onshore current conditions (1 $m \cdot s^{-1}$), most of the pulped paper discharge outside the 22 km (12 nmi) discharge limit could be expected to settle to the bottom about 12 to 21 km offshore in 20 to 120 m of water, depending on bottom topography.

Sea Floor Processes. Processes which will influence the fate of the pulped material on the sea floor are expected to include deposition rates, resuspension, transport, burial, degradation, and biological interactions. The analysis above suggests that deposition rates will be controlled primarily by the number of discharge events at a given location, and the depth dependent in ambient mixing of the material. Based on particle characteristics, lateral redistribution of the material due to resuspension and transport would appear to be likely in moderate to high energy environments such as coastal and shelf regions, and less likely in deep basins and quiescent regions where bottom currents are less than ~20 $cm \cdot s^{-1}$. Vertical mixing and burial of the pulped material will be determined by rates of natural sedimentation and bioturbation, with bioturbation being the primary controlling mechanisms except in regions near large sources of particulate input such as river mouths. Long term reduction of pulped material may occur through microbial degradation over periods of 1000 to 3000 days assuming aerobic conditions prevail. In anoxic basins such as exist in the Baltic, degradation rates may be reduced, and vertical mixing rates due to bioturbation may also be limited. Peak exposure levels in the sediment will most likely not exceed levels shown to be innocuous to representative benthic organisms, even assuming deposition from 100 to 1000 ships at the same location.

Operational Scenarios. Hypothetical operational profiles for four Special Areas were investigated using a simple steady-state box model. The overall partitioning of the material was controlled primarily by settling and advection. Of the total material input into the area, about 71% could be expected to settle to the sea floor within the same area, while the remaining ~29% would be advected out of the operational area. The results suggest that the operation of multiple ships within a limited area would not produce concentrations of pulped paper in the water column or on the sea floor which are greater than local exposures due to a single ship. Thus, significant biological effects would not be expected under operational scenarios such as those described above.

Basin Scale Scenario. An analysis of basin-wide inputs of pulped paper from U.S. Navy ships suggests that this source is insignificant in the overall constituent budgets of the Special Areas.

Estimated inputs from ships of TSS, BOD_5, nitrogen, and phosphorus represent much less than 1% of the over Special Area annual budgets. Thus, potential broad scale effects such as eutrophication due to nutrient inputs or oxygen depletion due to organic loading do not appear to be an issue on the basis of this source alone. In areas where these problems already exist, these inputs will probably not contribute to the existing imbalance to a measurable extent. Comparative data suggest that total annual input of pulped paper from all ships within a special area is roughly equivalent to spreading the entire discharge from a single sewage treatment plant over the entire Special Area.

Shredded Waste Stream

Discharge Conditions. The shreddded metal and glass waste stream discharge will vary mainly as a function of ship class, generation rate, and operational practices. Variations in ship speed, discharge rate, and duration affect the area over which the bags are dispersed. This area will likely extend over hundreds of kilometers long for a typical discharge from CVN 68 class ships. Discharging these materials in bags results in minimal dispersion of the individual components of the waste stream. By discharging in discrete packages, the material is likely to sink more quickly through the water column than if the material was discharged as individual pieces.

Waste Stream Characteristics. The rates at which the shredder bags sink through the water column suggests that sea floor processes are dominant in controlling their fate and effects. The process of shredding appears to be superior to that of compacting from a sinkability standpoint. The dominant component of the waste stream is tin-coated steel cans. Glass was next abundant while aluminum made up only a small fraction of the total. Corrosion of the metal portion of the waste stream is likely to occur over a period of a few years, although the rates can be highly variable. However, corrosion is not a removal process, but is a mechanism by which the materials are transformed into smaller particles. It will thus be a mechanism for changing the aesthetic nature of the waste stream from a component of litter to a component of typical sedimentary materials. Seawater leaching of the metal/glass may cause some effects under laboratory conditions, but because of the sink rates, it is unlikely that exposure in the water column is sufficient to be important. The diversity and abundance of organisms that colonized the metal/glass material on the bottom of San Diego Bay suggests that any negative effects seen in laboratory tests may not be important to a wide range of organisms.

Water Column Processes. The fate and effects of the metal/glass waste stream will not be important in the water column. The high sinking velocity minimizes the time spent in the water column; hence only lateral transport, its impact on the areal distribution of deposition, and potential for impacting the coastal zone are important. Because of the discrete nature of the shredder material and the relatively large surface area over which it is distributed under daily discharge conditions, the spatial scale of importance may be the bag size itself. Discharge of the metal/glass waste stream outside the 22-km limit should preclude it from being a source of coastal litter.

Sea Floor Processes. The chemical composition of the metal and glass waste stream is similar to natural crustal compositional characteristics. On a local scale, ie., the size of the bag, only Fe and Sn are enhanced relative to typical sediment compositions. On a daily discharge impact area scale, the materials will have an areal composition that is basically the same as typical sediments. As a result, the maximum impact of bags on bottom sediments can be considered on spatial scales equivalent to the size of an individual bag. Corrosion of the shredder materials will not

actually be a removal process, rather it will be a mechanism for redistribution mainly from a particle size change. It also will be a mechanism for changing the aesthetic nature of the waste stream from a component of litter to a component of typical sedimentary materials. From a liquid-phase aspect, the metal/glass may cause some effects under laboratory conditions, although the exposure levels in the environment that would cause some effect would only be found within the bags themselves. The diversity and abundance of organisms that were observe to colonize the metal/glass material on the bottom of San Diego Bay suggests that any negative effects seen in laboratory tests are likely unimportant on an ecosystem level.

Operational Scenarios. The potential effects of a hypothetical, multiship operational scenario was analyzed using the same operational conditions as that used for the pulped paper waste stream. There are differences in the conceptual model for the shredder from that of the pulper because of the lack of impacts in the water column and the fact that the bags are deposited quickly on the bottom. The operational scenario with a large number of ships operating over a reasonably long time frame in a limited area does not appear to have an impact that is spatially worse than the per bag impact. The coverage over the bottom is still exceptionally small orders of magnitude less than 1%. Biological effects would still be controlled by the size of the bag. These results could be altered if discharge practices acted to concentrate the discharges into particular areas that are significantly smaller than an operational area. This suggests that operational discharge practices should be minimized in areas that are constantly travelled such as before and after leaving Navy ports.

Basin Scale Scenario. The analysis above describes some possible outcomes for the discharge of shredded metal and glass waste for a single ship, or for several ships operating within a limited region. This analysis considers the total yearly input of metal and glass from all Navy shipboard operations for each Special Area. Because of the mobile nature of the discharge sources, the inputs are expected to be delivered to random locations over a wide spatial area. The discrete nature of the bag discharge still implies localized impacts will occur on a spatial scale equal to the size of the bag footprint, implying that the effect to marine organisms is limited to that extent. Annual discharges, from an areal coverage viewpoint are orders of magnitude less than 1%. This suggests that the loading from Navy sources is a small percentage of the loading from a single source in the Baltic and an even smaller percentage of the total loadings from all sources. Therefore, the input of shredded metal and glass from ships constitutes a distributed source which is not large enough to produce significant change in the overall budgets and processes within the Special Areas.

14.0 PLANNED STUDIES

Table 14-1. List of SSWD studies and completion dates.

STUDY	PERFORMER	RESULTS	DATES
Cellulose degradation using microbial and gravimetric methods	Dr. Mary Ann Moran Dept. of Marine Sciences University of Georgia Athens, GA	Initial degradation rates for white paper Initial cellulose composition percentages Matrix of degradation studies for mixed paper Final Report including indigenous populations	June 95 June 95 Oct 95 Oct 96
Benthic Organism Toxicity tests on amphipods and polychaetes	Dr. Tom Dean Coastal Resources Associates, Inc. San Diego, CA	Final Results	June 95
Liquid-phase Toxicity tests on bioluminescent marine bacteria and dinoflagellates, algae, mysid shrimp, and silver side minnows	Dave Lapota NCCOSC RDTE DIV Code 522 San Diego, CA	Final Results	June 95
Zooplankton feeding interference on two copepods, *Calanus* and *Acartia*, and one microzooplankton, *Polykrikos kofoidi*	Dr. Mike Mullin Dr. Hae Jin Jeong Scripps Institution of Oceanography (SIO) La Jolla, CA	Initial Report on feeding interference and recovery Final Report	June 95 Nov 95
Fish feeding interference, growth rate, mortality, and biochemical measures on sardines	Dr. Russ Vetter National Marine Fisheries Service (NMFS) La Jolla, CA	Initial Report on feeding interference, growth rate and mortality Final Report	June 95 Mar 96
Wake dilution model simulations for unstratified, stratified, and selected Special Area cases	Dr. Mark Hyman Naval Coastal System Station (NCSS) Panama City, FL	Data Results and Initial Report (2 cases) Final Report	June 95 June 96
Ambient model simulations extending to 10 days after discharge	Dr. Scott Jenkins Scripps Institution of Oceanography (SIO) La Jolla, CA	Data Results and Initial Report (2 cases) Final Report (all cases)	June 95 Mar 96
Benthic Ecology Sensitive Species	Merkel and Associates San Diego, CA	Initial Report Final Report	Feb 96 Mar 96

Because of the ongoing nature of this environmental analysis effort, there are several studies yet to be completed. Table 14-1 indicates the status of these studies with the exception of the full scale field work which is in the planning stages and will be executed in February 1996.

Unless otherwise directed, the physical and chemical characterization of the waste streams has been completed for this study. The follow-on work lies under the areas of degradation, biological interaction, modeling, field work, analysis, and reporting.

Microbial Degradation. The microbial degradation work being conducted at the University of Georgia is jointly funded by NAVSEA and ONR, and it will continue through September 1996. The second and third phase of the work will be accomplished during this time. This work will focus on studying the effect of the wide range of particle sizes on degradation within a matrix of oceanic conditions and on studying the rates of cellulose decomposition which are mediated by a variety of indigenous populations in seawater samples collected from Special Areas around the globe.

Biological Interaction. Two studies have ongoing work in the area of biological interaction: the zooplankton and clupeoid fish studies. Each has completed a portion of their work and provided initial data and reports. The zooplankton work has focused on two species of copepods and one microzooplankton species of dinoflagellates. The follow-on work will entail further feeding interference on other species in order to broaden the data on the range of potential effects. These studies will use the same concentrations of pulped material as the previous ones unless a NOEC is not determined, and then adjustments will be made as before in order to find the appropriate range of concentrations.

The clupeoid fish studies have focused on feeding interference using various concentrations of pulped material. Mortality was seen at higher concentrations, but because of the feeding methodology, growth rate was not directly obtained. The studies will continue to measure growth rate, recovery, and the effect of exposure duration on the fish. In addition, biochemical measures will also be taken for a more sensitive assessment of the health of the fish.

Additionally, a study has been initiated to identify sensitive end points and assess the worst-case benthic ecology impact in each of the Special Areas. This study is being approached as a literature search, rather than experimentally, given existing time constraints.

Wake and Ambient Dispersion Modeling. In addition to the stratified and unstratified wake dispersion cases, two representative Special Area cases have been run through the wake and ambient dispersion phases. This effort will be extended to include all of the Special Areas of interest to this analysis, and possibly more than one case in each area.

Field Testing. Several large scale field tests will be planned using the prototype equipment installed on a Navy frigate. The tests are being designed to obtain data for further model validation as well as to obtain *in-situ* data on the initial fate of the pulped material and to investigate the important processes involved.

Analysis and Reporting. Analysis and reporting will include the work to date, and the ongoing efforts described above will be included in a subsequent report by the end of FY96.

15.0 REFERENCES

Aijaz, S., S.A. Jenkins. *On the Electrokinetics of the Dynamic Shear Stress in Fluid Mud Suspensions.* Journal of Geophysical Research, V99, NC6, pp. 12,697-12,706, 1994.

Ailor, W.H. Jr. *Aluminum Alloys After Five Years in Seawater.* Materials Performance and the Deep Sea, ASTM STP 445, 115-130, American Society for Testing and Materials, 1969.

Alldredge, A. L., C.C. Gotshalk. *Bacterial Carbon Dynamics on Marine Snow.* Continental Shelf Research V10, pp. 41-58, 1990.

Aller, R.C. *Diagenetic Processes Near the Sediment-Water Interface of Long Island Sound I. Decomposition and Nutrient Element Geochemistry (S, N, P).* Ed. B. Saltzman, Estaurine Physics and Chemistry: Studies in Long Island Sound, Advances in Geophysics, V22, Academic Press, 1980.

American Society for Testing and Materials (ASTM). *Annual Book of ASTM Standards, ASTM Standard A 624.* ASTM, Philadelphia, PA. 1984.

Andrulewicz, E., K.H. Rohde. *Harmful Substances: Petroleum Hydrocarbons.* Helsinki: Baltic Marine Environment Protection Commission, Baltic Sea Environment Proceedings, N17 B, 351, pp. 170-198, 1987.

Apel, J.R. *Principles of Ocean Physics.* International Geophysics Series 38, Academic Press, 1-634, 1987.

Armi, L.A. *Effects of Variations in Eddy Diffusivity on Property Distributions in the Oceans.* Journal of Marine Research, V37, N3, pp. 515-530, 1979.

Ball, J., T. Reynolds. *Dispersion of Liquid Waste From a Moving Barge.* Journal WPCF, V48, N11, pp. 2541-2547, November, 1976.

Beavers, J.A., G.H. Koch, W.E. Berry. *Corrosion of Metals in Marine Environments.* MCIC Report 86-50, Battelle Columbus Division, Columbus, Ohio, July, 1986.

Benner, R,, A.E. MacCubbin, R.E. Hodson. *Temporal Relationship Between The Deposition and Microbial Degradation of Lignocellulosic Detritus in a Georgia Salt Marsh and The Okefenokee Swamp.* Microbiology Ecology, V12, pp. 291-298, 1986.

Benner, R., M.A. Moran, R.E. Hodson. *Effects of pH and Plant Source on Lignocellulose Biodegradation Rates In Two Wetland Ecosystems, The Okefenokee Swamp and a Georgia Salt Marsh.* Limnology Oceanography V30, pp. 489-499, 1985.

Benner, R., R.E. Hodson. *Microbial Degradation of The Leachable and Lignocellulosic Components of Leaves and Wood From Rhizophora Mangle in a Tropical Mangrove Swamp.* Marine Ecology Progress Series, V23, pp. 221-230, 1985.

Benner, R., S.Y. Newell, A.E. Maccubbin, R.E. Hodson. *Relative Contributions of Bacteria and Fungi To Rates of Degradation of Lignocellulosic Detritus in Salt Marsh Sediments.* Applied and Environmental Microbiology, V48, pp. 36-40, 1984.

Benninghoff, W.S. W.N. Bonner. *Man's Impact on The Antarctic Environment: A Procedure For Evaluation Impacts From Scientific and Logistic Activities*. Scientific Committee on Antarctic Research, Scott Polar Research Institute, 1985.

Berner, R.A. *Early Diagenesis, A Theoretical Approach.* Princeton University Press, Princeton, New Jersey, 1980.

Birkhoff, G.; Zarantonello. *Jets, Wakes and Cavities*. Academic Press, New York, pp. 353, 1957.

Blaxter, J.H.S., J.R. Hunter. *The Biology of the Clupeoid Fishes*. Off Print from Advances in Marine Biology, V20, pp.1-223, 1982.

Blough N., O. Zafiriou, J. Bonilla. *Optical Absorption Spectra of Waters From The Orinoco River Outflow-Terrestrial Input of Colored Organic Matter to The Caribbean.* Journal of Geophysical Research-Oceans, V98 Nc2, pp. 2271-2278, February, 1993.

Brick, R.M., J.J. Daly, E.L. Koehler, A.G. Skibbe. *The Selection of Tin Coatings for Steel Containers*. Ed. T. Lyman Metals Handbook, V1, pp. 1133-1141, Ohio, 1961.

Brockmann U., L. Rwpm, H. Postma. *Cycling of Nutrient Elements In The North Sea.* Netherlands Journal of Sea Research, V26 N2-4, pp. 239-264, 1990.

Brooks, N.H. R.G. Arnold, R.C.Y. Koh, G.A. Jackson, W.K. Faisst. *A Research Plan for Deep-Ocean Disposal of Sewage Sludge.* Robert E. Krieger Publishing Company, Malabar, Florida, 1987.

Brügmann L, P. Bernard, R. Vangrieken. *Geochemistry of Suspended Matter From The Baltic Sea .2. Results of Bulk Trace Metal Analysis By AAS.* Marine Chemistry, V38 N3-4 pp. 303-323, 1992.

Capuzzo, J.M., D.R. Kester. *Oceanic Processes in Marine Pollution Volume I, Biological Processes and Wastes in the Ocean.* Robert E. Krieger Publishing Company, Malabar, Florida, U.S., 1987.

Carlson, D.J. *A Field Evaluation of Plate and Screen Microlayer Sampling Techniques.* Marine Chemistry, V11, pp. 189-208, 1982.

Cederwall H., R. Elmgren. *Biological Effects of Eutrophication in The Baltic Sea, Particularly The Coastal Zone.* Ambio, V19 N3 pp. 109-112, 1990.

Chadwick, D.B., MH. Salazar. *Integrated Technologies for Monitoring the Marine Environment.* Ocean Proceedings 1991 Conference, pp. 343-350, 1991.

Charnock, H., K.R. Dyer, J.M. Huthnance, P.S. Liss, J.H. Simpson, P.B. Tett. *Understanding the North Sea System.* Chapman & Hall for the Royal Society, 1994.

Clark, R.B. *Marine Pollution, Third Edition.* Clarendon Press, Oxford, New York, 1992.

Committee on Merchant Marine and Fisheries House of Representatives One Hundred Third Congress First Session. *The Effectiveness of the Coast Guard's Efforts to Enforce Laws*

Which Prohibit the Dumping of Garbage into the Oceans and Examine the Two Publicized Cases of Illegal Dumping. U.S. Government Printing Office, 1993.

Cruz G., V. Lopez, C. Sosa. *Pollution By Solid Wastes Carried By Marine Currents To The Caribbean Coast Of Honduras.* Revista De Biologia Tropical, V38 N2, pp. 339-342. Language: Spanish, 1990.

Csanady, G.T, J.H. Churchill. *Environmental Engineering Analysis of Potential Dumpsites.* Robert E. Krieger Publishing Company, Malabar, Florida, 1987.

Csanady, G.T. *Accelerated Diffusion in the Skewed Shear Flow of Lake Currents.* Journal Geophysics Research, V71, pp. 411-420, 1966.

Csanady, G.T. *An Analysis of Dumpsite Diffusion Experiments: In Ocean Dumping of Industrial Wastes.* Eds. B.H. Ketchum, D.R. Kester, Plenum Press, New York and London, pp. 109-129, 1981.

Csanady, G.T. *Turbulent Diffusion in the Environment.* Journal Atmospheric Science, V26, pp. 414-426, 1973.

Dahl, J.B., O. Tollan. *Measurement of Dilution of Tank Waste Water in the Wake of M/T "Esso Bergen".* Institute for Atomic Energy, Kjeller, Norway, 1972.

Dahl, J.B., U. Haagensen, C. Qvenild, O. Tollan. *Dilution in the Ship's Wake of Tank Washings Released From M/T "Esso Slagen".* Institute of Atomic Energy, Kjeller, Norway, 1973.

Davidson, L., G. Kristina. *Special Area Status for the Wider Caribbean Region Under Annex I of the International Convention for the Prevention of Pollution From Ships.* U.S. Coast Guard, 1989.

Davis, R. *Sea Surface Films.* In a Report to the MITRE Corporation, JSR-86-105, McLean, Virginia, November, 1986.

De Wolfe, P., Zijlstra, J.J. *The Ecosystem.* Eds W. Salomons, B.L. Bayne, E.K. Duursma & U. Forstner, North Sea Pollution, pp. 118-151, Berlin, Springer-Verlag, 1988.

Defense Mapping Agency. *Ocean Basin Environment. Sailing Directions (Planning Guide) for the North Atlantic Ocean.* Defense Mapping Agency, 3rd Edition, 1988.

Defense Mapping Agency. *Ocean Basin Environment. Sailing Directions (Planning Guide) for the North Sea and Baltic Sea.* Defense Mapping Agency, 3rd Edition, 1990.

Defense Mapping Agency. *Ocean Basin Environment. Sailing Directions (Planning Guide) for Antarctica.* Defense Mapping Agency, 2nd Edition, 1992.

Defense Mapping Agency. *Ocean Basin Environment. Sailing Directions (Planning Guide) for the Mediterranean.* Defense Mapping Agency, 5th Edition, 1991.

Delft Hydraulics Laboratory. *Dilution of Liquids Discharged From A Ship.* Report M 1312. Delft Hydraulics Laboratory, Delft, The Netherlands, 1975.

Delvigne, G.A.L. *Experiments On The Dilution Capacity Of Wakes From Tankers Dumping In The North Sea.* Malabar, Krieger Publishing Company, pp. 235, Florida, 1987.

Devine, M. *Analysis of Mixing and Dispersion of Industrial Wastes Dumped into the Deep Sea.* Oceanic Processes in Marine Pollution, V2, pp. 63-70, Robert E. Krieger Publishing Co., Malabar, Florida, 1979.

Dexter, S.C. *Effect of Variation in Sea Water Upon the Corrosion of Aluminum.* Corrosion, V36, pp. 423-432. 1980.

Dixon, T.J., T.R. Dixon. *Marine Litter Distribution And Composition in The North Sea.* Marine Pollutant Bulletin V14(4), pp.145-148, 1983.

Dixon, T.R., T.J. Dixon. *Marine Litter Surveillance.* Marine Pollution Bulletin, V14, N4, pp. 145-148, 1983.

Drake, J., S. Gill, K. Bayer. *Technical Evaluation (TECHEVAL) Test Report for the Large Pulper Installed Onboard the USS George Washington (CVN 73).* Carderock Division, Naval Surface Warfare Center, CARDIVNSWC-TM-63-94/4, Washington. D.C., 1994.

Dubinsky, Z. *Coral Reefs.* Elsevier Science Publishers, Amsterdam, 1990.

Ducklow, H.W., D.L. Kirchman, G.T Rowe. *Production and Vertical Flux of Attached Bacteria in The New York Bight as Studied With Floating Sediment Traps.* Applied Environmental Microbiology, V43, pp. 769-776, 1982.

Durst, C.S. *The Relationship Between Current and Wind.* Quart. J. R. Met. Society, V50, pp. 113, London, 1924.

Earthscan. *The Improbable Treaty: The Cartagena Convention and The Caribbean Environment.* London: International Institute for Environment and Development, 1983.

Eisma D. *Transport and Deposition of Suspended Matter in The North Sea and The Relation To Coastal Siltation, Pollution, and Bottom Fauna Distribution.* Aquatic Sciences, V3 N2-3, pp. 181-216, 1990.

Elmgren R. *Mans Impact on The Ecosystem of The Baltic Sea - Energy Flows Today and at The Turn Of The Century.* Ambio, V18 N6 pp. 326-332, 1989.

El-Sayed, S.Z. *Plankton.* Elsevier, New York, New York, 1977.

Estrada M., M. Delgado. *Summer Phytoplankton Distributions In The Weddell Sea.* Polar Biology, V10 N6, pp. 441-449, 1990.

Evans, R.J. *Death in Hamburg. Society and Politics in the Cholera Years 1830-1910.* Oxford University Press, Oxford, 1987.

Farmer, D., D. Lemon. *Dispersion of Dyed Sea-Water Discharged from Moving Vessels in Coastal Waters.* Pacific Marine Science Report, Institute of Ocean Sciences, Patrician Bay, Victoria, BC., 1975.

Ferm, R. *Integrated Management of The Baltic Sea.* Marine Pollution Bulletin, V23, pp. 533-540, 1991.

Fischer G. *Stable Carbon Isotope Ratios of Plankton Carbon and Sinking Organic Matter From The Atlantic Sector of The Southern Ocean.* Marine Chemistry, V35 N1-4, pp. 581-596, 1991.

Fontana, M.G., *Corrosion Engineering.* McGraw Hill, New York, 1986.

Frankenhoff, C., C.A. Matos, E. Towle, J. McEachern, L.T. Giulini. *Environmental Planning and Development In The Caribbean: Analysis and Needs Assessment.* Project Coordinator, Duke E.E. Pollard, Contributors, Editorial Universitaria, Universidad De Puerto Rico, 1977.

Fransz H., J. Mommaerts, G. Radach. *Ecological Modeling of The North Sea.* Netherlands Journal of Sea Research, V28 N1-2, pp. 67-140, 1991.

Freestone, D. *Protection of Marine Species and Ecosystems in the Wider Caribbean, the Protocol on Specially Protected Areas and Wildlife.* Marine Pollution Bulletin, V22, N12, pp. 579-581, 1991.

Frost, B.W. *Effects of Size and Concentration of Food Particles on the Feeding Behavior of the Marine Planktonic Copepod Calanus pacificus.* Limnology Oceanography, 17:805-815, 1972.

Furness, R.W., P.S., Rainbow. *Heavy Metals in the Marine Environment.* CRC Press, Boca Raton, Florida, 1990.

Gabrielides, G. P., A. Golik, L. Loizides, M.G. Marino, F. Bingel, M.V. Torreg Rossa. *Man Made Garbage Pollution on the Mediterranean Coastline. Environmental Management And Appropriate Use Of Enclosed Coastal Seas Emecs'-90.* CODEN: International Conference on the Environmental Management of Enclosed Coastal Seas '90: EMECS '90, Kobe, Hyogo Prefect. (Japan), 3-6 August 1990 Marine Pollution Bulletin, V23, 1991

Garrity S., S. Levings. *Marine Debris Along The Caribbean Coast of Panama.* Marine Pollution Bulletin, V26 N6, pp. 317-324, 1993.

Gibbs, R.J. M. Angelidis. *Effect of Sludge Digestion on Metal Segregation During Ocean Dumping.* Marine Pollution Bulletin, V20, N10, pp. 503-508, 1989.

Glasby, G.P. *Antarctic Sector of the Pacific.* Elsevier, New York, New York, 1990.

Gordon, A.L. *Oceanography of Antarctic Waters.* Lamont-Doherty Geological Observatory of Columbia University, Palisades, New York, 1971.

Griffin, O.W., R.D. Peltzer, A.M. Reed, R.F. Beck. *Remote Sensing of Surface Ship Wakes.* Naval Engineers Journal, pp. 245-258, May, 1992.

Grogan, W.C., *Compiler. Input Of Contaminants To The North Sea From The United Kingdom.* Final Report Prepared for the Department of the Environment by the Institute of

Offshore Engineering. Institute of Offshore Engineering, Heriot-Watt University, Edinburgh, 203pp. 1984 Institute of Offshore Engineering., Heriot-Watt Univ., Edinburgh, EH14 4AS, U.K., 1984.

Hallberg R. *Environmental Implications of Metal Distribution In Baltic Sea Sediment.* Ambio, V20, N7 pp. 309-316, 1991.

Hammond, R.R., S.A. Jenkins, J.S. Cleveland, J.C. Talcott, A.L. Heath, J. Wasyl, S.G. Goosby, K.F. Schmitt, L.A. Levin. *Coastal Water Clarity Modeling.* SAIC, Technical Report 01-1349-03-4841-000, pp. 491, 1995.

Hardisty, J. *The British Seas: An Introduction To The Oceanography and Resources of The North West European Continental Shelf.* London: Routledge, pp. 272, 1990.

Hardy, J.T., C.W., Apts, E.A. Crecelius, N.S., Bloom. *Sea-Surface Microlayer Metals Enrichments in an Urban and Rural Bay.* Estuarine, Coastal and Shelf Science, V20, pp. 299-312, 1985.

Harris County 1994 Annual Sewage Discharge Monitoring Report. Harris County Wastewater Treatment Plant, Houston Texas, 1994.

Hill, H.W. *Currents and Water Masses.* North Sea Science, NATO North Sea Science Conference, MIT Press, Cambridge, Massachusetts, pp. 17-42, 1973.

Hill, R.T., I.T. Knight, M.S. Anikis, R.R., Colwell. *Benthic Distribution of Sewage Sludge Indicated by Clostridium Perfringens at a Deep-Ocean Dump Site.* Applied and Environmental Microbiology, V59, N1, pp. 47-51, 1993.

Hjulstrom, F. *Transportation of Detritus by Moving Water.* Recent Marine Sediments in Trask, pp. 5-31, 1939.

Hoekstra, M. *Macrowake Features of a Range of Ships.* Report N410461-1-PV, Maritime Research Institute, Netherlands, 1991.

Holm-Hansen, O., S.Z. El-Sayed. *Primary Production and the Factors Controlling Phytoplankton Growth in the Southern Ocean.* Applications within Antarctic Biology. Smithsonian Institution, pp. 11-50,Washington, D.C., 1977.

Horne, R.A.. *Marine Chemistry.* John Wiley and Sons, New York, 1969.

Hyman, M. *Modeling Ship Microbubble Wakes.* Dahlgren Division Naval Suffice Warfare Center, Panama City, Florida, 1994.

Hyman, M., J. Kamman, R. Smith, T.C. Nguyen. *Bubble Transport in Ship Wakes With Application to Wake Modification.* Naval Coastal System Center Technical Memorandum, June, 1987.

Hyman, M.C. *Initial Data Plane Estimation for Surface Ships-II.* NCSC Technical Note, NCSC TN 930-88, 1988.

Hyman, M.C. *Numerical Simulation of the Hydrodynamic Wake of a Surface Ship.* Naval Coastal System Center Technical Note, pp. 544-690, 1990.

Hyman, M.C. *Simulation of the Interaction Between A Wind-Driven Sea State and Surface Ship Wakes.* Naval Coastal System Center Technical Memorandum, CSS TM pp. 584-591. 1992.

Ijlstra, T., F. Jong. *Current Legal Developments. North Sea.* International J. Esturary Coast Law, V3, N3, pp. 246-265, 1988.

International Atomic Energy Agency. *An Oceanographic Model for the Dispersion of Wastes Disposed of in the Deep Sea.* Joint Group of Experts on the Scientific Aspects of Maine Pollution GESAMP Originally Approved at its Thirteenth Session Held in Geneva, 1983.

International Maritime Organization. *Articles, Protocols, Annexes, Unified Interpretations of the International Convention for the Prevention of Pollution from Ships, 1973, as modified by the Protocol of 1978 Relating Thereto.* MARPOL 73/78 Consolidated Edition 1991, IMO London, 1992.

Jansson, Bengt-Owe. *Ecosystem Approach to the Baltic problem.* Bulletins From the Ecological Research Committee, Stockholm, Ekologikommitten, Statens, 1972.

Jenkins, S.A., D.L. Inman,. *On a Submerged Sphere in a Viscous Fluid Excited by Small-Amplitude Motions.* Journal Fluid Mechanics, V157, pp. 199-224, 1985.

Jenkins, S.A., J. Wasyl. *Resuspension of Esturial Sediments by Tethered Wings.* Journal of Coastal Research, V6, N4, pp. 961-980, 1990.

Jenkins, S.A., J.A. Nichols, D.W. Skelly. *Coupled Physical-Biological Dispersion Model for the Fate of Suspended Solids in Sewage Discharged into the Ocean.* SIO Reference Series 89-3, pp. 53, 1989.

Joannessen, O.M. *Preliminary Results of Some Oceanographical Observations Carried Out Between Barbados and Tobago.* Marine Sciences Manuscript Report N8, McGill University, November, 1968.

Jones R., J. Amador. *Methane and Carbon Monoxide Production, Oxidation, and Turnover Times in The Caribbean Sea as Influenced by The Orinoco River.* Journal of Geophysical Research-Oceans, V98 N2, pp. 2353-2359, 1993.

Jonsson, I.G., N.A. Carlsen. *Experimental and Theoretical Investigations in an Oscillatory Turbulent Boundary Layer.* Journal Hydraulic Research, V14, N1, pp. 45-60, 1976.

Kastelein, R.A., M.S.S. Lavaleije. *Foreign Bodies In The Stomach Of A Female Harbour Porpoise (Phocoena phocoena) From The North Sea.* Aquatic Mammals, V18, N2, pp. 40-46, 1992.

Katz, C.N., D.B. Chadwick, G.S. Douglas. *Real-Time Fluorescence for Measurements Intercalibrated with GC-MS.* Ocean Proceedings 1991 Conference, pp. 351-358, 1991.

Kautsky H. *The Impact Of Pulp-Mill Effluents On Phytobenthic Communities In The Baltic Sea.* Ambio, V21 N4, pp. 308-313, 1992.

Kennett, J. *Marine Geology.* Prentice-Hall, Inc., Englewood Cliffs, New Jersey, 1982.

Kester, D.R., W.V. Burt, J.M. Capuzzo, P.K. Park, B.H. Ketchum, I.W. Duedall. *Wastes in the Ocean Volume 5.* John Wiley & Sons, New York, 1985.

Keys, J.R. *Antarctic Marine Environments and Offshore Oil.* Commission for the Environment Wellington, New Zealand, 1984.

Kjerfve, B. *Physical Flow Processes in Caribbean Waters Over a Range of Scales*, Belle W. Baruch Institute for Marine Biology and Coastal Research, University of South Carolina.

Kress N., A. Golik, G. Galil, M. Krom. *Monitoring The Disposal of Coal Fly Ash at a Deep Water Site in The Eastern Mediterranean Sea.* Marine Pollution Bulletin, V26, N8, pp. 447-456, 1993.

Kullenberg, G. *Entrainment Velocity in Natural Stratified Sheer Flow.* Estuary Coastal Marine Science, 5, pp. 329-338, 1977.

Kullenberg, G. *Overall Report On The Baltic Open Sea Experiment 1977 (BOSEX).* Copenhagen, Denmark: International Council for the Exploration of the Sea, 1984.

Kullenberg, G. *The State Of The Baltic.* Oxford, Pergamon Press, New York, 1981.

Laevastu, T. *Surface Water Types of the North Sea and its Characteristics.* Serial Atlas of the Marine Environment Folio, 4, American Geographic Society, 1963.

Laevastu, T. *Synopsis of Information on Oceanography of the North Sea.* FAO, Fisheries Division, Biology Branch, Report FB/60/SZ, 1960.

Lajczak A., M. Jansson. *Seasonal Variations In Suspended Sediment Yield In The Baltic Sea Drainage Basin.* Nordic Hydrology, V24 N1 pp. 53-64, 1993.

Lazaro, B.J., J.C. Lasheras. *Particle Dispersion in a Developing Free Shear Layer, Part I Forced Flow.* Journal of Fluid Mechanics, V235, pp. 179-221, 1992.

Lazaro, B.J., J.C. Lasheras. *Particle Dispersion in a Developing Free Shear Layer, Part 2 Forced Flow.* Journal of Fluid Mechanics, V235, pp. 179-221, 1992.

Lee, A.J. *The North Sea, Setting the Scene.* Eds. P.J. Newman, A.R. Agg, Environmental Protection of the North Sea, Professional Publishing, 1988.

Lee, A.J. *The North-West European Shelf Seas: The Sea Bed and the Sea in Motion, II.* In Newman, P.J.; Agg, A.R. Environmental Protection of the North Sea, Heinemann Professional Publishing, 1988.

Lee, A.J. *The Currents and Water Masses of the North Sea.* Oceanography, Marine Biology, 8, pp. 33-71, 1970.

Lee, A.J., J. Ramster. *The Hydrography of the North Sea. A Review of Our Knowledge in Relation of Pollution Problems.* Helgol. Wiss. Meeresunters, 17, pp. 44-63, 1968.

Lewis, R.E., A.M. Riddle. *Sea Disposal: Modeling Studies of Waste Field Dilution.* Marine Pollution Bulletin, V20, N3, pp. 124-129, 1989.

Lieberman, S.H., S. Clavell, D.B. Chadwick. *Techniques for Real-Time Environmental Monitoring.* Proceedings of the 16th Meeting U.S.-Japan Marine Facilities Panel: United States Cooperative Program in Natural Resources on Marine Facilities, pp. 495-499, 1989.

Lion, L.W., J.O. Leckie. *Accumulation and Transport of Cd, Cu, and Pb in an Estuarine Salt Marsh Surface Microlayer.* Limnology & Oceanography, V27(1), pp. 111-125, 1982.

Lipton, J., J.W. Gillett, J.W. *Uncertainty in Ocean-Dumping Health Risks: Influence of Bioconcentration, Commercial Fish Landings and Seafood Consumption.* Environmental Toxicology and Chemistry, V10, pp. 967-976, 1991.

Liss, P.S. *Chemistry of the Sea Surface Microlayer.* Eds. J.P. Riley, G. Skirrow, Chemical Oceanography, V2, 2nd Edition, Academic Press, New York, Pp. 193-243, 1975.

List, E.J., G. Gartrell, C.D. Winant. *Diffusion and Dispersion in Coastal Waters.* Journal of Hydraulic Engineering, V116, N10, pp. 1158-1179, 1990

Lithner, G. *Ronnskarsundersokningen.* Statens Naturvardsverk PM, 497, pp. 1-174, 1974.

Lizotte M., C. Sullivan. *Biochemical Composition and Photosynthate Distribution In Sea Ice Microalgae Of McMurdo-Sound, Antarctica - Evidence For Nutrient Stress During The Spring Bloom.* Antarctic Science, V4, N1, pp. 23-30, 1992.

Long, E.R., D.D. Mcdonald, S.L. Smith, F.D. Calder. *Incidence of Adverse Biological Effects Within Ranges of Chemical Concentrations in Marine and Estuarine Sediments.* Environmental Management, V19, N1, pp. 81-97, Springer-Verlad New York, Inc., 1995.

MacIntryre, F. *Chemical Fractionation and Sea-Surface Microlayer Processes.* Ed. E.D. Goldberg, The Sea, V5, Wiley, New York, pp. 245-299, 1974.

Manzi, D. *Shipboard-Generated Solid Waste Analysis-Naval Station, Norfolk,* 1994.

Martin, J.E., E. Meiburg. *The Accumulation and Dispersion of Heavy Particles in Forced Two-Dimensional Mixing Layers, 1: The Fundamental and Subharmonic Cases.* Physical Fluids, A-6, pp. 1116-1132, 1994.

Marvin, M., J. Burns, D.G. Capone. *Microbial Degradation of Sweetheart Cups in the Marine Environment.* A Report Submitted to the Sweetheart Cup Company, Inc., Chesapeake Biological Laboratory, University of Maryland, September, 1993.

McIntyre, A.D. *Pollution in the North Sea From Oil-Related Industry, an Overview.* Eds. P.J. Newman, A.R. Agg, Environmental Protection of the North Sea, Heinemann, Oxford, pp. 425, 1988.

McIntyre, A.D. *The Benthos of the Western North Sea.* Rapp. R.-v Reun. Cons. Internationa Expolorer, Mer, 172, pp. 405-417, 1978.

McLeay, D. *Aquatic Toxicity of Pulp and Paper Mill Effluent: A Review.* Environment Canada, Fisheries and Oceans, D. McLeay and Associates Ltd., 1987.

Meadows, G.A., D. Lyzenga, J. Lyden, R. Beck. *Nonintrusive, Multiple-Point Measurements of Water Surface Slope, Elevation and Velocity.* Proceedings of the Eighteenth ONR Symposium on Naval Hydrodynamics, National Academy Press, pp. 349-360, Washington, D.C., 1990.

Meadows, L., G. Meadows, A. Troesch, S. Cohen, K.P. Beier, G. Rot. *Lagranigian Velocity Profiles in the Wake of a High Speed Vessel.* Ocean Engineering, V21, N2, pp. 221-242, 1994

Melvasalo, T. *Assessment of the Effects of Pollution on the Natural Resources of the Baltic Sea.* Eds. J. Pawlak, K. Grasshoff, L. Thorell, A. Tsiban, Baltic Sea Environment, Proc. 5B, pp. 322-342, 1980.

Melvasalo, T. ed. *Assessment Of The Effects Of Pollution On The Natural Resources Of The Baltic Sea, 1980.* Helsinki: Baltic Marine Environment Protection Commission, Helsinki Commission, 1981.

Mercier, J.A., R.L. Hires. *Model Study of the Dilution of Soluble Liquids Discharged from Tankers.* Stevens Institute of Technology, Prepared for Coast Guard, September, 1973.

Merritt, G.E. *Wake Laboratory Experiment.* Cornell Aeronautical Laboratory Inc. New York, 1972.

Miner, W.E., S.E. Ramber. *A Method of Approximating the Initial Data Plane for Surface Ship Wake Simulations.* Naval Research Laboratory Report 6376, November, 1988.

Moraitou-Apostolopoulou, M., V. Kiortsis. *Mediterranean Marine Ecosystems.* Plenum Press, New York, 1985.

Moran, M.A., R. Benner, R.E. Hodson. *Kinetics Of Microbial Degradation Of Vascular Plant Material In Two Wetland Ecosystems.* Oecologia V79, pp. 158-167, 1989.

Muller-Karger F., C. Mcclain, T. Fisher, W. Esaias, R. Varela. *Pigment Distribution in The Caribbean Sea - Observations From Space.* Progress In Oceanography, V23, N1, pp. 23-64, 1989.

Mullin, M.M. *Particle Size Analysis on Mixed Paper Pulp, ETA.* Limnology and Oceanography, V10, pp. 459-462, 1965.

NAVSEA. *U.S. Navy Shipboard Solid and Plastics Waste Management Program Plan.* Naval Sea Systems Command, 1993.

Nehring D., W. Matthaus. *Current Trends in Hydrographic and Chemical Parameters and Eutrophication in The Baltic Sea.* Internationale Revue Der Gesamten Hydrobiologie, V76 N3, pp. 297-316, 1991.

Neumann, G. *Ober Die Komplexe Natr Des Seeganges, Teil 1 and 2.* Deut Hydrogr. Zeit., V5, N2/3, pp. 95-110, N5/6, pp. 252-277, 1952.

Nielsen, J.N. *Golfströmmen.* Geografisk Tidskrift, V28, N1, 1925.

Nielson, P. *Some Basic Concepts of Wave Sediment Transport.* Series Paper N20, Institute of Hydrodyn. and Hydr. Engineering, Technical University of Denmark, 1979.

North Sea Becomes MARPOL 'Special Area'. Marine Pollution Bulletin, 22 [5], 218-219, 1991.

Norton, R.L. *Assessment of Pollution Loads to the North Sea.* National Technical Information Service, 1982.

Office of Technology Assessment. *Wastes in Marine Environments, Summary.* Congress of the United States, Office of Technology Assessment, Washington D.C., U.S., 1987.

Okubo, A. *Oceanic Diffusion Diagrams.* Deep-Sea Research, V18, pp. 789, 1971.

Olson, T.M., S.E. Gill, C.S. Alig. *Study of Solid and Plastic Waste Management Aboard USS Emory S. Land (AS 39).* David Taylor Research Center, Bethesda, pp. 45, MD, 1989.

Otto L., J. Zimmerman, G. Furnes, M. Mork, R. Saetre, G. Becker. *Review of The Physical Oceanography of The North Sea.* Netherlands Journal of Sea Research, V26 N2-4, pp. 161-238, 1990.

Palanques A., D. Drake. *Distribution and Dispersal of Suspended Particulate Matter on The Ebro Continental Shelf, Northwestern Mediterranean Sea.* Marine Geology, V95 N3, pp. 193-206, 1990.

Park, P.K., T.P. O'Connor, B.H. Ketchum, eds. *Historical and International Considerations.* Plenum, New York, New York, 1980.

Parr, A.E. *A Contribution to the Hydrography of The Caribbean and Cayman Seas Based Upon the Observations Made by the Research Ship Atlantis, 1933-34.* Bingham Oceanography Collection, Bulletin, V5, 4, pp. 110, New Haven, 1937.

Peng, T.H., W.S. Broecker, G.G. Mathieu, Y.H. Li, A.E. Bainbridge. *Radon Evasion Rates in the Atlantic and Pacific Oceans as Determined During the GEOSECS Program.* Journal of Geophysics Research, 84, pp. 2471-2486, 1979.

Peterson, M.H., T.J. Lennox Jr. *Effects of Exposure Conditions on the Corrosion of Mild Steel, Copper, and Zinc in Seawater.* Materials Performance, V23, pp. 15-18, 1984.

Pitter, P., J. Chudoba. *Biodegradability of Organic Substances in the Aquatic Environment.* CRC Press, Inc., Boca Raton, Florida, 1990.

Portman, J. *The Chemical Pollution Status Of The North Sea.* Dana-A Journal of Fisheries and Marine Research, V8, pp. 95-108, 1989.

Postma, H. *Sediment and Pollution Interchange In Shallow Seas: Proceedings From ICES Workshop Held In Texel, 24-26, September 1979.* Copenhague, Danemark : Conseil International Pour L'exploration de la Mer, 1981.

Pritchard, D.W., A. Okubo. *Summary of Our Present Knowledge of the Physical Processes of Mixing in the Ocean and Coastal Waters, and a Set of Practical Guidelines for the Application of Existing Diffusion Equations in the Preparation of Nuclear Safety Evaluations of the Use of Nuclear Power Sources in the Sea.* Chesapeake Bay Institute, The Johns Hopkins University, Report No. NYO-3109-40, U.S. Atomic Energy Commission, Reference 69-1, September, 1969.

Proceedings of the FAO/UNEP/IAEA Consultation Meeting on the Accumulation and Transformation of Chemical Contaminants by Biotic and Biotic Processes in the Marine Environment. Edited by G.P. Gabrielidies, Mediterranean Action Plan, UNEP, MAP Technical Reports Series N59, La Spezia, Italy, pp. 24-28, September, 1990.

Progress Reports On Cadmium, Mercury, Copper and Zinc. Helsinki: Baltic Marine Environment Protection Commission, Helsinki Commission, 1987.

Pruter, A.T. *Sources, Quantities and Distribution of Persistent Plastics in the Marine Environment.* Marine Pollution Bulletin, V18, N6B, pp. 305-310, 1987.

Pyewipe 1992-1994 Sewage Discharge Monitoring Report. National Rivers Authority, Pyewipe Pumping Station, United Kingdom, 1992-1994.

Raudkivi, A.J. *Loose Boundary Hydraulics.* Third Edition, Pergamon Press, Inc., Maxwell House, Fairview Park, Elmsford, New York, 1990.

Rawn, A.M., F.R. Bowerman, N.H. Brooks. *Diffusers for Disposal of Seage in Sea Water. Diffusers for Disposal of Sewage in Sea Water.* Journal Sanitation Division, ASCE, 86, SA2, pp.65-105, 1960.

Redfield, A.C. *On the Proportions of Organic Derivatives in Sea Water and Their Relation to the Composition of Plankton.* James Johnstone Memorial Volume, Liverpool, University Press, pp. 348, 1934.

Reed, J.B. *Tracking Technologies for Radioactive Waste Shipments.* Denver, Colorado: National Conference of State Legislatures, Series title: State Legislative Report; V15, N4, 1990.

Rees H., A. Eleftheriou. *North Sea Benthos - A Review of Field Investigations Into The Biological Effects of Mans Activities.* Journal Du Conseil, V45 N3, pp. 284-305, 1989.

Reijnders P., K. Lankester. *Status of Marine Mammals in The North Sea.* Netherlands Journal of Sea Research, V26 N2-4, pp. 427-435, 1990.

Reinhart, F.M. *Corrosion of Metals and Alloys in the Deep Ocean.* Technical Report R 834, Civil Engineering Laboratory, Naval Construction Battalion Center, Port Hueneme, California, February, 1976.

Reinhart, F.M., J.F. Jenkins. *The Relationship Between the Concentration of Oxygen in Seawater and the Corrosion of Metals*. U.S. Naval Civil Engineering Laboratory Report, pp. 562-577, 1971.

Review of Several Plastic Dumping Incidents Involving the Navy, and What the Navy is Doing to End These Types of Incidents. Hearing Before the Subcommittee on Oceanography, Great Lakes and the Outer Continental Shelf of the Committee on Merchant Marine and Fisheries House of Representatives One Hundred Second Congress, U.S. Government Printing Office, 1991.

Saetre, R., M. Mork. *The Norwegian Coastal Current*. University Bergen, pp.795, 1981.

Salomons, W., B.L. Bayne, E.K. Duursma, U. Forstner. *Pollution of The North Sea: An Assessment*. Berlin, New York: Springer-Verlag, 1988.

Saydam, C., I. Salihoglu. *Dissolved/Dispersed Petroleum Hydrocarbons Suspended Sediment, Plastic Pelagic Tar and Other Litter in the North-Eastern Mediterranean.* Middle East Technical University Institute of Marine Sciences, P.K. 28, Erdemli-Ice 1, Turkey, VII Jounees Etud. Pollutions, Lucerne, 1984.

Schiewer U. *Eutrophication of The Baltic Sea* - Foreword. Internationale Revue Der Gesamten Hydrobiologie, V76 N3 pp. 293-294, 1991.

Schmidt D. *Mercury in Baltic and North Sea Waters.* Water Air and Soil Pollution, V62 N1-2 pp. 43-55, 1992.

Schoomaker, J.S., R.R. Hammond, A.L. Heath, J.S. Cleveland. *A Numerical Model for Prediction of Sub-Littoral Optical Visibility.* SPIE Ocean Optics XII, pp. 18, 1994

Scully-Power, P. *Navy Oceanographer Shuttle Observations STS41-G.* Naval Underwater Systems Center, NUSC Technology, Document 7611, 1986.

Sebek, V. *The North Sea and The Concept Of Special Areas.* Eds. T. Ijlstra, D. Freestone, The North Sea: Perspectives On Regional Environmental Cooperation, V5, N1-3 pp. 157-166, 1990.

Seibold, E., W.H. Berger. *The Sea Floor, An Introduction to Marine Geology*. Springer-Verlag Berlin Heidelberg, New York, 1982.

Seiwell, H.R. *Application of The Distribution of Oxygen To The Physical Oceanography of The Caribbean Sea Region.* Papers in Physical Oceanography and Meteorol., V6, N1, pp. 60, 1938.

Shimada, H., K. Miida, T. Yokooji. *The Relation Between the Corrosion Behavior of Steels and the Characteristics of Various Ocean Environments*. International Ocean Development Conference, V2, pp. 165-83, 1975.

Shumacher, M. *Seawater Corrosion Handbook.* Noyes Data Corporation, pp. 383, Park Ridge, New Jersey, 1979.

Simon, M., A.L. Alldredge, F. Azam. *Bacterial Carbon Dynamics on Marine Snow.* Marine Ecology Programe Series V65, pp. 205-211, 1990.

Slaczka, W., E. Andrulewicz, A. Trzosinska. *First Periodic Assessment of the State of the Marine Environment of the Baltic Sea Area, 1980-1985.* Helsinki: Baltic Marine Environment Protection Commission, Helsinki Commission, 1986-1987.

Smed, J. *History of International North Sea Research ICES.* J. Sundermann & W. Lenz. North Sea Dynamics, Springer Verlag, Heidelberg, pp. 1-25, 1983.

Smith, D.C., M. Simon, A.L. Alldredge, F. Azam. *Intense Hydrolytic Enzyme Activity On Marine Aggregates And Implications For Rapid Particle Dissolution.* Nature, V359, pp. 139-142, 1992.

Smith, R.W., M.C. Hyman. *Connective-Diffusive Bubble Transport in Ship Wakes.* Naval Coastal Systems Technical Note pp. 857-887, 1987.

Smookler, A., C. Alig. *The Navy's Shipboard Waste Management Research & Development Program.* Naval Engineers Journal, 1992.

Somer, E. *Heavy Metals in the Baltic.* ICES C.M., 1977.

Stefels J., H. Revier. *Protecting The North Sea Environment - Trends And Issues.* Water Science and Technology, V24 N10, pp. 277-281, 1991.

Stewart, M. *Numerical Prediction of Thermal Ship Wakes.* Naval Research Laboratory Memorandum Report 4955, Sept., 1987.

Storer, R. *Standard Guide E 12 18. 1992 Annual Book of ASTM Standards, American Society for testing & Materials.* ASTM, Philadelphia, pp. 874-883, 1992.

Sundermann, J., W. Lenz. *North Sea Dynamics.* Berlin; New York : Springer-Verlag, 1983.

Sverdrup, H.U., M.W. Johnson, R.H. Feming. *The Oceans.* Prentice Hall, New Jersey, 1942.

Swanson, R.L., R.R. Young, S.S. Ross. *An Analysis of Proposed Shipborne Waste Handling Practices Aboard United States Navy Vessels.* Marine Sciences Research Center, University at Stony Brook, Stony Brook, New York, 1994.

Tennekes, H., J.L. Lumley. *A First Course in Turbulence.* MIT Press, Cambridge, Massachusetts, pp. 300, 1972.

Thorade, H. *Die Geschwindigkeit van Triftstromungen and die Ekman'sche Theorie.* Ann. d. Hydr. u. Marit. Meteorol., V42, pp. 379, 1914.

Tilzer M., W. Gieskes, R. Heusel, N. Fenton. *The Impact Of Phytoplankton On Spectral Water Transparency In The Southern Ocean - Implications For Primary Productivity.* Polar Biology, V14, N2, pp. 127-136, 1994.

Traverso, E. *Effects of Rolling Direction and Tensile Stress on the Corrosion of Naval Carbon Steel.* Natural Marine Environments-I: Natural Seawater, British Corrosion Journal, V14 (2), pp. 97-102, 1979.

U.S. Coast Guard. *IMO Special Areas, Final Rule.* Draft, Antarctic Designation, 1994.

U.S. Environmental Protection Agency (EPA). *Evaluation of Dredged Material Proposed for Ocean Disposal - Testing Manual.* Environmental Protection Agency, Washington D.C. and Department of the Army, Washington D.C., 1991.

U.S. Environmental Protection Agency (EPA). *Short-Term Methods for Estimating the Chronic Toxicity of Effluents and Receiving Waters to Freshwater Organisms.* First Edition, EPA/600/4-89/001, 1988.

Underwood, P.C. *New Law of The Sea For The Caribbean - An Examination of Marine Law and Policy Issues In The Lesser Antilles.* E. Gold, Marine Policy, V13 N4, pp. 353-355, 1989.

UNEP. *Regional Seas Programme In Latin America and Wider Caribbean.* United Nations Environment, UNEP Regional Seas Reports and Studies N22 Rev. 22, 1985.

UNEP. *State of The Mediterranean Marine Environment.* United Nations Environment Programme, Mediterranean Action Plan, Athens: UNEP, 1989.

UNEP. *Technical Annexes to the Report on the State of the Marine Environment.* UNEP Regional Seas Reports and Studies N114/2, 1990.

UNESCO. *Coastal Ecosystems of Latin America and the Caribbean.* Objectives, Priorities and Activities of UNESCO's COMAR Project for the Latin American and Caribbean Region, Caracas, Venezuela, 1983.

Vesecky, J.F., R.H. Stewart. *The Observation of Ocean Surface Phenomena Using Imagery From the SEASAT Synthetic Aperture Radar: An Assessment.* Journal Geophysics, Research, V87(C5), pp. 3397-3430, 1982.

Voipio, A. *The Baltic Sea.* Elsevier Scientific Publication Co., New York, New York, 1981.

Waste Discharge Into The Marine Environment: Principles And Guidelines For The Mediterranean Action Plan. Prepared in Collaboration with the Institute of Sanitary Engineering, Polytechnic of Milan, Italy, 1st ed. Oxford, New York: Pergamon Press, 1982.

Wastewater Chemistry Laboratory. *Discharge Specifications for the Point Loma Ocean Outfall. City of San Diego.* Metropolitan Wastewater Department, 1994.

Weast, R. *CRC Handbook of Chemistry and Physics, 52nd Edition.* The Chemical Rubber Company, July, 1971.

West, J.M. *Basic Corrosion and Oxidation.* John Wiley and Sons, pp. 122, New York, 1980.

Williams, P.M. *Chemical and Microbiological Studies of Sea-Surface Films in the Southern Gulf of California and Off the West Coast of Baja California.* Marine Chemistry, V19, pp. 17-98, 1986.

World Bank. *The Environmental Program For The Mediterranean: Preserving A Shared Heritage and Managing A Common Resource.* World Bank, Luxembourg: European Investment Bank, Washington, D.C., USA, 1990.

Wulff, F., L. Rahm, P. Jonsson, L. Brydsten. *A Mass-Balance Model of Chlorinated Organic Matter for the Baltic Sea - A Challenge For Ecotoxicology.* Ambio, V22 N1, pp. 27-31, 1993.

Wust, G. *1890-Stratification and Circulation in The Antillean-Caribbean Basins.* New York, Columbia University Press, 1964.

Wyatt, J.R. *Tar Ball Pollution in the Western Caribbean.* University of the West Indies, Mona, Kingston, 7, Jamaica, 1982.

Zanke, U. *Seegang Erzeugte Kolke am Bauwerken, Sonderforschungsbereich 79, Teilsprojekt B9.* Pergamon Press, Inc., Maxwell House, Fairview Park, Elmsford, New York, 1977

Zar, J.H. *Biostatistical Analysis.* Prentice Hall, Englewood Cliffs, 1984.

Zmudzinski, L. *Environmental Quality in the Baltic Region.* University of Education, Slupsk, Poland, in Comprehensive Security for the Baltic, SAGE Publications, 1989.

REPORT DOCUMENTATION PAGE

Form Approved
OMB No. 0704-0188

1. AGENCY USE ONLY *(Leave blank)*	2. REPORT DATE	3. REPORT TYPE AND DATES COVERED
	January 1996	Final_

4. TITLE AND SUBTITLE
ENVIRONMENTAL ANALYSIS OF U.S. NAVY SHIPBOARD SOLID WASTE DISCHARGES: REPORT OF FINDINGS

5. FUNDING NUMBERS
PE: 0603721N
SUBPROJ: S0401
WU: DN309084

6. AUTHOR(S)
D. Bart Chadwick, Charles N. Katz, Stacey L. Curtis, Dr. James Rohr, Marissa Caballero, Aldis Valkirs, and Andrew Patterson

7. PERFORMING ORGANIZATION NAME(S) AND ADDRESS(ES)
Naval Command, Control and Ocean Surveillance Center (NCCOSC)
RDT&E Division
San Diego, CA 92152–5001

8. PERFORMING ORGANIZATION REPORT NUMBER
TR 1716

9. SPONSORING/MONITORING AGENCY NAME(S) AND ADDRESS(ES)
Naval Sea Systems Command
2531 Jefferson Davis Highway
Arlington, VA 22242–5160

10. SPONSORING/MONITORING AGENCY REPORT NUMBER

11. SUPPLEMENTARY NOTES

12a. DISTRIBUTION/AVAILABILITY STATEMENT
Approved for public release; distribution is unlimited.

12b. DISTRIBUTION CODE

13. ABSTRACT *(Maximum 200 words)*

This report describes a preliminary environmental analysis of selected shipboard solid waste discharges. It is part of the Navy's effort to determine whether their current solid waste discharge plan is environmentally sound. The potential impact/nonimpact of solid waste discharges from Navy ships is discussed, and the preliminary theoretical and experimental findings for the environmental analysis of U.S. Shipboard Solid Waste Discharges (SSWD) is presented. This study completes the physical and chemical characterization of the waste streams. Follow-on work lies under the areas of degradation, biological interaction, modeling, field work, analysis, and reporting.

Appendices are published in a separate document.

14. SUBJECT TERMS
Mission Area: Marine Environment

Shipboard Discharge
Cellulose Pulp
Solid Waste
Analytical Chemistry
Hazard Assessment
Environmental Analysis

15. NUMBER OF PAGES

16. PRICE CODE

17. SECURITY CLASSIFICATION OF REPORT	18. SECURITY CLASSIFICATION OF THIS PAGE	19. SECURITY CLASSIFICATION OF ABSTRACT	20. LIMITATION OF ABSTRACT
UNCLASSIFIED	UNCLASSIFIED	UNCLASSIFIED	SAME AS REPORT

21a. NAME OF RESPONSIBLE INDIVIDUAL	21b. TELEPHONE *(include Area Code)*	21c. OFFICE SYMBOL
Stacey L. Curtis	(619) 553–5255	Code 522

INITIAL DISTRIBUTION

Code 0012	Patent Counsel	(1)
Code 0274	Library	(2)
Code 0271	Archive/Stock	(6)
Code 522	Charles N. Katz	(28)

Defense Technical Information Center
Fort Belvoir, VA 22060–6218 (4)

Navy Acquisition, Research and Development
Information Center (NARDIC)
Arlington, VA 22244–5114

Center for Naval Analyses
Alexandria, VA 22302–0268

GIDEP Operations Center
Corona, CA 91718–8000

Naval Sea Systems Command
Arlington, VA 22242–5160 (6)

Deputy Assistant Secretary of the Navy (E&S)
Washington, DC 20350

Office of Naval Research
Arlington, VA 22217–5000

Commander in Chief
U. S. Atlantic Fleet
Norfolk, VA 23511–2487

Naval Surface Force
U. S. Atlantic Fleet
Norfolk, VA 23511–2494

Naval Surface Warfare Center
Annapolis, MD 01402–1198

GEO Centers – Consultants